Titre: Title:	A Comprehensive Review of Vertical Ground Heat Exchangers Sizing Models With Suggested Improvements
Auteur: Author:	Mohammadamin Ahmadfard
Date:	2018
Type:	Mémoire ou thèse / Dissertation or Thesis
Référence: Citation:	Ahmadfard, M. (2018). A Comprehensive Review of Vertical Ground Heat Exchangers Sizing Models With Suggested Improvements [Ph.D. thesis, École Polytechnique de Montréal]. PolyPublie. https://publications.polymtl.ca/3034/

UNIVERSITÉ DE MONTRÉAL

A COMPREHENSIVE REVIEW OF VERTICAL GROUND HEAT EXCHANGERS SIZING MODELS WITH SUGGESTED IMPROVEMENTS

MOHAMMADAMIN AHMADFARD

DÉPARTEMENT DE GÉNIE MÉCANIQUE

ÉCOLE POLYTECHNIQUE DE MONTRÉAL

THÈSE PRÉSENTÉE EN VUE DE L'OBTENTION

DU DIPLÔME DE PHILOSOPHIAE DOCTOR

(GÉNIE MÉCANIQUE)

AVRIL 2018

UNIVERSITÉ DE MONTRÉAL

ÉCOLE POLYTECHNIQUE DE MONTRÉAL

Cette thèse intitulée :

A COMPREHENSIVE REVIEW OF VERTICAL GROUND HEAT EXCHANGERS SIZING MODELS WITH SUGGESTED IMPROVEMENTS

présentée par : AHMADFARD Mohammadamin

en vue de l'obtention du diplôme de : Philosophiae Doctor

a été dûment acceptée par le jury d'examen constitué de :

M. CIMMINO Massimo, Ph. D., président

M. BERNIER Michel, Ph. D., membre et directeur de recherche

M. KUMMERT Michaël, Ph. D., membre

M. LAMARCHE Louis, D.Sc.A., membre externe

DEDICATION

To my parents for all their love, support, sacrifice and putting me through the best life possible.

ACKNOWLEDGEMENTS

This thesis is the results of four years of efforts that would certainly have been impossible to accomplish without the help and support of the people I met during my doctoral career.

To begin, I would like to thank my research supervisor, Professor Michel Bernier for his advice and support on this project. His words of encouragements and knowledge positively affected this research and his valuable words will follow me throughout all my life.

I would like to acknowledge the support of Professors Kummert and Pasquier who helped me to learn many things and to thank Professors Lamarche and Cimmino who accepted to be members of the jury.

Throughout these years, I enjoyed the company of *Massimo*, *Vivien*; *Nicolas*, *Bruno*, *Patricia*, *Pauline*, *Laurent*, *Corentin*, *Adam* and *Houaida*, my student colleagues of the Building and Energy Efficiency group of the Mechanical Engineering Department. Also, I would like to acknowledge the friendship that I developed over the years with *Parham*, *Ali*, *Kun*, *Katherine*, *Samuel* and *Behzad*.

Finally, I thank my family for their love, support and encouragement throughout the course of this research.

The project was made possible with funding from the Natural Sciences and Engineering Research Council of Canada (*NSERC*) and the NSERC Smart Net-Zero Energy Buildings Strategic Research Network (*SNEBRN*).

Mohammadamin Ahmadfard

Montréal, April 2018

RÉSUMÉ

L'objectif principal de ce travail est d'améliorer les outils de dimensionnement pour les échangeurs géothermiques verticaux en proposant plusieurs changements à l'équation de dimensionnement classique de l'ASHRAE, en adaptant un logiciel de simulation horaire pour en faire un outil de dimensionnement et en proposant des cas tests permettant une comparaison inter-modèle.

Il est suggéré de changer l'équation classique de dimensionnement de l'ASHRAE à trois impulsions afin que les résistances thermiques effectives au sol soient évaluées en utilisant des facteurs de réponse thermique basés sur les g-functions. Les trois g-functions requises sont évaluées dynamiquement à chaque itération jusqu'à convergence vers la longueur de puits finale. De plus, il est montré que les g-functions peuvent être évaluées sans superposition temporelle de l'historique thermique des puits géothermiques. Une autre contribution de la présente étude est l'inclusion de g-functions de courte durée dans la détermination des résistances thermiques effectives au sol. Comme le montre cette étude, négliger les effets à court terme peut entraîner un surdimensionnement d'environ 10% pour un champ de puits de 12×10 lorsque les charges de pointes ont une durée d'une heure.

Dans la seconde partie de cette thèse, le modèle de stockage thermique par puits géothermique connu sous le nom de DST est combiné avec GenOpt, un programme d'optimisation générique, pour permettre le dimensionnement du champ géothermique à l'intérieur de TRNSYS, un outil de simulation de systèmes thermiques. La combinaison résultante peut prendre en compte la variation horaire du coefficient de performance (COP) des pompes à chaleur et optimiser la longueur, le nombre de puits et leur espacement simultanément.

Enfin, une comparaison inter-modèle est présentée. Premièrement, les modèles de dimensionnement actuels sont classés en cinq niveaux ($L0$ à $L4$) de complexité croissante allant des règles du pouce aux outils de simulation horaire. Quatre cas tests, chacun répondant à une difficulté différente, sont sélectionnés pour la comparaison inter-modèle de douze outils de dimensionnement, dont six méthodes de niveau $L2$ utilisant des impulsions annuelles, mensuelles et horaires, quatre méthodes $L3$ utilisant des charges mensuelles moyennes et de pointe et deux méthodes $L4$ qui utilisent des impulsions de charge horaires. Le premier test montre que lorsque la durée de pointe est réduite à une heure, les effets à court terme sont importants et les longueurs minimale et maximale sont de 39.1 m (19.1% en dessous de la moyenne) et 59.7 m (23.5% au-

dessus de la moyenne). Il est également démontré qu'un nombre important d'outils sont incapables de prédire correctement la longueur maximale requise lorsque celle-ci est survient pendant la première année. Pour le dernier cas test, la charge annuelle au sol est fortement déséquilibrée. Les longueurs calculées pour ce test varient de 93.0 m à 128.9 m. Un groupe d'outils, montre un accord relativement bon avec des valeurs minimales et maximales de 121.0 et 128.9 m, soit une différence de 6%.

ABSTRACT

The main objective of this work is to improve sizing tools for vertical ground heat exchangers by proposing several enhancements to the classic ASHRAE sizing equation, adapting an hourly-based simulation software into a sizing tool, and providing test cases to compare various tools against each other.

It is suggested to change the classic three pulse ASHRAE sizing equation so that ground thermal resistances are evaluated using thermal response factors based on g-functions. The three required g-functions are evaluated dynamically at each iteration until a converged length is obtained. Also, it is shown that g-functions can be evaluated without temporal superposition of the bore field thermal history. Another contribution is the inclusion of short-time g-functions in the determination of the effective ground thermal resistances. As shown in this study, neglecting short-time effects can lead to oversizing of about 10% for a 12×10 bore field with one hour peak loads.

In the second part of this thesis, the duct ground heat storage (DST) model in TRNSYS is combined with GenOpt, a generic optimization program, to enable bore field sizing based on an hourly simulation tool. The resulting combination can account for hourly variation of the heat pump coefficient of performance (COP) and optimize the length, number of boreholes and their spacing simultaneously.

Finally, a comprehensive inter-model comparison is presented. First, current sizing models are categorized in to five levels ($L0$ to $L4$) of increasing complexity from rules-of-thumb to simulation-based tools. Four test cases, each addressing a different difficulty, are selected for the inter-model comparison of twelve sizing tools, including six $L2$ methods that use three yearly, monthly and hourly pulses, four $L3$ methods that use monthly average and peak loads and two $L4$ methods that use hourly load pulses. In the first test, it is shown that when the peak duration is reduced to one hour, short-term effects are important and the minimum and maximum lengths are 39.1 m (19.1% below the mean) and 59.7 m (23.5% above the mean). It is also shown that a significant number of tools are unable to correctly predict the maximum required length when it is needed in the first year of operation. In the final test, the annual ground load is highly imbalanced. The calculated lengths vary from 93.0 m to 128.9 m. One group of tools, shows a

relatively good agreement with minimum and maximum values of 121.0 and 128.9 m, a 6% difference.

TABLE OF CONTENTS

LIST OF TABLES

LIST OF FIGURES

LIST OF APPENDICES

CHAPTER 1 INTRODUCTION

Ground source heat pump (GSHP) systems are used increasingly in residential and commercial buildings as they lead to low energy consumption. A typical GSHP system consists of a series of heat pumps connected to a fluid loop and a series of vertical heat exchangers, often called boreholes, embedded in the ground. Compared to air source heat pumps, GSHP systems have higher initial costs. However, on the long term, they have a lower life cycle cost due to their low operating costs.

Given the relatively high costs associated with boreholes (drilling, pipe costs, etc.) it is essential to design them carefully. In particular, the required borehole length should be minimized while providing enough underground surface area to reject or collect heat associated with heat pumps operating in cooling and heating.

Vertical U-tube boreholes, which are the main focus of this research, typically have a length ranging from 50 to 120 meters and a diameter around 100 to 150 mm. Except for very small buildings. GSHP systems typically use multiple boreholes. Boreholes should be placed at least 6 to 7 meters away from each other to avoid thermal interaction. Boreholes are typically filled with a grout to protect the aquifer and improve heat transfer. The fluid temperature changes as it circulates in the borehole and fluid temperature in the downward and upward legs are different. This may cause a thermal short-circuit between the two legs. Figure 1-1 illustrates schematically a typical GSHP system that consists of seven U-tube boreholes that are connected to a heat pump. Since the U-tubes are connected in parallel to each other, they have the same inlet (T_{in}) and outlet (T_{out}) temperatures.

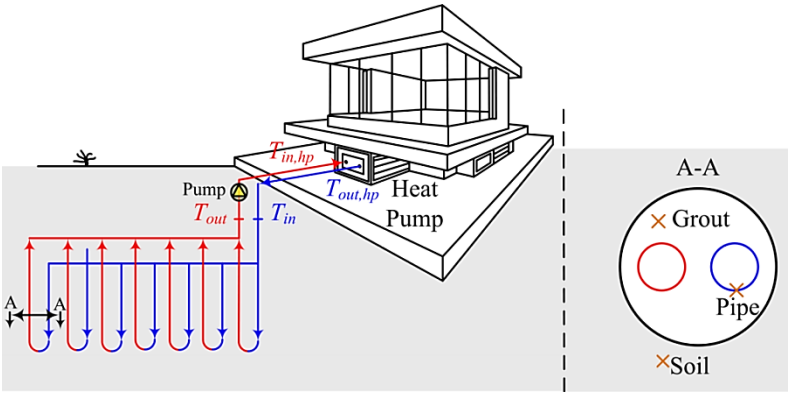

Figure 1-1: Schematic representation of a typical ground source heat pump system

In heating mode, the fluid temperature is lower than the ground temperature and heat is extracted from the ground. Conversely, in cooling mode, heat is rejected into the ground and the circulating fluid temperature is higher than the adjacent ground. The annual amounts of heat injected or rejected are most often unequal. This ground load imbalance can lead to long term ground temperature changes that can reduce the system efficiency or even lead to system failure.

The heat exchanged between the ground and the boreholes depends on many factors such as the ground temperature, the ground thermal properties, the borehole completion method, the bore field configuration and the fluid flow rate. The amount of heat exchanged in the ground depends on the building loads and the heat pump coefficient of performance (COP). Therefore, the required length of vertical ground heat exchangers depends on many factors. The boreholes should be sized so that the return temperature to the heat pumps is within the minimum and maximum operating temperatures.

To properly size vertical ground heat exchangers, many thermal phenomena that occur at different time scales during the operation of the geothermal system should be taken into account. In the short term, i.e. on a scale of several minutes to several hours, the thermal capacities of the fluid, the pipes and the grout are important as they dampen the minimum and maximum fluid temperatures that happen through the operation. In the longer term, i.e. over several years, the thermal interaction between boreholes and the annual ground load imbalances should be taken into account as they may have significant effects.

The main objectives of this study are to review and improve the current methods for sizing vertical ground heat exchangers. The first objective is to improve the ASHRAE sizing equation for vertical ground heat exchangers by removing its dependency on the use of temperature penalties. The proposed methodology uses g-functions to determine the effective ground thermal resistances and is not restricted to rectangular bore field configurations. The g-functions are evaluated “dynamically” as the solution progresses by using the Finite Line Source solution over borehole segments and without using temporal superposition. Indications are given as to the optimum number of segments and recommended convergence criteria. It is also shown how to account for borehole thermal capacity, through the use of short-time step g-functions.

The second objective is to develop an approach that sizes the ground heat exchangers based on multi-year hourly simulations. This is accomplished by combining the DST model in TRNSYS

with GenOpt, an optimization tool. With this approach, it is possible to minimize one or all three of the following parameters: borehole length, the number of boreholes, and the borehole spacing. The suggested method is able to account for the hourly evolution of the buildings/ground load as well as the changing value of the heat pump COP.

The third objective is to conduct a comparison of the current vertical ground heat exchanger sizing models. The models are first categorized into five levels ranging from rules-of-thumb to sizing methods based on hourly simulations. Then, a series of four test cases are proposed each addressing a particular difficulty. Finally, these test cases are used on twelve different sizing tools in a comprehensive inter-model comparison.

CHAPTER 2 LITERATURE REVIEW

The relevant literature not discussed in the following chapters is reviewed in this chapter. It covers heat transfer processes used for simulating vertical ground heat exchangers, various sizing models and some of the factors that have significant effects on sizing.

2.1 Heat transfer modeling of vertical ground heat exchangers

Accurate prediction of heat transfer in and around boreholes is essential for sizing vertical ground heat exchangers. Borehole heat transfer can be solved analytically or numerically or in some cases with a combination of both. Analytical models include the Infinite Line Source (ILS) solution (Ingersoll & Plass, 1948), the Infinite Cylindrical Source (ICS) solution (Carslaw & Jaeger, 1946), and the Finite Line Source (FLS) solution (Eskilson, 1987; Zeng et al., 2002), Numerical models can either be based on a Finite Difference method (Lei, 1993; Rottmayer et al., 1997), a Finite Element method (Muraya, 1994; Kohl et al., 2002), or a Finite Volume method (Rees, 2000). Due to computational time requirements and the complexity of their implementation, numerical models are generally not used for ground heat exchanger simulations. Consequently, current sizing models use analytical heat transfer models or pre-calculated numerical solution such as g-functions. It is customary to examine borehole heat transfer inside and outside the borehole separately.

2.1.1 Heat transfer outside the borehole

Heat transfer in the ground outside the boreholes includes heat conduction from the borehole wall to the ground and borehole-to-borehole thermal interaction in the case of bore fields. Heat conduction depends on the thermal conductivity and diffusivity of the ground, the borehole diameter as well as borehole spacing and length. Ground water movement can also be important in some cases.

Most of the GHEs sizing programs that are available today use g-functions that are either evaluated numerically or based on the FLS solution to model heat transfer outside the boreholes. Some programs use the ICS solutions and others use numerical or a combination of analytical and numerical solutions. In the following sections, the general concepts of some of these models are reviewed.

2.1.1.1 Infinite Line Source model

The ILS is the oldest approach used to calculate heat transfer from ground heat exchangers (Ingersoll & Plass, 1948). It applies Kelvin's line theory (1882) to obtain the temperature at any point in an infinite medium. The borehole is represented as an infinite long line that has a uniform heat transfer rate per unit length and is inserted in a medium (ground) at a uniform initial temperature. It is a one-dimensional model in the radial direction. Thus, it does not consider heat transfer in the borehole axis direction and thus end effects are neglected. In addition, the inside of the borehole (fluid, pipes, and grout) is not considered. With the ILS, the temperature at any radial point of the ground can be determined by a semi-infinite integral as follows:

$$T(r,t) - T_g = \frac{q'}{2\pi k} \int_{X=\frac{r}{2\sqrt{\alpha_g t}}}^{\infty} \frac{e^{-\beta^2}}{\beta} d\beta = \frac{q'}{2\pi k_g} I(X) \tag{2.1}$$

where r is the distance from the borehole's center line, $T(r,t)$ is the ground temperature at r for time t (when r is equal to the borehole radius, the temperature represents the borehole wall temperature at time t), T_g is the undisturbed ground temperature, α_g is thermal diffusivity of the ground, k_g is the ground thermal conductivity and q' is the heat transfer rate per unit length and $I(X)$ is the solution to the integral. Tabulated values of $I(X)$ are presented by Ingersoll et al. (1954). Ingersoll et al. (1954) mention that the ILS is accurate when t>$20r_b^2/\alpha_g$..

2.1.1.2 Infinite Cylindrical Source model

Ingersoll et al. (1950) used the solution suggested by Carslaw and Jaeger (1946) to simulate transient heat transfer from an infinite cylinder subjected to a constant heat transfer rate (or constant temperature, (Carslaw and Jaeger, 1959)) in a ground that has uniform initial temperature. Like the ILS, the ICS is a one-dimensional model in the radial direction and it neglects axial variations. The ICS solution is given by:

$$T - T_g = \frac{q'}{k_g} G_{\alpha_g t/r^2} \tag{2.2}$$

where G is the G-factor, $\alpha_g t/r^2$ is the Fourier number, r is the distance from the borehole center line and q' is the heat transfer rate per unit length. The determination of G-factors is a fairly

complex task since it includes integration from zero to infinity of an expression that contains Bessel functions (Eq. 2.3). G-factors have been calculated and are reported by Ingersoll et al. (1954) and Kavanaugh, (1985).

$$G_{\alpha_g t/r^2} = \frac{1}{\pi^2}\int_0^{\infty} \frac{e^{-z^2(\alpha_g t/r^2)} - 1}{z^2(J_1^2(z) + Y_1^2(z))}[J_0(z\,r/r_b)Y_1(z) - J_1(z)Y_0(z\,r/r_b)]dz \qquad (2.3)$$

The ILS and the ICS solutions (Eq. 2.1 and 2.2) are applicable to single boreholes and for a constant heat transfer rate per unit length. For multiple boreholes that have variable heat transfer rates, temporal and spatial superposition are needed to obtain the time evolution of the borehole wall temperature.

2.1.1.3 g-Functions

When the ground heat exchanger operates for a long time, the radial solutions presented by the ILS and the ICS are imprecise. Also, borehole-to-borehole thermal interference becomes important. One way to account for these two phenomenon is to use thermal response factors also known as g-functions based on the pioneering work of Eskilson (1987).

g-Functions are non-dimensional thermal response factors that relate the difference between the borehole wall temperature and the ground temperature to the heat transfer rate per unit length of the boreholes. The g-functions depend on the length and the radius of the boreholes as well as their spacing and are specific to particular bore field configurations. To obtain g-functions, Eskilson (1987) considered the boreholes as finite length cylinders with uniform boundary temperatures in a homogeneous ground at an initial uniform temperature. He used a transient finite-difference method on radial–axial coordinate system to solve the problem. The heat transfer rate per unit length of the boreholes varies along the borehole length and its variation is dependent on the position of the boreholes in the bore field as well as the operational time. Therefore, temporal and spatial superposition are needed to account for these effects. Equation 2.4 presents the classic definition of g-functions.

$$T_b - T_g = \frac{q'}{2\pi k_g} g\left(\frac{t}{t_s}, \frac{r_b}{H}, \frac{D}{H}, borefield\ configuration\right) \qquad (2.4)$$

where T_b is the borehole wall temperature, t_s is a characteristic time (= $H^2/9\alpha_g$), H is the borehole length, and D is the buried depth of the top of the borehole. As noted in Equation 2.4, g-functions depend on four non-dimensional parameters. Finally, according to Eskilson (1987), g-functions are valid for times greater than 5 r_b^2/α_g.

2.1.1.4 Finite Line Source solution

Eskilson (1987) and Zeng et al. (2002) presented the FLS solution. With this approach, the borehole is treated as a source of finite length subjected to a uniform heat transfer rate per unit length and immersed in a ground at an initial uniform temperature. The FLS model is thus a two-dimensional model where axial effects are considered. As shown in Figure 2-1, the FLS solution uses a mirror image above ground to account for the ground surface. When a constant ground surface temperature is assumed, the temperature at point (r, z) and at time t is given by (Eskilson, 1987):

$$T(r,z,t) - T_g = -\frac{q'}{4\pi k_g}\int_D^{D+H}\left[\frac{erfc\left(\frac{\sqrt{r^2+(z-h)^2}}{2\sqrt{\alpha_g t}}\right)}{\sqrt{r^2+(z-h)^2}} - \frac{erfc\left(\frac{\sqrt{r^2+(z+h)^2}}{2\sqrt{\alpha_g t}}\right)}{\sqrt{r^2+(z+h)^2}}\right]dh \qquad (2.5)$$

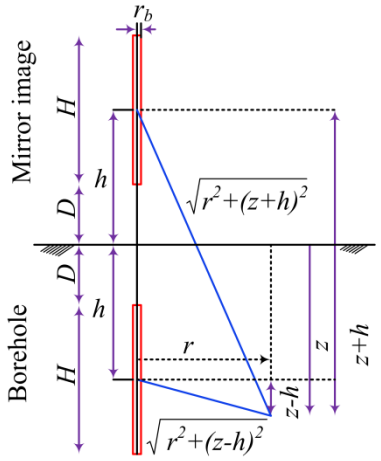

Figure 2-1: Nomenclature used in the Finite Line Source equation

Typically, Equation 2.5 is used to obtain the value of the borehole wall temperature ($r = r_b$) along the length of the borehole. It is often useful to evaluate the mean (often called the mean

integral) borehole wall temperature over the borehole length. In this case a second integral is required which lead to the following:

$$\bar{T}(r,t) - T_g = -\frac{q'}{4\pi k_g H}\int_D^{D+H}\int_D^{D+H}\left\{\frac{erfc\left(\frac{\sqrt{r^2+(z-h)^2}}{2\sqrt{\alpha_g t}}\right)}{\sqrt{r^2+(z-h)^2}} - \frac{erfc\left(\frac{\sqrt{r^2+(z+h)^2}}{2\sqrt{\alpha_g t}}\right)}{\sqrt{r^2+(z+h)^2}}\right\} dhdz \qquad (2.6)$$

Diao et al. (2004) used the borehole wall temperature at the mid-length instead of using the mean integral temperature along the borehole to simplify the solution to a single integral. Bandos et al. (2009, 2011) developed an approximation for the integral mean temperature and then used this approximation to evaluate the ground thermal properties based on data captured by a thermal response test. Their model accounts for the effects of the temperature variation on the ground surface as well as the geothermal gradients. Lamarche and Beauchamp (2007b) simplified the solution to Equation 2.6 to one integral for the case that the buried depth is zero ($D = 0$). Costes and Peysson (2008) extended the model presented by Lamarche and Beauchamp (2007b) for cases where $D > 0$. Claesson and Javed (2011) present an elegant approach to reduce the number of integrals form two to one for $D > 0$.

It is possible to use the FLS to generate g-functions. Cimmino and Bernier (2013a, 2014) initially used the FLS with a uniform heat transfer rate along the length of each borehole and one segment per borehole to obtain g-functions. The integral mean temperature is used to obtain the borehole wall temperatures. These temperatures are different for each borehole. This boundary condition, referred to as BC-I, leads to g-functions that can be largely overestimated for large bore fields. Improvements can be made to these predictions (Cimmino and Bernier 2013b, 2014) by imposing the same borehole wall temperature to every borehole and varying the heat transfer rate from borehole to borehole. This BC-II boundary condition improves the prediction of the g-functions. However, the borehole wall temperature is still calculated with the mean integral temperature even though the borehole wall temperature varies along the length of the boreholes. In order to adhere to the definition of a g-function as established by Eskilson (1987), the borehole wall temperature has to be uniform along the length of each borehole and constant in the bore field. Cimmino and Bernier (2014) applied this boundary condition, BC-III, by segmenting each borehole and applying the FLS over each of these segments to approach the true boundary condition of Eskilson (1987). With this approach, Cimmino and Bernier (2014) have shown that

it is possible to reproduce the original numerically-generated g-functions with relatively high accuracy. Their proposed methodology can account for boreholes that have different lengths and various buried depths. Recently, Lamarche (2017) modified the model presented by Cimmino and Bernier (2014) by introducing a linear heat transfer rate per unit length instead of a piecewise constant distribution profile along the borehole. The new model evaluates the results with the same precision as the model of Cimmino and Bernier (2014) with fewer segments.

2.1.2 Heat transfer inside the borehole

Various heat transfer processes occur inside the borehole including convective heat transfer between the fluid and the U-pipes inner wall, heat conduction in the pipe thickness and in the grout from the pipes to the borehole wall.

Generally, it is advantageous to have the lowest borehole thermal resistance to lower borehole length. When inlet conditions do not change significantly with time, it is possible to assume steady-state heat transfer in the borehole. For these cases, a steady-state borehole thermal resistance, R_b, is typically used. For rapidly changing inlet conditions (temperature and/or flow rate) it is necessary to model transient heat transfer in the borehole as the thermal capacitance of the grout/fluid have a significant impact in damping the fluid temperature variations. Ignoring these short-term thermal effects can lead to an error in determination of the energy consumption of the system (Salim-Shirazi and Bernier, 2013) and an overestimation of the required borehole length.

2.1.2.1 Steady-state

Javed and Spitler (2017) have provided an excellent review on methods to evaluate R_b. Values of R_b are local values. When heat transfer from the downward and upward legs is important (e.g. for low flow rates and/or long boreholes), the thermal short-circuit has to be considered. One way to achieve this is to calculate an effective borehole thermal resistance, R_b^*, Javed and Spitler (2016).

Steady-state borehole thermal resistances can be obtained experimentally from a thermal response tests (Shonder and Beck, 1999, Austin et al., 2000, Gehlin and Hellström, 2003) or analytically by using the borehole and ground thermal properties. Lamarche et al. (2007c, 2010) and Javed et al. (2009, 2010) have presented good reviews of the analytical methods that can be used for the evaluation of the boreholes thermal resistances.

Heat transfer inside the borehole has been treated as a quasi-three-dimensional problem (Dobson et al., 1995; Zeng et al., 2002). If one neglects the variation of the fluid temperature along the borehole length, the heat transfer inside the borehole can be simplified to a two-dimensional problem (Yavuzturk et al., 1999, Rees, 2000). It is also possible to reduce the problem to one-dimensional radial conduction by using an equivalent concentric cylinder (Deerman and Kavanaugh, 1991).

A conventional method for the evaluation of borehole thermal resistances is to use a circuit of thermal resistances connecting the fluid in each pipe to the borehole wall. Hellström (1991) used such an approach. He obtained the internal thermal resistances using two models: the line source model and its more general derivative, the multipole method. The multipole method was first suggested by Claesson and Bennet (1987) and Bennet et al. (1987) and recently improved by Claesson and Hellström (2011).

Hellström (1991) explains that the effect of varying fluid temperature along the U-tubes as well as the heat exchange between the legs can be evaluated by an effective fluid to ground thermal resistance R_b^*:

$$\overline{T_f}(t) - \overline{T_b}(t) = \overline{q'} R_b^* \tag{2.7}$$

where $\overline{T_f}$ is the average of the inlet and outlet temperatures, $\overline{T_b}$ is the average borehole wall temperature and $\overline{q'}$ is the heat transfer rate per unit length of the boreholes. In the case of Equation 2.7, the effective borehole thermal resistance, R_b^*, applies to the entire borehole and not locally like R_b.

Hellström (1991) then evaluates the effective thermal resistance for the two cases of uniform temperature and uniform heat flux along the borehole. For the uniform temperature case, R_b^* is determined as follows:

$$R_b^* = R_b \eta \, coth(\eta) \tag{2.8}$$

$$\eta = \frac{H}{C_f V_f 2R_b} \sqrt{1 + 4\frac{R_b}{R_{12}^{\Delta}}} \tag{2.9}$$

where H is the borehole length, C_f is the fluid specific heat, V_f is mass flow rate, R_b is the local borehole thermal resistance without the short circuit effects and R_{12}^{Δ} is the thermal resistance of the Δ circuit between the two pipes. The factor $\eta\, coth(\eta)$ gives the correction for the fluid temperature variation along the U-tubes and it can be estimated by $1+\eta^2/3$ when $\eta \leq 1$. A series expansion for small values of η gives:

$$R_b^* \approx R_b + \left[\frac{1}{3R_{12}^{\Delta}}\left(\frac{H}{C_f V_f}\right)^2 + \frac{1}{12R_b}\left(\frac{H}{C_f V_f}\right)^2\right] \qquad \eta \leq 1 \tag{2.10}$$

For the case of uniform heat flux along the borehole, R_b^* is evaluated as:

$$R_b^* \approx R_b + \left[\frac{1}{3R_a}\left(\frac{H}{C_f V_f}\right)^2\right] \tag{2.11}$$

where R_a is the product of a parallel-coupling of two parts: the thermal resistance between the pipes and the two thermal resistances between each pipe and the borehole wall that are coupled in series. In Equations 2.10 and 2.11, the terms that are in brackets account for the fluid temperature variation along the length as well as the heat exchange between the legs.

Zeng et al. (2003) and Diao et al. (2004) used a quasi-three-dimensional model to evaluate the heat transfer inside the boreholes that have uniform wall temperatures. The model accounts for the variations of the fluid temperature and pipe wall temperature through the axial direction and the impact of the short-circuiting among U-tube legs for different fluid circuit arrangements in double U-tubes boreholes. The results are obtained by Laplace transformation and it is showed that the double U-tubes arranged in parallel have better performance than the ones in series (Zeng et al. 2003).

Simplifying the two pipes into a single equivalent diameter pipe helps to simplify the heat transfer inside the borehole in the radial direction. Various approaches can be used to evaluate the equivalent diameter pipe (Bose et al., 1985, Gu and O'Neal, 1998, Kavanaugh, and Rafferty, 1997, Sutton et al., 2002).

Sutton et al. (2002) used the infinite cylindrical heat source solution to simulate heat transfer inside the boreholes. In their model, the convection thermal resistance of the fluid and the conductive thermal resistance of the pipes are neglected and the calculations are done just based

on the grout thermal properties. The U-tubes are simplified into an equivalent diameter pipe. The radius of this pipe is determined based on the borehole thermal resistance, which is evaluated with the solution proposed by Paul (1996).

2.1.2.1 Transient state

Beier and Smith (2003) developed a model that takes the thermal capacity of the fluid and the grout into account and neglects the conduction and the convection thermal resistances of the pipes and the contact resistances between the pipes and the grout. Based on these assumptions, the fluid and pipe temperatures are equal. The two pipes in the borehole are simplified to a single pipe with an equivalent diameter. The resulting one-dimensional model that simulates the temperature change in the grout and separately in the ground around the borehole is solved by Laplace transforms.

Young (2004) used the Buried Electrical Cable (BEC) model introduced by Carslaw and Jaeger (1959) for the evaluation of short-term effects in boreholes. In this model, called the borehole fluid thermal mass model (BFTM model), the boreholes are simulated as infinite cylinders inserted in a ground with uniform properties. The heat transfer inside each borehole is simulated by a core (with an equivalent diameter for the U-tubes) that is surrounded by insulation and a sheath. The core and the sheath are assumed to play the role of the fluid and the grout and have infinite conductivities and finite thermal capacitance. The insulation is assumed to play the role of the borehole thermal resistance evaluated based on the multipole method (Bennet et al., 1987). It has a finite thermal conductivity and no thermal capacitance. They used a fluid factor to account for fluid outside the borehole. In addition, they used a grout allocation factor (GAF) to adjust the grout thermal mass between the fluid and the grout and a logarithmic extrapolation procedure to improve the accuracy of the model. The grout allocation factor actually transfers a fraction of grout thermal capacity to the fluid and it depends on factors such as borehole diameter and shank spacing. Thus, it varies from case to case and is not easy to evaluate.

Lamarche and Beauchamp (2007c) solved a problem similar to the one considered by Beier and Smith (2003) in the time domain by using Laplace transforms. The model solves the exact solution for concentric cylinder heat exchangers and gives a good approximation for the U-tube heat exchangers. Heat transfer inside and outside the borehole are modeled with two different governing equations and the thermal properties of both the grout and the ground are accounted

for. The problem is solved for two conditions: i) imposed heat transfer rate per unit length at the pipes and ii) given mean fluid temperature and convention heat transfer through the pipes. For both cases, it is showed that the obtained solutions agree with the classic solutions when the grout and the ground materials are the same and these simplified cases are used for validation of the proposed method. In addition, the model is compared to four other methods including the buried cable method suggested by Young (2004), the compound model solution suggested by Sutton et al. (2002), a numerical solution based on COMSOL, and a model that uses a constant steady-state borehole thermal resistance. The suggested model matches perfectly the results from COMSOL. The buried cable model is shown to be more accurate than the classical methods but it deviates at very short time steps. The method suggested by Sutton et al. (2002) is accurate for short time steps but it has a deviation for longer time periods.

Bandyopadhyay et al. (2008a) used the classic Blackwell solution to solve heat transfer inside the borehole. In this model, the fluid is assumed to be virtual solid, with a diameter equivalent to the two pipes of the U-shaped loop, at a uniform temperature that injects constant heat at the borehole center. The model is only suitable for cases where the grout and ground have the same thermal properties. The same authors extend this approach with a semi-analytical model in which the properties of the grout and ground are different (Bandyopadhyay et al., 2008b). In this model, the solution is obtained in the Laplace domain and inverted with a numerical Gaver-Stehfest algorithm (Stehfest, 1970) in the time domain. The results of the model compare favorably well with the ones determined with a finite element method.

Yavuzturk et al. (2009) developed a finite element model to simulate transient heat transfer inside boreholes. The proposed model, developed as a TRNSYS component, uses the short time step temperature response factors (g-functions) coupled with a finite element model to simulate the inside of the borehole. The two-pipe geometry is converted into an equivalent diameter pipe. The borehole wall is actually the boundary that couples the finite element model to the ground thermal response factors and so the temperature and heat flux of this boundary should be similar in both models. The results issued from this model compares favorably well with the composite cylinder with fluid thermal mass solution introduced by Beier and Smith (2003). By comparing the model to the results obtained by Yavuzturk and Spitler (1999), it is observed that when the borehole thermal resistance is assumed to vary in time, the temperature profile takes 15 to 20 hours to follow the temperature profile modeled with a steady-state borehole thermal resistance.

Javed et al. (2010) and Javed and Claesson (2011) proposed an analytical model to simulate the short term temperature response of vertical ground heat exchangers. In the applied model, the U-tubes are replaced by a pipe with an equivalent diameter and the thermal resistance and thermal capacities of all ground heat exchanger elements are taken into account. Borehole heat transfer is solved in the Laplace domain with the use of a circuit of thermal resistances and by using inverse transforms to revert it back to the time domain. The authors compared their results to the BFTM of Young (2004), the solution suggested by Lamarche and Beauchamp (2007) and the virtual solid solution introduced by Bandyopadhyay et al. (2008a). These models are compared for three different borehole completion method: i) filled with ground water, ii) backfilled with thermally enhanced grout and iii) backfilled with borehole cuttings. The authors explained that the model suggested by Young assumes that the grout and the fluid have lumped thermal capacities and temperatures which is not correct in reality. In addition, the grout allocation factor and the logarithmic extrapolation that are suggested in this model are ambiguous to calculate and this model is the most inaccurate one for all three filling conditions. The model suggested by Lamarche and Beauchamp (2007) does not account for the fluid thermal capacity and this causes its results to be inaccurate for short times; however its results merge to the results of the suggested method on the long term. The model introduced by Bandyopadhyay et al. (2008a) is also shown to be inaccurate since the boreholes are assumed to be backfilled with borehole cuttings which does not happen often in reality.

So-called thermal resistance capacitance (TRC) models can also simulate the short-term behavior of boreholes. Bauer et al. (2010, 2011) made the initial contribution in this area followed by Zarella et al. (2011) and Pasquier and Marcotte (2012, 2014). In most cases, TRC models can also account for axial variations.

Li and Lai (2012) used the infinite linear source solution in a composite medium to obtain short-term response factors. The line sources are positioned according to the position of the pipes in the borehole and are superimposed spatially. The thermal responses are evaluated at the pipe wall and so the thermal resistance of the borehole is evaluated implicitly. The solution is mentioned to be valid until the axial effects appear. Later, Yang and Li (2014) used the finite volume method as well as some measured experimental data to check the validity of the composite medium line source model. The results showed that except for very short time periods, the results of both numerical and analytical models match each other but they are both higher than the experimental

data. For short periods (3 to 4 min), it is observed that the composite line source does not have the sufficient accuracy and so the authors have suggested to use this model for simulations of more than 3 minutes.

Salim-Shirazi and Bernier (2013) used the finite volume model coupled to the cylindrical source solution to simulate the boreholes outlet fluid temperature for varying inlet temperature and flow rate. In the applied model, the axial and azimuthal temperature variations are neglected and only the radial variations are accounted. The fluid and the grout thermal capacities are also accounted and an equivalent geometry consisting of a single pipe and a cylinder core filled with the grout is used. The developed model is compared to some analytical and numerical models as well as the experimental data presented by Spitler et al. (2009). Simulations of a building equipped with an on/off heat pump showed that neglecting the thermal capacity of the grout and the fluid leads to an overestimation of the heat pump energy consumption.

As described earlier, the original g-functions are used to evaluate heat transfer from the borehole wall to the ground. Therefore, they were not originally intended to predict the thermal behavior inside boreholes for short-time steps, i.e. for times less than $5r_b^2/\alpha_g$ (it is typically 9 hours when $r_b = 0.075$ m and α_g=0.075 m^2/day). However, for sizing or simulating the operation of vertical ground heat exchangers correctly, it is important to predict the short-term behavior of the borehole.

Yavuzturk and Spitler (1999) and Yavuzturk et al. (1999) extended the long-term g-function and presented so-called short-time g-functions. To evaluate the g-functions for short time steps, they used a two-dimensional (in polar coordinates), fully implicit finite volume formulation that uses "pie-sector" representation of the U-tubes. The thermal capacitance of the grout, the pipes and the fluid are included in the calculations. In order to follow the g-function definition introduced by Eskilson, the authors subtracted the contribution of the steady-state borehole thermal resistance of the borehole from the thermal response. This leads to negative g-functions for very short-time periods. In effect, when using short-time g-functions, the borehole wall temperature is obtained using:

$$T_b - T_g = q' \left(R_b + \frac{g_{sh}\left(\frac{t}{t_s}, \frac{r_b}{H}\right)}{2\pi k} \right) \tag{2.12}$$

where R_b is the borehole thermal resistance and g_{sh} is the short-time g-fucntion. The g-function takes the value of $-2\pi kR_b$ when $T_b = T_g$ for $t = 0$. As time progresses, the g-function values gradually increase and become positive after a certain time. The generated short time-step g-functions line up very well with Eskilson's long time-step g-functions indicating the validity of the approach proposed by (Yavuzturk and Spitler, 1999). Transient effects in the borehole can be considered negligible when the short-term and long-term g-function curve merges. This approach has also been modified to handle variations of borehole thermal resistance which can occur with fluid flow rate variations. The model has been validated successfully against the operational data of an elementary school (Yavuzturk and Spitler, 2001).

Xu and Spitler (2006) used a one-dimensional numerical model to calculate the short-term g-functions. The model uses an equivalent concentric cylinder geometry with five elements (a fluid layer, an artificial convective resistance layer, a tube layer, a grout layer and the surrounding ground) to represent the borehole. It is also possible to account for the thermal effects of the fluid outside the boreholes by using a fluid factor. The one-dimensional thermal resistances are calibrated so that they always match the total two-dimensional resistance that can be determined by the multipole method (Bennet et al., 1987). By controlling these parameters, the one-dimensional model compares favourably well with the two-dimensional boundary-fitted coordinates GEMS2D model (Rees, 2000) at a significantly lower computational cost (Xu, 2007).

2.2 Vertical ground heat exchanger sizing models

In this work, the sizing models are categorized into five levels based on the type of ground/building loads that they use. These levels are as follows:

Level 0- Rules of thumb, graphical charts and correlated equations

Level 1- Two load pulse methods

Level 2- Three load pulse methods

Level 3- Monthly average and peak load pulses

Level 4- Hourly loads

These levels and the most important underlying methods are reviewed in chapter seven. For completeness, the following section describes the models that are not discussed in chapter seven.

2.2.1 Level 0

2.2.1.1 Rules of thumb

The simplest way of sizing ground heat exchangers is to use rules of thumb. Rules of thumb relate the length of the ground heat exchangers to the peak heating or cooling loads of the building or to the installed capacity of the heat pump.

Rules of thumb are often used in small residential buildings where the experience of the installer dictates the required length based on the installed capacity of the heat pump. However, for large bore fields with large annual ground thermal imbalances, rules of thumb may result in large errors. In addition, rules of thumb do not account for the effects of design temperatures (maximum and minimum entering heat pump fluid temperatures) or many other design factors such as the borehole thermal resistance. Following is a review of rules of thumb used in various countries.

Rules of thumb up to 1983

Ball et al. (1983) reviewed borehole sizing models developed up to 1983 and categorized sizing models into three groups: rules of thumb, steady state models and transient models.

The authors state that rules of thumb have served well when the ground and weather conditions were fairly similar from one project to the next. However, they do not give good results for short boreholes, small borehole spacing, and high extraction rates. In addition, they mention that rules of thumb should not be extrapolated to other ground or weather conditions. The authors have presented various rules of thumb in a table similar to Table 2-1. Unfortunately, these rules are unclear and difficult to interpret.

The rules of thumb presented in Table 2-1 can be compared to the results of a study presented by Caneta (1998). In this study, the operational details of nine commercial/institutional buildings equipped with ground source heat pump systems located in the United States and Canada are analyzed. The results are summarized as follows: average building floor area 45900 ft^2 (range from 8000 ft^2 to 181069 ft^2), average heat pump capacity of 111 tons (range from 24 to 410 tons),

average flow rate of 2.46 gpm/ton (range from 0.4 to 3.2 gpm/ton), average vertical borehole length of 131 ft/ton (range from 92-176 ft/ton). By multiplying the last value by two, the average piping length is determined as 262 ft/ton (range of 184-352 ft/ton) which is within the values reported for copper/steel piping in Table 2-1.

Table 2-1: Rules of thumb reported by Ball et al. (1983)

Parameter	Reference
➢ **Piping length, m/kW (ft./ton) of heating or cooling**	
19 to 37 (215 to 430) with copper/ steel piping	(Ambrose, 1966)
28 to 37 (320 to 430) with plastic piping	(Bose, 1981)
9 (108) wetted vertical piping	(Bose, 1981)
36 (413) European experience (20 W/m) (21 Btu/(h.ft.)) average heat extraction rate at COP of 3.0	
➢ **Burial depth m (ft.)**	
1.3 (4.3) with cooling	
0.5 to 0.8 (1.6 to2.6) Without cooling	(Oskarsson, 1981)
➢ **Spacing m (ft.)**	
1.3 to 1.6 (4.3 to 5.2)	(Oskarsson, 1981)
➢ **Outside diameter of piping**	
Ground heat flow to piping is independent of diameter	(Vestal and Fluker, 1956)
Size inside diameter to minimize pumping power	
➢ **Circulation rate**	
0.04 to 0.07 L/(s.kW) (2 to 4 gpm/ton)	(Bose, 1982)
Reynolds number high enough to be above laminar flow but low enough to minimize pumping power i.e. 5000 to 10000	

Ball et al. (1983) also explained that up to the 1983 no general design guidelines or publicly available design methodology were available in the United States or in Europe. Furthermore, the available models are both too detailed and expensive to use or too simple and not much more accurate than rules of thumb.

Germany

In Germany, the lengths of borehole heat exchangers are often less than 100 m deep as longer boreholes need special permissions according to the German mining law. The temperature difference between the fluid in the boreholes and the undisturbed ground must not exceed ±10 °C under average load and ±15 °C under peak load conditions.

The German Guideline (Richtlinien, 2001) makes a distinction between small systems that have heating power less than 30 kW and larger ones. Small systems can be designed with a table of values and a nomogram, whereas the bigger systems should be designed by computer simulations. A part of this table is presented in Table 2-2. As can be seen, the specific heat extraction rates can be used for design of vertical ground heat exchangers in different geological conditions. As an example, based on Table 2-2, when a house has 2400 annual full load heating hours and the ground thermal conductivity is 2.0 W/m-K, the borehole heat extraction rate is about 50 W/m. If the heating power is assumed equal to 12 kW and the seasonal performance factor is 3.13, then the total required length would be 163.2 m (=12 kW/50 W/m ×(3.13-1)/3.13). As this length is more than 100 m, two boreholes of 81.6 m can be used.

Table 2-2 is restricted to the following conditions: Borehole lengths: 40 – 100 m, borehole spacing: 5 m for 40 –50 m and 6 m for 50 –100 m boreholes, double U pipes DN20, DN25 or DN32 or coaxial borehole with more than 60 mm in diameter. Only heat extraction (which may include production of hot water) is considered. The extraction power of boreholes that have thermal interferences has to be reduced by 10 –20 %. In cases that have less than 1000 hours of operation per year the length of the boreholes can be reduced by around 10 %. In summary, under the German guidelines, the required total length of the borehole should be determined based on the amount of heat that is to be withdrawn per meter. For grounds that have low thermal conductivities, such as dry sand, heat extraction rates are around 20 to 25 W/m while high thermal conductivity grounds, such as granite, heat extraction rates of 70 to 84 W/m are reported.

Table 2-2: Some typical rules of thumb based on German guidelines

Underground	**Specific heat extraction**	
General guideline values	1800 h/y	2400 h/y
Poor underground (dry sediment), k_g<1.5 W/m.K	25 W/m	20 W/m
Normal rocky underground and water saturated sediment, 1.5<k_g <3 W/m.K	60 W/m	50 W/m
Consolidated rock with high thermal conductivity, k_g >3 W/m.K	84 W/m	70 W/m
Individual rocks		
Gravel, Sand, dry	<25W/m	<20W/m
Gravel, Sand, water saturated	65-80 W/m	55-65 W/m
For strong groundwater flow in gravel and sand, for individual systems	80-100 W/m	80-100 W/m

Switzerland

The Swiss Bundesamt Für Energie wirtschaft (Stadler et al., 1995) has developed a nomogram, similar to the one reproduced in Figure 2-2, for sizing of small systems located in Switzerland. The nomogram is developed based on the results of computer simulations and was not validated by field monitoring. As can be seen, by using this nomogram, the length of single and double U-tube boreholes can be determined based on the annual heating energy, the heating power and the climatic conditions of the building which is defined based on the altitude of the building's location. A nomogram factor, a, defined in Equation 2.13 is required for using the nomogram.

$$a = \frac{Q_{Ha}}{Q_{Ha}/\beta_a - Q_{pa}} \tag{2.13}$$

where Q_{Ha} is the annual heating energy in kWh/year, Q_{pa} is the annual energy demand of peripheral components (circulation pump) in kWh/year, and β_a is seasonal performance factor.

The use of the nomogram is presented here with the example introduced in previous section. The house requires 2400 full load heating hours per year and the required power is 12 kW, then the annual heating energy, Q_{Ha}, is equal to 28.8 MWh/year (12 kW×2400 h) which is out of the specified range of heating energy (4–16 MWh/year) in the nomogram. Therefore, it is assumed that the total energy is provided by two boreholes with no thermal interactions (each provide 14.4 MWh/year with a heating power of 6 kW). Assuming that the power of peripheral components is

equal to 0.4 kW, the annual required energy (Q_{pa}) is 0.96 MWh/year (=0.4 kW×2400h). As a result, the nomogram factor is 4.0 (=14.4/(14.4/3.13-0.96)). If the house is assumed to be located at an altitude of 300 m, the resulting length of each borehole is around 75 m. This length can be compared to the length of 81.6 m determined earlier with Table 2.2.

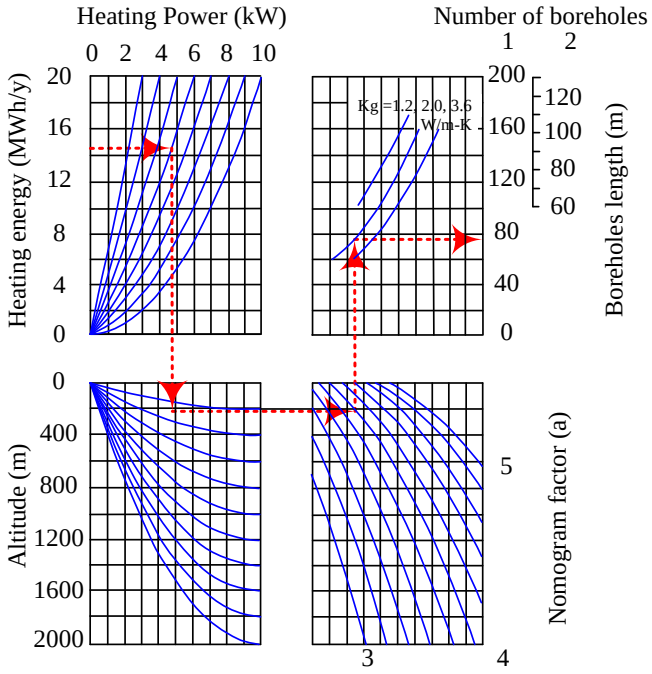

Figure 2-2: Nomogram for design of Vertical ground heat exchangers (adapted from Stadler et. al., 1995)

England

Banks (2012) has presented a figure, similar to the one reproduced in Figure 2-3, based on data gathered from some documented case studies. The figure reports the number of boreholes (left axis) and the total drilled meters (right axis) as a function of the heat pump delivery (in kW). It should be noted that all axes have logarithmic scales.

As mentioned by Banks (2012), most of these cases are either constructed or designed in the United Kingdom. The majority of data presented in Figure 2-3 are for heating dominated cases. However, some of the larger systems (more than 60 kW) are cooling dominated or provide both cooling and heating. As shown on this figure, the open loop systems extract more heat per borehole compared to closed loop systems. The installed capacity per borehole ranges from 2 to 17 kW. The smallest installed capacities are related to the shallowest (40 m) and the highest to

the deepest boreholes (180 m). The ratio of installed heat pump capacity over the total number of drilled meters ranges from 37 to 104 W per drilled meter, with an average of 67 W/m that corresponds to a ground peak heat extraction rate of 47 W/m for a heat pump COP of 3.4. As stated by Banks (2012) the heat extraction rate of 50 W/m (corresponding to a building peak requirement of 70 W/m) is the commonly used rule of thumb in the European ground source heat pump industry. However, this value may not result in very efficient systems. Banks (2012) has mentioned that the British guidelines recommend specific peak heat extraction rates of 25-40 W/m for ground thermal conductivities in the range of 1.5 to 2.5 W/m.K. These values are reported for small heating systems with 1800 to 2400 h/year equivalent full load operational hours.

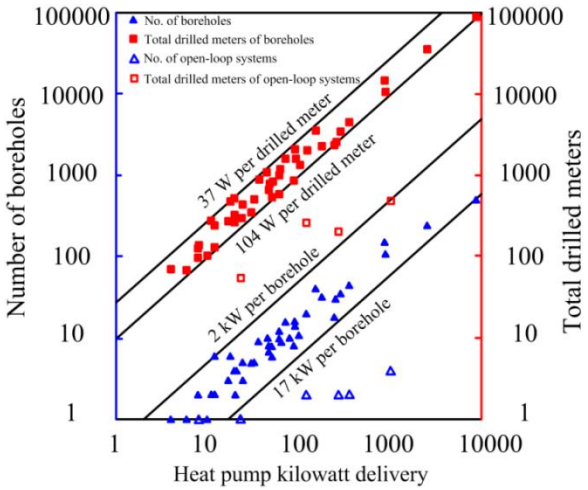

Figure 2-3: Number of drilled boreholes and their corresponding total drilled meters for a variety of vertical closed loop GSHP systems and a small number of open-loop systems as a function of installed heat pump kilowatt delivery (adapted from a figure presented by Banks (2012))

Banks (2012) has also summarized the rules of thumb reported by Rosén et al. (2001) who mention that in the United States, some installed single U-tube boreholes have a 68– 82 W/m heat exchange rate. In Austria, peak heat extraction rates of 30 W/m for dry sediments and 70 W/m for granite are recommended, when the temperature difference between the carrier fluid and the undisturbed ground is about 10 °C. Across Europe, the average peak heat extraction rates is typically about 62 W/m for systems with operating times of 1600– 2400 h/year.

Spitler and Cullin (2008) have questioned sizing of ground heat exchangers based on rules of thumb. The authors explained that rules of thumb are not applicable to buildings that have highly

variable relationships between peak and annual loads or to the ones which have an imbalance annual load that increases (or decreases) the heat pump entering fluid temperature in each year. To evaluate the effectiveness of rules of thumb a three-story office building, a hotel complex (Xu, 2007) and a school building (Chiasson et al., 2004) are considered in fourteen locations (Briggs et al., 2003). The Energyplus software program is used to determine the hourly building loads of each combination. The obtained loads are then used by HVACSIM+ (Clark, 1985) to determine iteratively the required length of the ground heat exchangers in a way that the heat pump entering fluid temperatures stay within prescribed bounds. The results are reported as the ratio of peak heat rates over the obtained total heat exchanger length. The results show that designing ground heat exchangers based on rules of thumb may result in oversized expensive systems or undersized heat exchangers that will fail quickly. The authors concluded that various combinations of ground properties, grout properties, working fluid, design temperature limits and building energy needs can vary peak heat transfer rates of boreholes significantly and no rules of thumb is able to consider the high degree of variability of these combinations.

2.2.1.2 Sizing with correlated equations

Aside from rules of thumb, it is possible to size ground heat exchangers using correlated equations resulting from the simulation of various cases. However, in general, correlated equations are very limited as they do not cover all climates, geological conditions and building sizes. For example, correlated equations cannot account for borehole thermal interactions or the annual ground load imbalances correctly and these parameters are very important in designing of large residential or commercial systems. In addition, borehole characteristics (radius, type of grout etc...) are rarely similar to the ones used in simulations. Therefore, reported correlations can only give the users an estimation of the heat exchanger length but they cannot be used in the final design of ground heat exchangers.

Cane et al. (1995) obtained three correlated equations based on simulation results for 396 cases obtained using an hourly building energy simulation software and a ground heat exchanger sizing tool. The ground heat exchanger sizing tool uses the infinite line source theory combined with the superposition principle and accounts for effects such as on-off cycling, pipe-to-pipe interference in U-tubes and earth temperature variations with depth and time of the year. The model is validated by actual system data collected from a large secondary school and several residential

building installations (Caneta Research Inc., 1992; Caneta Research Inc., 1993). The test cases cover various types of building types and sizes, two levels of heat pump efficiency and internal loads and seven locations (three in the United States and four in Canada).

Table 2-3 shows the resulting three correlated equations. In these equations, E_{Rej} is the annual rejected energy in cooling mode and E_{Ext} is the annual extracted energy in heating mode, T_H is set to $T_m + 20℃$ and T_L is set to $T_m - 10℃$ through simulations. Using these equations, two lengths are determined corresponding to the heating and cooling modes; the longer of the two is the final length of the ground heat exchangers. It should be noticed that the reported lengths show the total pipe length which is twice the borehole length. The boreholes are assumed to be far from each other so that there is no borehole-to-borehole thermal interference.

Table 2-3: Correlated equations obtained from the simulation of 396 cases

Scenario	The required heat exchanger length
Cooling without the hot water load	$L = 183.9 \times E_{Rej} / (T_H - T_m)$ (2.14.a)
Heating without the hot water load	$L = 198 \times E_{Ext} / (T_m - T_L)$ (1.14.b)
Heating with the hot water load	$L = 189.7 \times E_{Ext} / (T_{mean} - T_{min})$ (1.14.c)

To show the applicability of the correlated equations, a large office building in Philadelphia with low internal loads and low efficiency heat pumps is selected as an example. The peak cooling load of the building is determined to be 504 kW (143 tons) and its annual heat rejected is evaluated at 982 MWh (3044 MBTU). Using the correlated equations, a heat exchanger length of 8200 m (26900 ft.) is determined. The same problem is sized using the rule of thumb of 300 ft/ton of installed cooling capacity with a resulting the length of 13100 m (43000 ft.) which is about 60% more than the predicted length by the correlated equations.

O'Neal et al. (1994) have also suggested a correlated equation for borehole sizing in residential buildings in Texas. Since the cooling requirements are much more important in Texas, the heat exchangers are only sized for the summer period. The sizing procedure is developed using a ground coupled heat pump transient simulation (GSIM) model that uses the ICS solution to determine the borehole wall temperature. The heat exchanger is discretized axially. The heat flux over each element is assumed uniform but it varies along the length of the borehole. Thermal

short-circuiting between adjacent legs is also considered in the calculations. Hundreds of runs are executed with GSIM to evaluate the effects of various parameters such as outdoor weather, indoor temperature, soil density, ground thermal conductivity and temperature, cooling load and heat pump performance. Results are then used to develop the following correlated equation.

$$L_{ground\ coil} = L_b \times C_{it} \times C_{gt} \times C_{density} \tag{2.15}$$

where L_b is the heat exchanger base length, and C_{it}, C_{gt}, and $C_{density}$ are, respectively, the indoor air temperature, the ground temperature and the ground density correction factors. L_b is determined for the given ground thermal conductivity and average daily temperature swing and it is presented in two graphs for two different air temperature ranges. The three correction factors are also presented in three graphs.

An example is solved with the correlated equation and the results are compared with the ones obtained by the NWWA (Hart & Couvillion, 1986) and IGSHPA (1986) sizing methods. The required length is evaluated at 88.4 m (290 ft.) by the correlated equation, whereas the lengths obtained by the NWWA and IGSHPA methods are respectively 112.8 m (370 ft.) and 141.7 m (465 ft.). As can be seen, there are relatively large differences between the models. As mentioned by the authors, the methodology is limited only to cooling of residences in Texas and cannot be used elsewhere. The authors have reminded the users that the ground thermal properties and temperature may vary dramatically within a given city. Also, the average air temperatures and its amplitude variation may vary in time. In such cases, inaccurate inputs may affect the heat exchangers length noticeably. In addition, some parameters such as the cooling capacity, coefficient of performance (COP), water flow rate, and the maximum entering water temperature are considered constant in simulations. Such simplifications have limited the application of the correlation.

2.2.2 Sizing models for levels 1 to 4

In this section, sizing models in the levels 1 to 4 categories that are not examined in chapter seven are introduced below and are compared in a summary table.

2.2.2.1 Sizing based on a constant load (Level 1)

Bernier (2014) illustrates a simple sizing problem with a constant load for three different test conditions to show the impacts of axial effects and borehole-to-borehole thermal interferences. This can be considered to be a Level 1 method.

The problem is to determine the total required length of a bore field subjected to a constant heat injection of 9.63 kW if the mean fluid temperature is to be limited to 35 ℃ for a 20 year design period. In the first test, the axial heat transfer effects and the borehole-to-borehole thermal interferences are neglected and the result is determined using the cylindrical heat source solution. In the second test condition, a 3×2 bore field is used to dissipate the heat. The axial heat transfer effects are taken into account but the thermal interferences are neglected. Therefore, the g-functions are evaluated from the curve $B/H \rightarrow \infty$ (where B is the borehole spacing and H is the borehole length). As the g-functions depend on the borehole length which is unknown *a priori*, the borehole length is calculated iteratively. The iteration starts with a guessed value of the borehole length, H. Then Equation 2.16 is used to determine the g-function and it's corresponding logarithmic non-dimensional time (i.e. $ln(t/t_s)$, where t_s=$H^2/9\alpha$). Then a new length is found and this process is repeated until the value of H converges.

$$T_m = T_g - \frac{q}{H}\left(R_b + \frac{g}{2\pi k_g}\right) \tag{2.16}$$

In the third test condition, the borehole thermal interferences and the axial heat transfer effects are both accounted in the calculations. Similar to the second test, a 3×2 bore field is used and the borehole length is determined iteratively using g-functions. The total borehole length obtained for the first case by CHS is 312 m, while the lengths obtained for the second and third case by g-functions are respectively 275.4 m and 600 m. Thus, borehole-to-borehole thermal interactions have an important effect on the required length of this 3×2 bore field.

2.2.2.1 RETScreen (Level 1)

RETScreen is a software program that can evaluate the annual required energy, energy savings and costs of GSHP systems. It can also evaluate the length of horizontal, vertical and open loops for commercial or residential buildings

To determine the length of horizontal or vertical loops, RETScreen uses the IGSHPA method (to be described in chapter seven). The model first uses the bin method to distribute the hourly temperature occurrences and to determine the annual required energy and the annual average coefficient of performance of the system. Once the length is evaluated, the actual heat pump performance and capacity can be calculated for each bin and then the annual energy use and can be evaluated.

This model provides a quick estimate for sizing of ground heat exchangers. However, it uses some assumptions that limit its applicability. For example, complex building load profiles cannot be produced or analyzed with the RETScreen method. The long-term thermal imbalances are also ignored in the calculations. The bin method that is used for evaluating the buildings energy loads and peaks is very simplistic and the results may not represent real loads. For these reasons RETScreen tend to oversize ground heat exchangers compared to other commercial programs (CANMET, 2005).

2.2.2.2 GchpCalc (recently renamed as GshpCalc) level 2

GchpCalc is a ground heat exchanger sizing tool that has been used widely within the United States. The fundamental concepts behind the GchpCalc are reported in the book written by Kavanaugh and Rafferty (1997) and in the methodology described in the ASHRAE Handbook (ASHRAE, 2011) (described in chapter seven as the ASHRAE classic sizing equation). The method is based on the use of the ICS to model transient ground heat transfer for three load pulses (annually, monthly and hourly). For each pulse, GchpCalc calculates the ground thermal resistance using the ICS solution. The three ground thermal resistances are then used to determine the ground heat exchangers length. GchpCalc reports two lengths, one for heating and one for cooling. The procedure uses the user-defined annual equivalent full load hours and the building zone loads to calculate the load pulses. Next, the user specifies the desired maximum and minimum entering heat pump fluid temperatures, the nominal flow rates and the heat pump manufacture (from a data base). The program then selects the required heat pump for each zone and calculates its COP. The user enters the ground thermal properties as well as the bore field configuration. The tool then calculates the required ground heat exchanger length. The model gives the opportunity to evaluate design alternatives to reduce cost and land area or increase the system efficiency by changing one or more parameters without entering all of the original

information. These parameters can be the maximum and minimum loop temperatures, borehole dimensions, heat pumps efficiencies and operating hours. Other alternatives that can be examined are hybrid systems (cooling towers), less expensive and lower efficiency heat pumps. Groundwater movement effects are neglected in GchpCalc.

2.2.2.3 ASHRAE modified equation suggested by Li et al. (2017) (level 2)

Li et al. (2017) have developed an iterative sizing model derived by reformulating the ASHRAE classical equation. In their proposed method, the borehole lengths are evaluated so that the heat pump inlet temperature satisfies the two design temperature limits with a minimum borehole length. In addition, an effective fluid to pipe thermal resistance is applied instead of using a steady-state borehole thermal resistance. The fluid to pipe thermal resistance is evaluated by a quasi-3D model that accounts for the impact of the vertical temperature variation of the fluid inside the U-tubes and the effects of fluid flow rate. The authors evaluate G-factors (not to be confused with the ICS solution or g-functions) using three models: a so-called composite medium solution for evaluating the short term thermal response, the infinite line source solution for evaluating the mid-term thermal responses and the finite line source solution for calculating the long term thermal responses and also for evaluating the thermal interaction between the boreholes. Graphs are presented for simplifying the evaluation of the G-factors; however, it does not seem that using these graphs lead to an accurate result because: 1. interpolation between curves is necessary, 2. graphs are based only on square bore field patterns, 3. graphs are reported for very specific values for each parameter, 4. using these graphs manually, for each heat pulse, in each iteration, is difficult. The authors concluded that the new formula yields a less conservative and more accurate design length compared to the ones determined by the ASHRAE classical equation when sizing of the four test cases introduced by Cullin et al. (2015).

2.2.2.4 GLD (level 3)

Ground Loop Design (GLD) is a tool that sizes vertical, horizontal and surface water heat exchangers. GLD uses two methods to size vertical ground heat exchangers. The first method is based on the ICS solution. The model uses the method proposed by Deerman and Kavanaugh (1991) to account for the U-tube arrangement and hourly time steps. This method is described below in section 1.3.5. The second method is based on Eskilson’s g-function technique. Both

methods consider the long-term operation effects to evaluate the results. The availability of two models in a single program gives the users the opportunity to compare the results.

Loads can be entered using two approaches in GLD: average block load module and zone manager loads module. The average block loads module uses a particular, user-defined heat pump (or COP) and matches it in an average way to the entire installation. It accepts monthly loads (total and peak) data and it accepts 8760 hourly data in the new versions of GLD (2012).

The zone manager loads module has the ability to model various zones with different loads and equipment. It accepts average peak load data for every hour of a twenty-four hour day, however, for simplification, average peak loads for the design day can be summarized in four simple load pulses.

2.2.2.5 TRC model in TRNSYS (level 4)

Godefroy (2014) and Godefroy and Bernier (2014) have developed a model using a thermal resistance-capacitance (TRC) approach in the TRNSYS environment which has been successfully validated experimentally (Lecomte et al., 2016). The model is not actually a sizing tool, but similar to the procedure that is descried for the DST model in chapter six, the model can be used as a $L4$ design tool. In this TRC model, the borehole is divided into vertical sections. Heat transfer inside the borehole is evaluated at each time step using a thermal resistance and capacity network. The heat exchange with the ground can either be modeled using the ICS independently for each of the vertical sections of the borehole or by using specific g-functions.

2.2.3 Summary of sizing tools

The sizing models discussed in this thesis as well as their heat load types and heat transfer models are listed in Table 2.4. Some of the sizing models, listed in this table, are compared with four specific test cases in chapter seven. It is shown that sizing models exhibit large differences in cases where the thermal interaction between the boreholes and the annual load imbalances are relatively large or when the borehole thermal capacity has a significant effect on fluid temperature (for example when the peak durations have high magnitude but small duration). In the next section, some of the factors that may have important effects on the accuracy or calculation time of the sizing models are briefly reviewed.

Table 2-4: Comparison of the sizing methods discussed in the thesis

	Sizing model	Load type	Heat Transfer model
Level 0	Rules of thumb	Peak load or heat pump capacity	------
	Nomogram or correlated equations	Peak loads or heat pump capacity	Various models
Level 1	IGSHPA method*	Heat pump capacity	ILS
	Modified IGSHPA method*	Heat pump capacity	------
	Bernier's iterative method	A constant ground load	g-function
	RETScreen	Monthly average loads (Built in)	Bin Method and ILS
Level 2	ASHRAE equation*,**	Three ground pulses	CHS and ILS
	Modified ASHRAE equation*,** (excel spread sheet, (Philippe et al., 2010))	Three ground pulses	CHS and g-function
	Alternative method*,**	Three ground pulses	g-function
	Chiasson's Excel spread sheet*	Three ground pulses	g-function
	Modified ASHRAE equation Li et al. (2017)	Three ground pulses	G factors
	GchpCalc	Heating and cooling EFLHs and peak pulses (Tideload10v1 excel file)	Cylinder and line source method
Quasi level 3	Monthly ASHRAE modified method*,**	Monthly ground average and peak loads	CHS and g-function
	Monthly Alternative method*,**	Monthly ground average and peak loads	g-functions
Level 3	NWWA*	Monthly loads	ILS
	Chiasson's Excel spread sheet*	Monthly average and peak loads	g-function
	EED*	Monthly average and peak loads	g-function
	GLHEPro*	Monthly average and peak loads	g-function
	MLBDA*	Monthly average and peak loads	Developed based on Hellström's duct storage model
	GEOSTAR*	Monthly average and peak loads	Finite line source
	Spectral method**	Monthly average and peak loads	g-function and Fourier transform
	Load aggregation method**	Monthly average and peak loads	g-function
	Ground Loop Design	Hourly and monthly loads (LEADPlus)	Cylinder and line source method and g-function
Level 4	Hourly load simulation design model (HLSD) *	Hourly loads	the inverse Laplace transform of the g-function
	TRC model	Hourly loads	CHS and g-function
	DST model in TRNSYS*	Hourly loads	Analytical/numerical methods

* These models are presented in chapter seven.

** These models are used in a VBA Excel file presented in Appendix A.

2.3 Factors that have significant effects on sizing of vertical ground heat exchangers

Figure 2-4 illustrates schematically the steps that most sizing models need to follow to determine the length of ground heat exchangers. These steps are also presented in chapter seven (see Figure 7-2) as a function of the sizing level.

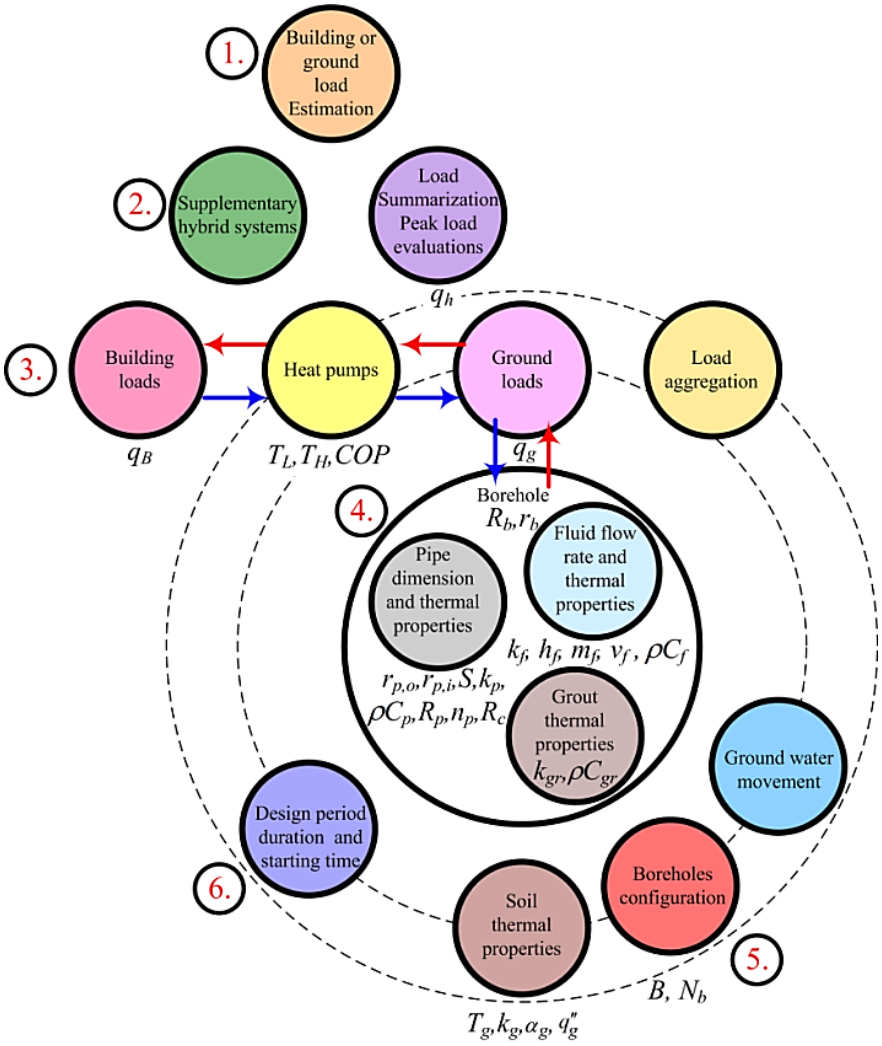

Figure 2-4: General input parameters of most sizing tools

As shown in Figure 2-4, the first step in any sizing method is the determination of the building or ground loads. These loads are generally evaluated by separate tools prior to sizing. In the second step, loads are analyzed and a supplementary system (heating boiler or cooling tower) may be needed because of a severe load imbalance. In that case, the monthly building peak loads may need to be revaluated. In the third step, the building or ground loads as well as the minimum and

maximum fluid temperature limits (T_L and T_H) for the heat pump are determined. When building loads are available, the heat pump coefficient of performances (COPs) in heating and cooling are required to calculate the ground loads. The simpler sizing models use fixed heating and cooling COPs (at T_L and T_H) while more precise ones use heating and cooling COPs as a function of inlet fluid temperature to the heat pumps. When hourly loads are provided, load aggregation or spectral methods are required to reduce the calculation time. This is explained further in section 1.3.2. In the fourth step, the thermal properties of the fluid, the pipes and the grout as well as the fluid flow rate, the size, the number and the distance of the pipes and the borehole size are to be specified. These parameters are used in the determination of steady-state and transient borehole thermal resistances as well as for the short-term ground thermal responses. In the fifth step, the parameters required for evaluating heat transfer outside the boreholes are quantified. These parameters are categorized into three groups: ground thermal properties (such as thermal conductivity and diffusivity as well as ground temperature), borehole spacing and bore field configuration and finally the ground water movement or saturation. Finally, in the sixth step, the design period and the starting month of operation should be specified.

Two topics, which are not covered in the next chapters, will be examined. These topics are: Evaluation of the peak loads and the effects of load aggregation.

2.3.1 Evaluation of the peak loads

Some of the most popular commercial $L3$ sizing tools use averaged monthly loads and monthly peak loads to evaluate the fluid temperature variation during the design period and calculate the required length of the VGHE. Thus, the magnitude and duration of the monthly peak loads should be evaluated so that they can match the actual hourly peak load profile as much as possible. While it might be relatively easy to determine the magnitude of the peak building loads, it is more difficult to estimate their duration. This is illustrated graphically in Figure 2-5.

Figure 2-5a shows an annual cooling and heating load profile obtained from hourly simulations. As shown, the heating and cooling peak loads occur in the first and eight months, respectively. More precise values of these peak loads are illustrated in Figures 2-5b and 2-5c over a 24 hour period. For the cooling peak load, the magnitude of the load can be determined easily but its duration is not as easy to evaluate and various values can be assumed for the peak load duration.

For the heating peak load, the load does not have a clear and distinct peak and this complicates the selection of the peak load magnitude as well as its duration.

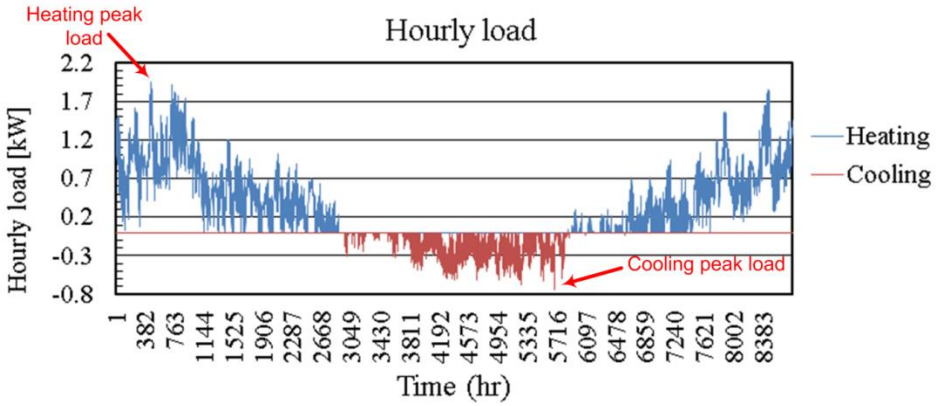

a.

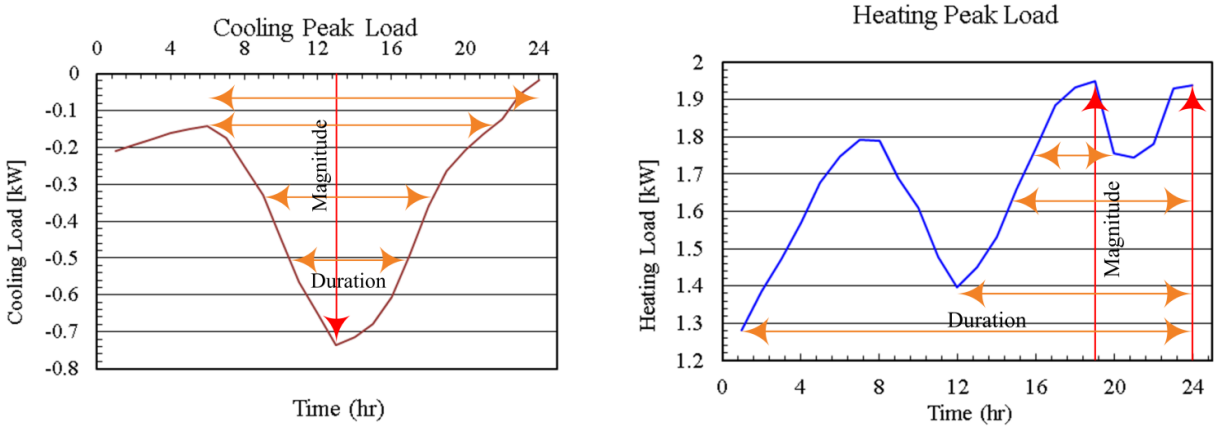

b. c.

Figure 2-5: a. A typical hourly load and its b. cooling and c. heating peak heat loads (adapted from content found in GLHEPRO 5.0 (2016))

To be conservative, designers may decide to select the real magnitude of the loads and apply it over a fixed duration even though this may not correspond to the actual load profile. This is more or less the approach taken with the ASHRAE sizing equation where a peak load duration of 6 hours is used regardless of the actual load profile. In effect, this corresponds to a rectangular load pulse of 6 hours.

Cullin and Spitler (2011) are at the origin of a study with the goal of determining appropriate values of peak load magnitude and duration to be used in $L3$ methods that would give the same required length as $L4$ methods. They used a hybrid time step approach to evaluate the monthly

peak loads from the hourly loads. They created an Excel spreadsheet (GLHEPRO 5.0, 2016) that automates the process. It is based on the fact that the temperature rise over the day is mainly dependent on the heat rejection and extraction of that particular day and to a lesser extent on the rejection and extraction of the previous day. Therefore, it is possible to find the day on which the peak load occurs and to run an hourly simulation for a one- or two-day period to find the resulting peak fluid temperature. Then, the best magnitude/duration pair for the rectangular load can be found in a way that the resultant fluid temperature follows the temperature profile obtained based on the hourly load as much as possible. The fluid temperature profiles are obtained based on the methodology introduced by Xu and Spitler (2006) which accounts borehole thermal capacity. The temperature change at any individual hour is normalized using the maximum temperature change during the simulation with the hourly load profile. The resulting temperature response of both the hourly load profile and the rectangular profile are plotted in a non-dimensional form as shown in Figures 2-6a and 2-6b. The reported fluid temperatures are obtained from the Excel spreadsheet (GLHEPRO 5.0, 2016) based on the cooling and heating peak loads presented earlier in Figures 2-5b and 2-5c.The fluid temperature responses obtained for three load durations are illustrated.

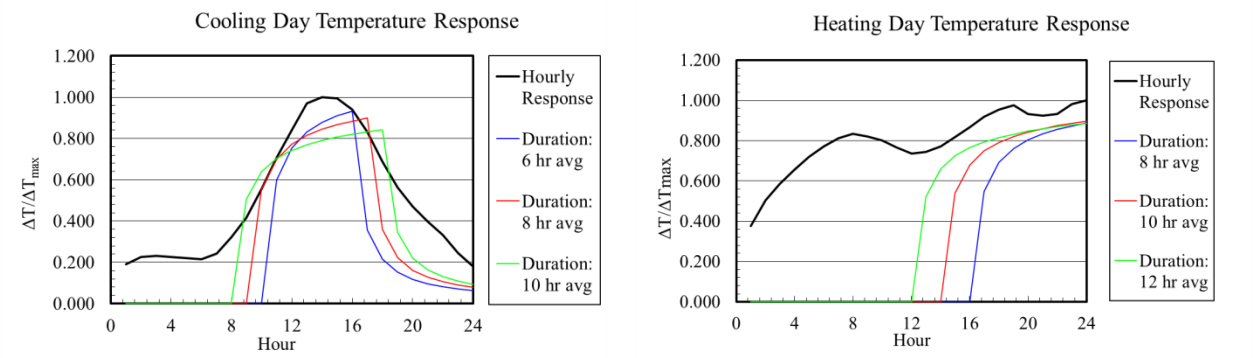

Figure 2-6: a. Temperature responses obtained based on hourly load and three peak load durations for a. cooling peak loads and b. heating peak loads. (Adapted from content found in GLHEPRO 5.0 (2016))

The magnitude and duration of the rectangular load pulses can be determined using two approaches. The first model, called “average over duration” uses a fixed specified duration and

takes the average of the hourly load changes in the specified duration to determine the peak load magnitude. The second model, called “maximum during duration”, finds the absolute maximum load in the specified duration and applies it to every hour of the specified duration. The fluid temperature profiles illustrated in Figure 2-6 are evaluated by the “average over duration” approach. The results for the “maximum during duration” model are reported in Figure 2-7. By comparing the results reported in Figures 2-6 and 2-7, it can be concluded that the “maximum during duration” model gives better results for this example as they are more close to the relative difference of 1 (see 6 hr max in Fig.2-7a or 12 hr max in Fig. 2-7b).

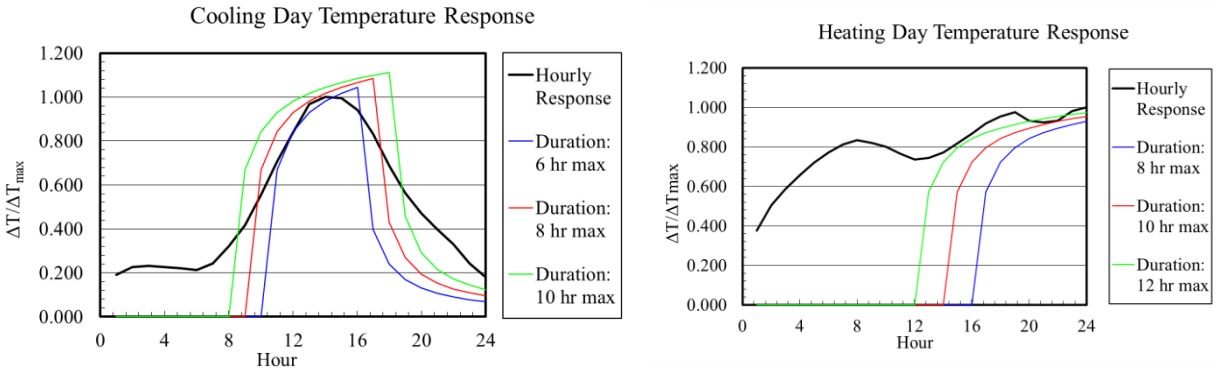

Figure 2-7: Temperature responses obtained by “maximum over duration” model (adapted from content found in GLHEPRO 5.0 (2016))

As such, the best fit that are the optimum peak duration and magnitude obtained from the two approaches will be used in sizing programs. For example, the best fit of the peak loads presented in Figure 2-5 are 14 hours heating load with the magnitude of 1.95kW and 4.8 hours cooling load with the magnitude of 0.73 kW that are obtained by “maximum during peak duration” method. Clearly, the best fit is case-dependent and so the user should do some iterations to find it.

Cullin and Spitler (2011) applied their proposed approaches to 48 cases and the results showed that the ground heat exchanger lengths obtained from monthly simulation were, on average, oversized by less than 1% (worst-cases: 5.7% undersized and 7.8% oversized) when compared with the ones obtained with the hourly simulations (Cullin and Spitler, 2011). The authors explained that some of the sources for the errors are: inability to estimate the load with rectangular pulses; the day with the peak load is not necessarily the same as the day with the peak

temperature response; and the peak load does not occur at the end of the month as is usually assumed in *L*3 methods.

2.3.2 The effects of load aggregation

When Level 4 methods are used, the borehole outlet fluid temperature is evaluated at each time step, typically every hour, by considering the past and recent thermal history since the start of the system operation. This temporal superposition leads to a summation of load pulses. Thus, for multi-year design periods, the number of terms in the summation is large and this summation needs to be re-evaluated at each time step since there is no recurrence. This may lead to large computational time. For these situations it is necessary to use load aggregation to limit the number of terms in the summation. Most of the load aggregation schemes use load averages that cover long periods of time when loads are part of the past history and progressively reduce the averaging period as temporal superposition moves towards the recent history. Some of the load aggregation strategies found in the literature are presented in the next paragraph.

Deerman and Kavanaugh (1991) introduced two methods to evaluate the cumulative effects of the ground heat transfer rates. They explained that these methods are useful in simulating the intermittent operations normally encountered in residential systems. The first method considers the ground heat transfer rates of the previous day while the second method utilises a fixed number of ground heat transfer rates from previous days based on the magnitude of the daily heat pump run time fraction for the current day. For run time fractions greater than 35%, no prior days are considered, while for run time fractions less than or equal to 10%, 15 prior days are considered. For run time fractions between these two values, the number of prior days is set proportionally. A comparison against measured data showed that the first method gives better results for both hourly and daily simulations.

Yavuzturk and Spitler (1999) used some user-defined block of loads with the same durations (730 hours) to reduce the time required for aggregation of hourly ground loads. For example, for the 2281st hour, three blocks of 730 hours are aggregated to simplify the loads and then the loads of the remaining 91 hours are superimposed in hourly steps. The authors observed that the results obtained based on this method have a deviation of about 1.1 °C. Therefore, they considered a "minimum hourly history period" which can be considered as a waiting period for recent loads before the load aggregation of blocks of 730 hours can start. For example, by considering a

minimum history period of 96 hours (instead of 91 hours), the temperature at the 2281st hour would be determined by two aggregated block loads of 730 hours and the remaining recent loads would remain intact and be superimposed in hourly steps. By comparing various minimum history periods, the authors selected a non-aggregated waiting period of 192 hours to perform the simulations. By using this period, the calculation time is decreased by 90% for a one-year simulation and 99% for a 20-year simulation. It is clear that by increasing this period, the results get more accurate but the calculation time also increases.

Bernier et al. (2004) used a similar methodology but with variable size block loads which is referred to as the multiple load aggregation algorithm (MLAA) method. In this method, five groups of yearly, monthly, weekly, daily and hourly block loads that respectively consist of N_y, N_m, N_w, N_d, and N_h hours are considered. Each of these blocks, except the yearly one, has a fixed length. In the beginning of the simulation, when the time step is smaller than N_h hours, the results are evaluated without any load aggregation. When the period exceeds N_h hours, the loads of the first N_h hours are averaged and this block is used in simulations. The same applies for the daily, weekly and monthly periods. The yearly period, N_y, does not have a fixed length since it contains the rest of the hours ($N_y = t - N_m - N_w - N_d - N_h$). The authors recommend to use N_m=360, N_w= 168, N_d=48, and N_h= 12 hours.

Liu (2005) used a hierarchical load aggregation. In this method, the hourly ground loads are aggregated into three small, medium and large blocks that have different time intervals. A large block contains a specific number of medium blocks, a medium block contains a specific number of small blocks and a small block contains some instantaneous individual ground loads. As the simulation progresses, the small blocks are accumulated into medium blocks and the medium blocks are grouped into the large blocks. Similar to the work of Yavuzturk and Spitler (1999), a waiting period is used for each level of time aggregation. Therefore, the aggregation of the individual loads (or smaller blocks) is performed when enough hourly loads have accumulated and their waiting time period has passed. The size and the waiting time of each block load will affect the computational efficiency and accuracy and so they should be selected carefully. This method presents an improvement over the multiple load aggregation method because it is not necessary to keep the entire history of ground loads. It needs also fewer load super position.

Claesson and Javed (2012) have also suggested a load aggregation method that uses some cells of loads that are organized in some levels for simulation of the fluid temperatures. The number of these cells can be considered to vary through each level. However, the authors have used a similar number of cells (5 cells) for all levels. The duration of the cells are assumed to be duplicated from one level to another. The load of each cell is dispersed from one cell to the next one when moving back in the load history and this dispersion is controlled based on weighting factors. The weighting factors for the first level of loads (the most recent) are kept unchanged. But the weighting factors of other levels are lumped together and their values are obtained directly from the step response functions that are calculated at the beginning of the simulation. To check the method, the authors have used the synthetic load profile introduced by Pinel (2003). For a 20 year simulation, the proposed method has evaluated the results in 25 s, while a calculation time of more than 88 minutes is obtained by not aggregating the loads.

Lamarche and Beauchamp (2007a) proposed a new methodology that does not need to use temporal superposition of all previous time steps. The proposed methodology uses the infinite cylindrical heat source model and to solve that the authors used Green's function technique instead of using the Laplace transform. This modification helped to evaluate the temperature at each time step based on the information from previous time steps. For example, a two-year simulation is performed in 1.39 s with the new technique whereas the same simulation requires 460 and 25.1 s with the techniques suggested by Yavuzturk and Spitler's (1999) and Bernier et al., 2004.

Lamarche (2009) generalized his previous work (Lamarche and Beauchamp, 2007a) to any type of step response factors. The author explained that the solution presented in his previous work had three main simplifications: axial effects and grout thermal capacitance were neglected and the analysis was restricted to a single borehole. The last simplifications can be lifted by using spatial superposition. As for the other two simplifications he suggests to use short and long term g-functions. By reformulating the equation that determine the borehole wall temperatures with the use of g-functions, he found a transformation that uses the same methodology developed in the previous study with the infinite cylindrical heat source model for g-functions. The resulting model is compared to the load aggregation suggested by Yavuzturk and Spitler's model (1999) and the multiple load aggregation method (Bernier et al., 2004). The results showed that the proposed model is faster and more accurate than the other two methods. For example, for a 2×2

bore field, a ten-year simulation is completed in just 1.9 s with the new model whereas calculation time of 3990 and 134 s are required with the models of Yavuzturk and Spitler (1999) and Bernier et al. (2004).

Marcotte and Pasquier (2008) explained that the temporal superposition of loads can be seen as a convolution in the time domain and so it can be solved more efficiently with the use by Fourier Transform (FFT). So, in their proposed model, the Fourier transform of the two terms required for evaluation of the temperatures (i.e. the load changes per unit length and the thermal responses) are evaluated first. Then the two series are multiplied and the inverse Fourier transform of the product is determined. Since the two series are discrete in time, discrete Fourier transforms are used. In order to reduce the calculation time, the authors suggested to use a subsample of the solution of the analytical model for the thermal response. Thus, the thermal response is calculated 76 times according to a geometric sequence. Then, a cubic spline interpolation scheme is used to generate the thermal response for all the required time steps. The combined approach, called the FFT-S model, can perform a 30-year hourly simulation in less than a second even if the computationally intensive finite line source solution is used to obtain the thermal response factors. The only difficulty with this method is that ground loads for the whole design period need to be known beforehand.

Cimmino et al. (2012) compared the computation time and accuracy of the multiple load aggregation method (Bernier et al., 2004) and the spectral method that is based on the Fourier transform method (Marcotte and Pasquier 2008) using some hourly simulations over periods of 1, 5, 10 and 20 years. The results showed that the Fourier transform method reduces the computational time by more than three orders of magnitude compared to the multiple load aggregation method. In addition, the Fourier transform model has a better accuracy since the method uses the real loads and not averaged loads.

Pasquier and Marcotte (2013) used an iterative method to determine the time-dependent heat fluxes of any number of heat sources that are kept at specific temperatures. The temporal superposition of heat transfer rates are performed as a convolution product and are evaluated with the Fast Fourier transform to reduce the computational time. The temperatures can be specified to change over time. In addition, different temperatures can be specified for each heat source. The

method is claimed to converge in just a few iterations. The algorithm can be applied to any analytical model (FLS, ICS, ILS) that uses the Neumann boundary condition for the heat sources.

Cimmino et al. (2013) used a spectral method to simulate the operation of a novel near-surface residential ground heat exchanger composed of 4 rows of 8 modules, each containing 18 tubes with a height of 2 m, distributed in 4 parallel rows. The thermal responses of these modules are evaluated with the use of the finite line source solution in the Laplace domain. The solution of a one-dimensional heat transfer model is superimposed on the thermal response of the field to consider the effect of the ambient air temperature changes. The temporal superposition required for simulation of the fluid temperatures is performed in the Laplace domain using a Fourier transform algorithm. The model is validated against measurements on a real system during a heating season. After an initial period ($t < 500$ h), the fluid temperatures predicted by the model is in good agreement with measurements, with average and maximum differences of 0.5 and 1.4 °C, respectively.

2.4 Conclusion

This literature presented the various levels of vertical ground heat exchangers sizing model and their differences. Sizing ground heat exchangers require different models that simulate various thermal phenomena occurring at different time scales. In the short term, the thermal capacity and the thermal conductivity of the fluid and the grout play an important role on the thermal response of the ground heat exchangers. In the long term, the thermal interaction between the boreholes and the annual load imbalances are important. The results of these models depend on the boundary condition and the simplifications as well as the input parameters and the mathematical solution that they use. Consequently, all these terms should be controlled or analyzed precisely for sizing ground heat exchangers accurately.

CHAPTER 3 OBJECTIVES OF THE RESEARCH WORK AND GENERAL ORGANIZATION OF THE THESIS

The main objective of this work is to review and improve the current vertical ground heat exchangers sizing methods. To meet this objective, three inter-related objectives are defined. Each of these objectives can be separated into secondary objectives as described below.

3.1 Objectives of the thesis

1- To improve the ASHRAE equation for sizing of vertical ground heat exchangers with the following sub-objectives:

a. Improve the evaluation of the ground thermal resistance using g-functions, eliminate the need to evaluate the temperature penalty and generalize the approach to be applicable to any bore field configuration.

b. Eliminate the need for the time consuming temporal superposition in determining g-functions.

c. Determine the best compromise between accuracy and computational time when calculating g-functions

d. Include the effects of borehole thermal capacity (short-term effects) in the ASHRAE equation.

2- Combine the DST model in TRNSYS with the GenOpt tool to automate a sizing procedure based on hourly simulation including possible changes of the heat pump COP.

3- Review and compare vertical ground heat exchangers sizing tools with the following sub-objectives:

a. Propose categories for the sizing tools.

b. Introduce sizing test cases which could cover most sizing difficulties.

c. Perform and inter-model comparison of some of the current sizing tools.

3.2 Organization of the thesis

The thesis consists of seven chapters and follows the format of a thesis by articles. Chapter 2 presents a complementary review of the literature on articles that are not described in the various articles. The review includes articles on modeling of heat transfer in geothermal bore fields, the various sizing levels and the related sizing programs. It also addresses some important factors that may affect the accuracy or calculation time of the sizing programs. Chapter 3 describes the objectives and organization of the thesis.

Chapter 4 presents the first article entitled "An alternative to ASHRAE's design length equation for sizing borehole heat exchangers" which was published in the ASHRAE annual conference (Ahmadfard & Bernier, 2014) proceedings. The paper reviews the classical ASHRAE sizing equation presented in the ASHRAE handbook and proposes an alternative to this equation. In this new approach, the ground thermal resistances are evaluated with the use of g-functions thus eliminating the need to calculate the temperature penalty. However, the equation has to be solved iteratively as the g-functions depend on the borehole length.

Chapter 5 presents the second article entitled "Modifications to ASHRAE's sizing method for vertical ground heat exchangers" which is "in press" in the journal of Science and Technology for the Built Environment (Ahmadfard & Bernier, 2018). This paper expands the analysis provided by Ahmadfard and Bernier (2014) and examines three aspects of this methodology. It is demonstrated that the time-consuming evaluation of the full g-function curve, typically obtained by temporal superposition, is not necessarily required. In addition, the effects of the convergence criteria and the number of borehole segments on the accuracy and calculation time are examined. Finally, the alternative method is modified to account for short-term effects and it is shown that the short-term effects can have an important impact on the required borehole length if the amplitude of the peak load is significant compared to the monthly and yearly loads.

Chapter 6 presents the third article entitled "Evaluation of the design length of vertical geothermal boreholes using annual simulations combined with GenOpt" which has been published in the proceedings of eSim 2016, the Canadian conference of the IBPSA (Ahmadfard et al., 2016). In this paper, a sizing model is developed in TRNSYS by combining the DST model and the GenOpt optimization tool. The proposed model uses the multi-annual building

hourly loads to determine the required borehole lengths. It can handle cases where the heat pump COPs varies as a function of the fluid inlet temperature.

Chapter 7 presents the fourth article entitled “A review of vertical ground heat exchanger sizing tools including an inter-model comparison” which has been submitted to the Renewable & Sustainable Energy Reviews journal. This article describes the important aspects that should be taken into account when comparing various vertical ground heat exchanger sizing tools. The current sizing programs are categorized in five levels which are described in the paper. Four test cases are proposed to cover the full spectrum of conditions from single boreholes to large bore fields with large annual ground thermal imbalance. The test cases are then used in a thorough inter-model comparison.

A general discussion is provided in Chapter 8 followed by conclusions and recommendations for future work.

Results obtained under objectives 3b and 3c are included in a Excel spreadsheet which is described in Appendix B. Some of the models described in the following chapters are programmed in a VBA-Excel spreadsheet that can be used for sizing vertical ground heat exchangers. The user manual of this spreadsheet is presented in Appendix A.

CHAPTER 4 ARTICLE 1: AN ALTERNATIVE TO ASHRAE'S DESIGN LENGTH EQUATION FOR SIZING BOREHOLE HEAT EXCHANGERS

Ahmadfard, M., Bernier, M. (2014). Proceedings of the ASHRAE annual conference, SE-14-C049.

ABSTRACT

An accurate determination of the required borehole length is an important step in the design of vertical ground heat exchangers used in ground-coupled heat pump systems. The ASHRAE Application Handbook presents a method to determine the design length. The method rests on three key calculations. First, effective ground thermal resistances corresponding to three thermal pulses of 10 years, 1 month and 6 hours need to be calculated. Second, the effective borehole resistance needs to be evaluated. Third, the ground temperature has to be corrected for borehole thermal interaction using a temperature penalty. The effective ground thermal resistances are evaluated using the so-called cylindrical heat source (CHS) analytical solution to transient heat transfer in the ground. This solution is relatively simple and effective ground thermal resistances can be calculated relatively easily as they do not depend on the length of the borehole. However, the CHS neglects axial heat conduction which can be a factor after a number of years. As for the temperature penalty, the handbook provides a table for estimating it. However, the table is incomplete and applies to a limited number of rectangular equally-spaced borehole configurations.

This paper proposes an alternative to the design length equation currently used in the ASHRAE handbook. In the proposed approach, the effective ground thermal resistances are evaluated using g-functions calculated based on the finite line source analytical solution. Because g-functions account for borehole thermal interaction, the correction provided by the temperature penalty is no longer needed. Furthermore, the determination of the effective ground thermal resistances is not restricted to rectangular bore fields of equally-spaced boreholes. However, as described in the paper an iterative calculation procedure is required as effective ground thermal resistances depend on the length of the borehole which is unknown a priori. In the last part of the paper, the proposed procedure is applied to determine the required length of 12×10 bore field. Results

indicate that the procedure predicts a bore field length which is in the range predicted by five other design software tools.

4.1 Introduction

An accurate determination of the required borehole length is an important step in the design of vertical ground heat exchangers used in ground-coupled heat pump systems. The ASHRAE handbook (ASHRAE, 2011) proposes an equation which is based on the work of Kavanaugh and Rafferty (1997) to determine the required length of vertical ground heat exchangers. This equation has been presented by Bernier (2006) and Philippe et al. (2010) in the following form:

$$L = \frac{q_h R_b + q_y R_y + q_m R_m + q_h R_h}{T_m - (T_g + T_p)} \tag{4.1}$$

where L is the required borehole length ($L = N_b \times H$, where H is the borehole length and N_b is the number of boreholes), T_m is the mean fluid temperature in the boreholes, T_g is the undisturbed ground temperature and T_p is a so-called temperature penalty. The first term in the numerator accounts for heat transfer (assumed to be in steady-state) in the borehole from the fluid to the borehole wall where R_b is the borehole thermal resistance (Kavanaugh, 2010). The next three terms in the numerator account for transient heat transfer in the ground. These three terms can be regarded as three consecutive ground thermal pulses q_y, q_m, and q_h each multiplied by their respective effective ground thermal resistance R_y, R_m, and R_h. The ground thermal pulses are considered negative when heat is extracted from the ground and positive for heat injection into the ground. The magnitude and duration of these pulses are project dependent but typically, t_1=3650 days, t_2=3680 days and t_f=3680.25 days. As shown in Figure 4-1, the ground thermal pulses correspond to three time periods. The assumed duration of the yearly average ground load, q_y, is equal to t_1. The average monthly ground load (during the month of the peak hourly load), q_m is assumed to last from t_1 to t_2. Finally, the peak hourly ground load, q_h, is assumed to last from t_2 to t_f.

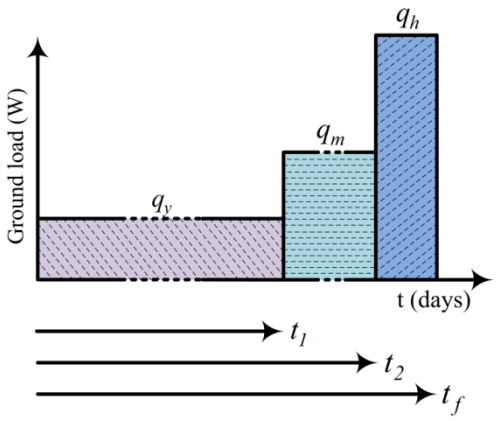

Figure 4-1: Three consecutive ground thermal pulses used in Equation 4.1

4.2 ASHRAE Handbook method

The determination of the effective ground thermal resistances associated with the three heat pulses can be done in several ways. The method described in the ASHRAE handbook (ASHRAE, 2011) suggests using a one-dimensional analytical solution to transient heat transfer in the ground. The analytical solution used in the ASHRAE handbook is the cylindrical heat source solution (Carslaw and Jaeger, 1947). It gives the temperature distribution in the ground, including at the borehole wall, for a given heat transfer rate per unit length applied at the cylinder diameter (Bernier, 2000). Under the cylindrical heat source solution, the borehole temperature, T_w, following a heat injection rate per unit length, q_y, for a period of time t is given by:

$$T_w - T_g = q_y(G_{Fo}/k) \tag{4.2}$$

where G_{Fo} is the analytical solution, also known as the G-factor, Fo is the Fourier number defined as $Fo = 4\alpha t/d^2$, α is the ground thermal diffusivity, d is the borehole diameter, and k is the ground thermal conductivity. Equation 4.2 can be written in terms of an equivalent ground thermal resistance, R_{ground}:

$$T_w - T_g = q_y R_{ground} \tag{4.3}$$

The effective ground thermal resistances used in Equation 4.1 are obtained based on the principle of superposition. For example, to determine the impact of q_y at the end of the calculation period

(i.e. at t_f), q_y is first assumed to prevail from 0 to t_f. Then its thermal influence from t_1 to t_f is subtracted. A similar procedure is applied for q_m and q_h resulting in the following:

$$\begin{aligned} R_y &= (G_{Fo_f} - G_{Fo_1})/k \\ R_m &= (G_{Fo_1} - G_{Fo_2})/k \\ R_h &= G_{Fo_2}/k \end{aligned} \tag{4.4}$$

with $Fo_f = 4\alpha(t_f)/d^2$, $Fo_1 = 4\alpha(t_f - t_1)/d^2$, and $Fo_2 = 4\alpha(t_f - t_2)/d^2$. The value of G is presented graphically in the ASHRAE Handbook. A correlation is also proposed by Bernier (2001). Finally, Philippe et al. (2010) have presented correlations to easily obtain R_y, R_m, and R_h for t_1=3650 days, t_2=3680 days and t_f=3680.25 days.

The determination of the design length of a bore field using Equation 4.1 is relatively simple. The values of R_y, R_m, and R_h are independent of the borehole length as the G-factors are based on a one-dimensional (radial) solution to ground heat transfer. Thus, contrary to the method proposed later, it does not involve an iterative solution procedure. However, as noted by Philippe et al. (2009) axial heat transfer effects start to play an important role after a few years of operation. Thus, values of R_y are not very accurate when t_1 is long. Luckily, the product $q_y R_y$ is usually small compared to the other terms in Equation 4.1 and any error in R_y is typically not significant in the determination of L.

The use of G-factors neglects thermal interactions among boreholes and may cause significant error in cases where there is a large annual thermal imbalance in the ground. Thus, a temperature penalty, T_p, has been introduced to account for these borehole thermal interactions. In effect, T_p is a temperature difference which corrects the value of the undisturbed ground temperature to account for the fact that boreholes do not "see" the undisturbed ground temperature when they are thermally interacting with each other. Two of the methods proposed for calculating T_p will now be described.

4.3 ASHRAE handbook method to estimate Tp

The ASHRAE handbook proposes a set of tabulated values for T_p. These values are given for a 10×10 bore field after 10 years of operation of a 350 kW (100 tons) load for various cooling and heating scenarios and borehole separations. Correction factors are provided for 1×10, 2×10, 5×5,

and 20×20 bore fields. Values were obtained for a ground thermal conductivity of 1.5 W/m-K but the ground thermal diffusivity is not given.

The calculation procedure to obtain these values of T_p is defined more precisely by Kavanaugh and Rafferty (1997) and it has been analyzed by a number of authors. Fossa and Rolando (2013) have compared the temperature penalty obtained using the ASHRAE method to the ones calculated using g-functions obtained with the finite line source solution. Results indicate that the ASHRAE method underestimates the temperature penalty by 40 to 50% for some particular cases leading to a typical average underestimation of the bore field lengths of around 12%.

Kurevija et al. (2012) have also compared the length obtained by the AHRAE method with what they called the "Lund-Eskilson" model based on the finite line source analytical solution. The authors note that there are distinguishable discrepancies between the two approaches as the ASHRAE method uses a somewhat simplistic borehole interaction model. They have analyzed the effects of different borehole distances as well as different operating time for two sets of borehole arrays (21×2 and 6×7). For a bore separation of 4 m, differences of the order of 10 and 20% are noted for 21×2 and 7×6 bore fields, respectively.

4.4 Evaluation of Tp based on g-functions

Bernier et al. (2008) evaluated the temperature penalty using 3-D thermal response factors, also known as g-functions, introduced by Eskilson's (1987). A complete description of g-functions follows in the next section. Bernier et al. (2008) defined the temperature penalty as the difference between the borehole wall temperatures in the bore field and in a single borehole subjected to the same heat transfer rate per unit length. Using Eskilson's g-functions for 144 configurations, a correlation was proposed to predict the value of the temperature penalty. Although the correlation covers a large spectrum of possible configurations and operating conditions, it has some restrictions relevant to the boreholes layout which limits its application to rectangular grids and equally spaced boreholes.

Much like Bernier et al. (2008), Capozza et al. (2012) have defined the temperature penalty as the difference from the value of the thermal disturbance averaged on the borehole walls of a bore field and the value of the thermal disturbance due to a single open-field borehole. The model uses the infinite line source and a correction factor which depends on the geometrical and physical

parameters. The results are compared to those obtained with the ASHRAE handbook method and the one presented by Bernier et al. (2008). Contrary to these two methods, the model presented by Capozza et al. (2012) doesn't have any limitation on the bore field configuration. It also has wider validity range for the thermo-physical parameters compared to the method of Bernier et al. (2008). Their results are in good agreement with the ones reported by Bernier et al. (2008). Their method was applied to a case study and they showed that the ASHRAE handbook method underestimates the required length by more than 10 %.

4.5 Alternative method

As indicated earlier, Equation 4.1 uses effective ground thermal resistances which are based on a one-dimensional (radial) analytical solution to heat transfer from a cylinder. This assumption can lead to errors, especially for R_y. Furthermore, as shown in the previous paragraphs, the value of Tp varies significantly depending on which method is used and is most often given for rectangular equally-spaced borehole grids. An alternative method is proposed here to alleviate these deficiencies. This alternative uses g-functions to determine the design length of bore fields. When g-functions are used, thermal interference among boreholes is implicitly accounted and there is no need to apply a temperature penalty. The values of R_y, R_m, and R_h are now based on g-functions and Equations 4.4(a-c) take the following forms:

$$\begin{aligned} R_{gy} &= \left(g_{(t_f)} - g_{(t_{f-t_1})}\right)/2\pi k \\ R_{gm} &= \left(g_{(t_{f-t_1})} - g_{(t_{f-t_2})}\right)/2\pi k, \\ R_{gh} &= g_{(t_{f-t_2})}/2\pi k \end{aligned} \tag{4.5}$$

where g_{t_i} is the g-function evaluated at $ln(t_i/t_s)$ with t_s equal to $H^2/9\alpha$ as defined by Eskilson (1987). The subscript g has been added to the R values to indicate that they are based on g-functions. Then, with the g-function concept, the alternative design length equation is as follows:

$$L = \frac{q_h R_b + q_y R_{gy} + q_m R_{gm} + q_h R_{gh}}{T_m - T_g} \tag{4.6}$$

Some design software tools use a similar g-function based approach but often with a greater number of thermal pulses (Hellström and Sanner (1994), Spitler (2000)).

The g-functions give a relation between the heat extracted from the ground per unit borehole length, q_L, and the borehole wall temperature T_w (Eskilson,1987). The borehole wall temperature is given by:

$$T_w = T_g - (q_L/2\pi k) \cdot g(t/t_s, r_b/H, B/H) \quad (4.7)$$

where g represents the g-function and q_L is the heat extracted from the ground per unit borehole length. As shown in Equation 4.7, g-functions depend on three non-dimensional parameters: B/H, the ratio of the borehole spacing over the borehole length; r_b/H, the ratio of the borehole radius over the borehole length; and t/t_s, a non-dimensional time where ts is a characteristic time. Typical g-functions curves are presented in Figure 4-2 for a 3×2 bore field as a function of ln(t/ts) for six bore field spacings, B/H, and for a particular value of r_b/H (=0.0005). The curve for B/H=∞ corresponds to the g-function of a single borehole. One of the major advantages of these non-dimensional curves is that they apply to any 3×2 bore field with the same non-dimensional parameters. Eskilson (1987) provides g-function curves for a number of bore field geometries. Design software tools that use the g-function concept have a relatively large data set of g-function curves to choose from. Eskilson (1987) calculated g-functions using two-dimensional transient finite-difference equations on a radial-axial coordinate system for a single borehole in homogeneous ground. The temperature fields for each individual borehole were superimposed in space to obtain a 3-D thermal response from a borehole field for a certain configuration.

g-function curves are relatively simple to use for the determination of R_{gy}, R_{gm}, and R_{gh}. For example, the evaluation of these ground thermal resistances for a 3×2 bore field with the following characteristics: r_b= 0.05 m (2 in.), B= 5 m (16.4 ft), H=100 m (328 ft), k=3.34 W/m-K (1.93 Btu/h-ft-°F), α =0.096 m^2/day (1.04 ft^2/day) and three consecutive heat pulses of 10 years, 1 month , and 6 hours lead to the following: t_s=11574 days, t_f= 3680.25 days, $ln(t_f/t_s)$=-1.14, t_1=3650 days, $ln((t_f - t_1)/t_s)$= -5.94, t_2= 3680 days, $ln((t_f - t_2)/t_s)$ =-10.74 , g_{t_f} = 12.34 , $g_{(t_f - t_1)}$=3.99, $g_{(t_f - t_2)}$ =1.55, and R_{gh}=0.074 m-K/W (0.128 h-ft-°F/Btu), R_{gm}= 0.116 m-K/W (0.201 h-ft-°F/Btu), and R_{gy}= 0.398 m-K/W (0.689 h-ft-°F/Btu).

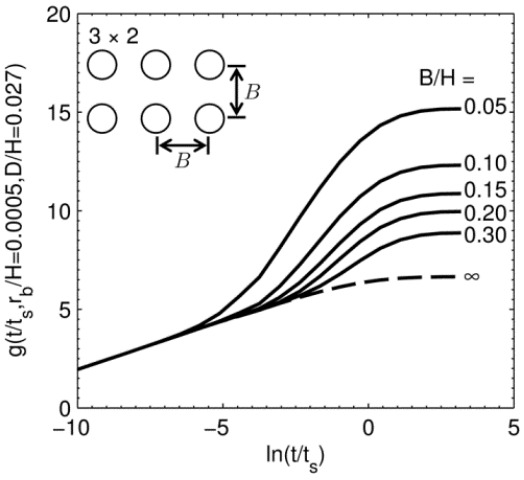

Figure 4-2: Six g-functions curves for a 3 x 2 bore field

The example just presented is somewhat idealistic as H is known. In practice, in a design length calculation, H is unknown a priori and R_{gy}, R_{gm}, and R_{gh} have to be obtained iteratively. This poses some difficulties in the solution procedure. First, g-function graphs are given for specific values of r_b/H and B/H. Eskilson recommends to apply a correction factor for values of r_b/H other than the ones associated with the g-function, but it is unclear if this correction factor applies to all cases. For values of B/H other than the ones associated with the g-function, an interpolation is possible. Malayappan and Spitler (2013) used logarithmic interpolations between pre-computed g-functions for various B/H ratios. They report sizing errors of a few percent when this interpolation scheme is used. Another difficulty is the limited number of g-functions which are publicly available.

In the approach proposed here, the required g-functions are calculated "on the fly" with the proper r_b/H and B/H ratios. There are no correction factors or interpolations. The whole g-function curve does not need to be calculated since only three g-functions values are required. Furthermore, in the proposed approach, the g-functions are not restricted to rectangular equally-spaced bore fields.

g-functions are evaluated based on the methodology proposed by Cimmino and Bernier (2013, 2014) which were able to reproduce Eskilson's g-function with a high level of accuracy using the finite-line source analytical solution. A full description of this technique is out of the scope of the present paper and only key features of the method will now be described. Eskislon's g-functions

are based on the assumption that all boreholes in a bore field have the same borehole wall temperature and that this temperature is uniform over the height of each borehole. In their approach, Cimmino and Bernier (2014) divided boreholes into axial segments and applied the finite line source to each of these segments. The integral mean temperature at a certain radius is obtained using a modified version of the finite line source solution proposed by Claesson and Javed (2011). A system of equation is obtained from the temporal and spatial superposition of the contribution of all borehole segments. The solution gives the wall temperature (equal for all segments of all boreholes) and the heat transfer rate of each borehole segment for a given total heat transfer rate in the bore field. In the present work, 12 axial segments are considered for each borehole. A simplified example of this procedure is provided in the Appendix.

As mentioned earlier, the required bore length has to be determined using an iterative procedure which is presented schematically in Figure 4-3. This procedure can either be used for heating or cooling applications with proper signs for ground loads. The iteration procedure is comprised of five steps. In the first step, parameters are initialized and a guess value for L is chosen. Using this value of L, the three g-functions are evaluated based on $H = L/N_b$. The third step involves the determination of the three effective ground thermal resistances (Equations (4.5)). In the fourth step, a new length is determined using Equation (4.6). Finally, this new length is compared to the previous length. If the two lengths agree to within a certain tolerance, typically set at 0.01%, then calculations are stopped, if not then a new iteration is started. Typically, less than 4 iterations are required to meet the convergence criteria.

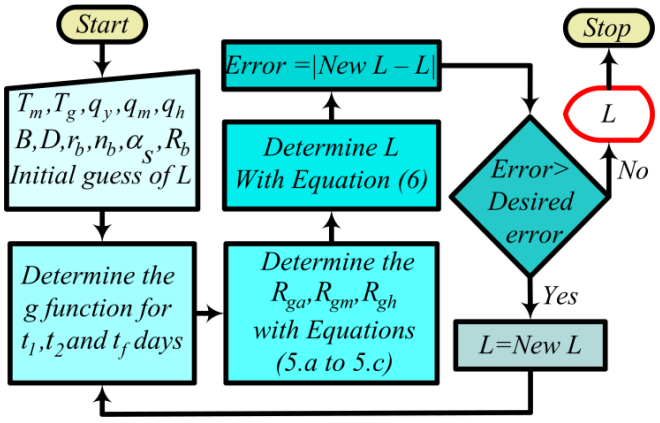

Figure 4-3: Flow diagram of the iterative procedure

4.6 Application of the procedure

The proposed procedure is verified against a test case originally presented by Shonder et al. (2000) who compared five different design software tools. The case is a heating application and the bore field consists of a 12×10 grid with a borehole spacing of 6.1 m (20 ft.). The three pulses q_h, q_m, and q_y pulses are equal to -392.25 kW (-1.338e+06 BTU/h), -100.0 kW (-.341e+06 BTU/h) and -1.762 kW (-6012 BTU/h), respectively. The required borehole length is determined for t_1=3650 days, t_2=3680 days, t_f =3680.25 days. Other parameters can be found in Shonder et al. (2000) and Philippe et al. (2010).

The solution process is illustrated on Figure 4-4 which shows a typical g-function graph and the 9 g-function points obtained after 3 iterations. The results for the 2nd and 3rd iterations are almost identical and each cross on the bottom curve represents two superposed points. The g-function curves are not required in the solution process but are drawn on Figure 4-4 to illustrate the location of the point of the curve. An initial guess of L = 120×150 m (120×492.1 ft.) was chosen and the top three points correspond to the pairs $[ln((t_f - t_2)/t_s), g(t_f - t_2)]$, $[ln((t_f - t_1)/t_s), g(t_f - t_1)]$, $[ln(t_f/t_s), g_{t_f}]$ with $ts = H^2/9\alpha$ = 36764 days. This leads to a new value of L = 120×82.19 m (120×269.6 ft.) and a second iteration is initiated. The process converges after 3 iterations with the final value of L = 120×81.55 m (12×267.5 ft). In their comparison exercise, Shonder et al. (2000) obtained results that ranged from 120×65 to 120×87 m (120×213.2 ft. to 120×285.4 ft.) for five different design software tools. Thus, the value obtained with the proposed procedure is in good agreement with other methodologies.

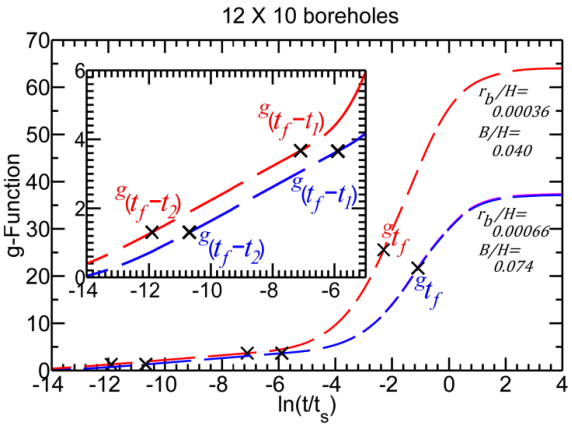

Figure 4-4: Determination of the three g functions related to the three thermal resistances in consecutive iterations

The computational time required for these three iterations is 340 s on a computer equipped with an Intel core i7 processor (2.80 GHz) and 4 GB of RAM. This relatively long computational time is due to the fact that the convergence criterion is strict (0.01%) and that 12 axial segments are used in the determination of the g-functions. Furthermore, the number of boreholes is relatively large which increases significantly the computational time associated with spatial superposition among boreholes. The same problem was solved by considering 1, 3, 6 and 9 segments for each borehole. The resulting borehole lengths for these cases are 81.98 m (268.89 ft.), 81.86 m (268.50 ft.), 81.68 m (267.91 ft.), and 81.60 m (267.65 ft.), respectively with corresponding calculation time of 6 s, 27 s, 92 s and 195 s, respectively. Thus, in this case, computational time can be reduced by approximately 2 orders of magnitude without a significant loss in accuracy by reducing the number of borehole segments.

4.7 Conclusion and recommendations

This paper proposes an alternative to the design length equation currently used in the ASHRAE handbook. In the proposed approach, the effective ground thermal resistances are evaluated using g-functions calculated based on the finite line source analytical solution. Because g-functions account for borehole thermal interference, the correction provided by the temperature penalty is no longer needed. Furthermore, the determination of the effective ground thermal resistances is not restricted to rectangular bore fields of equally-spaced boreholes. However, an iterative calculation procedure is required as effective ground thermal resistances depend on the length of the borehole which is unknown a priori. New g-functions are calculated as the iterative process progresses and there is no need to apply correction factors to account for the r_b/H ratio or to interpolate between different B/H curves. The proposed procedure has been checked against a well-known test case and results indicate that the procedure predicts a bore field length which is in the range predicted by five other software tools. More work is required to determine the best compromise between the number of borehole segments and the convergence criteria to obtain a reasonable computational time with an acceptable accuracy.

4.8 Acknowledgments

This work was funded by the National Sciences and Engineering Research Council of Canada under the Smart Net-Zero Energy Buildings Strategic Research Network (SNEBRN).

4.9 References

ASHRAE. (2011). ASHRAE Handbook-Application. Atlanta: American Society of Heating Refrigeration and Air Conditioning Engineers, Inc.

Bernier, M. (2000). A Review of the Cylindrical Heat Source Method for the Design and Analysis of Vertical Ground-Coupled Heat Pump Systems, Fourth international Conference on Heat Pumps in Cold Climates, Aylmer, Québec.

Bernier, M. (2001). Ground-Coupled Heat Pump System Simulation, ASHRAE Transactions, 106(1): 605-616.

Bernier, M. (2006). Closed-loop ground-coupled heat pump systems. ASHRAE Journal 48(9):12–19.

Bernier, M.A., Chahla, A. & P. Pinel. (2008). Long-term Ground Temperature Changes in Geo-Exchange Systems, ASHRAE Transactions, 114(2): 342-350.

Capozza A., De Carli M. & A. Zarrella. (2012). Design of borehole heat exchangers for ground-source heat pumps: A literature review, methodology comparison and analysis on the penalty temperature, Energy and Buildings 55, 369–379.

Carslaw, H. S. & J.C. Jaeger. (1947). Conduction of Heat in Solids, 2nd Ed. Chapter 13, The Laplace transformation: Problems on the cylinder and sphere. O. U. Press: Oxford University.

Cimmino, M. & Bernier, M. (2013). Preprocessor for the generation of g-functions used in the simulation of geothermal systems. Proceedings of the 13th International IBPSA conference, Chambéry, France, pp.2675-2682.

Cimmino, M. & M. Bernier. (2014). A semi-analytical method to generate g-functions for geothermal bore fields, Int. J. Heat Mass Transfer, 70(c):641-650.

Claesson, J. & S. Javed. (2011). An Analytical Method to Calculate Borehole Fluid Temperatures for Time Scales from Minutes to Decades. ASHRAE Transactions 117.2(2011) 279-288.

Eskilson, P. (1987). Thermal analysis of heat extraction bore-holes. PhD thesis, Lund University, Sweden

Fossa M. & D. Rolando. (2013). An improved method for vertical geothermal bore field design using the Temperature Penalty approach, European geothermal congress 2013.

Hellström, G. & B. Sanner. (1994). Software for dimensioning of deep boreholes for heat extraction. Proceedings of Calorstock 1994, Espoo/Helsinki, Finland, 195-202.

Kavanaugh, S.P., (2010). Determining thermal resistance. ASHRAE Journal 52(8):72–75.

Kavanaugh, S.P. & K. Rafferty. (1997). Ground-source heat pumps: Design of geothermal systems for commercial and institutional buildings. Atlanta: American Society of Heating, Refrigerating and Air-Conditioning Engineers, Inc.

Kurevija T., Vulin, D. & V. Krape. (2012). Effect of borehole array geometry and thermal interferences on geothermal heat pump system, Energy Conversion and Management, 60: 134-142.

Malayappan, V. & J.D. Spitler. (2013). Limitations of using uniform heat flux assumptions in sizing vertical borehole heat exchanger fields, Proceedings of Clima 2013, June 16-19, Prague, Czech Republic.

Philippe, M., Bernier, M. & D. Marchio. (2009). Validity ranges of three analytical solutions to heat transfer in the vicinity of single boreholes, Geothermics, 38(4): 407-413.

Philippe, M., Bernier, M. & D. Marchio. (2010). Sizing Calculation Spread sheet: Vertical Geothermal Borefields, ASHRAE Journal, 52(7): 20-28.

Shonder, J. A., Baxter, V. D., Hughes, P. J., & Thornton, J. W (2000). A comparison of vertical ground heat exchanger design software for commercial applications. ASHRAE Transactions 106(1):831–842.

Spitler, J. D. (2000). A design tool for commercial building loop heat exchangers. Paper presented at the Fourth International Heat Pumps in Cold Climates Conference, August 17-18, 2000. Aylmer, Québec.

4.10 Appendix

In this apppendix, a simplified example is provided to better understand how g-functions are calculated in the proposed method. The example is for a bore field composed of 3 boreholes in-line (3×1), each with a radius r_b=0.05 m (2 in.) and a height H=100 m (328 ft.). The boreholes are equally spaced by a distance B=5 m (16.4 ft). The ground thermal conductivity, k, and diffusivity, α, are equal to 1.0 W/m-K (0.577 Btu/h-ft-°F) and 0.1 m^2/day (1.07 ft^2/day), respectively. The evaluation of the g-function is required for t=10 years.

The determination of the g-function is independent of T_g and q_L and values of T_g= 0 °C and $q_L = 2\pi k$ are used here for convenience. In this simplified example, only one axial borehole segment is used to simplify calculations. However, in the approach proposed in this paper, 12 axial segments are used as suggested by Cimmino and Bernier (2014). Using the principle of spatial superposition, the borehole wall temperatures for boreholes 1, 2, and 3 (borehole #2 is the middle borehole) are given by:

$$\begin{aligned} T_{w1} &= q_1 \times MT_{q_1,r=0.05} + q_2 \times MT_{q_2,r=5} + q_3 \times MT_{q_3,r=10} \\ T_{w2} &= q_2 \times MT_{q_2,r=0.05} + q_1 \times MT_{q_1,r=5} + q_3 \times MT_{q_3,r=5} \\ T_{w3} &= q_3 \times MT_{q_3,r=0.05} + q_2 \times MT_{q_2,r=5} + q_1 \times MT_{q_1,r=10} \end{aligned} \tag{4.8}$$

Where $MT_{q_1,r=0.05}$ stands for the Mean Temperature over the segment length (= 100 m since only one segment is used in this simplified example) at a distance of 0.05 m from a line source having a heat transfer rate per unit length equal to q_1. The values of MT are obtained using the analytical solution to the finite line source proposed by Claesson and Javed (2011) with a borehole buried depth of D=4 m (13.1 ft). One of the underlying assumptions behind the g-funtion is that all borehole wall temperatures are equal. Furthermore, q_L is the average of the individual heat transfer rates:

$$\begin{aligned} T_{w1} &= T_{w2} \\ T_{w2} &= T_{w3} \\ q_L &= (q_1 + q_2 + q_3)/3 \end{aligned} \tag{4.9}$$

Solving the resulting system of 6 equations and 6 unknown results in the following: q_1=q_3= 6.593 W/m (6.857 Btu/h-ft), q_2=5.664 W/m (5.891 Btu/h-ft), T_{w1}=T_{w2}=T_{w3}=8.63 °C (47.5 °F) and the corresponding g-function is:

$$g = (T_w - T_g) \times (2\pi k/q_L) = 8.63$$

CHAPTER 5 ARTICLE 2: MODIFICATIONS TO ASHRAE'S SIZING METHOD FOR VERTICAL GROUND HEAT EXCHANGERS

Ahmadfard, M., & Bernier, M. (2018). In Press. Science and Technology for the Built Environment. (doi.org/10.1080/23744731.2018.1423816)

ABSTRACT

This paper proposes modifications to the ASHRAE sizing equation for vertical ground heat exchangers. The proposed method uses the same three pulse approach as the current sizing equation but uses g-functions to calculate the effective ground thermal resistances. One key feature of the iterative methodology is the ability to calculate new g-functions as the geometry morphs during the solution process. Long-term g-functions are evaluated analytically using the finite line source solution over borehole segments while so-called short-term g-functions are calculated based on an hybrid analytical/numerical method to account for the borehole thermal capacity. This paper examines three aspects of the proposed methodology. First, it is shown that the time-consuming evaluation of the full g-function curve, typically obtained by temporal superposition, is not necessarily required. Secondly, the optimum number of borehole segments to obtain an accurate bore field length with reasonable calculation time is examined. The selection of a convergence criteria and its impact on calculation time is also discussed. The excellent agreement between results obtained with the proposed alternative method and the ones obtained from other design software tools confirms the validity of the proposed method. Finally, it is shown that short-term effects can have a relatively significant effect on the calculation of the required borehole length.

5.1 Introduction

Accurate sizing of vertical ground heat exchangers (GHE) for ground source heat pump (GSHP) systems is important to limit drilling costs and avoid operational problems. A typical GSHP system is presented schematically in Figure 5-1 where a fluid loop links a series of heat pumps to six boreholes (in a 3×2 configuration). In this figure, D is the borehole buried depth, H is the borehole length, B is the borehole spacing, r_b is the boreholes radius, r_p is the pipe radius of the U-tube pipes and d_p is the center-to-center pipe distance. The important ground properties are the temperature T_g, the thermal conductivity k_g, and the thermal diffusivity, α_g.

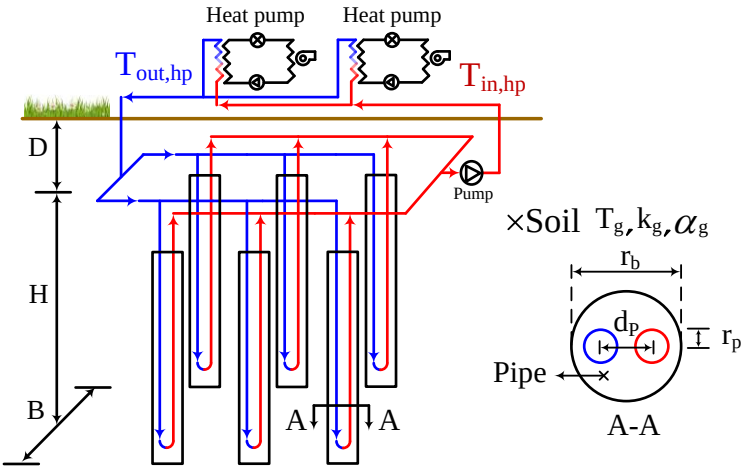

Figure 5-1: Schematic illustration of a typical GSHP system

As shown in Figure 5-1, GHEs are usually piped in parallel and it is generally assumed that the total flow rate is divided equally among all boreholes and that each borehole has the same inlet temperature. The heat pump inlet temperature, $T_{in,hp}$, is the average of the outlet temperatures of all boreholes. This temperature has to remain within limits set by heat pump manufacturers. The lower limit for the inlet temperature, T_L, can be as low as ≈ -5 °C while the high temperature limit T_H can reach ≈ 45°C.

Equation based design methods (Bose et al., 1985; ASHRAE Handbook, 1995) and simulation based design methods (Hellström and Sanner 2000; Spitler, 2000) can be used to size boreholes. Spitler and Bernier (2016) have categorized these methodologies into five levels (0 to 4) with increasing complexities and accuracy. Level 0 are rules-of-thumb sizing methods, level 1 and 2 cover the equation based models that use one or three ground load pulses while level 3 and 4 are

simulation based sizing models that use monthly or annual hourly ground loads. Most of these models use a derivative of Equation 5.1 for determination of the boreholes length:

$$L = \frac{\sum_{i=1}^{N} q_i R_i + q_h R_b}{T_m - (T_g + T_p)} \tag{5.1}$$

where L ($= N_b \times H$, N_b is the number of boreholes) is the total required borehole length, q_i is a ground thermal pulse associated with a certain time period, R_i is the corresponding effective ground thermal resistance, q_h is the peak ground thermal pulse, R_b is the effective steady-state borehole thermal resistance, T_m is the mean borehole fluid temperature ($= (T_{inHP} + T_{outHP})/2$), and T_p is a temperature penalty to account for the ground temperature increase (or decrease) caused by borehole-to-borehole thermal interaction when the annual ground load imbalance is important. This equation can be used by one pulse (level 1), three pulses (level 2), monthly pulses (level 3) and hourly pulses (level 4) and can be solved directly or iteratively. By increasing the number of load pulses the accuracy of the sizing model increases at the expense of increased mathematical complexity and calculation time. Among these models, the ASHRAE sizing equation, a level 2 method, is a good compromise between accuracy and calculation time.

The original ASHRAE sizing method, which is based on the work of Kavanaugh (1995), first appeared in the 1995 ASHRAE Handbook (1995). The original format of this equation has been reformatted by Bernier (2006) and is presented in Equation 5.2. This equation will be referred to as the ASHRAE classic sizing equation.

$$L = \frac{q_a R_{ga} + q_m R_{gm} + q_h R_{gh} + q_h R_b}{T_m - (T_g + T_p)} \tag{5.2}$$

The summation term includes three thermal pulses and their corresponding effective ground thermal resistances. The time periods of the three thermal pulses, q_a, q_m , and q_h are typically 10 years, 1 month, and 4 hours (or 6 hours in certain cases), respectively. The corresponding effective ground thermal resistances, R_{ga}, R_{gm}, and R_{gd} are calculated using the infinite 1-D (radial) cylindrical heat source (ICS) analytical solution and they do not depend on borehole length. Borehole-to-borehole thermal interaction is accounted for using the temperature penalty term in the denominator. The main advantage of the ASHRAE sizing equation is that it can be

solved directly and it does not require an iterative solution procedure when tabulated values of T_p are used directly. However, if T_p needs to be calculated for a specific geometry then Eq. 5.2 needs to be solved iteratively as T_p depends on the borehole length. It should be noted that if the annual ground load is balanced (i.e. $q_a = 0$), the calculations of T_p and R_{ga} are irrelevant and the ICS solution is adequate for sizing purposes. Despite its simplicity, several authors have noted important deficiencies in the ASHRAE sizing equation:

1- The infinite cylindrical heat source used for evaluating the ground thermal resistances neglects axial heat transfer.

2- The temperature penalty calculation is inaccurate.

3- It does not size the length correctly if the maximum length is required in the first year of operation.

4- It does not account for short term effects associated with borehole thermal capacity.

5- The value of the steady-state borehole thermal resistance does not account for the impact of the vertical temperature variation of the fluid inside the U-shaped tubes.

In the following paragraphs, solutions to these issues proposed by various authors are reviewed and then the proposed model is described.

Philippe et al. (2009) focused on the first point. They determined the impact of neglecting the axial effects on the three ground thermal resistances. Their analysis showed that the 10 year effective ground thermal resistance, R_{ga}, is the most affected and as noted by Spitler and Bernier (2016), the weight of R_{ga} in Equation 5.2 determines whether it has a significant impact on L or not.

The second drawback is much more important. It concerns the determination of the temperature penalty (T_p in equation 5.2) which is suggested to be evaluated based on a rudimentary table of values on a limited number of configurations (ASHRAE, 2015). This has motivated researchers Bernier et al. (2008), Fossa (2011), Fossa and Rolando (2013) and Capozza et al. (2012) to introduce various methodologies based on a more rigorous evaluation of the temperature penalty.

Bernier et al. (2008) evaluated T_p based on the difference between the g-function for a specific bore field with N_b boreholes, g_{Nb}, and the g-function of a single borehole, g_1. They proposed a

correlation that evaluates the temperature penalty of equally-spaced rectangular bore fields which is within ±10% of the exact values, when g_{Nb}-g_1>15. Their results show that the ASHRAE equation can underestimate the value of T_p significantly. This methodology was used by Philippe et al. (2010) in a simple spreadsheet tool to obtain the length of single boreholes and rectangular bore fields. Since the temperature penalties depend on borehole length, which is unknown a priori, iterations are required.

Fossa (2011) has proposed a different definition for T_p. He has defined a "true or reference" temperature penalty to correct the error introduced by the use of the infinite cylindrical heat source solution when compared to the g-function of the bore field under consideration. Therefore, the temperature penalty of a single borehole is not zero as was the case in the study by Bernier et al. (2008). Fossa and Rolando (2013, 2015, 2016) have suggested a correlated equation (called Tp8) which examines the influence of eight surrounding boreholes. They have reported that the ASHRAE equation typically underestimates the "true" temperature penalty values by more than 40% (Fossa and Rolando, 2015). The lengths evaluated based on the temperature penalties obtained from the ASHRAE equation have errors ranging from 17 to 50 % while the ones evaluated with their proposed correlated equation have an average error of 3 % with respect to reference values (Fossa and Rolando, 2015). Finally, they showed that the correlation suggested by Bernier et al. (2008) has a difference of less than 6% with their reference method for the rectangular and square bore fields.

Monzó et al. (2016) focused on the second and the third weak points. They proposed to use the same three-pulse technique used in the ASHRAE sizing method with two modifications. First, the yearly ground load is replaced by the average ground load of the previous months. Second, the temperature penalty, T_p, is based on the average ground load of the previous months and is evaluated using g-functions. The methodology involves a three step process. First, ground loads need to be analyzed and properly ordered. Then, using these loads, and assuming a temperature penalty $T_p = 0$, a first set of required lengths is determined for each month. Finally, an iterative process is initiated to account for the temperature penalty in each month to obtain the final required length for the worst condition. Monzó et al. (2016) have shown that the starting month can have a significant impact on the design length equation. Their proposed method compares favorably well with a commercial software tool.

Short term effects have been analyzed by several authors and a complete literature review on the subject has been presented by Li and Lai (2015). Yavuzturk and Spitler (1999) were among the first to evaluate these effects. They used a 2D finite volume method and calculated short term g-functions. Others (Zarrella, et. al, 2011, Pasquier and Marcotte, 2012, Ruiz-Calvo et. al, 2015) have used thermal resistance-capacity (TRC) networks to study these effects. This problem can also be solved by simplifying the geometry in the borehole with an equivalent-diameter hollow cylinder (Lamarche and Beauchamp, 2007, Salim-Shirazi and Bernier, 2013, Claesson and, Javed, 2011). Such models can be solved in the Laplace domain (Beier and Smith, 2003, Bandyopadhyay et al., 2008) or in the time domain (Lamarche and Beauchamp, 2007, Lamarche, 2015, Javed and Claesson, 2011). Another way of accounting for short term effects, without transforming the geometry into an equivalent diameter is to use the infinite line-source model in a cylindrical composite medium (Li and Lai, 2012, Yang and Li, 2014). This approach can be used for modeling various types of ground heat exchangers, including single and double U-shaped tubes, W-shaped channels, and helical-coils. However, since the infinite line-source model does not account for the annual load imbalances this model cannot be used for a long-term thermal processes.

Other authors have investigated the impacts of short term effects on the borehole length evaluated by the ASHRAE equation. Lamarche (2016) used an alternative model to the ASHRAE equation that uses g-function to determine the ground thermal resistances. He observed that by neglecting the thermal capacity of the boreholes the length is somewhat oversized especially when the hourly peak ground load is much larger than the monthly ground load. Gagné-Boisvert and Bernier (2016) took into account the thermal capacity inside the borehole and heat pump cycling. Running annual simulations with a TRC model they proposed to multiply the ASHRAE sizing equation by a correction factor. The correction factor can reach 0.69 when oversized heat pumps operate intermittently and 1.24 for undersized heat pumps and low thermal capacity boreholes.

Li et al. (2017) suggested an alternative to the ASHRAE sizing equation that considers not only the short term effects but also account for the vertical temperature variation of the fluid inside the U-tubes. The quasi-3D model uses a full-scale line source model for heat transfer outside the U-tubes that accounts for the short-term (with the use of the composite medium solution), the mid-term (with the use of the infinite line source solution), the long term temperature responses and also the thermal interaction between the boreholes (with the use of the finite line source solution).

The proposed method is applied to the four test cases introduced by Cullin et al. (2015) and it is shown that the borehole lengths evaluated with their proposed method are closer to the actual lengths and are also shorter than the ones evaluated by the classic ASHRAE sizing equation.

Some authors have argued that the errors in the ASHRAE sizing equation are caused by the use of only three load pulses. For instance, Cullin et al. (2014) compared the sizing ASHRAE equation with GLHEpro in sizing of a 3×2 bore field. The results showed that GLHEPro under predicted the required GHE length by 4% when compared to the actual length, while the ASHRAE sizing method lead to an over prediction of 103%. Later, Cullin et al. (2015) used the same design tool and the ASHRAE sizing equation to evaluate the design lengths of four different systems with operating data. The GLHEPro tool predicted the borehole lengths to within 6% in all four cases, while the ASHRAE sizing equation evaluated lengths with errors ranging from –21% to 167%. The authors explained that most of the error is related to the way that loads are represented in the ASHRAE sizing equation while the differences related to the borehole thermal resistance are less important.

In summary, past studies indicate that the ASHRAE sizing equation has several drawbacks including: i) the use of the 1-D infinite cylinder solution for long time which is inadequate for the long-term effective ground thermal resistances, ii) the inappropriate calculation of the temperature penalty, T_p, iii) the non-inclusion of borehole thermal capacity or variation of the vertical fluid temperature along the U-tubes, iv) the inability of the method to find the maximum length during the first year of operation. In this paper, an alternative to the ASHRAE sizing equation is proposed to alleviate the first three deficiencies. The fourth drawback has been examined by Monzó et al. (2016).

The alternative method proposed in this paper has first been introduced by Ahmadfard and Bernier (2014). It is also included in the latest version of the ASHRAE Handbook (ASHRAE, 2015) in a separate section entitled “Alternative sizing method”. This paper expands the analysis provided by Ahmadfard and Bernier (2014) and examines four aspects of this new methodology. First, it is shown that the time-consuming evaluation of the full g-function curve, typically obtained by temporal superposition, is not necessarily required. Secondly, the optimum number of borehole segments to obtain an accurate bore field length with reasonable calculation time is examined. In addition, the selection of a convergence criteria and its impact on calculation time is

discussed. Finally, the alternative method is modified to account for short-term effects. The proposed alternative method is presented in the next section and is then applied for sizing various bore field configurations and compared to other sizing tools in the following sections.

5.2 Modifications to ASHRAE's classic sizing equation

As shown in Equation 5.3, the alternative method uses the same three pulse methodology as the classic ASHRAE sizing equation.

$$L = \frac{q_a R_{ga,g} + q_m R_{gm,g} + q_h R_{gh,g} + q_h R_b}{T_m - T_g} \tag{5.3}$$

The three ground pulses, q_a, q_m and q_h are applied over time periods which are typically equal to 10 years (t_y), 1 month (t_m), and 4 or 6 hours (t_h), respectively. The corresponding ground thermal resistances, $R_{ga,g}$, $R_{gm,g}$, $R_{gd,g}$ are evaluated based on the principle of temporal superposition (ASHRAE, 1995, 2015):

$$\begin{aligned} R_{ga,g} &= \left[g_{(t_f)} - g_{(t_f - t_1)}\right]/2\pi k_g \\ R_{gm,g} &= \left[g_{(t_f - t_1)} - g_{(t_f - t_2)}\right]/2\pi k_g \\ R_{gd,g} &= \left[g_{(t_f - t_2)}\right]/2\pi k_g \end{aligned} \tag{5.4}$$

where $t_f = t_y + t_m + t_h$, $t_2 = t_y + t_m$ and $t_1 = t_y$. The subscript "g" denotes that the effective ground thermal resistances are evaluated using g-functions. g-Functions account for the thermal interactions among boreholes and the correction provided by the temperature penalty in the classic ASHRAE sizing equation is no longer required. When short-term effects caused by borehole thermal capacity are important, short-term g-functions should be used for the $g_{(t_f - t_2)}$ term which is present in $R_{gm,g}$, $R_{gd,g}$. The determination of short-term g-functions will be addressed later in this paper.

As explained by Bernier (2014), long-term g-functions depend mainly on three non-dimensional parameters: r_b/H, B/H, and t/t_s where t_s is the characteristic time (=$H^2/9\alpha$). The main drawback of the proposed alternative method is that an iterative procedure is required because g-functions depend on the length of the borehole which is unknown a priori. Most of the current

commercially available sizing programs use a pre-stored data base of g-functions with specific r_b/H and B/H ratios. For values of B/H other than the ones associated with the g-functions, logarithmic interpolation between pre-computed g-functions can be used. However, as stated by Malayappan and Spitler (2013), interpolation may result in sizing errors of a few percent. For values of r_b/H different than the ones associated with the g-functions, Eskilson (1987) recommends applying a correction factor but it is also unclear if this correction factor applies to all cases.

For cases where r_b/H and B/H ratios are different, correction factors for r_b/H or interpolation between different B/H curves are required. The method suggested in this paper does not need to use any correction factors or interpolation as it uses the exact values of r_b/H, B/H and $ln(t/t_s)$ in each iteration. In addition, the g-function values required at the various time are evaluated independently of previous g-functions as the temporal superposition is not used for evaluation of g-functions. In this way, g-functions are evaluated dynamically as the calculation to obtain L progresses from iteration to iteration.

Figure 5-2 shows schematically the five-step iteration procedure of the alternative method. A guess value of $L_i = (N_b \times H_i)$ is first selected. Using this guess value, three g-function are evaluated based on the proper values of $ln(t/t_{s,i})$, r_b/H_i and B/H_i. The whole g-function curve does not need to be evaluated since only three g-function values corresponding to three time periods, $t_f - t_2$, $t_f - t_1$ and t_f are required in each iteration. In the third step, the three g-functions are used to calculate the effective ground thermal resistances (Eq. 5.4) which are then used, in step 4, to evaluate the required boreholes length L_{ii} (Eq. 5.3). The resulting length L_{ii} is then compared to the guessed or the previous length L_i. If the two lengths agree to within a certain tolerance ε, then the solution is said to have converged. If not, the length L_{ii} is then used as the new guess value for the next iteration.

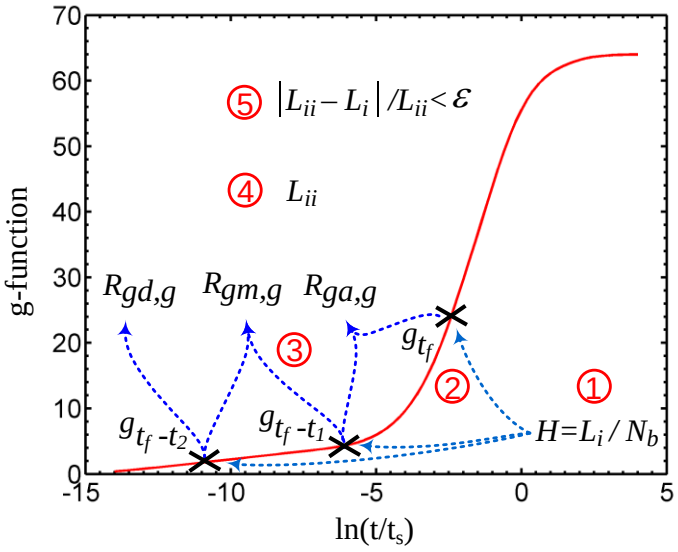

Figure 5-2: Illustration of the five step procedure for the alternative method

5.3 Evaluation of g-functions

The approach suggested by Cimmino and Bernier (2013, 2014) is first used to determine g-functions over the full time scale. This approach can generate g-functions for any bore field geometry. Each borehole is subdivided into a number of segments and the thermal response of every borehole segment is calculated using the finite line source analytical solution (FLS). Then, spatial superposition is used to calculate the total temperature variation at the borehole wall of every segment. While Cimmino and Bernier (2013, 2014) solved their equation in the Laplace domain, the equations developed here are solved in the time domain.

The process of generating g-functions is shown in Figure 5-3 for a 3×2 configuration where each borehole is subdivided into two equal length segments ($H_i = H/2$) giving a total of 12 segments. The thermal interactions of all segments towards segment #1, including segment #1 on itself, are illustrated schematically on this figure. In accordance with Eskilson's definition of the g-function, the borehole wall temperature T_b is the same for every borehole segments in the bore field. This condition is referred to as boundary condition #3 (BC-III) by Cimmino and Bernier (2014). The heat extraction rate per unit length Q_i of each segment is assumed uniform along its length. The total heat extraction rate per unit length $\bar{Q}$ of all boreholes is considered fixed and constant in time. The ground thermal properties are assumed to be isotropic and constant.

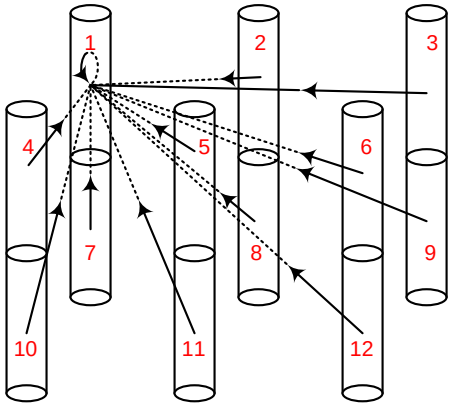

Figure 5-3: Schematic illustration of the thermal interaction of all boreholes segments towards segment #1

In order to evaluate the g-functions for a certain heat extraction rate $\bar{Q}$ at a certain time t_k, the thermal response, $h_{i,j}(t_k)$ among all segments i (1:12) toward each segment j (1:12) need to be calculated. These interactions are evaluated analytically using the FLS following the approach of Cimmino and Bernier (2013):

$$h_{i,j}(t_k) = \frac{1}{2}\int_{1/\sqrt{4\alpha_g t_k}}^{\infty} \exp(-r_{i,j}^2 s^2)\frac{Y(H_s s, D_i s, D_j s)}{H_j s^2} ds \qquad (5.5)$$

where, $Y(H_s s, D_i s, D_j s) = f\left((D_j - D_i + H_s)s\right) + f\left((D_j - D_i - H_s)s\right) + 2f\left((D_j + D_i + H_s)s\right) - 2f\left((D_j - D_i)s\right) - f\left((D_j + D_i)s\right) - f\left((D_j + D_i + 2H_s)s\right)$

and $f(x) = x.erf\,x - (1 - exp(-x^2))/\sqrt{\pi}$.

erf is the error function, H_s are the segment lengths, D_i and D_j are the depths of the borehole segments i and j from the ground surface, and $r_{i,j}$ is the radial distance between segments i and j. Cimmino and Bernier (2013) modified the original approach of Claesson and Javed (2011) to account for various borehole depth and heat extraction rate variation using borehole segments.

The radial distance of segments located in the same borehole is equal to r_b. Thermal response values can be reorganized in a square (12×12 in this example) matrix as follows:

$$\begin{bmatrix} h_{1,1} & h_{2,1} & \cdots & h_{11,1} & h_{12,1} \\ h_{1,2} & h_{2,2} & & h_{11,2} & h_{12,2} \\ \vdots & & \ddots & \vdots & \\ h_{1,11} & h_{2,11} & \cdots & h_{11,11} & h_{12,11} \\ h_{1,12} & h_{2,12} & & h_{11,12} & h_{12,12} \end{bmatrix} \quad (5.6)$$

Because of symmetry, some terms in this H-matrix are identical ($h_{1,12} = h_{3,10}$, for example). In these cases, the proposed methodology calculates h only once to limit calculation time. The segment-to-segment thermal response factor (Eq. 5.5) needs to be multiplied by the corresponding non-dimensional heat extraction rate of each segment. For a typical segment j the following equation is then applied:

$$h_{1,j}\widetilde{Q_1}(t_k) + h_{2,j}\widetilde{Q_2}(t_k) + \cdots + h_{11,j}\widetilde{Q_{11}}(t_k) + h_{12,j}\widetilde{Q_{12}}(t_k) + \theta^*_{b,j}(t_k) = \theta_b(t_k) \quad (5.7)$$

where $\theta_b(t_k)$ is the non-dimensional temperature variation at the borehole wall (which is the same for all segments) at time t_k . This value is in fact the g-function. The non-dimensional heat extraction rate per unit length of each segment i is given by $\tilde{Q}_i(t_k)(= Q_i(t_k)/\bar{Q})$. The product $h_{i,j}\tilde{Q}_i(t_k)$ accounts for the non-dimensional temperature variation at the borehole wall of the jth borehole segment due to the extraction/injection of heat by the ith borehole segment at time t_k. $\theta^*_{b,j}(t_k)$ is a term that accounts for the "history-effect" of the time variation of the heat extraction rates. This term has been determined by Cimmino and Bernier (2013) and can be evaluated with the following expression:

$$\theta^*_{b,j}(t_k) = \left[\sum_{p=1}^{k-1}\sum_{i=1}^{N_b.N_s=12} h_{i,j}(t_k - t_{p-1})\tilde{q}_i(t_p)\right] - h_{i,j}(t_k - t_{k-1})\tilde{Q}_i(t_{k-1}) \quad (5.8)$$

In this equation, $\tilde{q}_i(t_p)$ is equal to $\tilde{Q}_i(t_p) - \tilde{Q}_{i-1}(t_{p-1})$, where p is the time step counter. As shown in Eq. 5.8, $\theta^*_{b,j}$ uses temporal superposition. The heat extraction rates and the thermal interactions related to the $k-1$ previous time steps, are needed to evaluate the g-function at t_k.

In the $N_b \times N_s$ equations (Equation 5.7), there are $N_b \times N_s$ unknown heat extraction rates, $\tilde{Q}_{i=1:12}$, and one unknown g-function, $\theta_b(t_k)$. The last equation to close the problem is based on the fact that the total heat extraction rate is constant:

$$\sum_{i=1}^{N_b.N_s} \tilde{Q}_i\,(t_k) = N_b.N_s \rightarrow \tilde{Q}_1(t_k) + \tilde{Q}_2(t_k) + \cdots + \tilde{Q}_{11}(t_k) + \tilde{Q}_{12}(t_k) = 12 \qquad (5.9)$$

Finally, the system of equations can be re-casted in the following matrix form:

$$\begin{bmatrix} \begin{bmatrix} h_{1,1} & h_{2,1} & \cdots & h_{11,1} & h_{12,1} \\ h_{1,2} & h_{2,2} & & h_{11,2} & h_{12,2} \\ \vdots & & \ddots & \vdots & \\ h_{1,11} & h_{2,11} & \cdots & h_{11,11} & h_{12,11} \\ h_{1,12} & h_{2,12} & & h_{11,12} & h_{12,12} \end{bmatrix} \begin{matrix} -1 \\ -1 \\ \vdots \\ -1 \\ -1 \end{matrix} \\ \begin{matrix} 1 & 1 & \cdots & 1 & 1 \end{matrix} \quad 0 \end{bmatrix} \times \begin{bmatrix} \tilde{Q}_1(t_k) \\ \tilde{Q}_2(t_k) \\ \vdots \\ \tilde{Q}_{11}(t_k) \\ \tilde{Q}_{12}(t_k) \\ \theta_b(t_k) \end{bmatrix} = \begin{bmatrix} \theta^*_{b,1} \\ \theta^*_{b,2} \\ \vdots \\ \theta^*_{b,11} \\ \theta^*_{b,12} \\ N_b.N_s = 12 \end{bmatrix} \qquad (5.10)$$

By solving this system of equations, the 12 heat extractions $\tilde{Q}_i(t_k)$ as well as the g-function $\theta_b(t_k)$ are obtained at time t_k. Equation 5.10 is the resulting system of equations for the 3×2 configuration with 2 segments per borehole. As can be expected, calculation time increases significantly with an increase in the number of boreholes and borehole segments. In addition, as will be shown later, asymmetric bore fields also lead to long calculation times.

As shown below, the evaluation of $\theta^*_{b,j}$ can potentially be neglected for bore field sizing purposes. Consequently, g-functions can be evaluated without considering temporal superposition of heat extraction rates at previous time steps. Thus, the value of the heat extraction rates of all segments as well as the g-functions are evaluated directly at time t_k. As will be shown below, the generation of g-functions without temporal superposition reduces computational time significantly which is an important aspect of the proposed alternative method since g-functions are evaluated several times in the iterative process.

It should be pointed out that the methodology that is described here for the evaluation of g-functions is not specific to the ASHRAE sizing equation but can be used whenever g-functions are required.

5.4 Neglecting temporal superposition when generating g-functions values

Bore field sizing using the proposed alternative method (Eq. 5.3) requires g-function at three time values on the g-function curve (Fig. 5-2) for each iteration. Typically, as shown below, 3 to 5 iterations are required. Thus, 9 to 15 g-function values are required to size a bore field. There are

several ways to obtain these g-function values. First, as noted in the introduction, pre-calculated g-function curves can be used. However, these are typically valid for fixed values of B/H and r_b/H. It is possible to interpolate between B/H curves and correct for various r_b/H ratio but with a lost in accuracy which is difficult to quantify.

Secondly, one can generate the entire g-function curve for the exact B/H and r_b/H ratios by solving Equation 5.10 at several times, t_k. Temporal superposition is used to account for the "history-effect" of the time variation of the heat extraction rates of the borehole segments. Then, the three g-function values would be obtained by interpolation on the g-function curve. This process would have to be repeated 3 to 5 times depending on the number of iterations. Cimmino and Bernier (2013) evaluated the entire curve based on 71 individual values of t_k . They used time steps of one hour for the first 48th hours and then they doubled the time step for each subsequent time to cover the full time span of the g-function curve. In the present work, the same technique is employed but with 19 individual values of t_k evaluated at times corresponding to $ln(t/t_s)$= -14, -13, …, 3, 4. This accelerates the evaluation of the g-functions curve when compared to the technique of Cimmino and Bernier (2013). In sizing problems discussed below that are solved with temporal superposition, 19 g-functions values are calculated in each iteration and then the three g-functions are interpolated from these values.

The third method which is even faster and is the one recommended here, is to calculate the g-function directly at the required value of $ln(t_k/t_s)$ without temporal superposition. Thus, the $\theta^*_{b,j}(t_k)$ term in Equation 5.10 is considered to be equal to zero. Until now most researchers used temporal superposition to obtain g-functions (e.g. Cimmino and Bernier (2013). However, as shown below this is not necessary.

The accuracy of a direct calculation of the g-function without temporal superposition will now be evaluated for several bore field configurations. The first configuration to be studied is a 12×10 bore field with H = 100 m, D = 4 m, r_b = 75 mm and B = 6.5 m. The g-functions are calculated with 12 equal-length segments. Figure 5-4.a shows g-function curves evaluated using the three techniques just described with the bottom graph showing the relative difference between the technique without temporal superposition and two methods with temporal superposition where the entire g-function curve is generated with either 19 or 71 points. The maximum relative difference of the results is approximately 2.9% (with the 71 point curve) and occurs at a value of $\ln(t/t_s) \approx$

-1 where the g-function curve has its steepest slope. As shown on the top scale, this value corresponds to a time of 15 years for a 100 m borehole and a ground thermal diffusivity of 0.075 m^2/day. If this borehole is to be sized for a 10-20 year period, then the value of $R_{ga,g}$ will be the one most affected by this difference. However, as will be shown below, the overall effect of this difference on bore field length is minimum since the $R_{ga,g}$ term is typically not the dominant term in Equation 5.3.

Figure 5-4.b shows three series of curves. The upper and lower curves show, respectively, the time variation of $\sum_{p=1}^{k-1}\sum_{i=1}^{N_b.N_s=12} h_{i,j}(t_k - t_{p-1})\tilde{q}_i(t_p)$ and of $-h_{i,j}(t_k - t_{k-1})\tilde{Q}_i(t_{k-1})$ for all segments. The summation of these values is equal to $\theta^*_{b,j}$, represented by the middle curves. As expected, the values of $\theta^*_{b,j} \neq 0$ for $ln(t/t_s) \approx -1$ which explains the difference observed in the g-function value in Figure 5-4a.

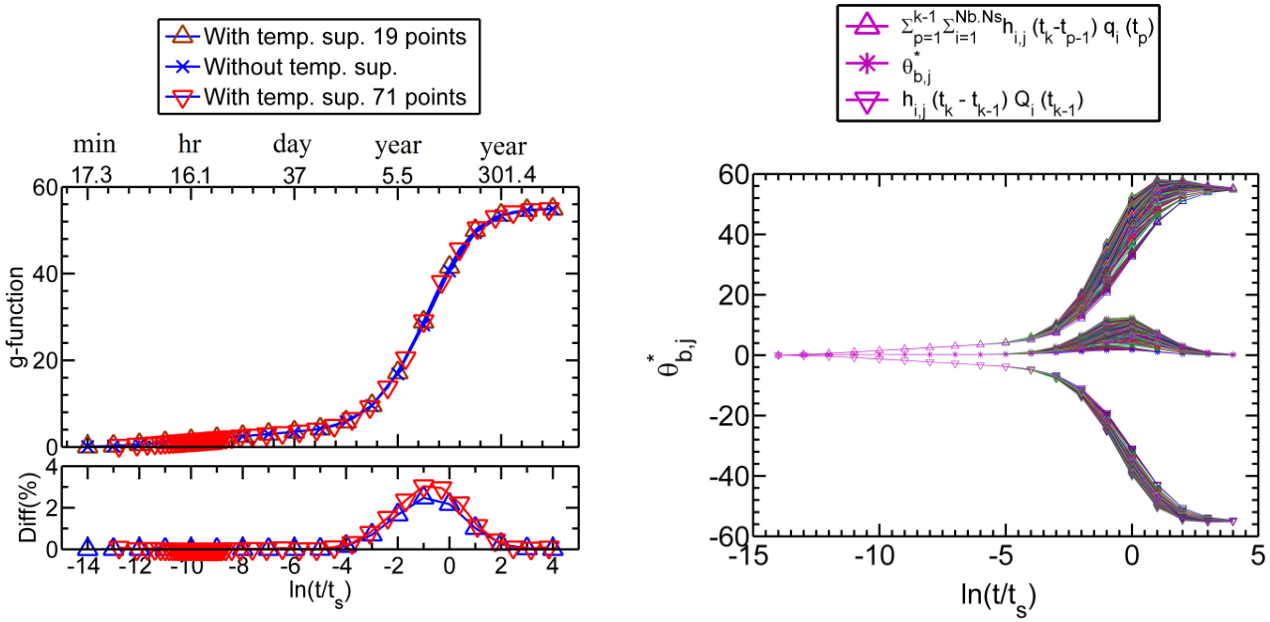

a. b.

Figure 5-4: a. g-Function curves determined with and without the temporal superposition and their relative difference b. Variation of θ^*_b as a function of non-dimensional time

Figure 5-5 presents the maximum relative difference of the g-functions obtained with temporal superposition for 19 t_k values and the ones that are evaluated without temporal superposition as a function of the number of segments. In addition to the 12×10 configuration, the comparisons are

done for two other configurations of 6×5 and 3×2 boreholes. For each of these cases, the input parameters are the same as those used for Fig. 5-4.

These results show that the maximum difference, typically occurring at $ln(t/t_s) \approx -1$, between the two methods increases with the number of boreholes. This is due to increased thermal interactions between boreholes that cause greater time variations of the heat extraction rates. The maximum difference also increases with the number of segments up to a certain point around 12-15 segments where the maximum difference stabilizes.

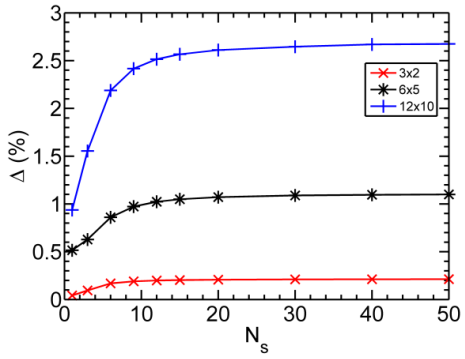

Figure 5-5: The effect of the number of segments and number of boreholes on Δ, the maximum difference between g-functions evaluated with and without temporal superposition

5.5 Verification of the proposed alternative method

The previous section examined the impact of calculating g-functions without temporal superposition. This section looks more closely at the accuracy of the proposed method for sizing of vertical ground heat exchangers. Therefore, the methodology is first compared with other sizing tools for six different borehole configurations. Then, the effects of temporal superposition, number of borehole segments, convergence criteria, and initial guesses are evaluated separately for a typical sizing problem. Finally, the effects of these parameters and also the effect of bore field symmetry on the calculation time and the boreholes overall length are discussed for two borehole configurations.

5.5.1 Ground loads and input parameters used in the comparisons

The ground load profile used in this work is presented in Figure 5-6 where negative loads indicate that the building is in heating mode and that the GHX collects heat from the ground. The same

annual load is repeated for a ten-year cycle. It is an unbalanced load which causes the ground to get progressively cooler from year to year.

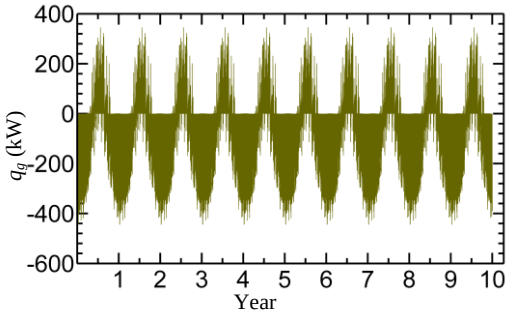

Figure 5-6: Ground loads used in the comparison cases

Table 5-1 provides a monthly summary of this load profile. The average ground loads of each month, q_m, are evaluated based on the average of all hourly loads of that month including the two heating and cooling peaks, $q_{h,C}$ and $q_{h,H}$, occurring during that month. Considering that the largest peak heating load (-443.9 kW) is larger than the largest peak cooling load (345.5 kW), and that there is a negative thermal imbalance, the required bore field length will be determined when the building is in peak heating mode. Therefore, only the required bore field length in heating will be evaluated here. Corresponding ground loads to be used for three pulse methods are presented in Table 5-2.

Table 5-1: Monthly average and peak ground loads in cooling and heating

	Jan	Feb	Mar	Apr	May	Jun	Jul	Aug	Sep	Oct	Nov	Dec
q_m (kW)	-146.4	-144.7	-123.0	-74.5	-17.6	31.0	41.9	30.6	-14.5	-62.3	-98.1	-136.0
$q_{h,C}$ (kW)	0.0	0.0	0.0	30.5	225.1	304.4	345.5	323.1	231.5	201.4	0.0	0.0
$q_{h,H}$ (kW)	-443.9	-428.0	-362.4	-309.2	-186.2	-108.9	-70.2	-170.1	-228.1	-297.2	-383.7	-415.8

Table 5-2: Annual, monthly and hourly ground loads used in for three pulse methods

Ground loads	(kW)
q_h	-443.9
q_m	-146.4
q_a	-59.0

The borehole parameters and ground properties used in the following analysis are reported in Table 5-3. It should be noted that the minimum entering fluid temperature limit, T_L and the undisturbed ground temperature are set to 0°C and 18°C, respectively. These loads are used for six different borehole configurations which are shown on the first row in Table 5-4.

Table 5-3: Borehole parameters and ground thermal properties

Parameter	Value
Ground	
Ground thermal conductivity (k_g)	1.8 W/(m.K)
Ground thermal diffusivity (α_g)	0.075 m2/day
Undisturbed ground temperature (T_g)	18 °C
Bore field	
Borehole buried depth (D)	4 m
Borehole spacing (B)	6.5 m
Borehole	
Borehole radius (r_b)	75 mm
Number of pipes	2
Pipe outer radius ($r_{p,out}$)	16.7 mm
Pipe inner radius ($r_{p,in}$)	13 mm
Center to center distance between pipes (d_p)	62 mm
Pipe thermal conductivity (k_p)	0.4 W/(m.K)
Pipe volumetric heat capacity	1540 kJ/(K.m3)
Grout thermal conductivity (k_{gr})	1 W/(m.K)
Grout volumetric heat capacity	3900 kJ/(K.m3)
Contact resistance (R_c)	0 W/(m.K)
Resulting borehole thermal resistance (R_b)	0.20 m.K/W
Fluid	
Fluid viscosity (μ_f)	0.00179 kg/(m.s)
Fluid density (ρ_f)	1016 kg/m3
Fluid specific heat capacity (C)	4000 J/(kg.K)
Fluid thermal conductivity (k_f)	0.513 W/(m.K)
Fluid flow rate ($\dot{m}$)	0.043 kg/s per kW of peak load
Minimum entering fluid temperature limit (T_L)	0 °C
Convection coefficient (h_{conv})	1000 W/(m2.K)

With the conditions presented in Table 5-3 and with the ground load profile given in Figure 5-6, 120 boreholes (12×10) each with a length of approximately 100 m are required. This

configuration represents the base case (5th column in Table 5-4). Other test cases, with a lower or larger number of boreholes, use a load profile which is proportional to the number of boreholes. Hence, a geometry with 25 boreholes will have values of q_a, q_m, and q_h which correspond to 25/120 times the value presented in Tables 5-1 and 5-2. Sizing with the proposed method is performed using three thermal pulses with t_y = 10 years, t_m = 1 month, and t_h = 6 hours.

5.5.2 Comparison with other sizing methods

In this section, the proposed method is compared with four other sizing tools/methods. These methods will now be briefly described. None of these methods account for short-term effects, i.e. for borehole thermal capacity. These effects will be discussed later.

The commercial sizing tool called Earth Energy Designer (EED) (Blomberg et al., 2015) uses a data base of pre-calculated g-functions to size bore fields. The program interpolates between g-function values by keeping the borehole spacing constant but changing borehole depth. The data base includes g-functions for the in-line, L, U, O and rectangular geometries. Thus, it cannot size the axisymmetric configuration shown in the last column of Table 5-4. EED requires user-defined average monthly heating and cooling loads and peak heating and cooling loads to determine the average and the peak monthly mean fluid temperatures. Peak heat loads are added to the average heat loads at the end of each month. It also assumes that the peak heat loads do not have any influence on the long-term behavior as they are already considered in the average load.

The next two sizing methods use the ASHRAE sizing equation but with better evaluations of the temperature penalties based on the methodologies suggested by Bernier et al. (2008) and Fossa and Rolando (2013). As mentioned earlier, Bernier et al. (2008) suggest to evaluate the temperature penalties T_p using $Q_u\left(g_{N_b} - g_1\right)/\left(2\pi k_g N_b H\right)$,while Fossa and Rolando (2013) suggest a slightly different method where T_p is equal to $Q_u\left(g_{N_b}/2\pi - G\right)/\left(k_g N_b H\right)$ The value of Q_u in these equations is the unbalanced load which is equal to $(q_a t_y + q_m t_m + q_h t_h)/\left(t_y + t_m + t_h\right)$.

The last sizing method uses the Duct ground STorage (DST) model in the TRNSYS environment as explained by Ahmadfard et al. (2016). The DST model is typically used for a known borehole length; it is not a sizing tool. However, when combined with GenOpt it is possible to find the optimum (i.e. minimum) borehole length such that the outlet temperature from the bore field is

within the temperature limits, T_L and T_H. For each iteration, GenOpt makes a new guess for the borehole length and then it calls the DST model to do a multiyear simulation. The objective functions as well as the optimization design parameters are the same as the ones used by Ahmadfard et al. (2016). The DST model is strictly valid for an axisymmetric configuration which explains the choice of the configuration shown in the last column in Table 5-4.

For the results reported in Table 5-4, the g-functions used in the proposed method and for the evaluation of the temperature penalties are calculated with twelve segments. The reported temperature penalties and borehole lengths are evaluated iteratively with the use of a convergence criterion of 0.1 % and an initial guess for the borehole length of 100 m.

Table 5-4: Comparison between the proposed method and four other sizing tool

Bore field geometry						
	19: (9,1,9)	25: (1×25)	28: (9,1,8,1,9)	36: (8,1,8,1,8,1,8,1)	120: (12×10)	127: axisymmetric
	Borehole length (m) (Percentage difference relative to the proposed method without temporal superposition)					
Proposed method without temporal superposition	77.0	76.8	77.6	78.9	106.1	112.6
Proposed method with temporal superposition	77.1 (0.1)	76.9 (0.1)	77.7 (0.1)	80.0 (0.1)	107.4 (1.2)	114.1 (1.3)
EED	79.8 (3.7)	77.4 (0.9)	77.2 (0.5)	78.1 (1.0)	111.6 (5.2)	-----
Classic ASHRAE equation with T_p from Fossa and Rolando (2013)	78.9 (2.6)	78.7 (2.6)	79.5 (2.6)	80.9 (2.5)	108.6 (2.3)	115.2 (2.3)
Classic ASHRAE equation with T_p from Bernier et al. (2008)	79.6 (3.4)	79.4 (3.4)	80.2 (3.4)	81.5 (3.4)	109.1 (2.8)	115.7 (2.7)
DST-GenOpt	-----	-----	-----	-----	-----	120.6 (7.1)

Results obtained by the proposed method with and without temporal superposition are very close to each other (within 0.1%) for non-dense bore fields but show slightly higher differences (1.2 to 1.3 %) for denser bore fields. This is not as high as the maximum difference, around 2.5%, shown in Figure 5-5 for 120 boreholes. This is due to the fact that the maximum difference in the g-function only affects the $q_a R_{ga,g}$ term in the sizing equation. This impact is presented in Table 5-5 where it is shown that the difference between g-functions evaluated with and without temporal superposition does not affect the short time periods and so the monthly and hourly effective ground thermal resistances of the two models are identical. Therefore, the main difference is related to the yearly ground thermal resistances. For non-dense bore fields, the difference in the value of $R_{ga,g}$ is small but for denser bore fields the difference is in-line with the values shown in Figure 5-5. For example, the difference in the value of $R_{ga,g}$ for the 120 borehole configuration in Table 5-5 is around 3%. However, this does not translate into a 3% difference in the bore field length as $R_{ga,g}$ is multiplied by q_a in the sizing equation (Eq. 5.3). Thus, depending on the weight of the $q_a R_{ga,g}$ term in Equation 5.3, the impact of the difference between g-functions evaluated with and without temporal superposition will be more or less significant. In the case reported in Table 5-4, the overall difference on the length is of the order of 1.2 to 1.3 %. Finally, the last line in Table 5-5 shows that calculation times with temporal superposition are 7 to 10 longer than without temporal superposition.

Table 5-5: Comparison of the three ground thermal resistances evaluated with and without temporal superposition

Bore field geometry	Without temporal superposition		With temporal superposition	
				
	19: (9,1,9)	120: (12×10)	19: (9,1,9)	120: (12×10)
Length (m)	77.0	106.1	77.1	107.4
$R_{gh,g}$ (m.K/W)	0.092	0.092	0.092	0.092
$R_{gm,g}$ (m.K/W)	0.209	0.209	0.209	0.209
$R_{ga,g}$ (m.K/W)	0.555	1.789	0.560	1.844
Calculation time (s)	36	50	240	486

The results evaluated without temporal superposition and the ones obtained using EED with the monthly pulses are in good agreement except for the L and rectangular bore field configurations where the differences are 3.7% and 5.2%. As shown previously, only 1.2 % of this difference is

related to the error associated with the generation of g-functions without temporal superposition. The remaining difference might be due to the fact that Eskilson's numerically generated g-functions, which were evaluated with 12 axial nodes, might not be grid independent as suggested by Cimmino and Bernier (2014).

Table 5-6 presents the results of a comparison between EED and the two proposed models with and without temporal superposition. In this comparison, the annual heat load is assumed to be zero. The results are also evaluated using 1 and 12 segments for the evaluation of the g-function. It can be seen that all methods lead to the same length of 63.9 m. This tends to demonstrate that when there is no annual ground thermal imbalance, the proposed method can be used with one segment and without temporal superposition. The calculation times in the last column in Table 5-6 show that it is clearly advantageous to reduce the number of segments and to perform the calculations without temporal superposition.

Table 5-6: Comparison of several methods when there is no annual ground thermal imbalance

Configuration	Method	Number of segments	Number of iterations	Length (m)	Calculation time (s)
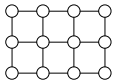	Proposed method without temporal superposition	1	2	63.9	1.1
		12	2	63.9	34.7
	Proposed method with temporal superposition	1	2	63.9	5.1
		12	2	63.9	270.6
	EED	------	----	63.9	1.0

Results presented in Table 5-4 also show that the borehole lengths obtained using the ASHRAE equation compare favorably well with other methods if the temperature penalties are evaluated properly. This is in contrast with the work of Cullin et (2015) who reported that the classic ASHRAE sizing equation evaluated with the original temperature penalty method showed differences ranging from –21% to 167% when compared to four different systems with operating data.

The last row of Table 5-4 is related to the result of the DST-GenOpt tool for an axisymmetric configuration. The difference between this method and the proposed method without temporal superposition is 7.1%. Sizing with the DST-GenOpt approach is achieved within the TRNSYS

environment using hourly time steps in order to mimic the three pulse approach. Hence, the hourly ground load contains 87600 hours at -59.0 kW, 744 hours at -146.4 kW and 6 hours at -443.9 kW. Figure 5-7 shows the evolution of the outlet fluid temperature from the bore field for the last iteration of the DST-GenOpt approach. As can be seen, the outlet temperature from the bore field decreases steadily for the first ten years, then there are two sudden decrease associated with the monthly and hourly pulses before the fluid temperature reaches a value of 0 °C, the minimum temperature limit. Finally, it should be mentioned that based on the results reported in Table 5-4, the proposed method has, on average, a 2.9 % difference with the other four sizing methods.

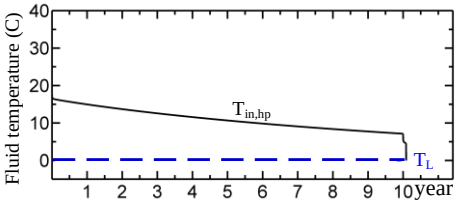

Figure 5-7: Evolution of the outlet fluid temperature for the last iteration of the DST-GenOpt method

5.5.3 Convergence criteria, initial guess values and number of segments

The proposed method is iterative in nature and results depend on the convergence criteria and initial guess values. The impact of these two factors are presented by examining the 12×10 sizing problem presented earlier with three different convergence criteria of 0.01, 0.1 and 1% and with two initial guess values for the borehole length, 50 and 200 m. Table5-7 presents the results of this analysis which was obtained without temporal superposition and with 12 borehole segments. As expected, a stricter convergence criteria leads to more iterations and longer calculation times. However, the evaluated lengths do not vary significantly. A 0.1% convergence criteria, i.e. a 0.1 m error for a 100 m borehole, appears to be a good compromise between accuracy and calculation time. Results also show that the alternative method converges to the same value whether the initial guess is significantly lower (50 m) or higher (200 m) than the final length.

Table 5-7: Analysis of the effects of various convergence criteria and initial guess values on the results

Convergence criteria, ε (%)	Initial guessed Length (m)	Number of iterations	Final length (m)	Calculation time (s)
1	50/200	3/3	106/106	52.9/52.8
0.1	50/200	4/4	106.1/106.1	70.9/70.0
0.01	50/200	5/5	106.07/106.07	87.6/87.4

The impact of the number of borehole segments is analyzed using the same 12×10 geometry by varying the number of segments from 1 to 25 and using a 0.1% convergence criteria. This problem is solved with and without temporal superposition and results are shown in Figures 5-8a and 8b. As can be seen, the results obtained with and without temporal superposition follow the same pattern; the relative differences in length between 1 and 25 segments are 3.4 and 4% with and without temporal superposition. The calculation time in both cases increases exponentially with the number of borehole segments. However, the calculation times obtained without temporal superposition are significantly shorter than the ones obtained using temporal superposition. For example, for 1 segment, the calculation times are 8 and 3.1 s with and without temporal superposition, respectively. The corresponding number for 25 segments are 2081 and 213 s. These results are obtained on a computer equipped with an Intel core i5 processor (2.70 GHz) and 8 GB of RAM. Twelve borehole segments appear to be a good compromise between accuracy and calculation time in line with the findings of Cimmino and Bernier (2014).

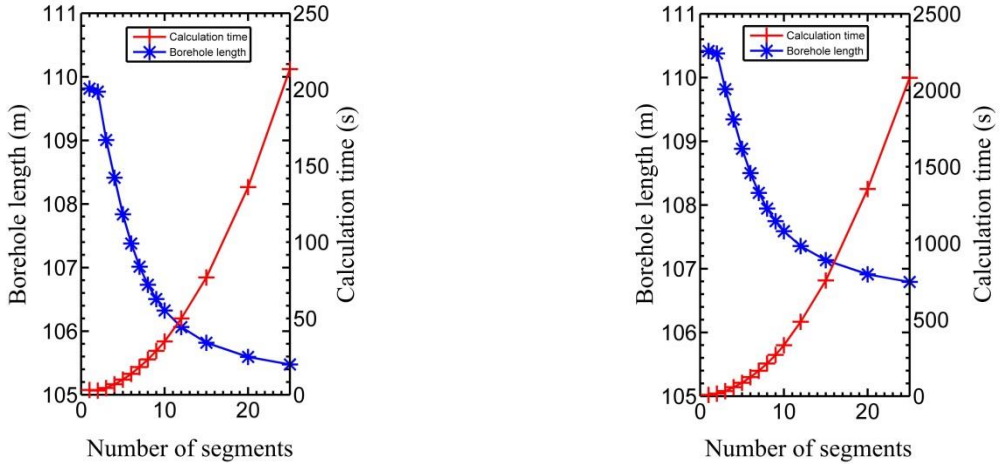

Figure 5-8: Borehole length and corresponding calculation time as a function of the number of segments obtained without (a) with (b) temporal superposition

It has also been observed that the optimum number of borehole segments is slightly dependent on the borehole length. For example, for the same geometry (12×10), if the loads are doubled, the resulting borehole length evaluated without temporal superposition is 197.8 m for one segment and 193.3 m for 25 segments, a 2.3% difference. If the loads are reduced in half, the resulting borehole length is 55.3 m for one segment and 52.3 m for 25 segments, a 5.7% difference. Thus it appears that fewer segments could be used for longer boreholes. This is due to the fact that

borehole end effects are proportionally less significant for longer boreholes. This fact can be used to reduce the calculation time of the proposed method. However, as the length of the boreholes is not known at the beginning of the iterations, the number of segments should be optimized during iterations. Hence, only one segment could be used in the first iteration and then the number of segments could be increased/decreased in the next iterations based on the evaluated borehole lengths.

5.5.4 The effect of symmetry on calculation time

As a final point regarding calculation time, it is interesting to examine a bore field composed of randomly placed boreholes with no symmetry, i.e. all segment-to-segment interactions are different. This was done using a bore field composed of 120 boreholes which are scattered arbitrarily in a 80×80 m^2 ground area with a minimum borehole separation of 6.5 m. The ground heat load and the input parameters are identical to those reported in Tables 5-2 and 5-3. This problem was solved with a convergence criteria of 0.1 % using 12 segments with and without temporal superposition with corresponding calculation times of 34070 and 5169 s which are, respectively, about 70 and 100 times longer than the ones for rectangular equally-spaced 12×10 bore field (486 and 50 s). Thus, symmetry plays a major role in the reduction of calculation time.

5.5.5 Short term effects

It is possible to account for short-term effects associated with borehole thermal capacity using the same sizing equations (Eq. 5.3 and 5.4) with so-called short-term g-functions. The method used here to evaluate short-term g-functions is based on the work of Xu and Spitler (2006) which finds its origin in the method proposed by Yavuzturk and Spitler (1999). Xu and Spitler (2006) approximated the U-tube geometry with a series of hollow cylinders representing the fluid, the fluid convective resistance, the pipe, the grout and the ground. The outer diameter of the equivalent pipe is simply taken as the square root of two multiplied by the outer diameter of the pipe. An equivalent grout thermal conductivity is used based on the determination of the grout thermal resistance obtained from the multipole method. Radial heat transfer from the fluid to the ground is then solved numerically to obtain g-functions using the definition given by Yavuzturk and Spitler (1999). Xu and Spitler (2006) have shown that results obtained with this technique

compare favorably well with the ones obtained with a two-dimensional model representing the real borehole geometry.

In this paper, the only modification to the Xu and Spitler (2006) approach is that heat transfer from the borehole wall to the ground is calculated using the infinite cylindrical source (ICS) solution. The required heat transfer rate at the borehole wall is obtained from the numerical solution and the borehole wall temperature boundary condition required by the numerical model is calculated from the ICS solution.

Figure 5-9 shows the short-time g-function curve obtained for the borehole described in Table 5-3. The g-function curve without short-term effects (for a 12×10 bore field) is also shown in this figure. The two curves merge into the same curve after a certain time ($ln(t/t_s) \approx -8$ in the case of figure 5-9. As shown on Figure 5-9, g-functions are lower when short-term effects are considered. Short-term g-functions are independent of borehole length and spacing as well as bore field configuration. Therefore, the evaluated g-functions (illustrated in Figure 5-9) can be used for any bore field configurations as long as the parameters are identical to the ones specified in Table 5-3.

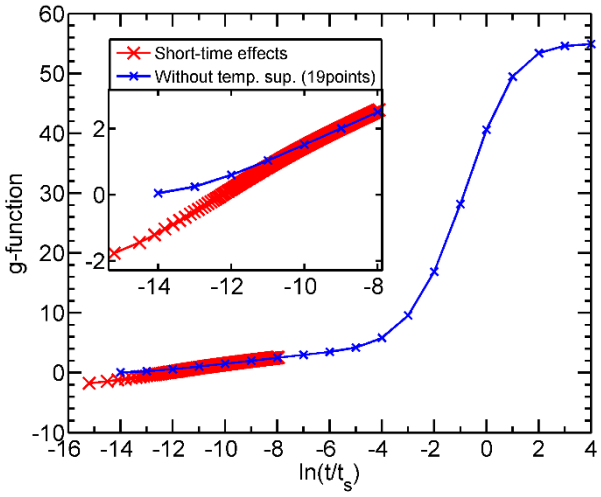

Figure 5-9: g-functions obtained with and without short-term effects for a 12×10 bore field

To show the impact of short time effects on the borehole lengths, results presented in Table 5-4 are recalculated using short-time g-functions for the $g_{(t_f - t_2)}$ term (see Equation 5.4). The monthly and yearly g-functions are calculated using the long-term g-functions based on 12 segment boreholes and without using temporal superposition. As shown in Table 5-8, the resulting

boreholes are shorter by about 2.8 to 3.9 % when short-term effects are considered. This is to be expected as borehole thermal capacity will dampen the change in the borehole wall temperature following a change in the amount of heat injected into a borehole. These differences are similar to the ones obtained by Lamarche (2016).

Table 5-8: Comparison of borehole lengths obtained with and without short time effects

Bore field geometry						
	19: (9,1,9)	25: (1×25)	28: (9,1,8,1,9)	36: (8,1,8,1,8,1,8,1)	120: (12×10)	127: axisymmetric
With short time effects (m)	74.0	73.8	74.6	75.9	102.9	109.5
Without short time effects (m)	77.0	76.8	77.6	78.9	106.1	112.6
Relative difference	-3.9 %	-3.9 %	-3.9%	-3.8%	-3.0 %	-2.8 %

The differences presented in Table 5-8 are problem dependent and cannot be generalized. In order to further examine these differences the values of the effective ground thermal resistances (Eq. 5.4) are presented in Table 5-9 for the 12×10 geometry for peak durations of one and six hours. As shown in this table there are significant differences in the values of $R_{gd,g}$ and $R_{gm,g}$. For example, for the 6 hour peak duration, $R_{gd,g}$ decreases from 0.092 to 0.068 m.K/W while $R_{gm,g}$ increases from 0.209 to 0.233 m.K/W. These differences are mainly due to the fact that short-term g-functions are slightly lower than the ones evaluated without short-term effects. The value of $R_{ga,g}$ changes slightly but in this case the variation is not due to short-term effects but to the fact that the borehole length has changed (due to short-term effects) which in turn changes the value of the long-term g-function. These changes in the three effective ground thermal resistances reduce the required borehole length by 3.0%. This difference is dependent on the relative strengths of $q_a, q_m,$ and q_h. Generally, when the value of q_h increases when compared to q_a and q_m, then the difference in the required borehole length with and without short-term effects will increase.

When the peak duration is only one hour, the required borehole length when the short-term effects are considered is 9.2% shorter than when short-term effects are not considered. As noted in Table 5-9, $R_{gh,g}$ is negative for a one hour peak duration, however the sum $R_b + R_{gh,g}$ is positive.

Table 5-9: The effects of short time effects and peak duration on the boreholes lengths of 12×10 bore field

Peak duration	6 hours		1 hour	
Short term effects	Without short term effects	With short term effects	Without short term effects	With short term effects
Length (m)	106.1	102.9	97.6	88.6
Relative difference	-3.0 %		-9.2 %	
$R_{gh,g}$ (m.K/W)	0.092	0.068	0.028	-0.039
$R_{gm,g}$ (m.K/W)	0.209	0.233	0.273	0.340
$R_{ga,g}$ (m.K/W)	1.789	1.777	1.754	1.711
$R_b + R_{gh,g}$ (m.K/W)	0.292	0.268	0.228	0.161

In addition to peak durations of 1 and 6 hours, the same sizing problem has been checked with peak durations ranging from one hour to 50 hours and the results are shown in Figure 5-10. It can be shown that length differences with and without short-term effects are negligible after 50 hours for this configuration and load pattern.

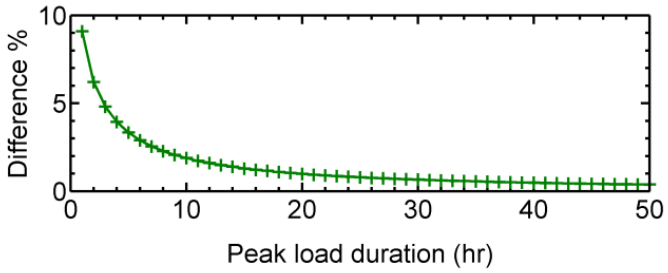

Figure 5-10: Relative length difference with and without short-term effects

5.6 Conclusions

This study proposes modifications to the ASHRAE sizing equation for vertical ground heat exchangers. The resultant method uses the same three pulse methodology as the classic ASHRAE sizing equation. The three effective ground thermal resistances corresponding to the three heat

pulses are evaluated with the use of three g-functions. Since g-functions evaluate the thermal interactions between the boreholes, there is no need to consider the "temperature penalty" present in the ASHRAE sizing equation. However, an iterative procedure is required as g-functions depend on the borehole length that is unknown a priori. One important aspect of the iterative procedure is that it is able to evaluate new g-functions dynamically as the solution progresses. Approximately 3 to 5 iterations are required to obtain a converged solution, thus the proposed methodology requires the evaluation of 9 to 15 single g-function values. These values are evaluated analytically using the finite line source by discretizing boreholes in axial segments and without applying any interpolation on the g-function curve or between pre-determined g-functions. In addition, contrary to previous works, temporal superposition is not used for evaluating the g-functions. Results show that the use of temporal superposition does not have a significant effect on the boreholes length, however, it affects the calculation time noticeably. For example, for a 12×10 bore field sized with 12 segments, the length evaluated with and without temporal superposition have a 1.2 % relative difference. However, calculation time is about 10 times longer with temporal superposition. It is also seen that longer boreholes need fewer boreholes segments. This is due the fact that the boreholes end effects are proportionally less significant for longer boreholes. It is also concluded that a convergence criteria of 0.1 % (0.1 m on a 100 m borehole) gives sufficiently accurate results with reasonable calculation time. The proposed methodology is compared against four other sizing methods including EED, the DST model of TRNSYS combined with GenOptl and the classic ASHRAE equation with appropriate temperature penalty calculations but without accounting for short-term effects. Six different borehole configurations ranging from a 19 borehole L-shape bore field to a 127 axisymmetric configuration are used in this comparison. The average relative difference between the results of the proposed method and the other sizing methods is 2.9 %. Finally, it is shown that short-term g-functions can be used to account for borehole thermal capacity. Short-term effects have an impact on the hourly and monthly effective ground thermal resistances. In one particular case studied here, the required length is 3.0 % shorter when short-term effects were considered for a 6 hour peak duration. When the peak duration is reduced to 1 hour, this difference reaches 9.2%.

5.7 Acknowledgements

This work was performed under a discovery grant provided by the Natural Sciences and Engineering Research Council of Canada (NSERC).

5.8 References

Ahmadfard, M. and Bernier, M. (2014) An alternative to ASHRAE's Design Length Equation for Sizing Borehole Heat Exchangers, ASHRAE Annual Conference, Seattle, USA, paper SE-14-C049, 8 pages.

Ahmadfard, M., Bernier, M., and Kummert, M., (2016) Evaluation of the design length of vertical geothermal boreholes using annual simulations combined with Genopt, Proceedings of eSim Building Performance Simulation Conference, May 3-6, McMaster University, Hamilton, Ontario, Canada, pp.46-57.

ASHRAE (1995) Chapter 32-Geothermal Energy. ASHRAE Handbook - Applications, Atlanta, GA: ASHRAE.

ASHRAE (2015) Chapter 34 – Geothermal Energy, ASHRAE Handbook - Applications, Atlanta, GA: ASHRAE.

Bandyopadhyay, G., Gosnold, W., Mann, M. (2008) Analytical and semi-analytical solutions for short-time transient response ground heat exchangers. Energy Build vol. 40, no.10, pp. 1816–1824.

Beier, R., Smith, M. 2003, Minimum duration of in-situ tests on vertical boreholes. ASHRAE Trans; vol. 109, no. 2, pp. 475–486.

Bernier, M. (2006). Closed-loop ground-coupled heat pump systems. ASHRAE Journal, vol. 48, no. 9, pp. 12–19.

Bernier, M. 2014. Sizing and simulating bore fields using thermal response factors. Proceedings of the 11th IEA Heat Pump conference, Montreal (Quebec), Canada, May 2014. Paper KN.3.1.1.

Bernier, M.A., Chahla, A., and Pinel, P. (2008) Long-term ground-temperature changes in geo-exchange systems, ASHRAE Transactions, vol. 114, no. 2, pp. 342-350.

Blomberg, T., Claesson, J., Eskilson, P., Hellström, G., Sanner, B., (2015) EED v3.2 - Earth Energy Designer, User Manual, BLOCON, Lund, Sweden.

Bose, J.E., Parker, J.D. McQuiston, F.C. (1985) Design/Data Manual for Closed-Loop Ground-Coupled Heat Pump Systems. Atlanta: ASHRAE.

Capozza, A., De Carli, M., and Zarrella, A., (2012) Design of borehole heat exchangers for ground-source heat pumps: A literature review, methodology comparison and analysis on the penalty temperature. Energy and Buildings, vol. 55, pp. 369-379.

Cimmino, M. and Bernier, M. (2013) Preprocessor for the generation of g-functions used in the simulation of geothermal systems, Proceedings of the 13th international IBPSA conference, Chambéry, France, pp.2675-2682. Cimmino, M. and Bernier, M. (2014) A semi-analytical method to generate g-functions for geothermal bore fields, International Journal of Heat and Mass Transfer, vol. 70, pp. 641-650.

Claesson, J., Javed, S. (2011) An analytical method to calculate borehole fluid temperatures for time-scales from minutes to decades. ASHRAE Transaction, vol. 117, pp. 279–88.

Cullin, J.R., Montagud, C., Ruiz-Calvo, F., and Spitler, J.D. (2014) Experimental validation of ground heat exchanger design methodologies using real, monitored data, ASHRAE Transactions, vol. 120, pp. 357-369.

Cullin, J.R., Spitler, J.D., Montagud, C., Ruiz-Calvo, F., Rees, S.J., Naicker, S.S., Konečný, P. and Southard, L.E., (2015) Validation of vertical ground heat exchanger design methodologies, Science and Technology for the Built Environment, vol. 21, no. 2, pp. 137–149.

Eskilson, P. (1987) Thermal Analysis of Heat Extraction Boreholes, Doctoral Thesis, Department of Mathematical Physics, University of Lund, Lund, Sweden.

Fossa, M. (2011) The temperature penalty approach to the design of borehole heat exchangers for heat pump applications. Energy and Buildings, vol. 43, no. 6, pp. 1473-1479.

Fossa, M. and Rolando, D. (2013) An improved method for vertical geothermal borefield design using the Temperature Penalty approach, European geothermal congress (EGC), pp. 1-8.

Fossa, M. and Rolando, D. (2015). Improving the Ashrae method for vertical geothermal bore field design. Energy and buildings, vol. 93, pp. 315-323.

Fossa, M. and Rolando, D. (2016). Improved Ashrae method for BHE field design at 10 tear horizon. Energy and buildings, vol. 116, pp. 114-121.

Gagné-Boisvert L. and Bernier, M. (2016) Accounting for borehole thermal capacity when designing vertical geothermal heat exchangers. ASHRAE summer conference, St-Louis, Missouri, June 2016. Paper ST-16-C027.

Hellström, G., and Sanner, B. (2000) Earth energy designer. User's Manual, version, 2.

Javed, S., Claesson, J. (2011) New analytical and numerical solutions for the short-term analysis of vertical ground heat exchangers. ASHRAE Transaction, vol. 117, no. 1, 3–12.

Kavanaugh, S.P. (1995) A design method for commercial ground-coupled heat pumps, ASHRAE Transactions, vol. 101, no.2, pp. 25-31.

Lamarche, L. (2015) Short-time analysis of vertical boreholes, new analytical solutions and choice of equivalent radius, International journal of heat and mass transfer, vol. 91, pp. 800-807.

Lamarche, L. (2016) Short-time modelling of geothermal systems. Proceedings of ECOS 2016, June 19-23, Portoroz, Slovenia. 9 pages.

Lamarche, L., Beauchamp, B. (2007) New solutions for the short-time analysis of geothermal vertical boreholes. Int. J. Heat Mass Transfer, vol. 50, pp. 1408–1419.

Li, M., Lai, A. (2012) New temperature response functions (G functions) for pile and borehole ground heat exchangers based on composite-medium line-source theory. Energy, vol. 38, pp. 255–63.

Li, M., Lai, A.C.K., (2015) Review of analytical models for heat transfer by vertical ground heat exchangers (GHEs): a perspective of time and space scales. Applied Energy, vol. 151, pp. 178-191.

Li, M., Zhuo, X. and Huang, G. (2017) Improvements on the American Society of Heating, Refrigeration, and Air-Conditioning Engineers Handbook equations for sizing borehole ground heat exchangers, Science and Technology for the Built Environment, published online on March 17th 2017.

Malayappan, V. and Spitler, J. D. (2013) Limitations of using uniform heat flux assumptions in sizing vertical borehole heat exchanger fields. Proceedings of Clima 2013, Prague, Czech Republic.

Monzó, P., Bernier, M., Acuna, J., and Mogensen, P. (2016) A monthly-based bore field sizing methodology with applications to optimum borehole spacing, ASHRAE Transactions, vol. 122, pp. 111-126.

Pasquier, P., and Marcotte, D., (2012) Short-term simulation of ground heat exchanger with an improved TRCM, Renewable Energy, vol. 46, pp. 92-99.

Philippe, M., Bernier, M., and Marchio, D. (2009) Validity ranges of three analytical solutions to heat transfer in the vicinity of single boreholes, Geothermics, vol. 38, no. 4, pp. 407–413.

Philippe, M., Bernier, M., and Marchio, D. (2010) Sizing calculation spreadsheet: vertical geothermal borefields. ASHRAE Journal, vol. 52, no. 7, pp. 20-28.

Ruiz-Calvo, F., De Rosa, M., Acunˇa, J., Corberan, JM., Montagud, C., (2015) Experimental validation of a short-term borehole-to-ground (B2G) dynamic model. Applied Energy, vol. 140, pp. 210–23.

Salim-Shirazi, A. and Bernier, M. (2013) Thermal capacity effects in borehole ground heat exchangers. Energy and Buildings, vol. 67, pp. 352-364.

Spitler, J. D. and Bernier, M. (2016) Advances in ground-source heat pump systems - Chapter 2: Vertical borehole ground heat exchanger design methods. Edited by S. Rees. Woodhead (Elsevier) Publishing, 29-61.

Spitler, J.D. (2000) GLHEPRO—A design tool for commercial building ground loop heat exchangers. Proceedings of the Fourth International Heat Pumps in Cold Climates Conference, Aylmer, Québec, August 17–18.

Xu, X. and Spitler, J.D. (2006). Modeling of vertical ground loop heat exchangers with variable convective resistance and thermal mass of the fluid. Proceedings of the 10th International Conference on Thermal Energy Storage – Ecostock 2006, Pomona, NJ.

Yang, Y., Li, M. (2014) Short-time performance of composite-medium line-source model for predicting responses of ground heat exchangers with single U shaped tube. Int. J Thermal Sciences, vol. 82, pp.130–7.

Yavuzturk, C. and Spitler, J.D. (1999). A short time step response factor model for vertical ground loop heat exchangers. ASHRAE Transactions, 105, 475-485.

Zarrella, A., Scarpa, M., De Carli, M. (2011) Short time step analysis of vertical ground coupled heat exchangers: the approach of CaRM. Renew Energy, vol. 36, no. 9, pp. 2357–67.

CHAPTER 6 ARTICLE 3: EVALUATION OF THE DESIGN LENGTH OF VERTICAL GEOTHERMAL BOREHOLES USING ANNUAL SIMULATIONS COMBINED WITH GENOPT

Ahmadfard, M., Bernier, M., & Kummert., M. (2016). Proceedings of the eSim 2016 Building Performance Simulation Conference, May 3-6, McMaster University, Hamilton, Ontario, Canada, 46-57.

ABSTRACT

Software tools to determine the design length of vertical geothermal boreholes typically use a limited set of averaged ground thermal loads and are decoupled from building simulations. In the present study, multi-annual building hourly loads are used to determine the required borehole lengths. This is accomplished within TRNSYS using GenOpt combined with the duct ground heat storage (DST) model for bore fields.

6.1 Introduction

The determination of the required total borehole length in a bore field is an important step in the design of vertical ground heat exchangers (GHE) used in ground-source heat pump (GSHP) systems. Undersized GHE may lead to system malfunction due to return fluid temperatures that may be outside the operating limits of the heat pumps. Oversized heat exchangers have high installation costs that may reduce the economic feasibility of GSHP systems.

Figure 6-1 illustrates schematically a typical GSHP system. It consists of eight boreholes and five heat pumps connected in parallel. Piping heat losses between the boreholes and the heat pumps are usually assumed to be negligible. Thus, the inlet temperature to the heat pumps, $T_{in,hp}$, is equal to the outlet temperature from the bore field T_{out}. Heat pumps can operate with $T_{in,hp}$ as low as ≈ -7 ℃ in heating and as high as ≈ 45 ℃ in cooling. However, most designers use a safety margin and try to limit $T_{in,hp}$ to a value of $T_L \approx 0$ ℃ in heating and $T_H \approx 35$ ℃ in cooling modes. Boreholes are typically connected in parallel and the inlet temperature to all boreholes, T_{in}, is equal to the outlet temperature from the internal heat pump fluid loop, $T_{out,hp}$.

The ground thermal conductivity, k_g, thermal diffusivity, α_g, and the undisturbed ground temperature, T_g, are usually evaluated (or estimated in the case of α_g) from a thermal response test (TRT) performed prior to the determination of the design length. The borehole thermal resistance (from the fluid to the borehole wall), R_b, can also be estimated from a TRT test or calculated from borehole heat transfer theory (Bennet et al., 1987).

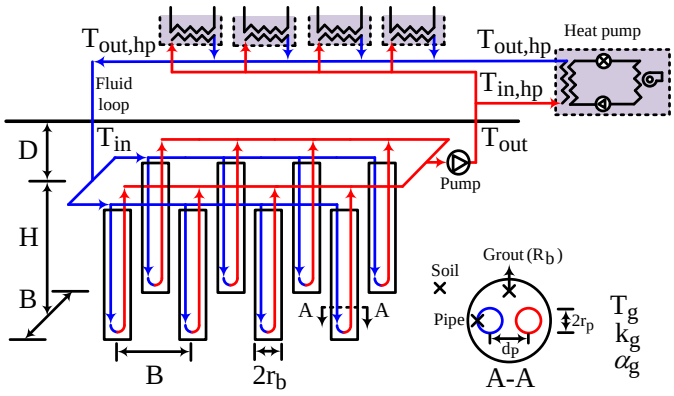

Figure 6-1: Schematic representation of a typical GSHP system

As shown in Figure 6-1, the bore field geometry is characterized by the number of boreholes, N_b, the borehole length, H, the borehole spacing, B, and the buried depth of the boreholes, D. Each borehole has a radius r_b (not to be confused with R_b, the borehole thermal resistance). As shown in section A-A, each borehole has two pipes with a radius r_p and a center-to-center distance equal to d_p. For typical boreholes, H varies from 50 to 150 m. For such long boreholes, the value of D has minimal effects on borehole heat transfer. In this work, it is assumed that D = 1 m and it is not considered to be a factor to determine the design length.

Designing a GHE consists in finding the "optimum" combination of H, N_b and B such that the inlet temperature to the heat pumps doesn't go below the minimum value of T_L or above the maximum value of T_H. In this work, the optimum combination is the one leading to the smallest overall length L (= $N_b \times H$).

In the first part of the paper, the basic design methodologies used in typical software tools are examined and categorized into five levels of increasing complexity. Then, the DST model and GenOpt are briefly reviewed. This is followed by the proposed methodology to obtain the optimum design length. The objective function involves the length and number of boreholes and T_L and T_H are considered as constraints. Contrary to most sizing methods, the heat pump

Coefficient of Performance (COP) is considered variable and so the ground loads are determined iteratively. Finally, the proposed methodology is applied and compared to other design software tools in three test cases.

6.2 Review of design methodologies

Spitler and Bernier (2016) categorized GHE sizing methodologies into five levels (0 to 4) of increasing complexity. The proposed methodology fits into the "level 4" category. These various levels will now be described with an emphasis on level 4.

6.2.1 Level 0 – Rules-of-Thumb

Rules-of-thumb relate the length of GHEs to the largest heating or cooling loads of the building or to the installed heat pump capacity. One popular rule-of-thumb in North America is to determine the length based on the simple formula: 150 feet of bore per ton of installed capacity (13 m of bore per kW of installed capacity). In the United Kingdom, look-up tables are used to obtain the maximum power that can be extracted per unit length for various ground conditions (Department of Energy and Climate Change, 2011). For example, for k_g = 2.5 W/m-K and $T_g = 12\,℃$, the recommended maximum power extraction is 50 W/m for 1200 hours of equivalent full load operating hours. The main problem with rules-of-thumb is that they only rely on peak loads and do not account for annual ground temperature increases (decreases) caused by load thermal imbalances.

6.2.2 Level 1 – Two ground load pulses

In level l methods, two lengths are calculated based on peak heating and cooling loads. Kavanaugh (1991) introduced a borehole thermal resistance in the analysis as well as an approximate factor to account for borehole-to-borehole thermal interference. Furthermore, the concept of temperature limits (T_L and T_H) is introduced. Despite these improvements, level 1 methods suffer from the same problem as level 0 methods as they do not properly account for the effects of ground load thermal imbalances.

6.2.3 Level 2 – Two set of three ground load pulses

The three pulse methodology (3 pulses in heating and 3 in cooling) is introduced by Kavanaugh (1995) along with the concept of temporal superposition which leads to the development of Eq.6.1. In order to keep the analysis simple, the borehole thermal resistance is assumed to be negligible and so it has been eliminated from the equation (it will be reintroduced later). In this equation, L is the overall borehole length ($= H \times N_B$), k is the ground thermal conductivity, T_f is the mean fluid temperature ($= [T_{in,hp}+T_{out,hp}]/2$) and T_g is the ground temperature. The temperature penalty, T_p, accounts for the borehole-to-borehole thermal interference (Bernier et al., 2008). Q_1, Q_2, and Q_3 are three consecutive ground load "pulses" with time durations t_1, t_2, t_3. The values of t_1', t_2' and t_3' are equal to t_1, $t_1 + t_2$, and $t_1 + t_2 + t_3$, respectively Finally, the function r_G is the thermal response of the ground which can be evaluated using several techniques. Figure 6-2 shows schematically three typical heat load pulses and their durations.

$$L = \frac{1}{k}\frac{Q_1 \mathrm{r}_G(t_3' - 0) + (Q_2 - Q_1)\mathrm{r}_G(t_3' - t_1') + (Q_3 - Q_2)\mathrm{r}_G(t_3' - t_2')}{T_f - (T_g + T_p)} \qquad (6.1)$$

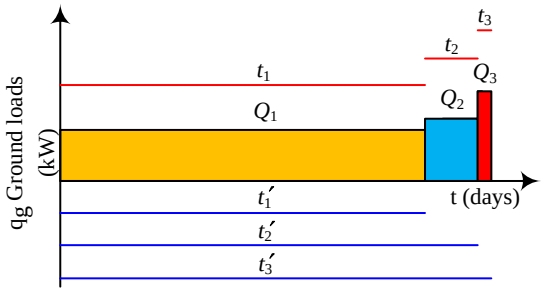

Figure 6-2: Three typical ground load pulses and their durations

In level 2 methods, the ground load pulses and their duration are typically assumed to be as follows: Q_1 is the annual amount of heat rejected (or collected) into the ground over a period t_1 (typically this period is 10 years). This is followed by a monthly ground load pulse Q_2 with a duration t_2 of one month. Finally, an "hourly" ground peak pulse Q_3 with a duration of $t_3 = 6$ hours is applied.

Building loads from energy simulation tools are generally not available in level 2 methods. Instead, peak building loads are calculated and the resulting peak ground loads, Q_3 are estimated. This estimation is based on a heat pump COP evaluated at peak conditions for $T_{in,hp} = T_H$ in

cooling and T_L in heating modes. Then, the average monthly ground load during the peak month, Q_2, is estimated assuming a run time fraction for the heat pump during that month. Finally, the average annual ground load, Q_1, is estimated. This can be done using the concept of equivalent full load heating and cooling hours as described by Spitler and Bernier (2016). It is to be noted that Q_1 and Q_2 are based on assumed constant COP values because the evolution of $T_{in,hp}$ is unknown in level 2 methods. These calculations are performed for both heating and cooling modes giving two sets of three ground load pulses. The end result of these calculations is illustrated in Figure 6-3a for a case where the building is mainly in cooling mode. In this example, Q_1, Q_2, and Q_3 have the following values: 19.2, 41.9, and 139.7 kW. These values are used in a test case to be examined shortly.

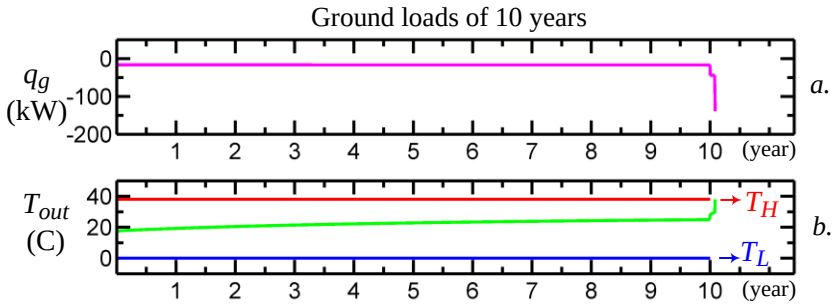

Figure 6-3: Typical ground loads related to level 2 sizing methods and the variation of T_{out} related to these loads

Eq. 6.1 forms the basis of the ASHRAE sizing method (ASHRAE, 2015) where r_G is based on the analytical solution to ground heat transfer referred to as the infinite cylindrical heat source or ICS (Bernier, 2000). Approximate values of T_p are tabulated for typical cases in the ASHRAE handbook (ASHRAE, 2015). Since the ICS and the tabulated values of T_p are independent of H, then L can be determined directly without iterations. The resulting value of L is the length required for the outlet temperature from the borehole, T_{out}, to remain below T_H (or above T_L for a heating case). This is illustrated in Figure 6-3b. This figure shows the evolution of T_{out} for the three ground load pulses of Figure 6-3a and shows that T_{out} reaches T_H at t_3'.

If more precise values of T_p are required in Eq. 6.1, then the approach suggested by Bernier et al. (2008) should be used. However, in this case T_p depends on H, and iterations are required to determine L. Typically, 3-4 iterations are necessary before convergence. This can be done for

rectangular bore fields automatically and rapidly with the Excel spreadsheet developed by Philippe et. al. (2010).

As suggested by Ahmadfard and Bernier (2014), the thermal response r_G in Eq. 6.1 can also be based on Eskilson's g-function (Eskilson, 1987). With this approach the temperature penalty, T_p, is no longer needed and Eq. 6.1 takes the following form where r_g is determined by the g-function of the bore field:

$$L = \frac{1}{2\pi k} \frac{Q_1 r_g(t'_3 - 0) + (Q_2 - Q_1) r_g(t'_3 - t'_1) + (Q_3 - Q_2) r_g(t'_3 - t'_2)}{T_f - T_g} \tag{6.2}$$

Since g-functions depend on H, an iterative process is required. This process can be computationally intensive if g-functions need to be evaluated during the process. Pre-calculated g-functions can be used to reduce computational time.

If average and peak ground heat loads are available for each month, Eqs. 6.1 or 6.2 can be modified to size the ground heat exchangers based on these pulses. In such cases, as suggested by Monzó et al. (2016), the monthly average and peak heat pulses can be rearranged into a format similar to Eqs. 6.1 and 6.2 as shown in Eqs. 6.3 and 6.4 where the overall length is evaluated for each month j:

$$L_j = \frac{1}{k} \frac{\begin{array}{c} Q_{1,j} r_G(t'_{3,j} - 0) + (Q_{2,j} - Q_{1,j}) r_G(t'_{3,j} - t'_{1,j}) + \\ (Q_{3,j} - Q_{2,j}) r_G(t'_{3,j} - t'_{2,j}) \end{array}}{T_f - (T_g + T_{p,j})} \tag{6.3}$$

$$L_j = \frac{1}{2\pi k} \frac{\begin{array}{c} Q_{1,j} r_g(t'_{3,j} - 0) + (Q_{2,j} - Q_{1,j}) r_g(t'_{3,j} - t'_{1,j}) + \\ (Q_{3,j} - Q_{2,j}) r_g(t'_{3,j} - t'_{2,j}) \end{array}}{T_f - T_g} \tag{6.4}$$

where $Q_{1,j}$ is the average of monthly heat loads, from the 1st month to the $j-1$ month, $Q_{2,j}$ is the monthly average heat load of month j, and the $Q_{3,j}$ is the cooling or heating peak of month j. $t'_{1,j} = t_{1,j}$, $t'_{2,j} = t_{1,j} + t_{2,j}$ and $t'_{3,j} = t_{1,j} + t_{2,j} + t_{3,j}$ where $t_{1,j} = \sum_{i=1}^{j-1} t_{m,i}$, $t_{2,j}$=$t_{m,j}$, $t_{3,j} = t_{h,j}$. $t_{m,i}$ is the duration of the month i and $t_{h,i}$ is the duration of the cooling or heating peak for month i.

Similar to previous cases, the effective borehole thermal resistance is neglected in these equations. Also, the duration of the peak heat loads, $t_{h,j}$, is usually considered to be 6 hours regardless of their actual duration. Since $T_{p,j}$ in Eq. 6.3 and the ground thermal response in Eq. 6.4 depend on H_j (=L_j/N_b) which is unknown, L_j is determined iteratively. The maximum value of L_j would be selected as the overall length of the ground heat exchangers.

Figure 6-4 illustrates schematically this concept with six monthly loads and six peak heat load pulses and their durations (bottom portion of the graph). They are summarized into three heat load pulses $Q_{1,j}$, $Q_{2,j}$ and $Q_{3,j}$ (top portion of the graph).

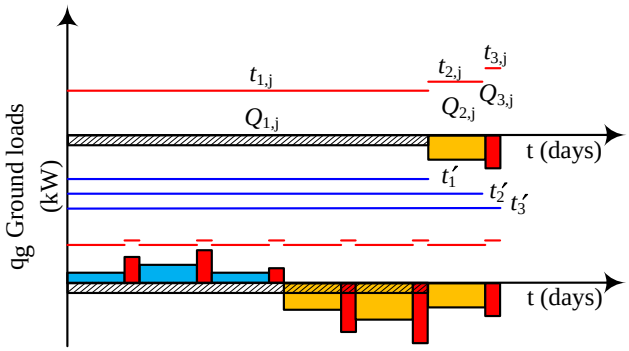

Figure 6-4: Evaluation of three ground heat load pulses and their durations for month j

6.2.4 Level 3 – Monthly average and peak heat pulses

Unlike level 2 methods which use three heat load pulses for the determination of borehole length, level 3 methods use a succession of monthly loads each followed by a peak load at the end of the month. This results in $24n$ terms where n is the number of years covered by the analysis. In level 2 methods, a fixed value of T_f is used to obtain L directly (or with some iterations if improved values of T_p are used). However, in level 3 methods, L is fixed and T_f is evaluated after each of the $24n$ ground heat pulses.

Eqs. 6.5 and 6.6 show the governing equations for level 3 methods. In this case, T_f is evaluated at the end of a 10 year analysis. Therefore, the numerator consists of a summation of 240 terms. Eq. 6.5 is used when the ground thermal response is given by the ICS while Eq. 6.6 is used when g-functions are used.

$$T_f = T_g + T_p + \frac{\begin{array}{c} Q_1 \mathrm{r}_G(t'_{240} - 0) + (Q_2 - Q_1)\mathrm{r}_G(t'_{240} - t'_1) + (Q_3 - Q_2)\mathrm{r}_G(t'_{240} - t'_2) + \\ \ldots + (Q_{239} - Q_{238})\mathrm{r}_G(t'_{240} - t'_{238}) + (Q_{240} - Q_{239})\mathrm{r}_G(t'_{240} - t'_{239}) \end{array}}{kL} \quad (6.5)$$

$$T_f = T_g + \frac{\begin{array}{c} Q_1 \mathrm{r}_g(t'_{240} - 0) + (Q_2 - Q_1)\mathrm{r}_g(t'_{240} - t'_1) + (Q_3 - Q_2)\mathrm{r}_g(t'_{240} - t'_2) + \\ \ldots + (Q_{239} - Q_{238})\mathrm{r}_g(t'_{240} - t'_{238}) + (Q_{240} - Q_{239})\mathrm{r}_g(t'_{240} - t'_{239}) \end{array}}{2\pi kL} \quad (6.6)$$

In Eqs. 6.5 and 6.6, $t'_n = \sum_{i=1}^{n} t_i$ and t_i is the duration of load Q_i.

Figure 6-5 presents schematically a sub-set of Eq. 6.5 and 6.6 with six monthly loads and six peak heat load pulses and their durations. The values of t'_n are also shown.

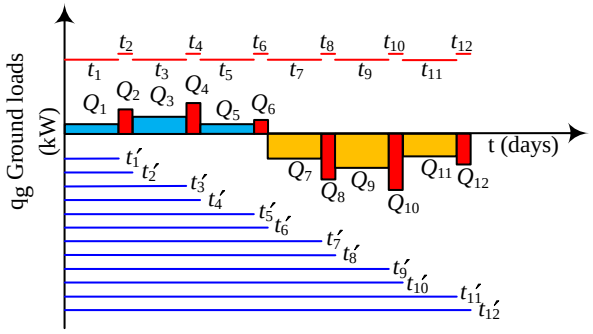

Figure 6-5: Six monthly average and peak ground heat load pulses and their durations

Eqs. 6.5 and 6.6 form the basis of some software design tools such as EED (Hellström and Sanner, 1997 and BLOCOM, 2015) and GLHEPRO (Spitler, 2000). Both of these tools use g-functions to calculate the ground thermal response factors. In such tools, ground loads can either be calculated separately or iteratively within Eqs. 6.5 or 6.6. In the former case, approximate values of the heat pump COP are used to calculate ground loads based on building loads. In most cases, two constant COP values (heating and cooling) are used. When ground loads are calculated iteratively within Eqs. 6.5 or 6.6, it is possible to use time-varying COPs as values of $T_{in,hp}$ are available during the calculation process.

Figure 6-6 shows an example of the various steps involved in a level 3 method. Figure 6-6a shows the building load variations used in the example for the 1st year of operation. It consists of 12 monthly average and 12 peak heat loads of a building with a cooling dominated load. These loads can be obtained by post-processing hourly loads obtained from a building simulation software tool or by simple approximations based on peak load calculations. Figure 6-6b shows

this load over the 10 year period of the analysis. Figure 6-6c and 6-6d present, respectively, the heating and cooling COP values used to convert the building loads into ground loads. In this particular case, constant values are used. Figure 6-6e shows the resulting series of ground loads to be used in Eqs 6.5 and 6.6.

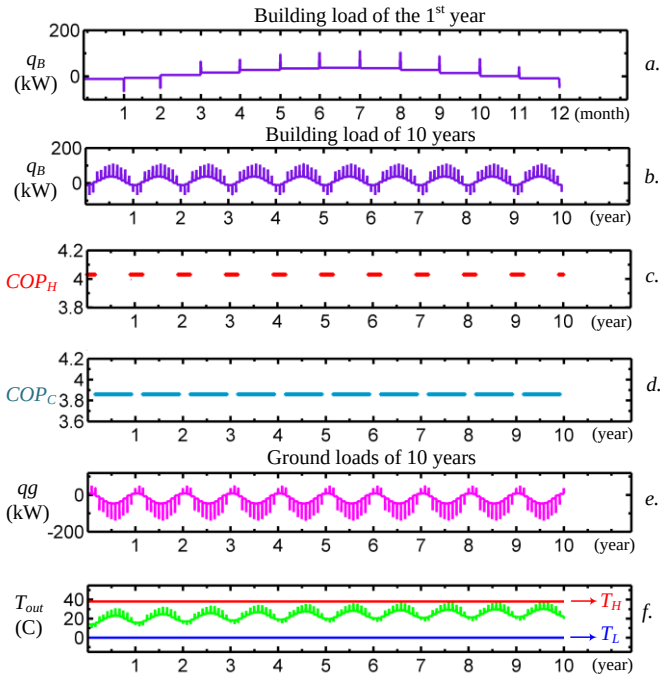

Figure 6-6: Various steps involved in the level 3 sizing methods

Eqs. 6.5 and 6.6 cannot be solved directly as T_p (in the case of Eq. 6.5) or g-functions (for Eq. 6.6) depend on L. Instead, a value of L is guessed and Eqs. 6.5 or 6.6 are solved to obtain T_{out} at the end of each individual time period (there are 240 evaluations of T_{out} in the case of a 10 year analysis). If T_{out} is outside the bounds fixed by T_H and T_L then a new value of L is chosen. This process is repeated until T_{out} reaches either T_H or T_L. For the case presented in Fig. 6-6, the evolution of T_{out} for the final iteration is presented in Fig. 6-6f where it is shown that T_H is reached in the summer of the 10th year.

If COPs are assumed to vary with $T_{in,hp}$ then there is second iterative process that goes through steps illustrated in Fig. 6-6b to 5-6f for each of the $24n$ ground heat pulses until COP values converge.

6.2.5 Level 4 – Hourly simulations

Level 4 methods push the level of granularity to hourly values. Thus, in essence, level 4 methods use equations similar to Eqs. 6.5 or 6.6, but with 87600 terms (in the case of a 10 year analysis). Level 4 methods should be more accurate but are also more computationally intensive. As in level 3 methods, an initial value of L is guessed and equations similar to Eqs. 6.5 or 6.6 are solved to obtain T_{out} at the end of each hour of the analysis period. If T_{out} is outside the bounds fixed by T_H and T_L then a new value of L is selected and a new iteration is initiated. This process is repeated until T_{out} reaches either T_H or T_L during the analysis period.

The solution process in a level 4 method is shown schematically in Figure 6-7 for the final iteration. Fig. 6-7a shows the hourly building loads for the first year. The same building load is repeated for 10 years in Fig. 6-7b. Fig. 6-7c and 6-7d show the calculated COP values used to obtain the ground loads which are shown in Fig. 6-7e. Finally, Fig. 6-7f shows the hourly variations of T_{out} (=$T_{in,hp}$) for the final iteration. This figure will also be used later in conjunction with test case 2.

Level 4 methods have been developed in recent years. For example, Nagano et al. (2006) have developed a sizing tool which applies the ICS to determine the hourly changes of temperature in the ground and in the heat carrier fluid. The model can also evaluate hourly variations of the ground load and COP. Henault et. al (2016) have suggested a method which predicts and optimizes the performance of hybrid GSHP systems on an hourly basis. This method uses spectral-based simulation tool (Pasquier et. al, 2013) that relies on g-functions and is applicable to variable heat pump COPs. The method gives the optimal number and location of vertical boreholes, the optimal number of heat pumps and their operating temperature limits as well as the optimal energy savings based on the financial performance of the system.

In a level 4 method, it is necessary to evaluate bore field heat transfer for each hour. One of the most widely used tools for such a task is the DST (Duct ground heat storage) model (Hellström, 1989), which has been implemented in the TRNSYS simulation environment. The DST model is not a GHE sizing program. However, it could be used repeatedly by changing borehole lengths “manually” until the temperature limits are reached. The objective of this paper is to show how to automate this process in combination with GenOpt.

Before addressing the proposed methodology, the DST model and GenOpt are briefly presented.

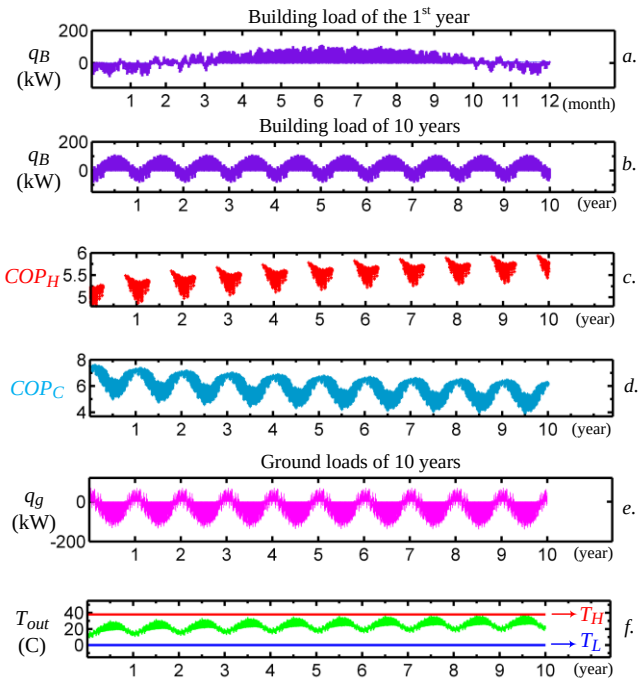

Figure 6-7: The solution procedure of a level 4 sizing method

6.3 DST model in trnsys

The vertical U-tube ground heat exchanger model in TRNSYS is type 557 and is based on Hellstrom's DST model (Hellström, 1989). It was originally developed to simulate seasonal thermal storage of densely packed boreholes in an axisymmetric cylindrical configuration with a given bore field volume, V_{BTES}. Chapuis and Bernier (2009) have provided a description of the calculations involved in the DST model. In summary, the DST model divides the ground formation into two parts: the local region around a single borehole and the global region located between the boundary of the storage volume and the far-field radius. The model uses a one dimensional numerical model to solve for the ground temperature in the local region and a two-dimensional finite difference model to simulate the ground temperature in the global region.

One of the very important limitations of the DST model has to do with borehole locations. The user selects H, N_b and one of the following two parameters: V_{BTES}, or B. The remaining fourth parameter is calculated internally by the DST model using Eq. 6.7.

$$V_{BTES} = \pi \times 0.525^2 \times B^2 \times H \times N_b \tag{6.7}$$

Figure 6-8 shows the borehole layout for a 37 borehole configuration and the origin of the value of 0.525 in Eq. 6.7. In this study, the borehole locations are evaluated based of this configuration.

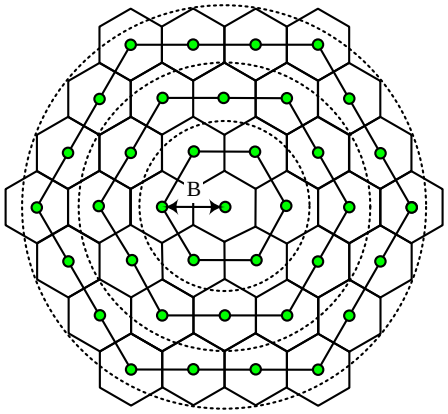

$$
\begin{aligned}
r_i &= B/2 \\
A_{hexagon} &= 2\sqrt{3}r_i^2 \\
&= \left(\sqrt{3}/2\right)\times B^2 \\
&= \pi r_1^2 \\
r_1 &= 0.525 \times B
\end{aligned}
$$

Figure 6-8: Geometry used by the DST model for a 37 borehole configuration

6.4 TRNOPT and GENOPT tools

GenOpt (Wetter, 2011) is a generic optimization program that was developed to address the class of optimization problems generally faced by Building Performance Simulation (BPS) users: a scalar cost function (e.g. the energy cost) must be minimized, the cost function (i.e. the BPS tool) is computationally intensive, and its derivatives are not known. The program offers a wealth of optimization algorithms capable of dealing with continuous and discrete variables, and uses multithreading when the algorithms allow it. Simple constraints (bounds) can be placed on optimization parameters, and more complex constraints can be implemented through penalty functions. The tool interfaces with BPS tools through text files, which makes it compatible with virtually all (batch-mode capable) BPS tools. GenOpt is also configured through text files. The "initialization file" defines the optimization problem at a high level (e.g. which simulation tool is used to evaluate the cost function, where to find the results, what to save, etc.). The "configuration file" provides specific information to interact with the BPS tool (e.g. the batch command to launch the program), and the "command file" provides detailed information on the optimization problem (variables, bounds, stopping criteria, and optimization algorithm). A "template" input file for the BPS tool must also be provided; where optimization parameters are replaced with special codes (e.g. "L" would replace the borehole length). GenOpt provides optimization results in a log file and also through a simple user interface that displays a graph of the current optimization parameters and cost function.

Configuring a GenOpt problem requires editing the 3 text files mentioned above, which can be intimidating and error-prone for non-expert users. To simplify this task, a dedicated GenOpt interface was created for TRNSYS. The interface, known as TRNOPT (TESS, 2014), automatically generates the text files required by GenOpt and also edits the TRNSYS input file (known as the deck file) to insert the special codes recognized by GenOpt to designate the optimization parameters. The interface also makes it easier to define the nature of the optimization variables (continuous or discrete, bounds and initial values, etc.) and the selected algorithm. Finally, TRNOPT comes with a dedicated "printer" component for TRNSYS that writes the value of the cost function in a text file easily interpreted by GenOpt.

The strength of GenOpt lies in its generic nature, which makes it compatible with virtually any program capable of reading and creating text files, and in the powerful optimization algorithms implemented in the program. However, selecting and configuring an algorithm for a specific problem requires some expertise and/or trial and error to avoid or minimize the impact of convergence issues, e.g. local minima or truncation of digits in the cost function. TRNOPT helps with the mechanics of setting up a GenOpt optimization problem with TRNSYS, but it does not reduce the difficulty of finding meaningful results when addressing a complex, multivariable optimization problem in the context of Building Performance Simulation.

6.5 Proposed methodology

A level 4 sizing method is proposed in this section. The objective is to find the required borehole length iteratively using the DST model combined with GenOpt in the TRNSYS environment.

Equation 6.8 shows the objective function that is applied in this work. This objective function can be used for minimizing only the height H for a given value of N_b or for minimizing the product of $H \times N_b$. It forces the optimization to find cases that satisfy the design temperature limits $T_L < T_{out} < T_H$. In Eq. 6.8, $T_{out,min}$ and $T_{out,max}$ are, respectively, the minimum and maximum outlet fluid temperatures from the bore field occurring during the selected period of the optimization.

$$\begin{aligned} \min Obj &= H \cdot N_b + C \times (P_1 + P_2) \\ P_1 &= \left[\left(T_L - T_{out,min}\right) LT\left(T_{out,min}, T_L\right)\right] \\ P_2 &= \left[\left(T_{out,max} - T_H\right) GT\left(T_{out,max}, T_H\right)\right] \end{aligned} \tag{6.8}$$

When T_{out} satisfies the temperature limits, this function reduces to $H \cdot N_b$. However, if the maximum fluid temperature, $T_{out,max}$, goes above T_H or the minimum fluid temperature, $T_{out,min}$, is below T_L then penalties equal to $C \times (T_{out,max} - T_H)$ or $C \times (T_L - T_{out,min})$ are applied to the objective function. C is a large coefficient assumed equal to 109 in the present work. The penalty is thus proportional to the temperature differences $(T_{out,max} - T_H)$ or $(T_L - T_{out,min})$. In this way, simulations that lead to $T_{out,max} \gg T_H$ (or $T_{out,min} \ll T_L$) will be heavily penalized.

In Eq. 6.8, the expressions $LT(T_{out,min}, T_L)$ and $GT(T_{out,max}, T_H)$ are "lower than" and "upper than" functions and are equal to 1 respectively when $T_{out,min} < T_L$ and $T_{out,max} > T_H$. For other values these functions are zero. It should be noted that only one of these two conditions may occur as the system can be either be sized in heating or cooling.

6.6 Implementation in TRNSYS

Figure 6-9 presents schematically the optimization procedure implemented in TRNSYS as well as some of the important scripts. This procedure can be used for optimizing one or all three design parameters (H, N_b and B). Numerical values used in the script refer to test cases presented in the next section. There are five blocks (0 to 4) of models and each will now be briefly described.

In blocks 0 to 2, the input parameters H, N_b and B are specified as well as the temperature design limits and the heat pump COPs. A parameter (COP_{cond}) is also defined to indicate whether a constant or a temperature-dependent COP is used. The storage volume, V_{BTES}, is also evaluated (see Eq. 6.7). Pre-calculated hourly building loads, q_b, are read by a standard data reader (Type 9a). A building model (Type 56) could also be used to determine the building loads. Next, the building loads are converted into ground loads, q_g, based on COP_{cond}. Note that if temperature-dependent COPs are used, they are evaluated each hour based on a performance map giving COPs as a function of T_{out} (see COP_{H-2} and COP_{C-2} in Figure 6-9a).

In block 3, ground heat transfer is evaluated using the DST model. The inlet and outlet fluid temperatures of the bore field are evaluated. If the COPs are temperature dependent, then TRNSYS will iterate at each time step until converged values of the fluid temperature, COPs, and ground loads are obtained.

The objective function is evaluated in block 4. At each time step, the outlet fluid temperature from the bore field is checked against the recorded values (Type 55) of $T_{out,min}$ and $T_{out,max}$ obtained up to that time step. If T_{out} is lower than $T_{out,min}$ or higher than $T_{out,max}$ then these parameters are updated with the value of T_{out} at the current time step. At each time step, the objective function is also calculated. The values of $T_{out,min}$ and $T_{out,max}$ are compared to T_L and T_H, respectively, and a penalty is applied according to Eq. 6.8. Then, the calculated objective function is compared with its recorded values. If it is higher than its recorded values it is updated.

At the end of the simulation period, the maximum recorded value of the objective function is sent to GenOpt, which analyzes the value of the objective function and updates the value of the design input parameters. Then, a new multi-year simulation is initiated. This process is repeated until the objective function converges to the user-specified tolerance or the iteration reaches its maximum number.

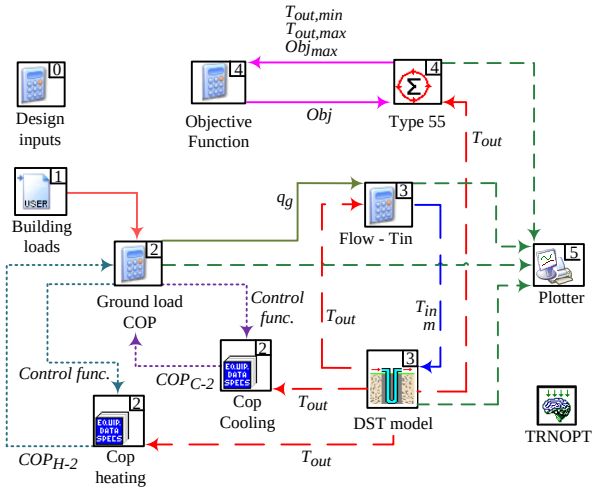

a.

Design inputs

H = 72
B = 7
N_b = 37
C = 4000 !J/kg.K
T_L = 0 !C
T_H= 38 !C
T_g = 15 !C
COP_{cond} = 1 !(1) is for constant COP and (-1) is for variable COP
COP_{C-1} = 3.86 !Constant COP for Cooling
COP_{H-1} = 4.03 !Constant COP for Heating
V_{BTES} = 3.14159. L. Nb. (0.525 . B)^2 (Eq. 7)

Ground load COP

$Func_{Heat}$= LT(q_b,0)
$Func_{Cool}$ = GT(q_b,0)
q_g= - [$Func_{Heat}$ (1-1/(max(COP_{H-F},1)))+ $Func_{Cool}$ (1+1/(max(COP_{C-F} ,1)))] . q_b
COP_{H-F}= EQL (COP_{cond} , -1). COP_{H-2}+EQL (COP_{cond},1). COP_{H-1}
COP_{C-F} = EQL (COP_{cond} , -1). COP_{C-2}+EQL (COP_{cond},1). COP_{C-1}

Flow - Tin

T_{in}= T_{out} - Del(T) !C
Del(T)= q_g /(m . C) !K
m = 5.549 !0.074 * 147.5 !kg/s

Objective Function

Obj = H . N_b +10^9 [(T_L - $T_{out,min}$) LT ($T_{out,min}$,T_L)]+ [($T_{out,max}$ - T_H) GT ($T_{out,max}$, T_H)] (Eq. 8)
Objective_function= Obj_{max}

b.

Figure 6-9: a. Schematic illustration of the TRNSYS project, b. Scripted equations used in some of the models.

6.7 Applications

Three sizing test cases are considered in this section to show the applicability of the proposed method and to compare results with other sizing methods. The reported calculation times are for a computer equipped with an Intel core i7 processor (2.80 GHz) and 4 GB of RAM.

6.7.1 Test case #1

The first test case is somewhat academic as it involves a perfectly balanced ground load. This case involves the optimization (i.e. minimization) of H for a 37 borehole configuration. The load profile is shown in Figure 6-10. This load is obtained using the methodology proposed by Bernier et al. (2004) with the following parameters: A=75000, B=2190, C=80, D=2, E=0.01, F=0 and G=0.95. On a yearly basis, the amount of heat injection in the summer is exactly equal to the amount of heat collected in the winter. This implies that the temperature penalty, T_p, due to borehole-to-borehole interference is zero. In addition, the ground temperature is chosen to be exactly at the midpoint between the values of T_L and T_H. So, in theory, the required borehole length should be the same for heating and cooling.

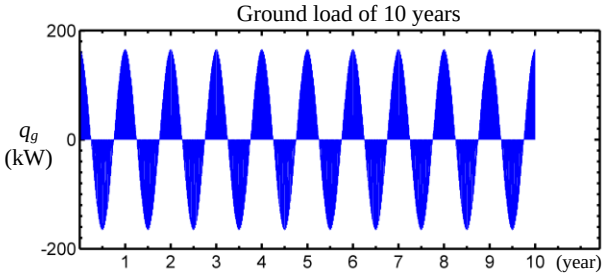

Figure 6-10: Ground load used for test case #1

Since ground loads are given directly, COPs do not need to be calculated. Therefore, block 2 (in Figure 6-9) is omitted.

Table 6-1 gives the value of the design parameters for test case #1. The coordinate search optimization method was selected based on a trial and error procedure which indicated that it required the smallest number of iterations. Table 6-2 shows the corresponding GenOpt parameters. The extent of the search domain is selected to be between 30 to 200 m with initial steps of 10 m.

Table 6-1: Design parameters used for test case #1

Parameter	Value	Parameter	Value
Borehole radius (r_b)	75 mm	Borehole buried depth (D)	1 m
Borehole spacing (B)	7 m	Borehole thermal resistance (R_b)	0.20 m.K/ W
Pipe nominal radius (r_p)	25 mm SDR-9	Center-to-center pipe distance (d_p)	8.3 cm (3.3 in.)
Number of pipes in each borehole	2	Pipe material	HDPE
Ground thermal conductivity (k_g)	1.9 W/m.K	Ground thermal diffusivity (α_g)	0.08 m2/da y
Undisturbed ground temperature (T_g)	17.5°C	Surface temperature (constant)	17.5° C
Minimum temperature limit (T_L)	0°C	Maximum temperature limit (T_H)	35°C
flow rate ($\dot{m}$)	5.55 kg/s	Fluid density (ρ)	1000 kg/m3
Fluid specific heat (C)	4 kJ/kg-k		

Table 6-2: Parameters used in optimization method for test case #1

Parameter	Value	Parameter	Value
Mesh size divider	2	Initial mesh size exponent	0
Mesh size exponent increment	1	Maximum number of step reductions	4

Table 6-3 presents the evolution of H calculated by GenOpt as well as the corresponding values of the objective function. The iterative process starts with an initial length of 40 m and converges to a final borehole length of 67.5 m and an overall bore field length of 2497.5 m. This is done in 13 iterations (i.e. 13 10-year simulations) and the calculation time is 3.5 minutes. For iterations 1, 2, 3, 7, 10, and 12, it can be seen that the guess values for H leads to high values of the objective function caused by values of T_{out} going beyond T_H or T_L.

Further optimization tests were performed with a smaller step size (2 m) and with two starting points (H=40 or H=200 m). As shown in Figure 6-11 the end result is the same whether H=40 or H=200 m are used as starting points. This graph shows a global minimum of 2471.6 at 66.8 m, a value close to the one obtained above for a coarser step size. However, this required 85 iterations.

Figure 6-12 shows the evolution of T_{out} for the final iteration for H = 67.5 m. As shown in this Figure, the profile for T_{out} of the 1st year (and also for the 10 year duration) is equally close to both T_L and T_H. This shows that both constraints are satisfied and, as expected with balanced ground loads and a ground temperature exactly equal to the mean of T_L and T_H, the borehole length required is exactly the same in heating and cooling. Thus, the proposed method is able to handle perfectly balanced loads.

Table 6-3: Borehole lengths determined by GenOpt and the corresponding objective function for test case #1

No.	H. (m)	Obj.	No.	H. (m)	Obj.
1	40	2.82E+10	8	72.5	2682.5
2	50	1.42E+10	9	67.5	2497.5
3	60	4.91E+09	10	66.3	5.29E+08
4	70	2590	11	68.8	2543.8
5	80	2960	12	66.9	1.37E+08
6	75	2775	13	68.1	2520.6
7	65	1.33E+09	final	67.5	2497.5

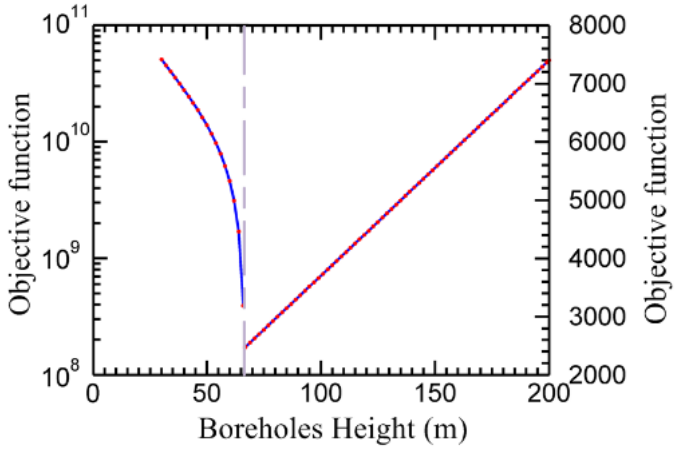

Figure 6-11: Plot of the objective function for test case #1

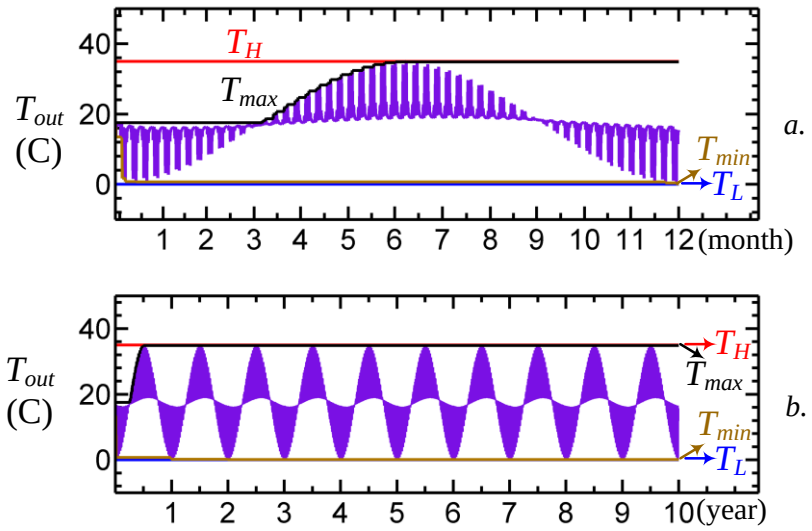

Figure 6-12: Evolution of the outlet fluid temperature for the first test case

6.7.2 Test case #2

For the second test case, the proposed methodology is used to determine the required borehole length of a GSHP system for a cooling dominated 1500 m2 building located in Atlanta (Bernier, 2006). Figure 6-7a shows the evolution of hourly building load for the 1st year. It is assumed that the operation starts on January 1st and that the same yearly load is repeated over a ten year period as shown in Figure 6-7b.

The design parameters are similar to the ones that are used for test case #1 and reported in Table 6-1. The only differences are the undisturbed ground and the ambient (surface) temperatures which are both set at 15 °C and T_H which is set equal to 38 °C.

This test case is solved using level 2 and 3 methods as well as the proposed level 4 methodology. For levels 2 and 3, the building load is converted into ground loads with two constant COPs of 3.86 and 4.03 for cooling and heating, respectively. The ground loads for the proposed methodology are evaluated iteratively using temperature dependent COPs which are evaluated based on the performance map given in Table 6-4.

Table 6-4: Performance map for the heat pump used in test case #2

$T_{in,hp}$ (°C)	Cop_H	$T_{in,hp}$ (°C)	Cop_H	$T_{in,hp}$ (°C)	Cop_C	$T_{in,hp}$ (°C)	Cop_C
-6.67	3.42	21.11	5.68	10	8.15	32.22	4.75
-1.11	3.91	26.67	6.04	15.56	7.36	37.78	3.96
4.44	4.4	29.44	6.2	21.11	6.51	43.33	3.31
10.00	4.85	32.22	6.35	26.67	5.63	48.89	2.75
15.56	5.29			29.44	5.16		

6.7.2.1 Level 2 results

The building load shown in Figure 6-7a has a cooling peak Q_p=111 kW during the month of July. With a COP of 3.86 in cooling this gives a peak ground load Q_3 of 139.7 kW. One common assumption is to assume that the average monthly ground load is equivalent to 30% of the peak load during that month. Thus, Q_2 = 0.3×Q_3 = 0.3×139.7 = 41.9 kW. To obtain Q_1, the annual average ground load, the concept of equivalent full load hours is used (Carlson and Thornton, 2002). For this type of building located in Atlanta, the equivalent full load hours of operation in heating and cooling are approximately, $EFLH_H$ = 500 h and $EFLH_C$ = 1500 h, respectively. This gives a value for Q_1 of 19.2 kW. The duration of Q_3 is considered to be 6 hours. This problem can be solved by using the spreadsheet developed by Philippe et al. (2010) with an appropriate

value of T_p for the axisymmetric geometry (Figure 6-8). The required length is calculated using Eq. 6.1:

$$L = \frac{1}{1.9}\frac{\begin{array}{c}19.2\mathrm{r}_G(88350-0)+(41.9-19.2)\mathrm{r}_G(88350-87600)\\+(139.7-41.9)\mathrm{r}_G(88350-88344)\ +\\139.7R_b)\end{array}}{38-(15+T_p)} \tag{6.9}$$

It should be noted that in this problem the borehole resistance is not zero, so a Q_3R_b term is added in Eq. 6.9 (with $R_b = 0.2$ m-K/W). The only unknown in this equation is T_p. It depends on the borehole length and it needs to be evaluated iteratively. Using the methodology suggested by Bernier et al. (2008), it can be shown that T_p is equal to +6.1 ℃ for a 10 year period. Solving Eq. 6.9, gives an overall length of 3185.8 m and a borehole length of 86.1 m. This calculation involves 6 iterations (to calculate T_p) with a convergence criteria on L set at 0.1%. This problem is solved in 35 seconds.

6.7.2.2 Level 3 results

The hourly building load profile given in Figure 6-7a is converted to 12 average monthly loads, Q_m, and 2×12 hourly cooling, $Q_{h,C}$, and heating, $Q_{h,H}$, peak heat loads. These loads are listed in Table 6-5. These building loads are further converted into ground loads assuming constant COPs for heating and cooling. This procedure is also illustrated in Figs 6-6.a to 6-6.e. Then, for each month, two lengths, one based on cooling peaks and another based on heating peaks, are evaluated using Eq. 6.3. Then, the maximum of the 240 lengths is selected as the final required length.

The results show that the required overall bore field length is 2848 m with individual borehole lengths equal to 77.0 m. The temperature penalty is also equal 6.9℃. The calculation time is approximately 2.5 minutes using the same convergence criteria and the same computer used in the level 2 results.

Table 6-5: Monthly average and peak building heating and cooling loads used in level 3 for test case #2

Period	Q_m (kW)	$Q_{h,C}$ (kW)	$Q_{h,H}$ (kW)
Jan.	-10.6	28.4	-86.4
Feb.	-5.0	42.5	-80.8
Mar.	6.4	66.0	-57.9
Apr.	16.8	74.3	-50.3
May.	27.8	95.9	0
Jun.	34.7	104.0	0
Jul.	37.3	111.0	0
Aug.	35.3	104.7	0
Sep.	27.5	88.8	0
Oct.	14.8	77.3	-7.6
Nov.	2.4	42.0	-56.3
Dec.	-7.8	27.2	-12.4

6.7.2.3 Level 4 results **(proposed methodology)**

Results are obtained using the same optimization method as in test case #1. COPs are evaluated each hour based on the calculated value of T_{out} for the corresponding hour. This implies some iterations within TRNSYS at each time step. Similar to test case #1, the length of each borehole is obtained in the search domain (from 30 to 200 m) with initial steps of 10 m. Results are presented in Table 6-6. The iteration process starts with a length of 40 m and converges to the borehole length of 75 m in 14 iterations with a calculation time of 5 minutes. The optimization process was also run with a smaller step size (2 m) with two starting points (H=40 or H=200 m). Figure 6-13 shows the shape of the objective function for various borehole lengths. This graph shows a global minimum for an objective function of 2765.8 at a corresponding borehole length of 74.8 m. This process required 82 iterations.

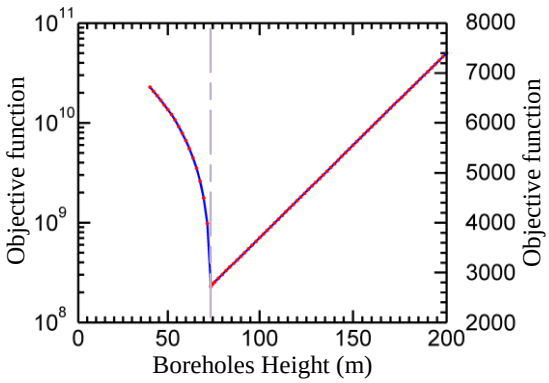

Figure 6-13: The objective function of the second test case

Table 6-6: Borehole lengths determined by the proposed methodology and the corresponding objective function for test case #2

No.	H. (m)	Obj.	No.	H. (m)	Obj.
1	40	2.28E+10	9	72.5	7.89E+08
2	50	1.36E+10	10	77.5	2867.5
3	60	6.64E+09	11	73.8	3.19E+08
4	70	1.76E+09	12	76.3	2821.3
5	80	2960	13	74.4	1.05E+08
6	90	3330	14	75.6	2798.1
7	85	3145	final	75	2775
8	75	2775			

Figure 6-14 illustrates the evolution of the maximum fluid temperature, $T_{out,max}$, for each of the 14 iterations. All of these cases satisfy the design limit of T_L ($T_{out,min} > T_L$) and so this constraint doesn't have any effect on the objective function. Lengths that do not satisfy the design limit of T_H (cases above $T_H = 38\,°C$) have received a penalty. A borehole length of 75 m is finally selected by the proposed methodology. Figure 6-7c and 6-7d show the variation of the

heating and cooling COPs and Figure 6-7f shows the evolution of T_{out} for a borehole length of 75 m.

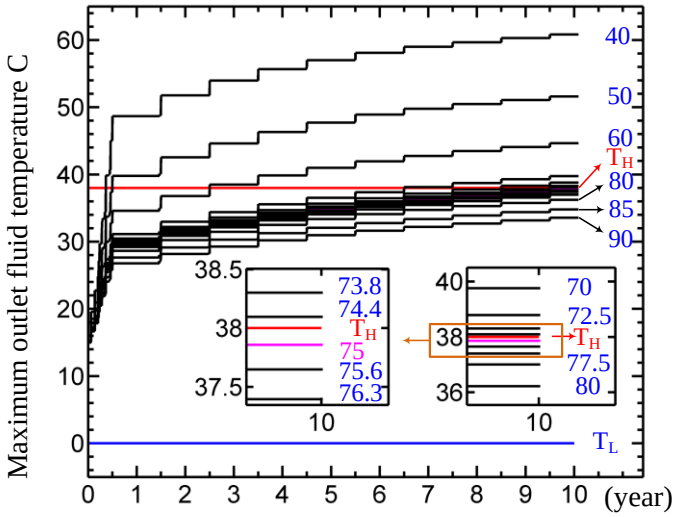

Figure 6-14: Variation of $T_{out,max}$ over 10 years for each iteration

Table 6-7 summarizes the results obtained with the three methods. As it can be seen, there are differences among the methods with the proposed method giving the shortest length.

Table 6-7: The results of the three sizing levels for test case 2

Sizing method	H (m)	L (m)
Level 2	86.1	3185.8
Level 3	77	2848
Proposed method (Level 4)	75	2775

6.7.3Test case #3

In the third test case, the number of boreholes is optimized for a fixed value of H. This case is important as the design variable, unlike the two previous test cases, is a discrete variable and therefore the coordinate search optimization method cannot be used.

For this case, the same design parameters as for the other two cases are used. The borehole length is considered fixed at 100 m and the number of boreholes is variable. The search domain for the optimum number of boreholes extends from 10 to 50 boreholes. Figure 6-15 shows the evolution of the objective function as a function of the number of boreholes. This graph is determined using 41 iterations and the global minimum of 2800 for 28 boreholes.

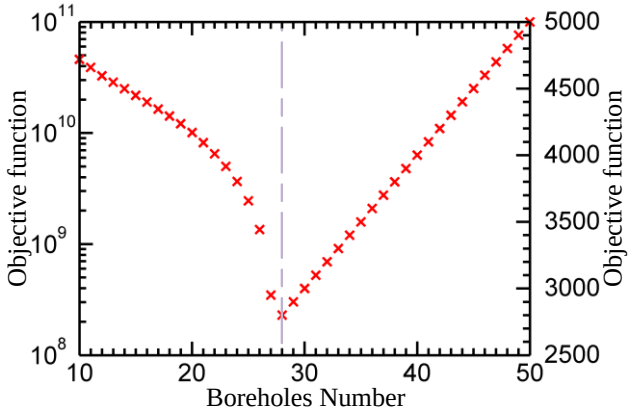

Figure 6-15: The objective function of the third test case

In this case the particle swarm optimization with inertia weight method is used. Table 6-8 illustrates the values of the parameters that are used in this optimization method. The parameter "number of particle" which is defined in Table 6-8 specifies the number of simulations that are run simultaneously. It is important for this number to be sufficiently large so as to search the whole domain for the design variable. Here, this number is defined as 5 and so 5 simulations with different guess values of borehole numbers are run simultaneously. Based on the results of these 5 simulations the optimization starts the next generation of simulations. As specified in Table 6-8 the "number of generations" is selected as 6. Therefore, the optimization should find the global minimum in 5×6 simulations. If these values are increased, the chance of finding the optimum is increased, but the number of simulations is also increased. If the optimization makes a guess that has already been analyzed it uses its history and does not simulate it again. When the optimization finds an "optimum" and if the "seed" number is greater than 1, then the algorithm starts a new set of optimization and uses this optimum as the initial guess value.

Table 6-8: Values of various parameters used in the optimization of test case #3

Parameter	Value	Parameter	Value
Neighborhood Topology	gbest	Social Acceleration	0.5
Neighborhood Size	1	Max Velocity Gain Continuous	2
Number Of Particle	5	Max Velocity Discrete	0.5
Number Of Generation	6	Initial Inertia Weight	0.5
Seed	1	Final Inertia Weight	0.5
Cognitive Acceleration	0.5		

For this case, the optimization has found the optimum of 28 boreholes with 17 iterations with a calculation time of 2 minutes. The initial guess for this problem was set at 40 boreholes.

6.8 Conclusions

In this work, the determination of the borehole length in ground-coupled heat pump systems with successive "manual" iterations using the duct ground heat storage (DST) model in TRNSYS is automated using GenOpt.

In the first part of the paper, the various design methods are reviewed starting with level 0 methods (rules-of-thumb based on peak loads) up to level 4 methods based on hourly simulations. The proposed methodology fits into the level 4 category.

Then, the paper explains how the objective function and related constraints are implemented in a TRNSYS/GenOPt configuration. The objective is to find the smallest overall length L ($= N_b \times H$) while satisfying two temperature constraints, the minimum and maximum allowable inlet temperature to the heat pumps. The method is adaptable, through a judicious choice of the optimization algorithm in GenOpt, to discrete or continuous design variables. The coordinate search method is used for determination of the borehole length (continuous variable) and the particle swarm optimization method is used for the determination of the number of boreholes (discrete variable).

Furthermore, the proposed method is able to handle cases where the heat pump COPs varies, as a function of the fluid inlet temperature, throughout the simulation.

To show the applicability of the method, three test cases are presented. In the first case, 37 boreholes are sized for perfectly balanced annual ground loads with a ground temperature chosen to be exactly at the midpoint between the minimum and maximum allowable temperature limits of the heat pumps. The proposed method was able to find, as it should in this symmetrical case, identical borehole lengths (67.5 m) in both heating and cooling. This was obtained after 13 iterations, i.e. 13 10-year simulations, in 3.5 minutes.

For the second and third test cases, the required overall length of a bore field for a cooling dominated 1500 m2 building located in Atlanta is determined for 10 years of operation. For the second test case, the number of boreholes is fixed (37) and the method is used to find the minimum borehole length. The optimization process found that the required length is 75 m. A total of 14 iterations are required with a calculation time of five minutes. This closely corresponds to the values of 86.1 m and 77.0 m obtained using two standard sizing, lower levels methods. In the third test case, the borehole length is fixed at 100 m and the number of boreholes is optimized. The proposed method evaluated the optimum boreholes number to be 28. This was done in 17 iterations and it required two minutes of calculation time.

The proposed methodology is relatively easy to use and applicable to cases where either continuous or discrete variables are optimized. However, more inter-model comparisons and perhaps validation cases with good experimental data are required to perform further checks of the proposed method.

6.9 Acknowledgements

The financial aid provided by the NSERC Smart Net-Zero Energy Buildings Research Network is gratefully acknowledged.

6.10References

Ahmadfard, M. and M. Bernier (2014), ‘An Alternative to ASHRAE's Design Length Equation for Sizing Borehole Heat Exchangers’, ASHRAE conf., Seattle, SE-14-C049.

ASHRAE (2015), Chapter 34 - Geothermal Energy. ASHRAE Handbook - Applications. Atlanta.

Bennet, J., J. Claesson, and G. Hellström. (1987), 'Multipole method to compute the conductive heat flows to and between pipes in a composite cylinder'. Technical report, University of Lund. Sweden.

Bernier, M. A., A. Chahla and P. Pinel. (2008), 'Long Term Ground Temperature Changes in Geo-Exchange Systems', ASHRAE Transactions 114(2):342-350.

Bernier, M. (2000), 'A review of the cylindrical heat source method for the design and analysis of vertical ground-coupled heat pump systems', 4th Int. Conf. on Heat Pumps in Cold Climates, Aylmer, Québec.

Bernier, M. (2006), 'Closed-loop ground-coupled heat pumps systems', ASHRAE Journal 48 (9):12–19.

Bernier, M., P. Pinel, R. Labib and R. Paillot. (2004), 'A Multiple Load Aggregation Algorithm for Annual Hourly Simulations of GCHP Systems'. HVAC&R Research 10(4):471-487.

BLOCON. (2015). EED v3.2. http://tinyurl.com/eed32.

Carlson, S. W. and J. W. Thornton. (2002), 'Development of equivalent full load heating and cooling hours for GCHPs'. ASHRAE Transactions 108(2):88-97.

Chapuis, S. and M. Bernier. (2009), 'Seasonal storage of solar energy in boreholes', Proceedings of the 11th International IBPSA conference, Glasgow, pp.599-606.

Department of Energy and Climate Change (2011), 'Microgeneration Installation Standard: MCS 022: Ground heat exchanger look-up tables - Supplementary material to MIS 3005', Issue 1.0., London, UK.

Eskilson, P. (1987), 'Thermal Analysis of Heat Extraction Boreholes'. PhD Doctoral Thesis, University of Lund.

Hellström, G. and B. Sanner B. (1997), EED - Earth Energy Designer. Version 1. User's manual.

Hellström, G. (1989), 'Duct ground heat storage model: Manual for computer code'. Lund, Sweden: University of Lund, Department of Mathematical Physics.

Hénault, B., P. Pasquier and M. Kummert (2016), 'Financial optimization and design of hybrid ground-coupled heat pump systems', Applied Thermal Engineering, 93:72-82.

Kavanaugh, S. (1995), ‘A Design Method for Commercial Ground-Coupled Heat Pumps’, ASHRAE Transactions 101(2):1088-1094.

Kavanaugh, S. P. (1991), ‘Ground and Water Source Heat Pumps - A Manual for the Design and Installation of Ground-Coupled, Ground Water and Lake Water Heating and Cooling Systems in Southern Climates’. University of Alabama.

Klein, S. A., et al. (2014), ‘TRNSYS 17 – A TRaNsient SYstem Simulation program, User manual. Version 17.2’. Madison, WI: University of Wisconsin-Madison.

Monzó, P., M. Bernier, J. Acuna and P. Mogensen. (2016), ‘A monthly-based bore field sizing methodology with applications to optimum borehole spacing’, ASHRAE Transactions, 122(1).

Nagano, K., T. Katsura and S. Takeda. (2006), ‘Development of a design and performance prediction for the ground source heat pump system’. Applied Thermal Eng., 26:1578-1592.

Pasquier, P., D.Marcotte, M. Bernier and M. Kummert. (2013), ‘Simulation of ground-coupled heat pump systems using a spectral approach’, Proceedings of the 13th International IBPSA conference, pp.2691-2698.

Philippe, M., M. Bernier and D. Marchio. (2010), ‘Sizing Calculation Spreadsheet: Vertical Geothermal Borefields’, ASHRAE Journal, 52(7):20-28.

Spitler J. D. and M. Bernier. (2016), Advances in ground-source heat pump systems - Chapter 2: Vertical borehole ground heat exchanger design methods. Edited by S. Rees. To be published.

Spitler, J. D. (2000), ‘GLHEPRO-A Design Tool for Commercial Building Ground Loop Heat Exchangers’. 4th Int. Conf. on Heat Pumps in Cold Climates, Aylmer, Québec.

Wetter, M. (2011), ‘GenOpt - Generic Optimization Program - User Manual, version 3.1.0’, Berkeley, CA, USA: Lawrence Berkeley National Laboratory.

TESS (2014), TRNOPT v17. Madison, WI, USA: Thermal Energy Systems Specialists.

CHAPTER 7 ARTICLE 4: A REVIEW OF VERTICAL GROUND HEAT EXCHANGER SIZING TOOLS INCLUDING AN INTER-MODEL COMPARISON

Ahmadfard, M., Bernier, M. (2018). Submitted to Renewable & Sustainable Energy Reviews on January 12th 2018.

Abstract

This study presents a methodology for comparing vertical ground heat exchanger sizing tools. In the first part of the paper, sizing tools are reviewed and categorized into five levels ($L0$ to $L4$) according to their level of complexity from tools based on rules-of-thumb ($L0$) to those using annual hourly simulations ($L4$). After review of available tests, four test cases are proposed to cover the full spectrum of conditions from single boreholes to large bore fields with various annual ground thermal imbalances. This is followed by an inter-model comparison of twelve sizing tools including some commercially-available software programs and various forms of the ASHRAE sizing equation. In one of the tests on a single borehole subjected to a one-hour peak load duration, it is shown that the minimum and maximum lengths obtained by the various tools are 39.1 m and 59.7 m (19.1% below and 23.5% above the mean). Tools that include short-term effects tend to calculate smaller lengths while longer lengths are predicted by tools that evaluate effective ground thermal resistances using the cylindrical heat source solution. In another test involving a large annual ground imbalance on a 5×5 borehole field, it is shown that results vary from 93.0 m to 128.9 m among the twelve tools which represents values that are respectively 21.7% below and 8.5% above the mean. A group of seven tools, including $L2$, $L3$, and $L4$ tools are in good agreement with a minimum of 121.0 m and a maximum of 128.9 m, thus a maximum difference of 6%. Two tools have determined lengths that are much lower than the rest of the tools (103.9 and 93.0 m). Clearly, these two tools cannot properly account for borehole thermal interaction caused by large annual imbalanced loads. Finally, a sensitivity analysis shows that tools react differently to a change in certain parameters.

Keywords: sizing tools, vertical ground heat exchangers, inter-model comparison, test cases.

7.1 Introduction

A ground source heat pump (GSHP) system equipped with vertical ground heat exchangers (GHE) is depicted in Figure 7-1. This system is composed of a series of boreholes and heat pumps which provide heating and cooling to a building. The bore field consists of a number of boreholes, N_b, with length H, spaced apart by a distance B and buried at a depth D. The overall length of the bore field, L, is thus equal to $N_b \times H$. Boreholes have a radius r_b and typically contain one or two U-tubes with a thermal conductivity, k_p. In the case of Figure 7-1, two pipes (one U-tube) with internal and external diameters, $r_{p,i}$ and $r_{p,o}$, are used. They are separated by a distance $2d_p$. The borehole is usually filled with grout with a thermal conductivity, k_{gr}, and a thermal capacity, MCp_{gr}. The ground is characterized by its thermal conductivity, k_g, thermal diffusivity, α_g, and undisturbed temperature, T_g.

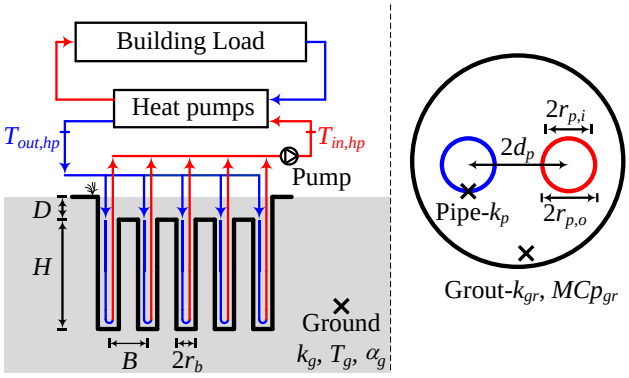

Figure 7-1: Schematic representation of a ground-source heat pump system (left) and a borehole cross-section with one U-tube (right)

Boreholes are typically connected in parallel. The fluid inlet temperatures and flow rates are usually assumed to be identical for all boreholes. Assuming negligible heat gains/losses in the piping between the boreholes and the heat pumps, the bore field outlet temperature is equal to the heat pump inlet temperature, $T_{in,hp}$, and the heat pump outlet temperature, $T_{out,hp}$, is equal to the bore field inlet temperature. The flow rate in each borehole is equal to $\dot{m}_f/N_b$, where $\dot{m}_f$ is the total bore field flow rate. For commercially available heat pumps, $T_{in,hp}$ can be as low as −7°C in heating and as high as 45°C in cooling. However, designers most often plan their system so that $T_{in,hp} \geq 0$°C in heating and $T_{in,hp} \leq 35$°C in cooling. These two limiting temperatures will be referred to T_L and T_H, respectively. Unlike HVAC equipment which are typically sized only for

peak load conditions, bore field sizing has to account for the thermal history of heat injection/collection into the ground and the period of the year when the system starts to operate (Monzó et al., 2016).

A number of input parameters, listed in Table 7-1, need to be determined prior to using sizing tools. Building or ground loads are generally determined using separate tools. Inaccurate loads will have an impact on the accuracy of L. For instance, Bernier (2002) has shown, for a particular case, that an uncertainty of ± 10% on the peak, monthly and annual ground loads (q_h, q_m, q_y in equation 7.4 – to be described later) translates into a cumulative uncertainty of ± 8.9% on L. The duration of peak loads has also an influence on L: typical values range from 4 to 6 hours. The next required input parameters are the target heat pump inlet temperature limits, T_H and T_L, that should not be exceeded during the expected lifetime of the system. The user has also to decide on the bore field geometry which is often dictated by the available land area. Cimmino and Bernier (2014) have shown that borehole placement within a given rectangular land area is not crucial in terms of total borehole length. An accurate value of the ground thermal conductivity is important to properly size a bore field while the ground thermal diffusivity is less important. Bernier (2002) has shown that a ± 10% uncertainty on k_g and α_g lead, respectively, to uncertainties of ± 7.1%, and ± 1.0% on the bore field length for a particular case. An accurate value for the ground temperature is also important and when it's value is close to T_H or T_L, longer boreholes are required. The borehole characteristics need to be carefully selected to optimize the borehole thermal resistance and the overall length. Some sizing tools account for borehole thermal capacity and in these cases, the thermal capacities of the pipes, the fluid and the grout are required. If building loads are used as inputs in sizing tools, heat pump coefficient of performances ($COPs$) in heating and cooling are required to calculate ground loads. The simpler methods will only require COP_H and COP_C at T_L and T_H while more elaborate tools will evaluate COP_H and COP_C as a function of $T_{in,hp}$. The selection of a flow rate has an influence on borehole heat transfer and on the ΔT across the borehole. A high flow rate reduces the borehole thermal resistance and the ΔT but increases pumping power. Low flow rates may lead to laminar flows in the borehole pipes which should be avoided at peak ground load conditions. For sizing purposes, the flow rate is typically around 0.05-1.0 L/s per kW of peak load. The required borehole length is not necessarily obtained at the end of the design period (typically 10 to 20 years). Indeed,

Monzó et al. (2016) have shown that the maximum length can occur during the first year of operation depending on the starting month of operation.

Table 7-1: Required input parameters for most sizing tools

Building or ground loads and peak load duration
Target temperature limits for heat pumps (T_L and T_H)
Bore field geometry (number of boreholes and location)
Ground thermal properties (k_g α_g and T_g)
Borehole characteristics (geometry, thermal properties)
Heat pump characteristics (COP_H and COP_C)
Flow rate
Design period
Starting month of operation

Sizing tools take different paths to obtain L with various levels of complexity and accuracy. Spitler and Bernier (2016) have identified five such levels ($L0$ to $L4$). Figure 7-2 presents typical calculation sequences associated with tools in the $L1$ to $L4$ categories. These levels are described in the next section including a presentation of some available sizing tools within each level. This is followed by a literature review on comparisons of bore field sizing tools. Then, a series of test cases are proposed. Finally, these test cases are used in an inter-model comparison of several existing tools.

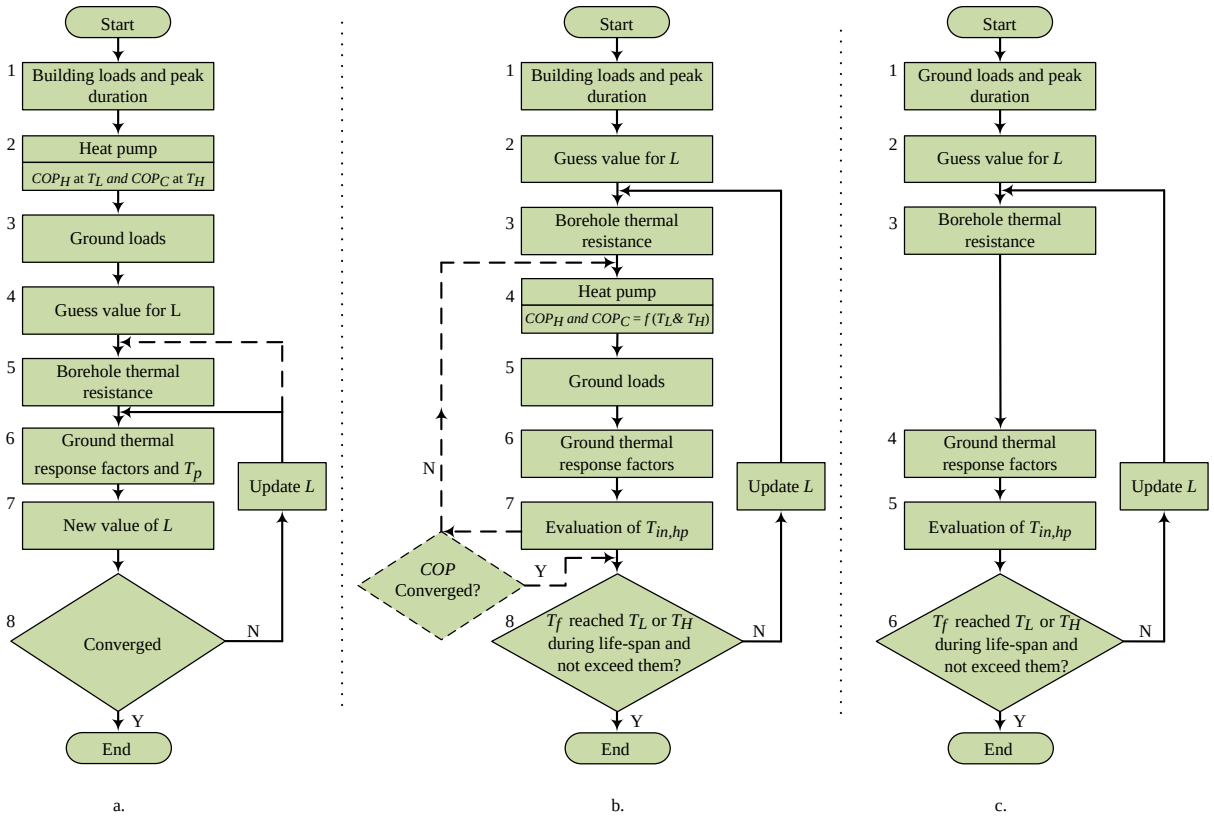

Figure 7-2: Typical steps required to size a bore field for a) $L1$ and $L2$ methods, b) $L3$ and $L4$ methods with building loads as input, and c) $L3$ and $L4$ methods with ground loads as inputs

7.2 Categories of sizing tools

7.2.1 L0 – Rules-of-thumb

Level $L0$ tools are simple rules-of-thumb. They typically relate the borehole length to the building peak heating or cooling loads or installed capacity, typically expressed as W/m or ft/ton. Spitler and Bernier (2016) mention that $L0$ tools are mostly used for small systems in heating only applications. They are bound to give erroneous results in large systems where borehole-to-borehole thermal interaction, caused by ground thermal imbalance and/or small borehole spacing, is large. Also, they do not consider the borehole thermal resistance. They should only be used as a reality check for more advanced sizing tools.

Excluding $L0$ tools, most sizing methods are derived from Equation 7.1:

$$L = \frac{\sum_{i=1}^{N} q_i R_i + q_h R_b}{T_m - (T_g + T_p)} \tag{7.1}$$

where q_i is a ground thermal pulse associated with a certain time period, R_i is the corresponding ground thermal response which takes the form of an effective ground thermal resistance, q_h is the peak ground thermal pulse, R_b is the borehole thermal resistance, T_m is the mean borehole fluid temperature (=$(T_{inHP} + T_{outHP})/2$)), and T_p is a temperature penalty to account for borehole-to-borehole thermal interaction. In some methods, this thermal interaction is included in R_i values and for such methods, T_p = 0. Equation 7.1 can be used for heating or cooling applications with appropriate signs for ground loads (negative when heat is extracted from the ground).

7.2.2 L1 – Two pulses –peak heating and cooling loads

$L1$ methods use two heat pulses which are either the maximum heating and cooling heat pump capacities or the building peak heating and cooling loads. They are somewhat outdated but it is interesting to present them from an historical perspective. $L1$ methods have been described by ose et al. (1985), OSU (1988), and Kavanaugh (1991). With reference to Figure 7-2a, a $L1$ tool would typically go through the six step process starting with the peak building loads or in some cases with the installed heat pump capacity. In step 2, values of COP_H and COP_C are determined based on values of T_L and T_H and used in the determination of the ground loads in step 3. Heat pump compressor power is either added or subtracted from the building to obtain ground loads. Thus, the heat pump COP, which is the ratio of the capacity (heating or cooling) over compressor power, has an impact on bore field sizing. For example, the overall length of a bore field will decrease with an increase of heat pump COP when a bore field is sized in cooling. Conversely, when a bore field is sized for heating conditions, an increase in the COP value will lead to an increase in the bore field length. Rudimentary values, by today's standards, of the borehole thermal resistance and ground thermal response factors are typically evaluated in steps 4 and 6. Finally, L is obtained directly in step 7 and iterations on L are generaly not required. $L1$ tools are perhaps best explained by examining the so-called IGSHPA method which is thoroughly described by Bose et al. (1985). This method follows the sequence presented in Figure 7-2a except that building loads are replaced by heat pump capacities in step 1. In this method, the lengths in heating (L_H) and cooling (L_C) are determined using Equation 7.2 with the longest of two giving the required borehole length, L. As shown in Equation 7.2, the heat pump capacities in heating and cooling, Cap_H and Cap_C, are multiplied by a factor involving $COPs$ in heating and cooling (COP_H and COP_C) to obtain peak ground loads in heating and cooling, respectively.

These loads are then multiplied by the sum of the pipe (borehole) resistance, R_p, and of the ground thermal response (ground thermal resistance), R_s. This last value is multiplied by the runtime fraction, ($Run_{f,H}$ or $Run_{f,C}$). The denominator of Equation 7.2.c is the difference between T_g and T_L in heating or between T_H and T_g in cooling.

$$L_H = \frac{Cap_H \frac{(COP_H - 1)}{COP_H}\left(R_p + R_s Run_{f,H}\right)}{\left(T_g - T_L\right)} \tag{7.2.a}$$

$$L_C = \frac{Cap_C \frac{(COP_C + 1)}{COP_C}\left(R_p + R_s Run_{f,C}\right)}{COP_C\left(T_H - T_g\right)} \tag{6.2.b}$$

$$L = max(L_H, L_C) \tag{6.2.c}$$

The ground thermal resistance, R_s, is determined using the infinite line source solution. Its value depends on the time period over which the ground load is applied. Also, spatial superposition can be used to account for borehole thermal interaction as discussed by Bose et al. (1985). The pipe resistance, R_p, is the ancestor of the modern borehole thermal resistance. For a U-tube geometry, it is approximated using the concept of an equivalent diameter.

Equation 7.2 is applied for winter and summer design periods. Cap_H and COP_H are evaluated at T_L while Cap_C and COP_C are evaluated at T_H. Accurate values of L are largely dependent on the selection of the design period duration, which influences R_s, and on the estimation of the run time fraction for the heat pumps during that period, ($Run_{f,H}$ or $Run_{f,C}$). Typically, the extent of the design period is of the order of one to three months.

The ground thermal resistances evaluated by this approach are not precise for long-term estimations since the one-dimensional (radial) infinite line source solution does not account for increased heat transfer at the borehole extremities which can be important after several months of operation. These simplifications, as explained by Cane and Forgas (1991) and Caneta (1992) lead to borehole oversizing.

7.2.3 L2 – Three pulse methods

L2 methods use temporal superposition of three successive load pulses to size bore fields. These pulses are: i) peak ground load; ii) average monthly ground load during the month in which the peak load occurs; and iii) the yearly average ground load. With reference to Equation 7.1, the summation term would then involve three terms. Each of these pulses is applied over a certain time period which typically corresponds to: 4 to 6 hours for the peak load; 30 days for the monthly load; and 10 years for the yearly ground load. Thus, the lengths L determined with L2 methods are the lengths required to reach the temperature limits (T_L or T_H) when the bore field is subjected to 10 years of the yearly average ground load followed by 30 days of the average monthly ground load and finally 4 o 6 hours of the peak ground load.

With reference to Figure 7-2a, $L2$ methods start either at step 1 or 3. Step 1 involves the determination of three building loads associated with the three thermal pulses, i.e. the peak building loads in heating and cooling and their duration, the monthly averaged building loads in heating and cooling during the peak month and the total annual heating/cooling loads. Then, peak ground loads are obtained in step 3 using the COP_H and COP_C values determined in step 2. Monthly ground loads are evaluated as a fraction (often called the Part-Load Factor – PLF) of the peak loads and the annual average ground load can be calculated using the concept of equivalent full load hours using the peak loads and COP_H and COP_C determined in step 2. Then, three ground thermal response factors (or ground thermal resistances) and T_p are evaluated in step 6. As shown below in the description of some $L2$ tools, these values are determined using either the infinite cylindrical heat source analytical solution or g-functions. If the ground thermal resistances (and T_p) depend on the borehole length then an iterative process is required and ground thermal response factors are re-evaluated until convergence as indicated in Figure 7-2a. In some methods, the borehole thermal resistance depends also on L, in which case the calculations are reinitiated in step 4 as indicated by the dotted line in Figure 7-2a. Three L2 methods (and their variations) will now be reviewed.

7.2.3.1 ASHRAE sizing equation

Equation 7.3 will be referred here as the ASHRAE sizing equation. This equation first appeared in the 1995 ASHRAE Handbook-Applications and in a paper by Kavanaugh (1995) and is still used in the latest version (2015) of the ASHRAE Handbook-Applications. Earlier versions of

these equations were presented by Kavanaugh (1988, 1991). Equation 7.3 can either be used for heating or cooling applications: $T_{in,hp}$ is replaced by T_L or T_H, the design temperature limits in heating and cooling, respectively, and $T_{out,hp}$ is determined from an energy balance on the bore field.

$$L = \frac{q_y R_y + (q_h - W)(R_b + PLF_m R_m + R_h F_{sc})}{T_g - \frac{\left(T_{in,hp} + T_{out,hp}\right)}{2} - T_p} \tag{7.3}$$

In Equation 7.3, the annual, monthly and peak load pulses are given by: i) q_y, the net annual average heat transfer to the ground, ii) $(q_h - W)PLF_m$, the monthly average heat transfer to the ground, and iii) $(q_h - W)$, the peak heat transfer rate to the ground. Note that q_y is a ground load and that q_h is a building load which is converted into a ground load by subtracting the compressor power at peak load, W. PLF_m is the part load factor during the design month and finally F_{sc} is the short circuit heat loss factor in the borehole. This last value, which is typically very close to 1, is tabulated in the ASHRAE handbook (2015). R_y, R_m and R_h are the yearly, monthly and hourly effective ground thermal resistances which are evaluated using the infinite cylindrical source (ICS) analytical solution. With the use of the ICS, the ASHRAE equation is relatively simple to calculate as the ground thermal resistances do not depend on the heat exchanger length and so the result can be determined directly without iterations. However, the use of the ICS implies that borehole-to-borehole thermal interaction is not accounted for. The equation thus needs a correction factor, referred to as a temperature penalty, T_p.

Values of T_p are tabulated in the ASHRAE Handbook (2015) for a limited number of bore field configurations and annual ground thermal imbalances (q_y). These values are based on a calculation procedure developed by Kavanaugh and Rafferty (1997) which was recently slightly modified (Kavanaugh and Rafferty, 2015) to account for heat transfer from the bottom of the bore field. This last method of calculating T_p will be used later in the inter-model comparison. With this method, T_p can be regarded as the increase/decrease of the temperature in the ground volume occupied by the boreholes caused by the annual ground thermal imbalance. This method of calculating T_p has been criticized by a number of authors (e.g. Bernier et al. 2008, Fossa 2011) and has been shown to underestimate T_p.

As for the determination of the borehole thermal resistance, R_b, the ASHRAE handbook proposes a table of R_b values for two (one U-tube) and four pipes (two U-tubes) for three different grout conductivities, three different fluid flow regimes (laminar, transition, and fully turbulent), three different U-tubes sizes, and three different bore diameters. Various pipe locations within the borehole are also considered. Reported values are calculated using a publicly-available spreadsheet program (Kavanaugh, 2010). The ASHRAE equation has been implemented in a tool called GCHPcalc (Kavanaugh, 1995).

7.2.3.2 Modified and modified+ ASHRAE sizing equation

Bernier (2006) suggested to rewrite the ASHRAE sizing equation as follows:

$$L = \frac{q_y R_y + q_m R_m + q_h R_h + q_h R_b}{T_m - \left(T_g + T_p\right)} \tag{7.4}$$

This will be referred as the modified ASHRAE sizing equations. In Equation 7.4, $T_m = (T_{in,hp} + T_{out,hp})/2$, q_m is the monthly average heat transfer to the ground, and q_h is the peak ground load, in contrast with q_h in Equation 7.3 which is the peak building load. There are three other differences between Equations 7.3 and 7.4: the F_{sc} term has been dropped, the borehole thermal resistance is calculated based on the zeroth order expression of the multipole method (Javed and Spitler, 2017), and T_p is obtained using a correlation based on g-functions (Bernier et al. 2008) which accounts for the three dimensional nature of heat transfer in a bore field. This value of T_p corrects the borehole temperature obtain with the ICS to account for borehole-to-borehole thermal interactions. Since g-functions depend on borehole length, an iterative procedure is required as discussed earlier in conjunction with Figure 7-2a.

Philippe et al. (2010) developed a user-friendly spreadsheet for sizing bore fields based on Equation 7.4 for three fixed pulses of 10 years, 30 days, and 6 hours. The spreadsheet can perform up to five iterations which is usually sufficient to obtain a converged solution for L. However, there are some limitations associated with this tool. First, the correlated equation for T_p is limited to rectangular bore fields of less than 144 equally-spaced boreholes. Secondly, it is not possible to change the duration of the three heat pulses. Monzó et al. (2016) overcame this limitation by implementing a marching solution where Equation 7.4 is applied month after month with the value of q_y replaced by the ground load averages of the proceeding months. Finally, the

value of R_b does not account for the possible thermal short-circuit between the upward and downward legs in the borehole. An improved version of the original spreadsheet of Philipe et al. (2010), refered to as the modified+ ASHRAE sizing equation, has been developed. First, the duration of the three pulses are user-defined. Secondly, values of T_p are not restricted to rectangular geometries and equally-spaced boreholes. They can be evaluated using either the method of Bernier et al. (2008) of Fossa's approach (2011) which are summrarized in Equations 7.5 and 7.6.

$$T_p = \frac{q_y}{2\pi k_g L}[g_N(t) - g_1(t)] \tag{7.5}$$

$$T_p = \frac{q_y}{k_g L}\left[\frac{g_N(t)}{2\pi} - G(t)\right] \tag{7.6}$$

where g_N and g_1 are the g-functions for the entire field (composed of N boreholes) and for a single borehole, respectively; G is the ICS solution for one borehole. The time t at which T_p is evaluated is not restricted to 10 years.

The third improvement included in the modified+ ASHRAE sizing equation is related to the borehole thermal resistance, R_b, which is calculated using the first-order expression of the multipole equation (equation 13 in Javed and Spitler, 2017). Furthermore, these R_b values are corrected to account for possible thermal short-circuiting in the borehole. The corrected values are usually referred to as an effective borehole thermal resistance, R_b^* which can either be based on a constant heat flux or constant temperature boundary condition at the borehole wall (equations 4.67 and 4.68 in Javed and Spitler, 2016). Typically, the average of the two R_b^* values is used and this will be the case in the tools used in the inter-model comparison reported below.

7.2.3.3 ASHRAE's Alternative method

Ahmadfard and Bernier (2014, 2018) suggested a further improvement to the modified ASHRAE sizing equation to eliminate the need to evaluate the temperature penalty. The resulting alternative equation is:

$$L = \frac{q_y R_{gy} + q_m R_{gm} + q_h R_{gh} + q_h R_b}{T_m - T_g} \tag{7.7}$$

This $L2$ method uses g-functions to calculate the three effective ground thermal resistances corresponding to the three ground loads. As g-functions account for borehole thermal interactions, the temperature penalty is no longer needed. However, an iterative calculation procedure is required as g-functions depend on the borehole length. The method can be applied to any bore field configuration as it calculates g-functions dynamically as the solution evolves. Since only three g-function values corresponding to the three heat load periods are required the whole g-functions curve does not need to be evaluated (Ahmadfard and Bernier 2014, 2018). Recently, Ahmadfard and Bernier (2018) introduced the concept of short-term g-function into this equation to account for borehole thermal capacity (fluid, pipe and grout).

With this technique, R_{gh} and R_{gm} are based on short-term g-functions. These values are obtained in a way similar to the one used by GLHEPro with the use of an equivalent diameter.

7.2.3.4 GHX Design Toolbox (in L2 mode)

In his book, Chiasson (2016) provides access to a spreadsheet-based design tool which can size vertical GHE with either $L2$ or $L3$ approaches. For $L2$ (Figure 7-2a), hourly peak building loads in heating and cooling as well as their duration are provided by the user along with monthly and yearly load factors and a constant borehole thermal resistance. These values are then used along with constant values of COP_H and COP_C to calculate various ground loads: peak loads in heating and cooling, average monthly heating and cooling loads during the peak months, and annual load. Then, a g-function based approach similar to the one proposed by Ahmadfard and Bernier (2014), i.e., Equation 7.7, is used to obtain L. An iterative procedure on L is required. It takes the form of a single variable optimization, using the golden section search method. The g-functions are calculated using the analytical g-functions obtained by Claesson and Eskilson (1987) as the base and the Incomplete Bessel Function (i.e. the Leaky Well Function) for evaluating the borehole-to-borehole thermal interactions. The borehole locations are user-defined and are not limited to rectangular configurations.

7.2.4 L3 -Monthly and peak pulses

Some of the most popular software tools use $L3$ methods which rely on monthly averaged loads and monthly peak loads. The objective of $L3$ methods is to obtain T_m (or T_{inHP}) for a given bore

field length (Equation 7.8). Since the ground thermal response (values of R_i) vary with borehole length, an iterative process is required as shown in Figure 7-2b.

$$T_m = \frac{T_{inHP} + T_{outHP}}{2} = \frac{\sum_{i=1}^{N} q_i R_i + q_h R_b}{L} + T_g \tag{7.8}$$

Typically, Equation 7.8 would be evaluated month by month for the entire design period. For example, Equation 7.9 would be used to obtain $T_{m,2}$ after the second month of operation:

$$T_{m,2} = \frac{T_{inHP,2} + T_{outHP,2}}{2} = \frac{q_{m,1}R_{m,1} + q_{m,2}R_{m,2} + q_{h,2}R_{h,2} + q_{h,2}R_b}{L} + T_g \tag{7.9}$$

where $q_{m,1}$ and $q_{m,2}$ are the average ground loads for the first two months, $q_{h,2}$ is the peak ground load of the second month (typically applied at the end of the month), $R_{m,1}$, $R_{m,2}$, and $R_{h,2}$ are the ground thermal responses corresponding to the duration of $q_{m,1}$, $q_{m,2}$, and $q_{h,2}$, respectively.

In theory, $L3$ methods should be more accurate than level L2 methods as they follow more closely the time evolution of the loads. The calculation sequence for a typical $L3$ method can be explained using Figures 7-2b and 7-2c. Two approaches are typically used: one which starts with building loads and the other with ground loads. In the first approach (Figure 7-2b), the user typically inputs 48 building loads, i.e. 12 monthly averaged building loads and 12 monthly peak loads for both heating and cooling conditions. These values are assumed to repeat each year for the design period of the system. It is important for the user to carefully select the duration of the peak loads as this has a relatively important influence on the results. The reader is referred to the work of Cullins and Spitler (2011) who have formulated a method to determine peak loads and their duration using hourly building load profile.

It should be noted that the calculation process described in this paragraph applies to $L3$ and $L4$ (to be described shortly) methods. Calculations start in step 2 with a first estimate of the borehole length. Then, the borehole thermal resistance (which in some tools depend on L) is evaluated in step 3. Then, COP_H and COP_C are typically evaluated each month (each hour in $L4$ methods) based on values of T_{inHP} prevailing at peak conditions during that month (or during the given hour in $L4$ methods). With known values of $COPs$, ground loads can be evaluated in step 5 followed by the calculation of the ground thermal response factors in step 6. Then, Equation 7.8 (Equation 7.1 for $L4$ methods) is applied sequentially from month to month (hour to hour in $L4$

methods) for the expected lifetime of the system to determine T_{inHP} in step 7. If calculated values of T_{inHP} have not converged then the process goes back to step 4 for an update on the COP values. If T_{inHP} has converged then a check is made to verify if the temperature limits (T_L or T_H) have been reached. If not, then the value of L is updated and calculations proceed back to step 3. When the method starts with the ground loads (Figure 7-2c), the calculation sequence is simpler. The tool sets a guess value for L then evaluates the borehole thermal resistance for this value of L. Ground thermal response factors are calculated in step 4 and Equation 7.8 (equation 7.1 for $L4$ methods) is used to evaluate T_{inHP} in step 5. As shown in step 6, if either T_L or T_H has been reached then a converged value of L is obtained, if not, L is updated and the sequence goes back to step 3. Note that if the tools assume that the borehole thermal resistance is independent of L, then iterations go back to step 4 instead of step 3 in both paths (Figures 7-2b and 7-2c). If $COPs$ are dependent on the fluid temperature, the ground loads are evaluated iteratively at each time step. The iterative procedure uses an initial guess value for the $COPs$ and iterates until convergence as shown in Figure 7-2b. Four $L3$ methods will now be described.

7.2.4.1 NWWA method

The National Water Well Association (NWWA) method is a L3 method where ground loads are used directly. It has been described by Hart and Couvillion (1986). The NWWA method applies Kelvin's line source model to evaluate ground heat transfer. It takes into account the effects of cyclic on-off operation as well as thermal interferences of adjacent boreholes. As reported by Cane and Forgas (1991) the entering heat pump fluid temperature at month k (T_{f_k}) obtained by the NWWA method is evaluated using the following equation:

$$T_{f_k} = \sum_{i=0}^{i=k} \left(\left(\frac{q}{\sum_{j=1}^{layers} \left(\frac{L_j}{(L_M/L_s)_j R_{s_j} + R_p} \right)} \right)_i \Delta RTR_i \right) + \frac{q\ RTR}{2\left(\dot{m}\ SG\ Cp_f\right)} + \Delta T_{g_k} + T_{g_k} \quad (7.10)$$

The term $q/\sum_{j=1}^{layers}\left(L_j/\left((L_M/L_s)_j R_{s_j} + R_p\right)\right)$ represents the heat transfer between the heat exchanger fluid and the ground. q is the heat exchanged with the ground, L_s is the length of single-pipe heat exchanger and L_M is the length of multiple heat exchangers, L_j is the length of pipe in the jth ground layer, $(L_s/L_M)_j$ is the length multiplier for a multiple system in the jth

layer of the ground, R_{s_j} is the ground thermal resistance in the jth ground layer surrounding the borehole, R_p is the pipe thermal resistance, i is any month from the beginning of the period up to month k, RTR_i represents the ratio of run time to the cycle time of month i, ΔRTR_i is the change in run time ratio from one month to the next, $\dot{m}$ is the fluid flow rate in the pipe, SG and Cp_f are the specific gravity and specific heat of the fluid, respectively, T_{g_k} represents the average far field temperature in month k, ΔT_{g_k} is the average seasonal variation of the far field temperature in month k. The obtained fluid temperatures are compared to the user specified lowest and highest entering fluid temperatures. If the difference satisfies the specified convergence criterion, the iterative procedure stops, otherwise, a new heat exchanger length is selected and the procedure is repeated until convergence. The NWWA has been shown to be more precise than the IGSHPA method (Caneta, 1992). However, it does not reach the accuracy that can be achieved with modern techniques.

7.2.4.2 Quasi-three pulse method with running average

Monzó et al. (2016) have proposed a methodology which accounts for monthly loads but that still uses the three-pulse approach of $L2$ methods. The resulting sizing method is shown in Equation 7.11. In their approach, the length is determined for each month i over the design period. The yearly load and corresponding value of the effective ground thermal resistances (product $q_y\ R_y$ in Equation 7.4) is replaced by a running average of the loads of the previous months multiplied by the corresponding effective ground thermal resistance ($\bar{q}_{pm,i}R_{pm,i}$). The monthly pulse term in Equation 7.4 ($q_m\ R_m$) is replaced with the monthly pulse of the current month and the corresponding monthly effective ground thermal resistance ($q_{cm,i}R_{cm}$). The temperature penalty ($T_{p,i}$) is evaluated iteratively for each month using the technique described in Equation 7.5.

$$L_i = \frac{\bar{q}_{pm,i}R_{pm,i} + q_{cm,i}R_{cm} + q_{h,i}R_h + q_{h,i}R_b}{T_m - \left(T_g + T_{p,i}\right)} \tag{7.11}$$

Even though this method uses the three pulse approach of $L2$ methods it is considered here as a quasi $L3$ method because monthly loads are considered.

It is also possible to extend the $L2$ alternative method described earlier to a quasi $L3$ method using the approach proposed by Monzó et al. (2016) but using g-functions instead of T_p. The resulting equation is given in Equation 7.12,

$$L = \frac{\bar{q}_{pm,i} R_{g,pm,i} + q_{cm,i} R_{g,cm} + q_{h,i} R_{gh} + q_{h,i} R_b}{T_m - T_g} \tag{7.12}$$

where the index g has been added to the effective ground thermal resistance to indicate that they are based on g-functions. Finally, much like for the alternative method described earlier, it is possible to account for borehole thermal capacity by evaluating R_{gh} and $R_{g,cm}$ with short-term g-functions.

7.2.4.3 GHX Design Toolbox (in L3 mode)

In addition to the $L2$ approach described earlier, Chiasson's (2016) spreadsheet has $L3$ capabilities. The user can either specify 48 monthly values (average building loads and peak loads for heating and cooling) directly or enter the hourly building load values which are then pre-processed to obtain the 48 monthly building loads. The building loads are then converted to ground loads based on the user defined COP values as a function of $T_{in,HP}$. The peak load durations in heating and cooling are also specified by the user. Once these values are entered, the calculation proceeds as shown in Figure 7-2b. More specifically, Equations 7.13.a to 7.13.d are solved for both heating and cooling conditions to obtain L.

$$T_{f,avg} = T_g + \sum_{i=1}^{n} \frac{(q'_i - q'_{i-1})}{2\pi k_g} g\left(\frac{t_n - t_{i-1}}{t_s}, \frac{r_b}{H}, \frac{B}{H}\right) + q'_n R_b \tag{7.13.a}$$

$$T_{f,peak} = T_{f,avg} + \frac{q_{rej,peak}}{H.N_b} R_q \tag{6.13.b}$$

$$R_q = \frac{ln\left(4\alpha t_p / r_b^2\right) - 0.5772}{4\pi k_g} \tag{6.13.c}$$

$$T_{in,hp,peak} = T_{f,peak} + \frac{q_{rej,peak}}{2\dot{m}C_p} \tag{6.13.d}$$

where $T_{f,avg}$ and $T_{f,peak}$ are the average and the peak mean fluid temperature in the boreholes and $T_{in,hp,peak}$ is the peak inlet fluid temperature to the heat pumps determined for the nth month of operation, q'_i is the net average ground load per unit borehole length for the ith month, g is the ground thermal response factor (g-function), which is a function t/t_s, r_b/H, and B/H and t_s is the net peak ground load. It is obtained by subtracting the average cooling or heating loads from the cooling or heating peak loads. R_q is estimated by an approximation of the infinite line source solution and is dependent on the peak load duration. Equations 7.13.b to 7.13.d are calculated each month over the expected life time of the system. Then, as shown in Figure 7-2b, L is

updated if convergence has not been reached. It is updated using the golden section search optimization method where the objective function is defined as the square of the error of the calculated and target values of T_L and T_H

7.2.4.4 EED

EED (v3.2) is a $L3$ sizing tool which sizes the ground heat exchangers based on either the building or the ground loads (BLOCON, 2015). It should be noted that the newest version of EED (v4) can also operate as a $L4$ tool. With EED in $L3$ mode, the sequences presented in Figure 7-2b or 7-2c are used. When building loads are specified, constant COP values are used to obtain the ground loads. Thus, the inner iteration loop on T_{inHP} shown in Figure 7-2b is not used. The duration of peak loads can be set to different values for each month. When ground loads are specified (Figure 7-2c), heat pump characteristics are not required. The borehole thermal resistance can be entered directly by the user or it can be evaluated within the sizing sequence. The user can choose if borehole short circuiting effects should be accounted or not. EED calculates effective borehole resistances and so iterations go back to step 3 (Figures 7-2.b and 7-2.c). Ground thermal response factors are derived using pre-calculated g-functions stored in an extensive database with various bore field geometries including boreholes positioned in various configurations (in-line, L- and U-shape, open rectangular or rectangular). EED v4 can approximate irregular borehole patterns with regular ones. The data base of g-functions are for specific values of r_b/H, B/H. During the course of a calculation, if values of r_b/H and B/H do not match these values, then a correction factor (Eskilson, 1987) is applied to account for different values of r_b/H and the tool interpolates between g-function values for different B/H by keeping the borehole distance spacing constant and changing boreholes depth.

The tool evaluates the average and the peak monthly mean fluid temperatures over the design period of the system and determines the minimum required bore field length which satisfies the heat pump temperature limits as shown in Figures 7-2b and 7-2c.

7.2.4.5 GLHEPro

GLHEPro (GLHEPro V4.0, 2007 and Spitler, 2000) is a $L3$ sizing tool which uses average and peak monthly heat loads. Note that GLHEPro V.5 can also perform hourly simulations ($L4$ level) for a given bore field length. Much like EED, two paths are possible either with the building

loads or directly using ground loads. The heat pump $COPs$ can either be defined as constant or dependent on the inlet fluid temperatures. In this later case, an inner iteration is required, as shown by the dash line in Figure 7-2b. The calculation methodology for GLHEPro is similar to the one presented in Equations 7.13.a to 7.13.d. However, as noted by Cullins and Spitler (2011) the evaluation of $T_{f,peak}$ uses R_b in addition to R_q.

$$T_{f,peak} = T_{f,avg} + \frac{q_{rej,peak}}{H.N_b}(R_q + R_b) \tag{7.14}$$

where $R_q = g(t/t_s, r_b/H)/(2\pi k_g)$ which is the effective ground thermal resistance for the peak load duration. R_q is evaluated based on short-term g-functions determined by a technique elaborated by Xu and Spitler (2006).This technique is based on an earlier methodology developed by Yavuzturk et al. (1999) and Yavuzturk and Spitler (1999). In effect, this method accounts for thermal capacity of the fluid, the pipe and grout inside the borehole.

The method finds the maximum and minimum heat pump inlet fluid temperatures for each month by superimposing the temperature response of the peak loads on the obtained average fluid temperature (Equation 7.13.d). Then, these maximum and minimum values are compared to the specified temperature limits until convergence. The tool uses 307 pre-calculated g-functions (GLHEPRO 4.0, 2007) that are stored in a database for various types of bore field. GLHEPro evaluates the effective borehole thermal resistance using 10th order multipole method (Javed and Spitler, 2017).

7.2.5 L4 –Hourly loads

Hourly building or ground loads are used as the starting point in $L4$ methods. Typically, the same hourly loads are used from year to year for the design period. With reference to the general sizing equation (Equation 7.1), $L4$ methods involve 8760 terms in the summation for each year of calculation. This makes the calculations computationally intensive and most often loads are aggregated to reduce the number of terms in the summation. Aside from the different time scale of the loads, the calculation sequence of $L4$ methods is identical to $L3$ methods and follows the sequence presented earlier depending on whether building (Figure 7-2b) or ground loads (Figure 7-2c) are provided.

As indicated above, the newest versions of EED has an option to perform L4 calculations. A number of tools can be considered to be quasi $L4$ tools. For instance, GLHEPro V5.0, Energy

Plus, eQuest all provide hourly simulations but for a fixed bore field length. It is possible to update "manually" this length until T_L and T_H are reached to get the design length. The Duct ground heat STorage (DST) model, which is part of the TRNSYS package, is not considered to be a ground heat exchanger sizing tool. However, it can predict the hourly fluid temperature evolutions over the expected life of the system. Recently, Ahmadfard et al. (2016) have combined the DST model with GenOpt to automate this iterative procedure to make it a $L4$ method. It will now be briefly described.

7.2.5.1 DST model used a sizing tool In TRNSYS

The Duct ground heat STorage (DST) model has been developed originally by Hellström (1989) to simulate seasonal thermal storage of densely packed boreholes configured in an axisymmetric pattern. It is part of the TESS library (TESS, 2012) of TRNSYS (Klein, et al. 2014) and is known as Type 557. The ground thermal response is calculated using a one dimensional analytical model to solve for the ground temperature in the local region and a two-dimensional explicit finite difference model to simulate the ground temperature in the global region.

With the approach suggested by Ahmadfard et al. (2016), GenOpt starts the iteration with a guess value for the length. It then calls the DST model and runs a simulation for the expected design period of the system. Next, it analyzes the results and updates the guessed length and runs a new iteration. This iterative procedure continues until the minimum borehole length that satisfies the maximum and minimum fluid temperature limits is obtained. The model can handle both constant and variable $COPs$. In the latter case, the tool has an inner hourly iteration loop (steps 7 to 3 in Figure 7-2.b). There are two major drawbacks when using the DST model. First, it is only strictly applicable to axisymmetric configurations. Secondly, borehole thermal capacity is not considered and the borehole thermal resistance remains constant throughout a simulation.

7.3 Literature review of inter-model comparisons

Caneta (1992) performed one of the earliest comparative studies where the IGSHPA and NWWA methods were compared to a rule-of-thumb. A real installation composed of three boreholes with an actual total borehole length of 274.3 m was used. The evaluations were based on monthly loads including eight heating months and four cooling months. The resulting borehole lengths obtained from the sizing tools were: 271.7, 330 and 365.8 m for the NWWA, IGSHPA, and rule-

of-thumb methods, respectively. This represents differences of 0.94, 20.3, and 33.35 % when compared to the real installation.

Thornton et al. (1997) are at the origin of the first serious efforts to compare modern vertical GHE sizing tools. They used one year of site-collected data from a single-family residence at Fort Polk, Louisiana to first calibrate the inputs to the DST model to obtain "best-fit" thermal properties. These inputs where then used to compare one-year design lengths obtained with five commercially-available sizing tools for eight values of T_H and two ground temperatures. The most important spread in the results is obtained when T_H = 29.5°C, where differences of about 83 and 88 % are observed for ground temperature of 16.7°C and 20.6°C, respectively.

Shonder et al. (1999) repeated the comparison exercises for residential applications with updated version of the five sizing tools used by Thornton et al. (1997) and one new tool. Two sites, in cooling- and heating-dominated applications are examined. The DST model is used as the benchmark and it is first calibrated with site collected data. For the cooling-dominated application, four values of T_H are considered and the GHE length is determined for 1 and 10 years of operation. Results show a much better agreement compared with the previous results of Thornton et al. (1997). For T_H = 35°C, the six sizing tools determined the borehole length within 7% for a one-year operation. However, all six programs seem to undersize the GHE to some extent when compared to the DST model. The ten-year design lengths obtained by four programs vary by about 17% for T_H = 35°C. For the heating-dominated case and for T_L = -1.1°C, the one-year and ten-year design lengths vary by about ±16% and ±15%, respectively.

Shonder et al. (2000) compared four GHE sizing tools for a relatively large bore field (12×10) in an elementary school in Lincoln, Nebraska. The authors first used the DST model in TRNSYS as a benchmark and calibrated its inputs with one year of site-collected data. Since this is a heating-dominated application, the four design tools were compared for values of T_L equal to -1.1°C, 1.7°C, and 4.4°C for one and ten year design periods. On average, there is a ±16% difference between the four sizing tools and the DST model. Overall, the GHE lengths differ by an average of ±12% from the TRNSYS benchmark, somewhat less than the ±16% difference for the one-year lengths. The ten-year GHE design lengths are on average, about 7% higher than the one-year lengths, indicating only modest multi-year effects. Indeed the annual ground thermal imbalance is 1.76 kW (in heating mode) which leads to a relatively small temperature penalty, T_p = 0.35 °C. It should also be noted that the DST model is designed to simulate boreholes in an axisymmetric

pattern not a rectangular 12×10 geometry. The resulting error from this approximation has not been documented by the authors.

Spitler et al. (2009) performed an inter-model comparison of six different simulation tools including the DST model, three g-function based models implemented in EnergyPlus, eQuest, and HVACsim+, and two proprietary models. Two set of data were used: The first set comes from a three-borehole ground heat exchanger at Oklahoma State University, with 15 months of hourly-averaged experimental data. The second set is composed of one-year of hourly ground load data obtained by simulating an office building in Tulsa. A 196 borehole configuration is used in this second case. Results for the first set of data indicate that all models show higher oscillation amplitudes than the experiment, probably indicating that the dampening effect associated with borehole thermal capacity is not properly accounted for in the models. In addition, the authors indicate that the use of hourly time steps that do not correspond to the heat pump on/off cycles, may have causes these differences. The authors cite model assumptions that may not have been encountered in the experiments: uniform undisturbed ground temperature, no ground water flow, no moisture transport in the upper, unsaturated region of the ground, and uniform heat transfer along the borehole length.

For the second test with the 196 borehole configuration, substantial differences in the evaluation of the long-term temperature rise and monthly fluid temperature changes at the heat pump inlet are observed after 20 years of simulated operation. It is speculated that the assumptions used for superposition of individual boreholes, boundary conditions and heat transfer variations along the borehole are the likely causes of discrepancies. Finally, the authors note that user input and post-processing errors should not be ruled out in such a comparison.

Bertagnolio et al. (2012) presented test cases for comparing the time evolution of borehole wall temperatures obtained using three analytical solutions (infinite line source (ILS), infinite cylindrical heat source (ICS), and finite line source (FLS), two numerical models (g-functions and DST) and a hybrid model (ICS/Tp/MLAA) based on a combination of the infinite cylindrical heat source, and improved calculation of T_p and a so-called multiple load aggregation algorithm (MLAA). The authors defined two series of test cases for single and multiple boreholes. Synthetic load profiles are used in all cases. They are generated using a relatively simple mathematical function which enables reproducible profiles. The same approach will be used later in the paper for some test cases. For single boreholes, constant heat rejection load, symmetric

cyclic heat load, asymmetric heat load (cooling dominated for 20-year) and non-continuous (heating only) heat load are considered. The results show that analytical one-dimensional radial models (ILS, ICS) are in good agreement with three dimensional models for relatively short-simulation periods. However, for longer time periods the results are not as accurate since the axial effects become more significant and only the FLS, g-functions and DST models have good accuracies. Cyclic heat load tests proved to be useful in evaluating the accuracy and the computational performance of different load aggregation algorithms. Results obtained with the asymmetric load revealed that ICS-based models predict borehole wall temperatures within ±1ºC of the DST model.

For multiple boreholes, constant heat rejection and asymmetric loads (cooling dominated for 20-year) are considered. Constant load tests illustrated significant differences among the two numerical and hybrid models. These differences are due to two factors. First, the ICS/Tp/MLAA model cannot account for axial effects and these effects become important over the long term. Secondly, the DST model arranges the boreholes in an axisymmetric configuration which resulted in some error for in-line configurations.

Kurevija et al. (2012) compared the ASHRAE sizing equation (Equation 7.3 – $L2$ method) with $L3$ sizing methods based on g-functions. Two borehole arrangements, 6×7 and 21×2, are considered for a Croatian building. Borehole spacing is varied from 4 to 9 m giving a total of 12 comparisons. Peak and monthly building loads are given as well as the estimated peak duration and the equivalent full load operating hours (to obtain the annual ground loads). The bore field is sized for a 30-year operation. The lengths obtained with the g-function based methods are 8.8% to 10.7% (for the 21×2 configuration) and 10.7 to 19.3% (for the 7×6 configuration) greater than the ones obtained with the ASHRAE sizing equation with the largest differences occurring for small borehole spacing. The authors explain that these discrepancies are due to the fact that the ASHRAE sizing equation uses a simplistic borehole interaction model for predicting the heat buildup in the ground over time.

Cullin et al. (2014) used six years of experimentally measured data on a 3×2 ground heat exchanger, located in Valencia, Spain, to compare the sizing results of a simulation-based design tool (GLHEPro) and the classic ASHRAE sizing equation against the known borehole length (50 m). Results indicate that the simulation tool under predicts the required heat exchanger length by 4%, while the ASHRAE sizing equation over predicts it by 103%. A sensitivity study on the

input uncertainties revealed that the simulation-based method could under predict the results by about 2 % and over predict them by as much as 12%. However, only 9% of the over prediction obtained with the ASHRAE sizing equation could be attributed to inputs inaccuracies.

Cullin et al. (2015) extended their study to compare the design results of the simulation-based tool (GLHEPro) with the ASHRAE equation using experimental data from four systems. In addition to the Valencia case, data from systems located in Stillwater (USA), Atlanta (USA) and Leicester (UK) are used. Results show that the simulation-based tool predicts the actual installed borehole length to within 6% in all cases. Use of the ASHRAE sizing equation resulted in predicted borehole lengths which were significantly different from the actual lengths. Differences of -21%, +26%, +60%, and +103% were observed (negative/positive values represent undersizing/oversizing, respectively). The authors explained that the load representation and, to a lesser extent, the calculation of the borehole thermal resistance explain much of the differences between the ASHRAE sizing equation and the simulation-based tool. The authors also point out to the inherent uncertainty in reading values from the G-factor chart provided by Kavanaugh and Rafferty (1997) which is used to determine the effective ground thermal resistances. As indicated above, the ASHRAE sizing equation has been developed to calculate the required length based on three thermal pulses with durations of 10 years, 30 days, and 6 hours, respectively. The four cases represent measurement periods of six years or less. Therefore, the ground thermal resistance for the 10 year pulse in the ASHRAE sizing equation has to be adapted.

The present authors have also looked at the data for the Valencia case and determined the required borehole length based on their own interpretation of the data. Table 7-2 summarizes the results of these calculations and a comparison is made with the results provided by Cullin et al. (2015). As shown in Table 7-2, there are some significant differences in the evaluation of the parameters used in Equation 7.3.

First, the value of q_a is estimated to be -17.4 kW based on an analysis of the raw data. The PLF_m value of 0.192 is obtained from 2405/(17.4×720), where the value of 2405 kWh is the total heat injected during the 6th month of the third year of operation (Cullin et al., 2015) and 720 is the number of hours in the month of June. Values of R_h, R_m, R_y are also different. In the present case, they are obtained using calculated values of the G-factor based on the solution of the ICS solution provided by Cooper (1976) based on a borehole radius of 75 mm, a thermal conductivity of 1.6 W/m-K (Cullin et al., 2015), and a ground volumetric heat capacity of 2250 kJ/m^3-K

(Cullin et al., 2014). The values of T_{inhp}/T_{outhp} (30/35.5°C) are taken from the raw data at the peak conditions. The calculated value of -0.27°C for T_p is obtained using the original concentric ring technique proposed by Kavanaugh and Rafferty (1997) with a borehole separation distance of 3 m, a period of 3 years, and a borehole length of 61.1 m.

Table 7-2: Two different set of inputs to be used with the ASHRAE sizing equation for the Valencia case

Parameter	Units	Values used by Cullin et al. (2015)	Values used in the present study
q_h	kW	-17.0	-17.4
$q_h \times PLF_m$	kW	-17.0×0.27	-17.4×0.192
q_a	kW	-0.469	-0.469
$R_h/R_m/R_y$	m.K.W^{-1}	0.169/0.244/0.193	0.113/0.217/0.179
R_b	m.K.W^{-1}	0.11	0.11
$t_h/t_m/t_a$	hours/days/years	6/30/3	6/30/3
T_{inhp}/T_{outhp}	°C	27.2/32.7	30/35.5
T_g	°C	19.5	19.5
F_{SC}	-	1.04	1.04
T_p	°C	-0.5	-0.27
L	m	101	61.1

The final calculated length (61.1 m) obtained using the ASHRAE sizing equation with the current set of inputs is much closer to the actual length (50 m) than the results of calculations performed by Cullin et al. (2015) using the same ASHRAE sizing equation (100 m) but with a different set of inputs. If the duration of the peak heat load is assumed equal to 3 hours (GLHEpro V5.0, 2016), the length obtained by the ASHRAE equation goes down to 56.8 m. These discrepancies show the importance of human interpretation of the raw data on the final results. This is one reason why all loads are pre-treated in the inter-model comparison so that all tools have the same inputs. Li et al. (2017) have also used the four cases introduced by Cullin et al. (2015) to validate their methodology which is based on a reformulation of the ASHRAE sizing equation. For the Valencia case presented in Table 7-2, they obtain a length of 77 m. Finally, as mentioned by Spitler (2016), these four cases have reasonably balanced annual heat extraction and rejection loads with no significant long-term heat build-up or draw-down. Therefore, these data sets are not necessarily suited to check long-term effects.

7.4 Proposed test cases

One of the goals of this work is to propose a set of test cases that could be used to compare vertical GHE sizing tools against each other. With reference to the BESTEST terminology (Judkoff and Neymark, 1995, 1998) for building simulation software tools, three types of sizing test cases can be defined for comparisons: 1- simple analytical test cases, 2- comparative test cases and 3- real/experimental cases. Analytical test cases can only be applied for the simplest conditions (e.g. single borehole with constant load). Good long-term experimental data suitable for comparative testing could not be found in the literature. Therefore, only comparative test cases are examined in this work.

Differences in the required bore field length calculated by sizing tools can be the result of input errors or modeling differences. Input errors may be the results of human errors (e.g. different users may enter different ground thermal conductivities) or differences of interpretation for the raw data (e.g. different user may select different peak load duration or may convert building loads to ground loads differently). In an effort to avoid input errors, all test cases reported here are performed using a common set of data entered in each software by the same user and checked by another. Differences in results are thus presumed to be mainly due to the use of different modeling approaches or coding errors.

It should be noted that a spreadsheet containing all the loads and input data accompanies this paper so that other users can test other sizing tools with the same data. This spreadsheet also includes the test results of the inter-model comparison presented below. With reference to the general sizing equation (Equation 7.1), sizing tools will differ in the way they calculate the values of the ground thermal response, R_i, including in some cases the value of T_p, and the borehole thermal resistance, R_b. Also, software tools from the same level will handle the summation term (in Equation 7.1) differently. In order to separate problems linked to the evaluation of R_b from the rest of the calculation methodologies, most of the test cases are solved with imposed values of R_b. There are many data sets in the literature that could be used for inter-model comparative testing. A total of four data sets have been selected for the present study, each addressing a specific difficulty. A summary table of other data sets found in the literature is provided in Appendix A. The four data sets include: i) a synthetic perfectly balanced hourly load profile; ii) the monthly and peak load data provided by Shonder et al. (2000) for a school in Lincoln,

Nebraska; iii) the set of monthly and peak load values presented by Monzó et al. (2016); iv) the hourly load profile used by Bernier (2006) for a simulated building in Atlanta.

7.4.1 Input parameters

Table 7-3 shows the input parameters used for all test cases. Some tools need specific parameters that are not required by other tools. These parameters are listed at the bottom of Table 7-3.

Table 7-3: Input parameters for the four test cases

Parameter	Test 1 Synthetic balanced load	Test 2 Shonder et al. (2000)	Test 3 Monzó et al. (2016)	Test 4 Bernier (2006)	units
N_b	1	12×10	7×7	5×5	------
B	6	6	5	8	m
D	4	3	2.5	4	m
r_b	75	54	75	75	mm
$r_{p,i}$, $r_{p,o}$	16.7, 13.7	16.7, 13.7	16.7, 13	16.7, 13	mm
$2d_p$	75	47.1	75	83	mm
$\dot{m}_f$	0.443 (ground load) 0.559 (building load)	29	33.1	10.34	$kg.s^{-1}$
ρ_f	1052	1026	1026	1026	$kg.m^{-3}$
Cp_f	3795	4019	4019	4019	$J.kg^{-1}.K^{-1}$
μ_f	0.0052	0.00337	0.00337	0.00337	$kg.m^{-1}.s^{-1}$
k_f	0.480	0.468	0.468	0.468	$W.m^{-1}.K^{-1}$
$c_{p,g}$	2073.6	2877	2592	2052	$kJ.m^{-3}.K^{-1}$
α_g	0.075	0.068	0.075	0.08	$m^2.day^{-1}$
k_g	1.8	2.25	2.25	1.9	$W.m^{-1}.K^{-1}$
k_{gr}	1.4	1.73	1.73	0.69	$W.m^{-1}.K^{-1}$
k_p	0.43	0.45	0.4	0.4	$W.m^{-1}.K^{-1}$
T_g	17.5	12.41	10	15	°C
T_L	0	4.4	0	0	°C
T_H	35	35	35	38	°C
R_b	0.13	0.113	0.1	0.2	$m.K.W^{-1}$
t	10	10	10	20	years
COP_C	3.825 (building load)	3.643	------	3.86	------
COP_H	3.49 (building load)	4.09	------	4.03	------
When required by some tools, the following parameters are used: F_{sc}=1.04, $q_g'' = 0$ W/m^2 (geothermal heat flux), MCp_{gr} = 3900 $kJ.m^{-3}.K^{-1}$ (grout volumetric heat capacity) MCp_p = 1540 $kJ.m^{-3}.K^{-1}$ (pipe volumetric heat capacity), $R_c = 0$ $m.K.W^{-1}$ (contact resistance) $h_{\text{conv}} = 1000$ $W.m^{-2}.K^{-1}$ (Internal convection coefficient in pipes)					

7.4.2 Test 1 -Synthetic balanced load – one borehole

The first test case uses a synthetically generated balanced load profile either as a ground load or as a building load. For this test, it is assumed that the load is handled by just one borehole. The sizing tools are compared on their ability to predict the length of a single borehole when the borehole-to-borehole thermal interference is inexistent. Thus, T_p= 0 since q_y is zero (Equations 7.5 and 7.6).The balanced load is generated based on the methodology proposed by Bernier et al. (2004) using the following parameters: A=2000, B=2190, C=80, D=2, E=0.01, F=0 and G=0.95. The resulting sine profile with daily and weekly variations is shown in Figure 7-3a (a positive value represent a heating load). Figure 7-3b represents the cumulative energy of this load over the year. It can be seen that the cumulative energy is zero at the end of the year. This means, for example, that when the load is used as a ground load, the cumulative annual amount of energy injected/retrieved from the ground is zero.

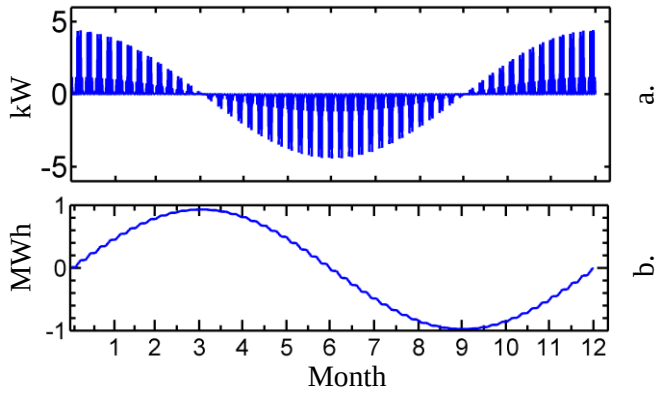

Figure 7-3: a) Hourly loads for the synthetic profile; b) Cumulative energy exchange resulting from the hourly loads

In the inter-model comparison of L4 methods, this hourly load profile has been used either directly as a ground load (Test1a) or as a building load (Test1b). Monthly and peak values have been extracted from hourly values for use with $L3$ methods (Table 7-4). The three loads used for $L2$ methods have also been determined and are presented in Table 7-5. When the input load is a building load (Test 1b), it is converted to a ground load using Equations 7.15.a and 7.15.b where T_{inHP} is in ℃ (Bertagnolio et al. 2012). When constant heating and cooling $COPs$ are assumed, COP_H and COP_C are evaluated at T_L (0 ℃) and T_H (35℃) giving COP values of 3.49 and 3.825 in heating and cooling, respectively. For $L4$ tools that use a variable COP, Equations 7.15.a and 7.15.b are used with the current value of T_{inHP} during a given time step.

$$COP_H = 3.49 + 0.061 \times T_{inHP} \quad (7.15.a)$$

$$COP_C = 7.92 - 0.117 \times T_{inHP} \quad (6.15.b)$$

The nominal flow rate is assumed to be 0.1 kg/s per kW of peak load to ensure turbulent flow. Since the peak ground loads in Tests 1a and 1b are 4.428 and 5.586 kW, respectively, the corresponding flow rates are 0.443 and 0.559 kg/s. The borehole is sized for a 10-year design period.

Table 7-4: Monthly average and peak ground loads to be used with $L3$ methods (all loads are in kW)

Month	Test 1				Test 2			Test 3		Test 4	
	1a-ground		1b-building								
	q_m	q_h	q_m	q_h	q_m	q_h	Peak duration (h)	q_m	q_h	q_m	q_h
1	0.604	4.401	0.431	0.000	100.003	395.127	11	105.374	238.670	7.938	-35.770
2	0.492	3.707	0.351	0.000	77.624	375.484	5	91.741	214.170	3.784	-53.548
3	0.202	2.208	0.144	0.000	37.794	374.729	2	55.245	181.170	-8.085	-83.086
4	-0.168	-2.002	-0.212	-2.525	9.705	200.208	3	0.051	107.330	-21.107	-93.549
5	-0.430	-3.605	-0.543	-4.548	-35.161	108.792	1	-65.165	80.420	-35.048	-120.782
6	-0.685	-4.387	-0.864	-5.533	-81.056	50.619	1	-122.411	0.000	-43.666	-130.893
7	-0.648	-4.428	-0.818	-5.586	-105.101	46.841	1	-150.538	0.000	-46.983	-139.731
8	-0.478	-3.726	-0.603	-4.701	-108.986	33.998	1	-103.258	0.000	-44.389	-131.761
9	-0.186	-2.137	-0.235	-2.695	-36.244	63.462	6	-51.053	57.080	-34.678	-111.780
10	0.160	1.968	0.114	-0.009	-2.861	239.494	1	4.382	111.500	-18.686	-97.338
11	0.478	3.746	0.341	0.000	59.615	243.271	2	50.366	150.670	-2.983	-52.843
12	0.680	4.427	0.485	0.000	111.392	281.802	4	92.720	198.000	5.853	-34.284

Table 7-5: Synthesis of the data for each Test used in L2 methods (negative values indicate that cooling conditions determine the required length)

	Test 1		Test 2	Test 3	Test 4
	1a-ground	1b-building			
	kW	kW	kW	kW	kW
q_h	-4.428	-5.586	---	-139.731	---
q_m	-0.648	-0.818	---	-46.983	---
q_a	-0.001	-0.120	---	-19.968	---
q_h	4.427	---	395.127	---	238.670
q_m	0.680	---	100.003	---	105.374
q_a	-0.001	---	1.763	---	-7.712

Data presented in Tables 7-4 and 7-5 need some further explanations. First, data are presented sequentially starting with January as month #1 which is also the starting date of operation. The monthly loads are the average of all hourly loads including the peak load. The monthly peak load is found by searching for the maximum load during a given month. Thus, taking the first month of the synthetic load as an example, the average monthly load is 0.604 kW and the peak load is 4.401 kW. The duration of the peak loads is assumed to be 6 hours in $L2$ and $L3$ methods. It is not necessary to assume peak load duration in $L4$ methods as the calculation methods follow the hourly loads. In some test cases, the peak load durations are reduced to 1 hour or, in the case of Test 2, the actual peak durations are used (see Table 7-4). Some tools require the monthly loads to be entered as cumulative energy values. In this example, the monthly energy load for January would then be 0.604×31×24 = 449.376 kWh. In $L3$ methods, the monthly peak is typically superimposed at the end of the month. Again, using the synthetic load profile as an example, and referring back to Equation 7.9, $T_{m,2}$ (mean fluid temperature in the borehole at the end of February) would be calculated using $q_{m,1}$= 0.604 kW, $q_{m,2}$=0.492 kW, and $q_{h,2}$=3.707 kW with corresponding durations of 31 days, 28 days minus 6 hours (in some models 28 days), and 6 hours. It should be noted that only the dominant loads that lead to longer lengths are reported in Table 7-5 which explains why either heating or cooling loads are presented.

7.4.3 Test 2 – Shonder's test – 120 boreholes

Shonder et al. (2000) used the data from an elementary school located in Lincoln, Nebraska to perform an inter-model comparison. Since this comparison is almost two decades old, it was felt that it needed to be revisited with the current state of sizing tools. This test case concerns an installation with a 12×10 borehole field. Boreholes are 73 m deep and are spaced 6 m apart. Table 7-4 presents the loads obtained from the data reported by Shonder et al. (2000). In their article, Shonder et al. (2000) provide peak building loads but not peak ground loads. They do provide a table of COP values as a function of T_{inhp} which was used here to convert building loads to ground loads heating and cooling $COPs$ of 4.09 and 3.643 for T_L = 4.44 °C and T_H = 35 °C where assumed but other COP values may have been used by Shonder et al. (2000). The monthly peak load durations are assumed equal to the measured values reported by these authors (see Table 7-4). Peak load durations of 6 hours are also considered in the comparison. In addition, the shank spacing and pipe thermal conductivity are assumed to be 47.1 mm and 0.45 $W.m^{-1}.K^{-1}$, respectively. The properties of the heat transfer fluid (propylene glycol, 22%) are evaluated at 10 °C. As was done by Shonder et al. (2000), the bore field is sized for the heating case. Test 2 is not particularly severe in terms of borehole-to-borehole thermal interference since there is a relatively small annual ground thermal imbalance (1.76 kW). The monthly and peak loads reported in Table 7-4 are used to generate an hourly load shown in Figure 7-4 with a 6 hour peak duration.

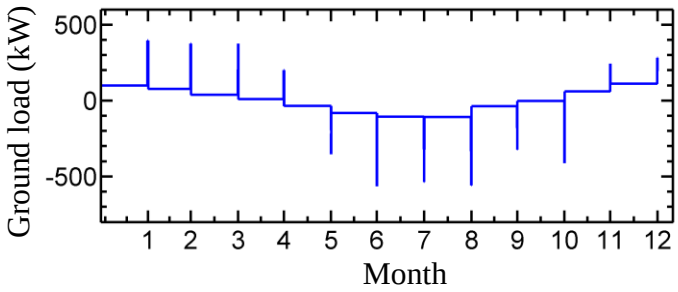

Figure 7-4: Hourly ground loads generated from monthly and peak loads for L4 methods used in Test 2

7.4.4 Test 3 – Required length during the first year

Monzó et al. (2016) proposed a methodology, presented earlier (Equation 7.13), which accounts for monthly loads but that still uses the three-pulse approach of L2 methods. Their methodology was tested using an hourly, cooling dominated, ground load profile which will be used as a test case in the present study. The profile, shown in Figure 7-5, was analysed to obtain monthly averaged and monthly peak values (Table 7-4) and the three load pulses (Table 7-5). This profile is interesting in that the required length occurs in the first year of operation. Thus, as will be shown in the results section, methods that do not calculate the required length in the first year, will lead to inaccurate results. The monthly peak heat loads are defined as the maximum heating and cooling loads of each month and their durations are assumed to be 6 hours. In order to simplify calculations, Monzó et al. (2016) assumed that every month had an equal duration of 30.42 days. However, in this work the monthly ground loads are evaluated based on the exact number of days for each month.

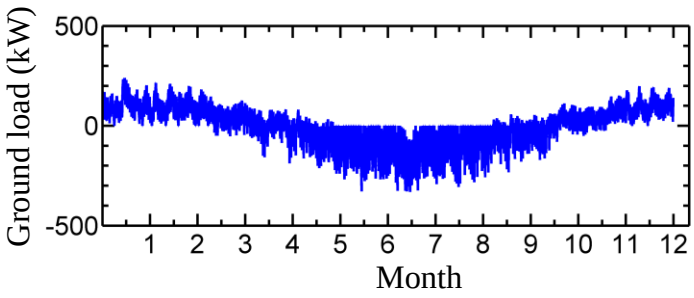

Figure 7-5: Hourly ground load profile for Test 3

7.4.5 Test 4 – High annual ground load imbalance

Test 4 has a relatively high annual ground load imbalance. Building loads for this case are generated using TRNSYS based on a building that is part of the TESS library (TESS, 2005). Figure 7-6 shows the hourly building load profile. The building has an area of 1486 m^2 and is assumed to be located in Atlanta. Bernier (2006) has shown that this profile has an annual ground load imbalance which leads to relatively high values of T_p of the order of +7.0 °C after a 20 year period. Thus, this profile should provide a good test to evaluate the long-term borehole thermal

interference effects of the various tools. Using constant COP values of 4.03 and 3.86 in heating and cooling, respectively, monthly average ground loads and monthly peak ground loads have been evaluated (Table 7-4). Finally, the monthly pulses required for $L3$ methods and the three pulses required for $L2$ methods have been evaluated and are presented in Tables 7-4 and 7-5.

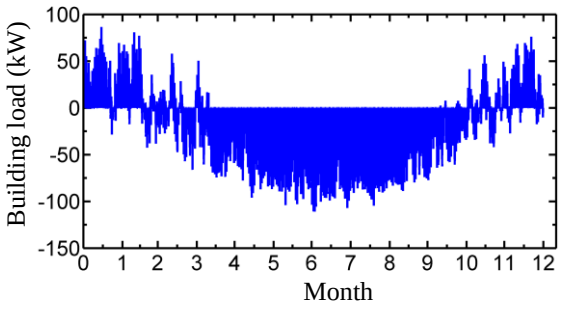

Figure 7-6: Hourly building loads considered for Test 4

7.4.6 Results of the inter-model comparison

The four test cases are used in an inter-model comparison of twelve different sizing tools covering the range from $L2$ to $L4$ methods. These sizing tools are listed in Table 7-6 with their main characteristics. The results of the four test cases are presented graphically in Figure 7-7 while exact lengths are presented in appendix B. It should be noted that some tools could not be used for particular tests. Tool B could not be used for Test 1a with a one hour peak duration, for Test 2 and for Test 4, because it has fixed pulse durations. Also, tool L with an hourly varying COP was only used for Test 1b.

Table 7-6: Sizing tools used in the inter-model comparison

Identifying letter	Tool	Main characteristics	Level
A	Classic ASHRAE sizing equation	- Based on Equation 7.3 - Ground thermal resistance evaluated using the ICS - T_p evaluated using the modified concentric ring technique (Kavanaugh and Rafferty, 2015) - First-order multipole for the effective borehole thermal resistance	$L2$
B	Modified ASHRAE sizing equation	- EXCEL tool of Philippe et al. (2010) is used (Equation 7.4) - Ground thermal resistance evaluated using the ICS - Rectangular geometries - Fixed pulse durations - Zeroth order multipole for borehole thermal resistance	$L2$

Table 7-6 (continued): Sizing tools used in the inter-model comparison

C	Modified + ASHRAE sizing equation-B	- Based on Equation 7.4 - Ground thermal resistance evaluated using the ICS - T_p evaluated with Equation 7.5 (Bernier's approach) - User defined pulse durations - Not restricted to rectangular geometries - First-order multipole for the effective borehole thermal resistance	*L*2
D	Modified + ASHRAE sizing equation-F	- Same as C expect that T_p is evaluated with Equation 7.6 (Fossa's approach)	*L*2
E (E_{st})	Alternative method	- Based on Equation 7.7 - Ground thermal resistance evaluated using g-functions - User defined pulse durations - Not restricted to rectangular geometries - First-order multipole for the effective borehole thermal resistance - A modified version, (E_{st}), accounts for short-term effects	*L*2
F	GHX design tool box	- Based on Equation 7.7 - Ground thermal resistance evaluated using g-functions - User defined pulse durations - Not restricted to rectangular geometries - First-order multipole for the effective borehole thermal resistance	*L*2
G	Quasi *L*3 method – Equation 7.13	- Based on Equation 7.11 - Effective ground thermal resistances are calculated using the ICS - User defined pulse durations - Not restricted to rectangular geometries - First-order multipole for the effective borehole thermal resistance	*L*3
H (H_{st})	Quasi *L*3 method - Equation 7.14	- Based on Equation 7.12 - Effective ground thermal resistances are calculated using g-functions - User defined pulse durations - Not restricted to rectangular geometries - First-order multipole for the effective borehole thermal resistance - A modified version, (H_{st}), accounts for short-term effects	*L*3
I	EED – monthly (v.4.17)	- g-function based method - Pre-defined geometries are used - Effective borehole thermal resistance based on 10 multipoles	*L*3
J	GLHEpro (v 5.0)	- g-function based method - Pre-defined geometries - Effective borehole thermal resistance based on 10 multipoles - Accounts for short-term effects using short-term g-functions	*L*3
K	EED – hourly (v.4.17)	- g-function based method - Pre-defined geometries - Effective borehole thermal resistance based on 10 multipoles	*L*4
L	DST	- Numerical/Analytical model - Strictly valid for axisymmetric geometries - First-order multipole for the effective borehole thermal resistance	*L*4

Test 1a. Synthetic balanced ground load – one borehole

As shown in Figure 7-7, three variations of Test 1a are reported. In the first two sets, the peak load durations are assumed equal to 6 hours and the borehole thermal resistance is evaluated either internally by the tool or is entered as a constant value (=0.13 m.K.W^{-1}) in all tools. In the third set, the peak load duration is assumed to be one hour and the results are evaluated with the same borehole thermal resistance (=0.13 m.K.W^{-1}) for all sizing tools.

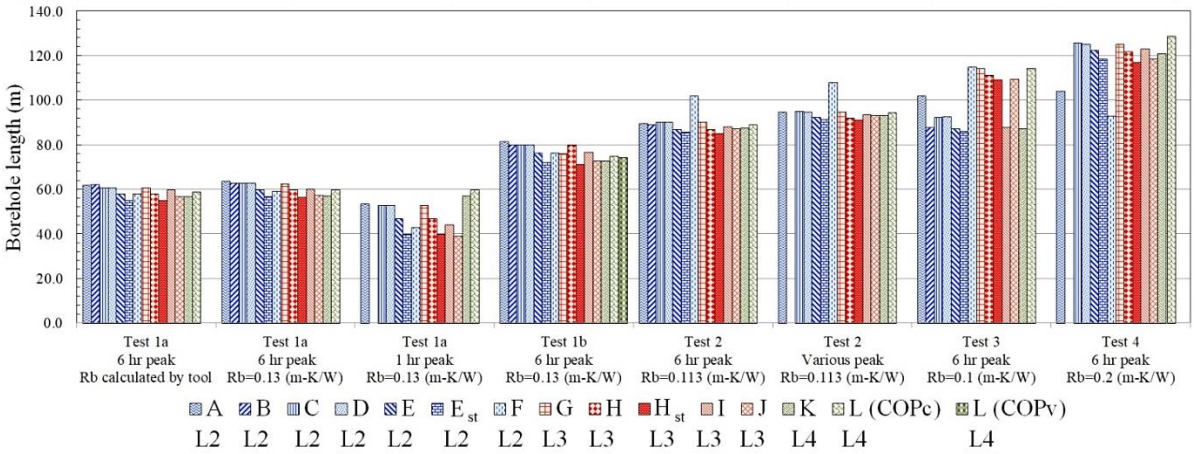

Figure 7-7: Inter-model comparison of twelve sizing tools for four test cases

An analysis of the first two sets in Test 1a reveals that the results obtained by the various sizing tools are in a relatively good agreement. The minimum and maximum lengths in the first set are 54.8 and 62.1 m, respectively. These lengths are 6.6% below and 5.9% above the mean value. Tools Est ($L2$), Hst ($L3$), J ($L3$), K ($L4$) and L ($L4$) give results that are lower than the mean. This is most likely due to the fact that E_{st}, H_{st} and J account for short-term effects (i.e. borehole thermal capacity) and that $L4$ tools use hourly values, not a 6-hour peak duration. For L2 methods, tool B has a higher predicted length because the value of R_b calculated by the tool is higher than other $L2$ tools. The borehole thermal resistances evaluated by the tools vary from 0.120 to 0.127 m.K.W^{-1}, a 5.8% difference, as reported in Table 7-8. When the same value of R_b (=0.13 m.K.W^{-1}) is used for all tools (second set of cases for Test 1a), the minimum and maximum lengths are 56.5 m (5.8% below the average) and 63.7 m (6.2% above the average), respectively. It can be seen that using an identical borehole thermal resistance for all tools reduces the differences marginally by about 0.5 %. The differences among sizing tools in the evaluation of R_b experienced for Test 1a is typical of what was encountered for all test cases. In other words, no apparent flaw was detected among tools in the evaluation of R_b. Therefore, the

remainder of the inter-model comparison will be performed for identical values of R_b for every sizing tool. The reader is referred to the spreadsheet which contains the values of R_b obtained by the various tools for every test case. Aside from short term effects and the differences in the value of R_b, it is difficult to pinpoint other reasons that could explain the differences for this second set for Test 1a. One modeling difference that might have an impact is the use of the ICS for the evaluation of the ground thermal resistance in some of the tools (A, B, C, D, and G) which implies that axial heat transfer effects are not accounted.

The third block of results for Test 1a is obtained using a peak duration of one hour. As shown in Figure 7-7, the required length decreases and the relative difference among results increases. The minimum and maximum lengths are 39.1 m (19.1% below the mean) and 59.7 m (23.5% above the mean). The main reason for these significant differences is related to the short term effects (borehole thermal capacity). This was already observed above for the 6 hour peak duration. However, the impact is much greater when the peak duration is only one hour as shown with results obtained with tools E_{st} ($L2$), H_{st} ($L3$) and J ($L3$) which have the smallest lengths. If tools E and E_{st}, which are identical except for the inclusion of short term effects in Est, are compared, they show a difference of about 14.7%. The magnitude of this difference depends on the magnitude of q_h. For example, if the value of q_h is doubled and halved (everything else remaining the same) the differences in required lengths between tools E and E_{st} increases to 18% and decreases to 9.9%, respectively.

Test 1b. Synthetic balanced building load – one borehole

The synthetic load is used as a building load in Test 1b. This test is mainly used to detect if $L3$ tools are using heating and cooling $COPs$ correctly to evaluate ground loads and to test the impact of an hourly varying COP on the results of $L4$ tools. The calculated lengths are also higher than the ones evaluated for Test 1a because of larger ground loads. Test 1b is solved by considering one borehole, a six hour peak duration, R_b =0.13 m.K.W^{-1} and a 10-year design period. As shown in Figure 7-7, the length varies from 71.3 m to 81.3 m, 6.5% below and 6.6% above the average, respectively. Similar to Test 1a, tools E_{st}, H_{st} and J have determined the smallest lengths as they account for the short term effects. Tools K and L have also determined small lengths; however, this is mainly due to the fact that they use hourly-based loads. The

lengths determined by tool L with constant or variable $COPs$ have about a 0.8 % difference. So it appears from this test that the use of constant COP values evaluated at T_L and T_H is more than adequate to predict the required length.

Test 2. Elementary school in Lincoln, Nebraska – 120 boreholes

Test 2 examines the differences among the various tools for a large bore field (12 ×10). It is based on the original comparison of Shonder et al. (2000). Sizing is performed for heating for a 10 year design period with identical borehole thermal resistances (= 0.113 m.K.W^{-1}) once by assuming a peak load duration equal to six hours and once by using the original peak load durations provided by Shonder et al. (2000) which are presented in Table 7-4.

As shown in Figure 7-7 for the case in which the peak duration is assumed to be six hours, the results vary from 85.1 m to 102.0 m which are, respectively, 4.5% below and 14.5% above the mean value. The results calculated using the original peak durations vary from 91.1 m to 108.0 m, i.e. 3.6% below and 14.3% above the mean. In both cases, tools E_{st} and F have calculated the minimum and maximum lengths, respectively. The length calculated by tool F is about 12 meters higher than the next higher value. After examination of the results, it was found that the g-functions evaluated by this program are not sufficiently accurate. By ignoring the results of program F, the results vary from 85.1 m to 90.2 m when the peak load duration is considered to be six hours and they vary from 91.1 m to 94.9 m when the original peak load durations are assumed for each month. In their original paper, Shonder et al. (2000) obtained lengths ranging from 65.6 m to 87.3 m. As mentioned earlier, it is not clear what values of $COPs$ they used to convert building loads to ground loads which might explain the observed differences. Nonetheless, it appears that current tools are in closer agreement than in the original comparison of Shonder et al. (2000). However, the ground load imbalance is not severe so any deficiency in the borehole thermal interference calculation in a tool would not have a significant impact on the results. Test 4 will tackle the issue of a large ground load thermal imbalance. The results of the tools C and D do not have a significant difference. Recall that these tools only differ in the way they calculate T_p (Equations 7.5 and 7.6). This behavior can be seen in the other test cases for multiple boreholes. Overall, the difference observed between tools C and D is less than 1% for all test cases.

Test 3. Length required in the first year– 49 boreholes

Test 3 involves the sizing of a 49 borehole field over a 10 year period with a constant value of R_b (= 0.1 m.K.W^{-1}) and a six hour peak duration. Therefore, in all sizing tools, the design period is given as 10 years and the goal is to see if the sizing tools can adapt to the fact that the maximum required length occurs during the first year of operation.

As shown in Figure 7-7, the required length varies from 85.9 m to 115 m. These values are 13.9% below and 15.3% above the mean. This test shows that $L2$ sizing tools underestimate the required length when the maximum length is required in the first year. Tool A appears to give better results that other $L2$ tools, however the result is due to an underestimation of the temperature penalty (+1.18 °C, while the T_p evaluated by other tools is about +2.24 °C). Thus, two effects (wrong T_p and inability to size during the first year) tend to somewhat compensate each other for Tool A. The same can be said about tool F which appears to give good results but the inaccurate g-function determination mentioned earlier has a tendency to compensate for other factors. Surprisingly, tools I and K, which are $L3$ and $L4$ tools (thus not constrained by the 10 year period) calculate lengths below the average.

Test 4. Large annual ground load imbalance– 25 boreholes

Test 4 is based on the loads used by Bernier (2006). The required length is calculated for a 20 year design period for a 5×5 borehole field and a borehole thermal resistance of 0.2 m.K.W^{-1}. As mentioned earlier, the annual load is highly imbalanced and peak load conditions occur in cooling. As shown in Figure 7-7, results vary from 93.0 m to 128.9 m which represents values that are, respectively, 21.7% below and 8.5% above the mean. Three different group of results can be seen. First, results from tools C ($L2$), D($L2$), E($L2$), G($L3$), H ($L3$), I($L3$), K($L4$), L(($L4$) are in good agreement with a minimum of 121.0 m and a maximum of 128.9 m, thus a maximum difference of 6%. This tends to indicate that even though L2 methods appear to be less sophisticated that $L4$ methods, they give similar results. The second group concerns the tools that account for short-term effects, i.e. tools E_{st} ($L2$), H_{st} ($L3$), and J ($L3$). The agreement among these tools is excellent with calculated lengths of 118.4 m, 117.0 m, and 118.5 m, respectively. Finally, tools A ($L2$) and F ($L2$) have determined lengths that are much lower than the rest of the

tools (103.9 m and 93.0 m). These values are, respectively, 13 and 24 m lower than next lowest result (117 m). Clearly, these two tools cannot properly account for borehole thermal interaction caused by large annual imbalanced loads.

7.4.7 Sensitivity analysis

In this section, a sensitivity analysis is performed on Test 4 to check the variation of five parameters: peak load magnitude, q_h, thermal conductivity, k_g, borehole spacing, B, ground temperature, T_g, and the total number of boreholes, N_b. In this analysis, parameters are varied one at a time, and the new lengths are compared with the original Test 4 results for each tool. Results are shown in Figures 7-8.a to 7-8.e where relative differences from the original Test 4 results are shown. Each curve in these Figures is composed of three points including the pivot points which are the results obtained for the original Test 4. It should be mentioned that results for tool B are not presented because it is unable to calculate a 20-year design period. In addition, it is not possible to change the peak load magnitude for $L4$ tools (since the loads are hourly based) and, therefore, they are not included in the analysis of the peak load variation (Figure 7-8.a).

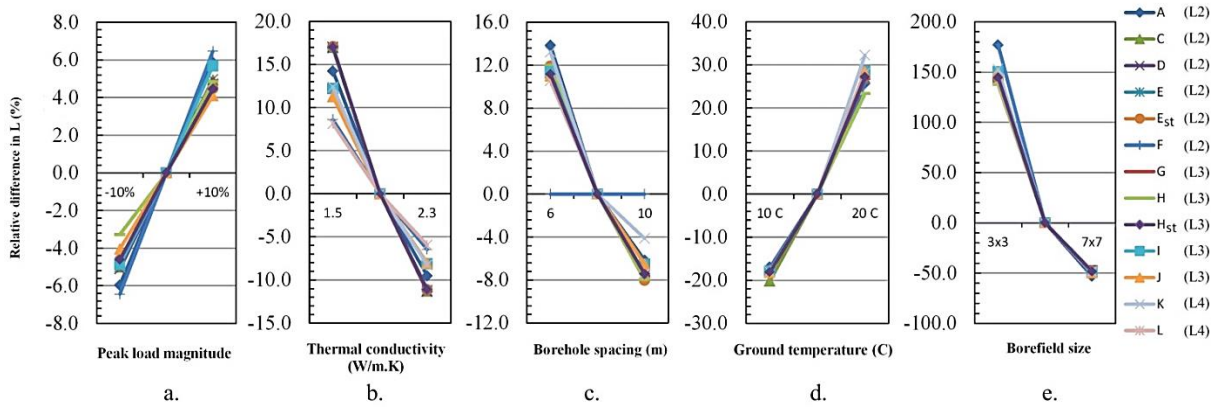

Figure 7-8: Sensitivity analysis for five parameters compared to the original Test 4 results obtained by each tool

In Figure 7-8.a, the value of q_h has been varied by ± 10%. As shown, some tools are more sensitive to peak load variations. For example, tool F predicts variations of - 6.5% and +6.5%, while tools G or H show variations about half as important (- 3.3% and +4.8%). In Figure 7-8.b, the original thermal conductivity, 1.9 $W.m^{-1}.K^{-1}$ is varied upward and downward by ± 0.4 $W.m^{-1}.K^{-1}$. Here again, the slopes are different and tools react differently to a change in thermal

conductivity. $L2$ tools are more sensitive to the thermal conductivity variation and they vary on average by +17.0% and -11.3%.Tools F and L predict lower variations. The results for tool F vary by +8.6% and -6.5 % and tool A vary by +14.2% and -9.5 % and the ones evaluated by tool L vary by +8.1% and -5.9 %. In Figure 7-8.c, the borehole spacing is varied by ± 2 m. All tools exhibit a similar trend except tools A, F, K. First, tool F shows no variations with borehole spacing which seems to indicate a problem with the tool. Tool A shows a higher relative difference than other tools when borehole spacing is reduced to 6 m but has approximately the same relative difference compared to the other tools when borehole spacing is 10 m. This tends to corroborate the fact that tool A cannot accurately predict borehole thermal interference which increases as borehole spacing decreases. Tool K behaves much like tool A when the borehole spacing is 6 m and shows a smaller relative difference than all the other tools when borehole spacing is 10 m. In Figure 7-8.d, the original ground temperature of 15 ºC is varied by ± 5 ºC. This has the effect of decreasing/increasing the denominator in Equation 7.1. When the denominator is changed, the length changes which, in turn, changes the effective ground thermal resistances (which are length dependent) and also the value of T_p in some tools. For the case where the ground temperature is reduced to 10 ºC (from 15 ºC), tools show about the same variations in length (-17.0 % to -18.2 % with an average of -17.9 %).With a ground temperature of 20 ºC (thus reducing the magnitude of the denominator), tools show different variations, from 23.3% to 32.2% with an average of 27.2%. Finally, the original 5×5 borehole field is changed to 3×3 and 7×7 configurations. All tools show approximately the same relative variations when the 7×7 configuration is examined. However, when borehole thermal interference becomes important for the 3×3 configuration, tools A (+177.0 %) and F (+177.4 %) show a marked difference when compared to the average of all tools (+145.5%).

7.5 Conclusion

The present study provides a general methodology for comparing vertical ground heat exchanger sizing tools. In the first part of the paper, sizing tools are categorized into five levels ($L0$ to $L4$) with increasing complexities: rules-of-thumb ($L0$), one-pulse ($L1$), three-pulse ($L2$), monthly-based ($L3$), and finally hourly-based annual simulations tools ($L4$). The calculation methodologies involved in $L1$ to $L4$ methods are presented in details and summarized schematically (see Figure 7-2). Descriptions of some of the available tools are given. Then, the

literature on comparative testing of sizing tools is reviewed. The most important study to date remains the work of Shonder et al. (2000) but it is almost two decades old and is revisited here with current sizing tools.

The second part of the paper presents the four test cases selected for the inter-model comparison. Test 1 uses a synthetically-generated balanced ground/building load for a single borehole for a 10-year design period; Test 2 revisits the Shonder et al. (2000) comparison which consists of a 12×10 borehole field for a heating dominated load; Test 3 has a peculiar load profile which leads to a maximum required length in the first year of operation that is used for a 7×7 geometry; Test 4 involves sizing of a 5×5 configuration with a high annual ground load imbalance for a 20-year design period. A total of twelve different sizing tools (described in Table 7-6), some of them commercially-available, are then compared against each other. A summary of the comparison is presented in Figure 7-7. These tools cover the $L2$ to $L4$ range with three of them including short-term effects (i.e. borehole thermal capacity). A spreadsheet has been constructed to archive the various loads of each test and report the results obtained with the various tools. A link is provided at the end of the paper to get access to this spreadsheet.

Test 1 is actually composed of four sub-tests. In the first of these sub-tests, the borehole thermal resistance, R_b, is evaluated by each tool and the peak duration is set at six hours. Results indicate a difference of 5.8% in the evaluation of R_b among all tools. This difference is typical for all the tests considered in this study and the reminders of the tests are performed assuming the same value of R_b for all tools. When the same value of R_b (=0.13 m.K.W^{-1}) is used for all tools, the minimum and maximum lengths are 56.5 m (5.8% below the average) and 63.7 m (6.2% above the average), respectively. Tools that include short-term effects tend to calculate smaller lengths while longer lengths are predicted by tools that evaluate effective ground thermal resistances using the cylindrical heat source solution which neglects axial heat transfer in boreholes. When the peak duration is reduced to one hour, short-term effects are much more important and results indicate that minimum and maximum lengths are 39.1 m (19.1% below the mean) and 59.7 m (23.5% above the mean). The fourth sub-test reveals that tools can correctly convert building loads to ground loads. Furthermore, it appears that using a constant value of COP evaluated at the design heat pump inlet temperature, T_L and T_H, to convert building loads to ground loads gives essentially the same results as the length obtained using a variable COP.

For Test 2, and using the peak durations provided by Shonder et al. (2000), the results vary from 91.1 m to 108.0 m, i.e. 3.6% below and 14.3% above the mean. The upper limit of 108.0 m is reduced to 94.9 m when the results of one of the tools are excluded. When compared to the original comparison of Shonder et al. (2000), it appears that current tools are in closer agreement. However, this test is not severe with a relatively small annual ground load imbalance.

For Test 3, the required length varies from 85.9 m to 115 m. These values are 13.9% below and 15.3% above the mean. It is shown that all of the $L2$ tools as well as one $L3$ and one $L4$ tool were unable to detect that the maximum required length is needed in the first year.

In Test 4, the cooling dominated load used by Bernier (2006) is applied to check if the sizing models can account accurately for the thermal interactions between the boreholes when the annual ground load is relatively highly imbalanced. The calculated lengths vary from 93.0 m to 128.9 m which represents values that are, respectively, 21.7% below and 8.5% above the mean. One group of tools, which includes $L2$, $L3$ and $L4$ tools, shows a relatively good agreement with minimum and maximum values of 121.0 and 128.9 m., a 6% difference. This tends to indicate that even though $L2$ methods (three-pulse method) appear to be less sophisticated that $L4$ methods (hourly simulations), they give similar results if used with the correct set of inputs. A second group of tools that account for short-term effects show excellent agreement with calculated lengths of 118.4 m, 117.0 m, and 118.5 m, respectively. Finally, two tools have determined lengths that are much lower than the rest of the tools (103.9 m and 93.0 m). Clearly, these two tools cannot properly account for borehole thermal interaction caused by a large annual ground load imbalanced.

In the final part of the paper, a sensitivity analysis is performed on Test 4. The main conclusion of this sensitivity analysis is that tools vary differently to a change in parameters. For example, when the peak load magnitude is varied by ± 10%, some tools predict length variations of + 6.5% and -6.5%, while other tools predict variations about half as important.

This work provides a set of test cases that can be used to compare other software tools against the ones used in the present study with the ultimate goal of improving the reliability of design methods for sizing vertical ground heat exchangers.

Acknowledgments

The authors would like to thank Professor Jeffrey Spitler from Oklahoma State University for providing a temporary GLHEPro license for this study. Furthermore, the authors would like to express their appreciation to Carla Isabel Montagud Montalva for letting us get access to the experimental data of the Valencia case. Finally, the financial support provided by the Natural Science and Engineering Research Council of Canada through a discovery grant and the Smart Net-Zero Energy Buildings Strategic Research Network is gratefully acknowledged.

7.6 Nomenclature

Capital letters

B = distance between the boreholes (m)

Cp_f = thermal heat capacity of the circulating fluid (kJ.kg^{-1}K^{-1})

Cp_{gr}= thermal heat capacity of the backfilling material (kJ.kg^{-1}K^{-1})

Cp_p= thermal heat capacity of the pipe (kJ.kg^{-1}K^{-1})

Cap_H, Cap_C= heat pump capacities in heating and cooling (kW)

COP_H, COP_C= heat pump coefficient of performances in heating and cooling (---)

D = distance between the ground surface and the top of boreholes (m)

F_{sc}= short circuit heat loss factor in the borehole (---)

G= thermal response factors calculated by the infinite cylindrical source model (---)

H = borehole depth (m)

L = total overall length of boreholes (m)

L_s, L_M, L_j= length of single and multiple heat exchangers and the length of pipe in the jth ground layer (m)

N_b = total number of boreholes (---)

N_U = number of U tubes in each borehole (---)

PLF_m= part load factor during the design month (---)

R_b = effective thermal resistance of the boreholes (m.K.W^{-1})

R_c = contact thermal resistance (m.K.W^{-1})

R_p= pipe thermal resistance (m.K.W^{-1})

R_y, R_m, R_h, yearly, monthly and hourly peak load ground thermal responses (m.K.W^{-1})

R_{s_j}= ground thermal resistance related to the jth ground layer surrounding the borehole (m.K.W^{-1})

RTR_i= ratio of run time to the cycle time of month i (---)

$Run_{f,H}$, $Run_{f,C}$= heating and cooling runtime fractions (---)

SG = specific gravity of the fluid (---)

T_g, T_{g_k}= initial temperature of the ground and the average ground temperature in month k (°C)

$T_{in,hp}$ = inlet fluid temperature of the heat pump (°C)

$T_{out,hp}$ = outlet fluid temperature of the heat pump (°C)

T_H = maximum inlet fluid temperature to the heat pump (°C)

T_L = minimum inlet fluid temperature to the heat pump (°C)

T_m, $T_{f,avg}$ = mean fluid temperature in the borehole (°C)

T_P = Temperature penalty (°C)

W= compressor power at peak load condition (kW)

Small letters

d_p = half of the center-to-center spacing between the legs of a U-tube (mm)

g_N, g_1= thermal response factors evaluated for N and 1 boreholes by the finite line source method (---)

h_{conv}= internal convection coefficient in pipes ($W.m^{-2}K^{-1}$)

k_f = fluid thermal conductivity ($W.m^{-1}K^{-1}$)

k_g = soil thermal conductivity ($W.m^{-1}K^{-1}$)

k_{gr} = thermal conductivity of the backfilling material ($W.m^{-1}K^{-1}$)

k_p = pipe thermal conductivity ($W.m^{-1}K^{-1}$)

$\dot{m}_f$ = flow rate of the circulating fluid ($kg.s^{-1}$)

q_g'' = geothermal heat flux ($W.m^{-2}$)

q_y, q_m, q_h= yearly, monthly and hourly building or ground loads (kW)

r_b = borehole radius (mm)

$r_{p,i}$ = inner radius of U-pipe legs (mm)

$r_{p,o}$ = outer radius of U-pipe legs (mm)

t_y, t_m, t_h = duration of yearly, monthly and hourly peak load pulses (h)

Greek letters

α_g = soil thermal diffusivity ($m^2.day^{-1}$)

ρ_f = density of the heat carrier fluid ($kg.m^{-3}$)

μ_f = viscosity of the heat carrier fluid ($Kg.m^{-1}s^{-1}$)

7.7 References

ASHRAE, (2015). Chapter 34 - Geothermal Energy. ASHRAE Handbook - Applications. Atlanta, Georgia, ASHRAE.

ASHRAE, (1995). Chapter 32 - Geothermal Energy. ASHRAE Handbook - Applications. Atlanta, Georgia, ASHRAE.

Ahmadfard, M., and Bernier, M. (2018). Modifications to ASHRAE's sizing method for vertical ground heat exchangers. In press. Science and Technology for the Built Environment. (doi.org/10.1080/23744731.2018.1423816)

Ahmadfard, M., Bernier, M., and Kummert, M. (2016). Evaluation of the design length of vertical geothermal boreholes using annual simulations combined with GenOpt. Proceedings of the eSim 2016 Building Performance Simulation Conference, May 3-6, McMaster University, Hamilton, Ontario, Canada, pp. 46-57.

Ahmadfard, M., and Bernier, M. (2014). An alternative to ASHRAE's design length equation for sizing borehole heat exchangers. ASHRAE Annual Conference, Seattle, WA, 1–8.

Banks, D. (2008). An introduction to thermogeology: ground source heating and cooling, Blackwell Publishing Ltd, Oxford, UK.

Bernier, M.A., Chahla, A. and Pinel, P. (2008). Long-term ground temperature changes in geo-exchange systems. ASHRAE Transactions, 114(2):342-350.

Bernier, M. (2006). Closed-loop ground-coupled heat pump systems. ASHRAE Journal, 48:12-19.

Bernier, M.A., Pinel, P., Labib, R., and Paillot, R. (2004). A multiple load aggregation algorithm for annual hourly simulations of GCHP systems. HVAC&R Res, 10(4):471–487.

Bernier, M. (2002). Uncertainty in the Design Length Calculation for Vertical Ground Heat Exchangers, ASHRAE Transactions, 108(1): 939-944.

Bernier, M. (2000). A review of the cylindrical heat source method for the design and analysis of vertical ground-coupled heat pump systems. In Fourth International Conference on Heat Pumps in Cold Climates.

Bertagnolio, S., Bernier, and M., Kummert, M. (2012). Comparing vertical ground heat exchanger models. Journal of Building Performance Simulation. 5: 369-383.

BlOCON, (2015). Earth Energy Designer (EED) v3.2.

Bose, J. E., Parker, J. D., and McQuiston, F. C. (1985). Design/Data Manual for Closed-Loop Ground-Coupled Heat Pump Systems. Atlanta, Georgia: ASHRAE.

Capozza, A., Zarrella, A., and De Carli, M. (2015a). Analysis of Vertical Ground Heat Exchangers: The New CaRM Tool. Energy Procedia, 81, 288-297.

Capozza, A., Zarrella, A., and De Carli, M. (2015b). Long-term analysis of two GSHP systems using validated numerical models and proposals to optimize the operating parameters. Energy and Buildings, 93, 50-64.

Capozza, A., De Carli, M. and Zarrella, A., (2012). Design of borehole heat exchangers for ground-source heat pumps: A literature review, methodology comparison and analysis on the penalty temperature. Energy and Buildings, 55, 369-379.

Cane, R. L. D., and Forgas, D. A. (1991). Modeling of ground-source heat pump performance. ASHRAE Transactions, 97(1), 909-925.

Caneta Research Inc., (1992). Development of algorithms for GSHP heat exchanger length prediction and energy analysis, Efficiency and Alternatives Energy Analysis Technology Branch, Natural Resources Canada, Ottawa, Ontario.

Chiasson, A.D. (2016).Geothermal heat pump and heat engine systems: theory and practice. Asme press and John Wiley & Sons, Ltd.

Cimmino, M., and Bernier, M. (2014). Effects of unequal borehole spacing on the required borehole length, ASHRAE Transactions, 120(2):158-173.

Claesson, J., Eskilson, P. (1987). Conductive heat extraction by a deep borehole. Analytical studies, in Eskilson, P. (ed.), Thermal Analysis of Heat Extraction Boreholes, Lund, Sweden: Department of Mathematical Physics, University of Lund.

Cooper, L.Y. (1976). Heating of a cylindrical cavity. International Journal of Heat and Mass Transfer, 19:575-577.

Cui, P., Sun, C., Diao, N. and Fang, Z., (2015). Simulation modelling and design optimisation of vertical ground heat exchanger-GEOSTAR program. Procedia Engineering, 121, 906-914.

Cullin, J.R. Spitler, J.D. Montagud, C. Ruiz-Calvo, F. Rees, S.J. Naicker, S.S. Konečný, P. Southard L.E., (2015). Validation of vertical ground heat exchanger design methodologies, Sci. Technol. Built Environ., 21(2):137–149.

Cullin, J. R. Ruiz-calvo, F. Montagud, C. and Spitler, J. D. (2014). Experimental validation of ground heat exchanger design methodologies using real, monitored data. ASHRAE Transactions 120:1-13.

Cullin, J.R. and Spitler, J.D. (2011). A computationally efficient hybrid time step methodology for simulation of ground heat exchangers. Geothermics, 40:144-156.

Eskilson, P. (1987). Thermal Analysis of Heat Extraction Boreholes," Doctoral Thesis, Department of Mathematical Physics, University of Lund, Lund.

Fossa, M. (2017). Correct design of vertical borehole heat exchanger systems through the improvement of the ASHRAE method, Science and Technology for the Built Environment, 23(7):1080-1089.

Fossa, M., Rolando, D. (2016). Improved Ashrae method for BHE field design at 10 tear horizon. Energy and buildings, 116:114-121.

Fossa, M., Rolando, D. (2015). Improving the Ashrae method for vertical geothermal bore field design. Energy and buildings, 93:315-323.

Fossa, M., Rolando, D. (2013). An improved method for vertical geothermal borefield design using the Temperature Penalty approach, European geothermal congress (EGC), 1-8.

Fossa, M. (2011). The temperature penalty approach to the design of borehole heat exchangers for heat pump applications. Energy and Buildings, 43(6):1473-1479.

GLHEPRO 5.0. (2016). GLHEPRO 5.0 for Windows. International Ground Source Heat Pump Association, School of Mechanical and Aerospace Engineering: Oklahoma State University.

GLHEPRO 4.0. (2007). GLHEPRO 4.0 for Windows. International Ground Source Heat Pump Association, School of Mechanical and Aerospace Engineering: Oklahoma State University.

Hart, D. P., and Couvillion, R. (1986). Earth-coupled heat transfer. prepared for the National Water Well Association, Dublin, OH.

Hellström, G., Sanner, B., Klugescheid, M., Gonka, T., Mårtensson, S., (1997). Experiences with the borehole heat exchanger software EED. Proceedings MEGASTOCK 97, Sapporo, 247–252.

Hellström, G., Sanner, B., (1994). Software for dimensioning of deep boreholes for heat extraction. Proceedings CALORSTOCK 94, Espoo/Helsinki, 195–202.

Hellström, G., (1991). Ground heat storage: thermal analyses of duct storage systems. Department of Mathematical Physics, Lund University, Sweden.

Hellström, G. (1989). Duct ground heat storage model: Manual for computer code. Lund, Sweden: University of Lund, Department of Mathematical Physics.

Javed, S., and Spitler. J., (2017). Accuracy of borehole thermal resistance calculation methods for grouted single U-tube ground heat exchangers. Applied Energy, 187: 790-806.

Javed, S. and J. Spitler. (2016). Calculation of borehole thermal resistance. In: Simon J. Rees, editor. Advances in ground-source heat pump systems. Woodhead Publishing. P.63-95.

Judkoff, R. Neymark, J., (1998). The BESTEST method for evaluating and diagnosing building energy software, in: Proceedings of the ACEEE Summer Study on Energy Efficiency in Buildings, 5:175–190.

Judkoff, R. Neymark, J., (1995). IEA-BESTEST and diagnostic method. Golden, CO: NREL.

Kavanaugh, S. P. and K. Rafferty 2015. Geothermal Heating and Cooling - Design of Ground-Source Heat Pump Systems. Atlanta, Georgia: ASHRAE.

Kavanaugh, S.P., (2010). Groud Heat Exchangers – Determining Thermal Resistance, ASHRAE Journal, 52(8), 72-75.

Kavanaugh, S. P. and K. Rafferty (1997). Ground-Source Heat Pumps-Design of Geothermal Systems for Commercial and Institutional Buildings. Atlanta: ASHRAE.

Kavanaugh, S., (1995), A design method for commercial groundcoupled heat pumps. ASHRAE Transactions, 101(2), 1088-1094.

Kavanaugh, S.P. and Calvert, T.H., (1995). Performance of ground source heat pumps in North Alabama. Final Report, Alabama Universities and Tennessee Valley Authority Research Consortium. University of Alabama, Tuscaloosa.

Kavanaugh, S. P. (1991). Ground and Water Source Heat Pumps - A Manual for the Design and Installation of Ground-Coupled, Ground Water and Lake Water Heating and Cooling Systems in Southern Climates. Tuscaloosa, AL: University of Alabama.

Kavanaugh, S. P. (1988). Ground and water source heat pump performance and design for southern climates. Fifth Symposium on Improving Building Systems in Hot and Humid Climates, Houston, Texas.

Klein, S. A., et al. (2014). 'TRNSYS 17 – A Transient System Simulation program, User manual. Version 17.2. Madison, WI: University of Wisconsin-Madison.

Kurevija, T. Vulin, D. and Krapec, V. (2012). Effect of borehole array geometry and thermal interferences on geothermal heat pump system. Energy Conversion and Management, 60, 134-42.

Lamarche, L. (2016). Short-time modelling of geothermal systems, proceedings of ECOS, the 29th international conference on efficiency, cost, optimization, simulation and environmental impact of energy systems, Portorož, Slovenia.

Lamarche, L. Dupré, G. Kajl, S. (2008). A new design approach for ground source heat pumps based on hourly load simulations, ICREPQ Conference, Santander, 338/1–5.

Li, M., Zhuo, X. and Huang, G. (2017). Improvements on the American Society of Heating, Refrigeration, and Air-Conditioning Engineers Handbook equations for sizing borehole ground heat exchangers, Science and Technology for the Built Environment, 23:8, 1267-1281.

Monzó, P. Bernier, M. Acuña, J. Mogensen, P. (2016). A monthly based bore field sizing methodology with applications to optimum borehole spacing. ASHRAE Trans, 122 (1), 111–126.

OSU, (1988). Closed-Loop/Ground-Source Heat Pump Systems Installation Guide.

Philippe, M. Bernier, M. and Marchio, D. (2010). Sizing calculation spreadsheet vertical geothermal borefields. ASHRAE Journal, 20-28.

Ping, C., Hongxing, Y. and Zhaohong, F., (2007). Simulation modelling and design optimisation of ground source heat pump systems. HKIE transactions, 14(1), 1-6.

Sanaye, S. and Niroomand, B., (2009). Thermal-economic modeling and optimization of vertical ground-coupled heat pump. Energy Conversion and Management, 50(4), 1136-1147.

Sanner, B., (2012). Gshp design: design methods, calculations, software demo. International Geothermal days, Romania.

Shonder, J. A. Baxter, V. D. Hughes, P. J. and Thornton, J. W. (2000). A comparison of vertical ground heat exchanger design software for commercial applications. ASHRAE Transactions, 106:831-842.

Shonder, J. A. Baxter, V. Thornton, J. and Hughes, P. (1999). A new comparison of vertical ground heat exchanger design methods for residential applications, ASHRAE transactions, 105, 1179–1188.

Spitler, J.D. (2016). Latest Developments and Trends in Ground-Source Heat Pump Technology, Proceedings of the European geothermal Congress, Strasbourg, France, 19-24 sepr. 2016.

Spitler J. D. and Bernier., M. (2016). Advances in ground-source heat pump systems - Chapter 2: Vertical borehole ground heat exchanger design methods. Edited by S. Rees. To be published.

Spitler, J. D., Bernier, M., Kummert, M., Cui, P., Liu, X. (2009). Preliminary intermodel comparison of ground heat exchanger simulation models. Effstock 2009, Stockholm, paper#115, 8 pages.

Spitler, J. D. (2000). GLHEPRO-A Design Tool for Commercial Building Ground Loop Heat Exchangers. in Proceedings of the Fourth International Heat Pumps in Cold Climates Conference, Aylmer, Québec.

Staiti M., Angelotti A., (2015). Design of Borehole Heat Exchangers for Ground Source Heat Pumps: A Comparison between Two Methods, Energy Procedia, 78, 1147-1152.

Sutton, M.G., Nutter, D.W., Couvillion, R.J. and Davis, R.K., (2002). Comparison of multilayer borefield design algorithm (MLBDA) to available GCHP benchmark data/Discussion. ASHRAE Transactions, 108, 82.

TESS. (2012). TESS Component Libraries. Madison, Wisconsin: Thermal Energy Systems Specialists.

TESS, (2005). TESS Libraries Version 2.02, Reference Manuals (13 Volumes). Thermal Energy Systems Specialists, Madison, WI. http://tess-inc.com.

Thornton, J. W., McDowell, T. P. and Hughes, P. J., (1997). Comparison of five practical vertical ground heat exchanger sizing methods to a Fort Polk data/model benchmark, ASHRAE Transactions, 103, 675-83.

UNI 11466. (2012). Sistemi geotermici a pompa di calore- Requisiti per il dimensionamento e la progettazione. Milano: UNI.

Xu, X., Spitler, J.D. (2006). Modeling of vertical ground loop heat exchangers with variable convective resistance and thermal mass of the fluid. Proceedings of the 10th International Conference on Thermal Energy Storage – Ecostock 2006, Pomona, NJ.

Yavuzturk, C., Spitler, J. D. (1999). A short time step response factor model for vertical ground loop heat exchangers. ASHRAE Transactions, 105, 475-485.

Yavuzturk, C., Spitler, J. D., and Rees, S. J. (1999). A transient two dimensional finite volume model for the simulation of vertical U-tube ground heat exchangers. ASHRAE Transactions, 105(2), 465-474.

7.8 Appendix A

Table 7-7 presents test cases found in the literature and used for validation of different sizing tools.

Table 7-7: Sizing test cases found in the literature

Level	Reference	Main caracteristic	Bore field	Solved by
L1	Sanaye, and Niroomand (2009)	Synthetic problem	Single borehole	Modified version of IGSHPA method
The model is modified to account for the thermal short-circuit and the convection effects. The method is applied to a synthetic example and then the results are compared with the ones evaluated by the IGSHPA and ASHRAE methods and the recommendations presented by Kavanaugh and Calvert (1995). The results had respectively 1.01, 3.9 % and 7.51 % difference.				
L2	Kavanaugh (1995)	An office building in Birmingham	5×6	GchpCalc, developed based on Eq. 7.3
Designed for 10 years. Load pulses are calculated using a design day in cooling and the annual equivalent full load hours of each zone. Constant COPs are applied. The equivalent diameter concept is used to calculate the borehole thermal resistance. Solved with and without ground water movements. Some design alternatives for minimizing costs are also examined.				
L2	Italian standard UNI 11466 (2012)	A residential and an office buidlings	3 and 15 boreholes	ASHRAE equation (Eq. 7.3)
Designed for 10 years. Uses monthly average building loads, annual heating and cooling equivalent full hours, part load factors, constant COPs. The maximum heating and cooling power of the system are used as peak loads.				
L2 and L3	Staiti and Adriana (2015)	A residential and an office buidlings	Single borehole and various rectangular patterns from 1×5 to 4×5	ASHRAE classical equation and GLHEpro
Designed for 10 years, The authors applied two sizing models to the two sizing problems introduced in Italian standard and checked the effects of various design alternatives such as the two temperature limits of the heat pumps, borehole spacing and the thermal conductivity of the ground. Compared to GLHEPRO, the results show that the ASHRAE sizing equation over estimates the boreholes length up by up to 27%.				
L2	Bernier (2000)	Bernier (2000)	-----	Modified ASHRAE equation
Designed for 10 years. Building loads are converted to ground loads using a constant COP. It is suggested to calculate ground loads using hourly simulations instead of a design day load. It is also suggested to use the real borehole diameter instead of the equivalent U-tube diameter. In the modified ASHRAE equation, the part load factor (PLF) is eliminated, the bore field configuration or borehole spacing is not specified and a value is just assumed for the temperature penalty.				
L2	Lamarche (2016)	Cooling dominated building	Single borehole	Alternative method (Eq. 7.7)
It is showed that the effect of short time g-functions appears both in R_{gm} and R_{gh}. For the term $q_h(R_{gh} + R_b)$ in numerator of Eq. 7.7, three alternatives are suggested and by each one the problem is solved and the final results are compared. Designed for 10 years. The problem is introduced to show the impact of short-term effects on the overall length. The sizing problem introduced by Philippe (2010) is used with some modifications. It is showed that by neglecting the thermal capacity of the boreholes the length is oversized.				
L2	Li et al. (2017)	Four cases introduced by Cullin et al. (2015)	1×3, 2×3, 2×6 and 7×8	An iterative alternative model based on the ASHRAE equation
Level 3, Designed for various numbers of years, It is shown that results evaluated by the proposed method are shorter (Due to using short time effects) and in three cases closer to the actual lengths compared to the values determined by Cullin et al. (2015) by using ASHRAE equation.				

Table 7-7 (continued): Sizing test cases found in the literature

L2	Fossa and Rolando (2013, 2015, 2016), Fossa (2017)	Cooling and heating cases	Various arrangements	Modified ASHRAE equation (Eq. 7.4) with correlated temperature penalties
In these papers, a series of correlated equations are developed and modified for evaluation of the temperature penalty required in ASHRAE equation.				
L3	Bank (2008)	Synthetic problem	3×5	EED
The test case is not solved as a sizing problem. It is introduced to show the effects of various design parameters as the average and peak heat loads, balanced or unbalanced loads, boreholes configuration and boreholes spacing. It is first solved based on the heating loads and next based on both heating and cooling loads. The system is sized for one and twenty five years and as the system has a small net annual ground load the results do not vary significantly.				
L3	Hellstrom and Sanner (1994), Hellström et al. (1997) and Sanner (2012)	Various synthetic problems	-----	EED
These papers introduce the functionality of different versions of the EED.				
L3	Spitler (2000)	A two floor office in Ottawa divided into seven zones	5×9	GLHEPRO
Designed for 12 years. Building loads are converted to ground loads using a correlation for the COP which depends on the inlet temperature. Ground loads are relatively balanced. The relatively small difference between T_g and T_L caused the boreholes length to be sensitive to T_L.				
L3	Sutton et al. (2002)	An elementary school located in Lincoln, Nebraska	12×10	Multilayer bore field design algorithm (MLBDA)
The model is based on Hellström's duct storage model (1991) but can be applied to a series of geological layers. Level 3. Designed for 10 years. Problem based on the work of Shonder et al. (2000) except that two heating and cooling scenarios are defined for the building, Ground loads are applied, The peak heat loads are assumed to occur on the 21st of each month and their duration is assumed to be 8 hours. For the heating dominated case, the model is compared against five sizing tools including the DST model but for the cooling case only the DST model is used for comparisons.				
L3	Ping et al. (2007)	Commercial building in the city of Shandong in China	-----	GEOSTAR
The sizing program uses the finite line source and a quasi-three dimensional models for the heat transfer inside and outside of the boreholes, the quasi-3d model accounts for the fluid temperature variation along the boreholes depth and the thermal interaction between the boreholes legs. The sizing problem is related to a real GSHP installation. Two values are reported for the cooling and heating peak loads but the peak durations are not reported. Borehole configuration is not mentioned. The system is sized for 20 years and the effects of certain parameters as the ground and grout thermal conductivities, borehole spacing, shank distance and annual load imbalance load are examined. More details about the GEOSTAR program are provided by Cui et al. (2015).				
L4	Lamarche et al. (2008)	Residential building in Montreal	2×2	Hourly load simulation design model (HLSD)
The HLSD model simulates the thermal response of the hourly loads with the use of inverse Laplace transform of the g-functions instead of using load aggregation. The method can take into account the short time effects and can accept variable COPs and determine iteratively the ground loads at each hourly step. Designed for 10 years using building loads. The problem is also solved using DST, EED and GS2000. GS2000 is a level three sizing model which uses cylindrical and line source models. For HLSD and DST models hourly loads and for EED and GS2000 monthly average and peak heat loads are used. The ground heat loads are evaluated iteratively based on the COP values provided by TRNSYS and HLSD models. For EED and GS2000, they are evaluated based on the average COP values. The borehole thermal resistance evaluated by the DST was used in EED and HLSD simulations. For GS2000, it is not possible to enter the borehole thermal resistance as an input. Some parameters are also missing: i.e. B, $C_{p,g}$, R_b , ṁ and peak durations.				

Table 7-7 (continued): Sizing test cases found in the literature

L4	Capozza et al. (2015a and b)	Heating dominated office in Padova and a cooling dominated office near Milan	16 boreholes in a semi L-shape pattern, 51 boreholes in a semi rectangular pattern	CARM model and ASHRAE equation (Eq. 7.3)
CARM is a thermal capacity and resistances model; it is not a sizing model. However, it determines the entering fluid temperature of the heat pumps on hourly basis. The authors used their CARM method to model two real cases and also check the effects of possible modifications such as increasing the number of boreholes or the use of hybrid systems. The ASHRAE equation is used to size the boreholes and then the obtained lengths are compared with real boreholes lengths. Designed for 10 years. Building loads are used with constant COPs. In both problems the peak loads and their durations are not reported. For the 51 borehole case, only the monthly average loads were available. The temperature penalty required in ASHRAE sizing equation is obtained by the model suggested Capozza et al. (2012). For the 16 borehole case, the ASHRAE equation underestimated the result by 4% while for the other case it oversized the boreholes by 41.5%. The authors explain this difference due to inaccuracy of the ground loads.				

7.9 Appendix B

Table 7-8: Results presented in Figure 7-7 in addition to the mean and individual differences from the mean

Scenario:	Sizing model	A	B	C	D	E	Est	F	G	H	Hst	I	J	K	L COPc	L COPv	mean
Level		L2	L2	L2	L2	L2	L2	L2	L3	L3	L3	L3	L3	L4	L4	L4	
Test 1-a, 6 hr peak -R_b calculated by tool	L (m)	61.7	62.1	60.7	60.7	57.8	54.8	58.0	60.7	57.8	54.8	59.8	56.7	56.8	58.7	----	58.6
	Dif. %	5.2	5.9	3.5	3.5	-1.4	-6.6	-1.1	3.5	-1.4	-6.6	2.0	-3.4	-3.1	0.1	----	
	Rb (m-K/W)	0.122	0.127	0.122	0.122	0.122	0.122	0.126	0.12	0.12	0.12	0.127	0.127	0.127	0.125	----	0.123
Test 1-a, 6 hr peak -R_b=0.13 (m-K/W)	L (m)	63.7	62.7	62.7	62.7	59.8	56.6	59.0	62.6	59.7	56.5	60.0	57.3	57.0	59.7	----	60.0
	Dif. %	6.2	4.5	4.5	4.5	-0.3	-5.7	-1.7	4.3	-0.5	-5.8	0.0	-4.5	-5.0	-0.5	----	
Test 1-a, 1 hr peak -R_b=0.13 (m-K/W)	L (m)	53.4	----	52.8	52.8	46.9	40.0	43.0	52.7	46.8	39.9	44.1	39.1	57.0	59.7	----	48.3
	Dif. %	10.5	----	9.3	9.3	-2.9	-17.2	-11.0	9.1	-3.2	-17.4	-8.7	-19.1	18.0	23.5	----	
Test 1-b, 6 hr peak -R_b=0.13 (m-K/W)	L (m)	81.3	80.0	80.0	79.9	76.2	72.1	76.2	75.9	80.0	71.3	76.7	72.6	72.6	74.8	74.2	76.3
	Dif. %	6.6	4.9	4.9	4.8	-0.1	-5.5	-0.1	-0.5	4.9	-6.5	0.6	-4.7	-4.8	-1.9	-2.7	
Test 2, 6 hr peak -R_b=0.113 (m-K/W)	L (m)	89.7	89.1	90.2	90.2	86.9	85.5	102.0	90.1	86.7	85.1	88.0	87.2	87.3	88.9	----	89.1
	Dif. %	0.7	0.0	1.3	1.3	-2.4	-4.0	14.5	1.2	-2.7	-4.5	-1.2	-2.1	-2.0	-0.2	----	
Test 2, various peak -R_b=0.113 (m-K/W)	L (m)	94.6	----	94.9	94.8	92.2	91.4	108.0	94.7	92.1	91.1	93.6	93.2	93.2	94.5	----	94.5
	Dif. %	0.1	----	0.4	0.3	-2.4	-3.3	14.3	0.2	-2.5	-3.6	-0.9	-1.3	-1.4	0	----	
Test 3, 6 hr peak -R_b=0.1 (m-K/W)	L (m)	101.9	87.9	92.4	92.6	87.2	85.9	115.0	114.2	111.1	109.0	87.8	109.6	87.2	114.4	----	99.7
	Dif. %	2.2	-11.9	-7.3	-7.1	-12.6	-13.9	15.3	14.5	11.4	9.3	-12.0	9.9	-12.6	14.7	----	
Test 4, 6 hr peak -R_b=0.2 (m-K/W)	L (m)	103.9	----	125.8	125.1	122.5	118.4	93.0	125.1	121.7	117.0	123.0	118.5	121.0	128.9	----	118.8
	Dif. %	-12.5	----	5.9	5.3	3.1	-0.3	-21.7	5.3	2.5	-1.5	3.6	-0.2	1.9	8.5	----	

CHAPTER 8 GENERAL DISCUSSION

The overarching goal of this thesis is to improve vertical ground heat exchanger sizing tools. Steps towards achieving this goal have been accomplished by: improving the ASHRAE sizing equation; developing an hourly simulation based sizing model; providing test cases for comparing various tools against each other; and performing a thorough inter-model comparison.

The first contribution of this work is the use of g-functions, calculated based on the finite line source analytical solution, to evaluate the effective ground thermal resistances required in the ASHRAE sizing equation. Thus, the temperature penalty, which is the subject of some debate among ground heat exchanger modellers, is no longer needed since g-functions intrinsically account for borehole-to-borehole thermal interferences. In addition, the equation is no more restricted to rectangular bore fields of equally-spaced boreholes. However, due to the dependency of the g-functions on the borehole length, an iterative procedure is required.

The second contribution of this work is related to the way that the g-functions are evaluated through the sizing procedure. The required g-functions do not need to be evaluated over the full g-function curve. It is shown that they can be evaluated dynamically in each iteration without using temporal superposition, correction factors or interpolation of pre-determined g-functions. Thus, the ASHRAE sizing equation will require only three g-function values at each iteration. Aside from the effect of temporal superposition on g-functions, bore field symmetry and the optimum number of segments as well as the convergence criteria have been examined to reduce calculation time while maintaining accuracy. For example, for a 12×10 bore field sized with 12 segments, the length evaluated with and without temporal superposition have a 1.2 % relative difference. However, calculation time is about 10 times longer with temporal superposition. It is also shown that longer boreholes need fewer borehole segments. This is due to the fact that the borehole end effects are proportionally less significant for longer boreholes.

The third contribution of this work concerns the inclusion of short term effects in the ASHRAE sizing equation using the concept of short-term g-functions. It is shown that the short term effects have an impact on the hourly and monthly effective ground thermal resistances. In one particular example, accounting for borehole thermal capacity lead to a reduction of about 10% of the required length when a one-hour peak load is used. Based on this work it is suggested to modify the ASHRAE sizing equation to include short-term effects.

The fourth contribution of this work is related to combining the duct ground heat storage (DST) model in TRNSYS to GenOpt. This combination enables the DST model to size bore fields automatically through an optimization process. This work provided an additional $L4$ tool to the limited arsenal of hourly-based simulation tools. In addition, with this approach, it is possible to examine heat pump COP variations with the inlet temperature. This capability proved to be useful in the inter-model comparison to assess the importance of this variation.

Finally, this work makes an important contribution in the area of inter-model comparison by providing a series of test cases which are then used in the comparison. A spreadsheet tool summarizes the loads used in the test cases and shows the obtained results with various sizing tools. It is hoped that this tool will serve the GSHP community as benchmark tests for current and future VGHE sizing models. In the meantime, the inter-model comparison shows that a significant number of surveyed tools are unable to predict the borehole required length correctly when the maximum length is needed in the first year of operation. Also, when the annual ground load is relatively highly imbalanced, sizing tools exhibit differences of up to 30%. Finally, significant differences are noted among tools that account for short term effects and those that do not.

CHAPTER 9 CONCLUSION AND RECOMMENDATIONS

Based on the present work, a number of recommendations can be made for future studies.

The main theme of this thesis is a comparison of sizing models for long vertical boreholes that are connected in parallel and have one internal U-tube. A similar exercise should be done for boreholes that have two or three U-tubes and that are connected in series or in a combination of parallel and series circuits. For short boreholes, end effects are much more important and checks should be made to see if all sizing programs account for these effects. Also, the inter-model comparisons could be extended to horizontal systems.

The comparisons made in this thesis are implemented with a limited number of sizing methods. It would be appropriate to complete the inter-model comparison with every sizing tool on the market.

For long boreholes (>200 m) or when the fluid flow rate in boreholes is small, short-circuit effects become more important and it is unclear if all sizing tools can handle such effects.

The g-functions that are evaluated in this work are calculated by assuming a constant and uniform borehole wall temperature for all boreholes in accordance with the original g-function definition. However, this assumption does not necessarily correspond to all cases in reality. Therefore, it would be interesting to test other boundary conditions and quantify their impact on borehole length.

Last but not least, as mentioned in the literature review, not much work has been done on the approximation of peak loads. More research is required on this topic as peak loads have an important effect on the results of sizing programs.

BIBLIOGRAPHY

Ahmadfard, M., Bernier, M. (2014). An alternative to ASHRAE's Design Length Equation for Sizing Borehole Heat Exchangers, Proceedings of the ASHRAE annual conference, SE-14-C049, Seattle, USA.

Ahmadfard, M., Bernier, M., and Kummert, M. (2016). Evaluation of the design length of vertical geothermal boreholes using annual simulations combined with GenOpt. Proceedings of the eSim 2016 Building Performance Simulation Conference, May 3-6, McMaster University, Hamilton, Ontario, Canada, 46-57.

Ahmadfard, M. and Bernier, M. (2018). Modifications to ASHRAE's sizing method for vertical ground heat exchangers. In press. Science and Technology for the Built Environment. (doi.org/10.1080/23744731.2018.1423816).

Ahmadfard, M., Bernier, M. (2018). A review of vertical ground heat exchanger sizing tools including an inter-model comparison. Submitted to Renewable & Sustainable Energy Reviews on January 12th 2018.

Ambrose, E. R. (1966). Heat pumps and electric heating. New York: John Wiley and Sons, Inc.

ASHRAE Handbook, (2011). HVAC Applications, Geothermal Energy, Chapter 32.

Austin, W. A. I., Yavuzturk, C., and Spitler, J. D. (2000). Development of an in-situ system and analysis procedure for measuring ground thermal properties. ASHRAE Transactions, 106, 365-379.

Ball, D. A., Fischer, R. D., and Hodgett, D. L. (1983). Design methods for ground-source heat pumps, ASHRAE Transactions, 89, 416-440.

Bandos, T. V., Montero, Á., Fernández de Córdoba, P. J., and Urchueguía, J. F. (2011). Improving parameter estimates obtained from thermal response tests: Effect of ambient air temperature variations. Geothermics, 40(2), 136-143.

Bandos, T. V., Montero, Á., Fernández, E., Santander, J. L. G., Isidro, J. M., Pérez, J. (2009). Finite line-source model for borehole heat exchangers: effect of vertical temperature variations. Geothermics, 38(2), 263-270.

Bandyopadhyay, G., Kulkarni, M., and Mann, M. (2008a). A New Approach to Modeling Ground Heat Exchangers in the Initial Phase of Heat-Flux Build Up. ASHRAE Transactions, 114(2), 428-439.

Bandyopadhyay, G., Gosnold, W., and Mann, M. (2008b). Analytical and semi-analytical solutions for short-time transient response of ground heat exchangers. Energy and Buildings, 40(10), 1816-1824.

Banks, D. (2012). An introduction to thermogeology: ground source heating and cooling, 2nd edition. Somerset, NJ, USA, John Wiley & Sons.

Bauer, D., Heidemann, W., and Diersch, H.-J. (2011). Transient 3D analysis of borehole heat exchanger modeling. Geothermics, 40(4), 250-260.

Bauer, D., Heidemann, W., Müller-Steinhagen, H., and Diersch, H.-J. (2010). Thermal resistance and capacity models for borehole heat exchangers. International Journal of Energy Research, 35(4), 312-320.

Beier, R. A., and Smith, M. D. (2003). Minimum duration of in-situ tests on vertical boreholes. ASHRAE Transactions, 109(2), 475-486.

Bennet, J., Claesson, J. and Hellström, G. (1987). Multipole Method to Compute the Conductive Heat Flows to and Between Pipes in a Composite Cylinder. Notes on Heat Transfer 3-1987, Department of Building Technology and Mathematical Physics, University of Lund, Sweden.

Bernier, M. (2014). Sizing and simulating geothermal bore fields using thermal response factors, Proceedings of the 11th IEA Heat Pump conference, Montreal (Quebec), Canada, May 2014. Paper KN.3.1.1.

Bernier, M., Chahla, A., and Pinel, P. (2008). Long-term ground temperature changes in geo-exchange systems, ASHRAE Transactions, 114, 342-350.

Bernier, M. (2006). Closed-loop ground-coupled heat pump systems, ASHRAE Journal, 48, 12-19.

Bernier, M., Pinel, P., Labib, R., and Paillot, R. (2004). A multiple load aggregation algorithm for annual hourly simulations of GCHP systems. HVAC&R Research, 10(4), 471-487.

Bernier, M. A. (2002). Uncertainty in the design length calculation for vertical ground heat exchangers, in ASHRAE Winter Meeting, Atlantic City, NJ, United States, 939-944.

Bernier, M. A. (2001). Ground-coupled heat pump system simulation, ASHRAE Transactions, 107, 605-616.

Bose, J. (1982). Water source HVAC manual, University extension, Oklahoma State University, Stillwater, OK: Oklahoma State Univ.

Bose, J. E. (1981) Design and testing of solar assisted earth coils, Final report to DOE, Contract EM-78-S-01-4257.

Bose, J. E., Parker, J. D., and McQuiston, F. C. (1985). Design/data manual for closed-loop ground-coupled heat pump systems. Atlanta: Oklahoma State University for ASHRAE.

Briggs, R. S., Lucas, R. G., and Taylor, T. (2003). Climate Classification for Building Energy Codes and Standards: Part 2 - Zone Definitions, Maps and Comparisons, ASHRAE Transactions, 109, 122-130.

Cane, R. L. D., Clemes, S. B., Morrison, A. and Hughes, P. J. (1995). Heat exchanger sizing for vertical closed loop ground source heat pumps, presented at the ASME/JSME/JSES international Solar Energy Conference, Maui, Hawaii.

Caneta Research Inc., (1992). Development of algorithms for GSHP heat exchanger length prediction and energy analysis, Efficiency and Alternatives Energy Analysis Technology Branch, Natural Resources Canada, Ottawa, Ontario.

Caneta Research Inc., (1993). Validation of ground source heat pump models for large buildings, Public works Canada, Ottawa, Ontario.

Caneta Research Inc., (1998). Cadmus Group Inc., and Science applications International Corp., Operating experiences with commercial ground-source heat pump systems. Atlanta, Georgia: American Society of Heating, Refrigeration and Air conditioning Engineers, Inc.

CANMET, (2005). Clean Energy Project Analysis: RETScreen Engineering & Cases Textbook-ground-source heat pump project analysis chapter. Minister of Natural Resources Canada, CANMET Energy Technology Center, Varennes.

Carslaw, H. S. and Jaeger, J. C. (1946). Conduction of Heat in Solids. Oxford, UK: Claremore Press.

Carslaw, H. S. and J. C. Jaeger. (1959). Conduction of heat in solids. Oxford, U.K.:Claremore Press.

Chiasson, A. D., Yavuzturk, C., and Talbert., W. J. (2004). Design of School Building HVAC Retrofit with Hybrid Geothermal Heat-Pump System, Journal of Architectural Engineering, 10, 103-111.

Cho, H., and Choi, J.M. (2014). The quantitative evaluation of design parameter's effects on a ground source heat pump system, Renewable energy, 65, 2-6.

Cimmino, M., and Bernier, M. (2014). A semi-analytical method to generate g-functions for geothermal bore fields, International Journal of Heat and Mass Transfer, 70, 641-650.

Cimmino, M., and Bernier, M., Adams, F.A., (2013a). A contribution towards the determination of g-function using the finite line source, Appl. Therm. Eng., 51, 401-412.

Cimmino, M., Bernier, M. (2013b). Preprocessor for the generation of g-functions used in the simulation of geothermal systems, in: Proceedings of BS2013, Chambéry, France, 2675-2682.

Cimmino, M., Bernier, M., and Cauret, O. (2013c). Validation d'un modèle pour la simulation de capteurs géothermiques compacts. XIe Colloque Interuniversitaire Franco-Québécois sur la Thermique des Systèmes, Reims, France., 277-282.

Cimmino, M., Bernier, M., and Pasquier, P. (2012). Utilisation des g-functions de Eskilson pour la simulation de systèmes géothermiques. Proceedings of eSim 2012, Halifax NS., 282-295.

Claesson, J., and Bennet, J. (1987). Multipole method to compute the conductive heat flows to and between pipes in a cylinder. Department of Building Technology and Mathematical Physics, University of Lund, Sweden.

Claesson, J., and Hellström, G. (2011). Multipole method to calculate borehole thermal resistances in a borehole heat exchanger. HVAC&R Research, 17(6), 895-911.

Claesson, J., and Javed, S. (2011). An analytical method to calculate borehole fluid temperatures for time-scales from minutes to decades. ASHRAE Transactions, 117(2), 279-288.

Claesson, J., and Javed, S. (2012). A load-aggregation method to calculate extraction temperatures of borehole heat exchangers. ASHRAE Transactions, 118(1), 530-539.

Clark, D. R. (1985). HVACSIM+ Building Systems and Equipment Simulation Program Reference Manual. NBSIR 84-2996. National Bureau of Standards.

Costes, V., and Peysson, P. (2008). Capteurs géothermiques verticaux enterrés: Validation expérimentale de nouveaux modèles développés dans l'environnement TRNSYS. École Polytechnique de Montréal.

Cui, P., Yang, H., and Fang, Z. (2006). Heat transfer analysis of ground heat exchangers with inclined boreholes. Applied Thermal Engineering, 26(11-12), 1169-1175.

Cullin, J.R., Spitler, J.D. Montagud, C. Ruiz-Calvo, F. Rees, S.J. Naicker, S.S. Konečný, P. Southard L.E., (2015). Validation of vertical ground heat exchanger design methodologies, Science and technology for the Built Environment, 21(2),137-149.

Cullin, J. R., and Spitler, J. D. A. (2011). Computationally efficient hybrid time step methodology for simulation of ground heat exchangers, Geothermics, 40, 144-156.

Deerman, J. D., and Kavanaugh. S. P. (1991). Simulation of vertical U-tube ground-couple heat pump systems using the cylindrical heat source solution. ASHRAE Transactions. 97, 287-295.

Diao, N. R., Zeng, H. Y., and Fang, Z. H. (2004). Improvement in modeling of heat transfer in vertical ground heat exchangers. HVAC&R Research, 10(4), 459-470.

Dobson, M. K. O'Neal, D. L. and Aldred, W. (1995). Modified analytical method for simulating cyclic operation of vertical U-tube ground-coupled heat pumps, in ASME/JSME/JSES International Solar Energy Conference, Maui, HI, USA, 69-76.

Eskilson, P. (1987). Thermal analysis of heat extraction boreholes. Doctoral Thesis. University of Lund, Department of Mathematical Physics. Lund, Sweden.

Fossa, M. (2011). The temperature penalty approach to the design of borehole heat exchangers for heat pump applications, Energy and Buildings, 43, 1473-1479.

Gehlin, S. E. A., and Hellström, G. (2003). Comparison of four models for thermal response test evaluation. ASHRAE Transactions, 109, 131-142.

GLD. (2012). Ground Loop Design Premier 2012 User's Guide, Gaia Geothermal LLC, 337 pages.

Godefroy, V. (2014). Élaboration et validation d'une suite évolutive de modèles d'échangeurs géothermiques verticaux. Mémoire de maîtrise, École Polytechnique de Montréal.

Godefroy, V., and M. Bernier. (2014). A simple model to account for thermal capacity in boreholes. Proceedings of the 11th IEA Heat Pump Conference, Montreal, Qc, Canada. Paper #P.4.8.

Gu, Y., and O'Neal, D. L. (1998). Development of an equivalent diameter expression for vertical U-tubes used in ground-coupled heat pumps. ASHRAE Transactions. 104(2), 347-355.

Hart, D. P., and Couvillion, R. (1986). Earth-coupled heat transfer, prepared for the National Water Well Association, Dublin, OH.

Hellström, G. (1991). Ground Heat Storage-Thermal Analyses of Duct Storage Systems, Ph.D. , Department of Mathematical Physics, University of Lund, Lund, Sweden.

IGSHPA, (1986). Closed-Loop Ground-Coupled Heat Pump Design Manual, Oklahoma State University, Engineering Technology Extension, Stillwater, Oklahoma

Ingersoll, L. R., Adler, F. T., Plass, H. J., and Ingersoll, A. C. (1950). Theory of earth heat exchangers for the heat pump. Heating, Piping & Air Conditioning, 22, 113-122.

Ingersoll, L. R. and Plass, H. J. (1948). Theory of the ground pipe heat source for the heat pump, Heating, Piping & Air Conditioning, 20, 119-122.

Ingersoll, L. R., Zobel, O. J., and Ingersoll, A. C. (1954). Heat Conduction with Engineering Geological and other Applications. New York, NY, USA: Mc Graw-Hill.

Javed, S., and Spitler. J., (2017). Accuracy of borehole thermal resistance calculation methods for grouted single U-tube ground heat exchangers. Applied Energy, 187: 790-806.

Javed, S. and J. Spitler. (2016). Calculation of borehole thermal resistance. In: Simon J. Rees, editor. Advances in ground-source heat pump systems. Woodhead Publishing. P.63-95.

Javed, S. and Claesson, J. (2011). New Analytical and Numerical Solutions for the Short Term Analysis of Vertical Ground Heat Exchangers, ASHRAE Transactions, 117.1, 3-12,

Javed, S., Claesson, J., and Fahlén, P. (2010). Analytical modelling of short-term response of ground heat exchangers in ground source heat pump systems. Proceedings of the 10th REHVA world congress; Clima 2010, Antalya Turkey. Clima 2010.

Javed, S., Fahlén, P., and Claesson, J. (2009). Vertical ground heat exchangers: A review of heat flow models. Proceedings of the 11th international conference on thermal energy storage; Effstock 2009, Stockholm Sweden. Effstock 2009.

Kavanaugh, S. P., and K., Rafferty (2015). Geothermal Heating and Cooling - Design of Ground-Source Heat Pump Systems. Atlanta, Georgia: ASHRAE.

Kavanaugh, S. P., and Rafferty, K. (1997). Ground-source heat pumps, design of geothermal systems for commercial and institutional buildings. Atlanta, GA: American Society of Heating, Refrigerating and Air-Conditioning Engineers (ASHRAE).

Kavanaugh, S. P. (1995). A Design Method for Commercial Ground-Source Heat Pumps, ASHRAE Transactions, 101,

Kavanaugh, S. P. (1985). Simulation and experimental verification of vertical ground coupled heat pump systems. Ph.D. Oklahoma State University. Stillwater, Oklahoma.

Kelvin, W. T. (1882). Mathematical and Physical Papers. Cited by Ingersoll et al. (1954), 41.

Kohl, T., Brenni, R., and Eugester., W. (2002). System performance of a deep borehole heat exchanger. Geothermics. 31: 687-708.

Kurevija, T., Vulin, D., and Krapec, V. (2012). Effect of borehole array geometry and thermal interferences on geothermal heat pump system, Energy Conversion and Management, 60, 134-42,

Lamarche, L. (2017). g-function generation using a piecewise-linear profile applied to ground heat exchangers, International Journal of Heat and Mass Transfer, 115(Part B), 354-360.

Lamarche, L. (2011). Analytical g-function for inclined boreholes in ground-source heat pump systems. Geothermics, 40(4), 241-249.

Lamarche, L. (2009). A fast algorithm for the hourly simulations of ground-source heat pumps using arbitrary response factors. Renewable Energy, 34(10), 2252-2258.

Lamarche, L., Kajl, S., and Beauchamp, B. (2010). A review of methods to evaluate borehole thermal resistances in geothermal heat-pump systems. Geothermics, 39(2), 187-200.

Lamarche, L., and Beauchamp, B. (2007a). A fast algorithm for the simulation of GCHP systems. ASHRAE Transactions, 113, 470-476.

Lamarche, L., and Beauchamp, B. (2007b). A new contribution to the finite line-source model for geothermal boreholes. Energy and Buildings, 39(2), 188-198.

Lamarche, L., and Beauchamp, B. (2007c). New solutions for the short-time analysis of geothermal vertical boreholes. International Journal of Heat and Mass Transfer, 50(7-8), 1408-1419.

Lei, T. K. (1993). Development of a computational model for a ground-coupled heat exchanger. ASHRAE Transactions. 99(1), 149-159.

Li, M., and Lai, A. C. K. (2012). New temperature response functions (G functions) for pile and borehole ground heat exchangers based on composite-medium line-source theory. Energy, 38(1), 255-263.

Li, M., Zhuo, X. and Huang, G. (2017). Improvements on the American Society of Heating, Refrigeration, and Air-Conditioning Engineers Handbook equations for sizing borehole ground heat exchangers, Science and Technology for the Built Environment, 23(8), 1267-1281.

Liu, X. (2005). Development and experimental validation of simulation of hydronic snow melting systems for bridges. Ph.D. Thesis, Oklahoma State University, Stillwater, OK.

Marcotte, D., and Pasquier, P. (2009). The effect of borehole inclination on fluid and ground temperature for GLHE systems. Geothermics, 38(4), 392-398.

Marcotte, D., and Pasquier, P. (2008). Fast fluid and ground temperature computation for geothermal ground-loop heat exchanger systems. Geothermics, 37(6), 651-665.

Montagud, C., Corberán, J.M., Montero, Á., Urchueguía, J.F. (2011), Analysis of the energy performance of a ground source heat pump system after five years of operation, In Energy and Buildings, 43(12), 3618-3626.

Muraya, N. K., O'Neal, D. L., and Heffington. W. M. (1996). Thermal interference of adjacent legs in a vertical U-tube heat exchanger for a ground-coupled heat pump. ASHRAE Transactions. 102(2), 12-21.

Muraya, N. K. (1994). Numerical modeling of the transient thermal interference of vertical U-tube heat exchangers. Ph.D. Dissertation. Texas A&M University.

Oskarsson, S. V. (1981). Ground coupled heat pump systems, presented at the National Water Well Association conference

O'Neal, D. L., Gonzalez, J. and Aldred, W. A. (1994). Simplified Procedure for Sizing Vertical Ground Coupled Heat Pump Heat Exchangers for Residences in Texas, in Proceedings of the Ninth Symposium on Improving Building Systems in Hot and Humid Climates, Arlington, TX,

Pasquier, P., and Marcotte, D. (2012). Short-term simulation of ground heat exchanger with an improved TRCM. Renewable Energy, 46, 92-99.

Pasquier, P., and Marcotte, D. (2013). Efficient computation of heat flux signals to ensure the reproduction of prescribed temperatures at several interacting heat sources. Applied Thermal Engineering, 59(1), 515-526.

Pasquier, P., and Marcotte, D. (2014). Joint use of quasi-3D response model and spectral method to simulate borehole heat exchanger. Geothermics, 51, 281-299.

Paul, N.D. (1996). The Effect of Grout Thermal Conductivity on Vertical Geothermal Heat Exchanger Design and Performance, Master's thesis, South Dakota State University, USA.

Philippe, M., Bernier, M. and Marchio, D. (2010). Sizing calculation spreadsheet vertical geothermal borefields, ASHRAE, 20-28,

Pinel, P. (2003). Amélioration, validation et implantation d'un algorithme de calcul pour évaluer le transfert thermique dans les puits verticaux de systèmes de pompes à chaleur géothermiques. M.Sc. Thesis, École Polytechnique de Montréal, Canada

Richtlinien V.D.I. 4640, (2001). Thermal use of the ground. Ground source heat pump systems, ed. Verein Deutscher Ingenieure, Part 2, Beuth Verlag GmbH, 10772 Berlin.

Rottmayer, S. P., Beckman W. A. and Mitchell. J. W. (1997). Simulation of a single vertical U-tube ground heat exchanger in an infinite medium. ASHRAE Transactions. 103(2): 651-659.

Rees, S. J. (2000). An introduction to the finite volume method: Tutorial series. Report. Oklahoma State University. Stillwater, OK.

Rosén, B., Gabrielsson, A., Fallsvik, J., Hellström, G. and Nilsson, G. (2001). System för värme och kyla ur mark – En nulägesbeskrivning [Systems for Ground Source Heating and Cooling – A Status Report – in Swedish] Varia 511 , Statens Geotekniska Institut, Linköping, Sweden.,

Salim-Shirazi, A., and Bernier, M. (2013) Thermal capacity effects in borehole ground heat exchangers. Energy and Buildings, 67, 352-364.

Shonder, J. A., Baxter, V. D., Hughes, P. J. and Thornton, J. W. (2000). A comparison of vertical ground heat exchanger design software for commercial applications. ASHRAE Transactions, 106, 831-842.

Shonder, J. A., and Beck, J. V. (1999). Determining effective soil formation thermal properties from field data using parameter estimation technique. ASHRAE Transactions, 105, 458-466.

Spitler J. D., and Bernier, M. (2016). Advances in ground-source heat pump systems - Chapter 2: Vertical borehole ground heat exchanger design methods. Edited by S. Rees. Woodhead Publishing.

Spitler, J., Cullin, J., Lee, E., Fisher, D., Bernier, M., Kummert, M., Cui, P., Liu, X. (2009), Preliminary intermodel comparison of ground heat exchanger simulation models, in: 11th International Conference on Thermal Energy Storage; Effstock 2009, Stockholm, Sweden, (paper #115, 8 pages).

Spitler J. D., and Cullin, J., (2008). Misconceptions Regarding Design of Ground-source Heat Pump Systems, in Proceedings of the World Renewable Energy Congress, Glasgow, Scotland.

Stadler, T., Hopkirk, R. J., and Hess, K. (1995). Auswirkungen von Klima, Bodentyp, Standorthöhe auf die Dimensionierung von Erdwärmesonden in der Schweiz. Schlußbericht ET-FOER(93)033, BEW, Bern.

Staiti, M., Angelotti, A., (2015). Design of Borehole Heat Exchangers for Ground Source Heat Pumps: A Comparison between Two Methods, Energy Procedia, 78, 1147-1152.

Stehfest, H. (1970). Algorithm 368, Numerical inversion of the Laplace transforms [D5]. Communications of the ACM, 13(1), 47-49.

Sutton, M G, Couvillion, D W, Nutter, D. W., and Davis, R K. (2002). An algorithm for approximating the performance of vertical bore heat exchangers installed in a stratified regime. ASHRAE Transactions. Vol. 108(2), 177-184.

Vestal, D. M., and Fluker, B. J. (1956). Earth as heat source and sink for heat pumps, Heating, piping and Air Conditioning

Xu, X., and Spitler, J.D. (2006). Modeling of vertical ground loop heat exchangers with variable convective resistance and thermal mass of the fluid. Proceedings of Ecostock 2006.

Xu, X. (2007). Simulation and optimal control of hybrid ground source heat pump systems. Ph.D. dissertation, Oklahoma State University, Stillwater, Oklahoma.

Yang, Y., and Li, M. (2014). Short-time performance of composite-medium line-source model for predicting responses of ground heat exchangers with single U-shaped tube. International Journal of Thermal Sciences, 82, 130-137.

Yavuzturk, C., Chiasson, A. D., and Nydahl, J. E. (2009). Simulation model for ground loop heat exchangers. ASHRAE Transactions, 115(2), 45-59.

Yavuzturk, C., and Spitler, J. D. (1999). A short time step response factor model for vertical ground Loop heat exchangers. ASHRAE Transactions. 105(2), 475-485.

Yavuzturk C. and Spitler, J. (2001). Field validation of a short time step model for vertical ground-loop heat exchangers. ASHRAE Transactions, 107, 617-25.

Yavuzturk, C., Spitler J. D., and Rees, S. J. (1999). A transient two-dimensional finite volume model for the simulation of vertical U-tube ground heat exchangers. ASHRAE Transactions. 105(2), 465-474.

Young, R. (2004). Development, verification, and design analysis of the borehole fluid thermal mass model for approximating short-term borehole thermal Response. Master Thesis. Oklahoma State University. Stillwater, OK.

Zarrella, A., Scarpa, M., and De Carli, M. (2011). Short time step analysis of vertical ground-coupled heat exchangers: The approach of CaRM. Renewable Energy, 39(9), 2357-2367.

Zeng, H. Y., Diao, N. R., and Fang, Z. (2003). Heat transfer analysis of boreholes in vertical ground heat exchangers. International Journal of Heat and Mass Transfer, 46(23), 4467-4481.

Zeng, H., Diao, N., and Fang, Z. (2002). A finite line-source model for boreholes in geothermal heat exchangers. Heat Transfer- Asian Research. 31(7), 558-567.

Zhang, X., Huang, G., Jiang, Y., and Zhang, T. (2015). Ground heat exchanger design subject to uncertainties arising from thermal response test parameter estimation. Energy and buidings. 102, 442-452.

APPENDICES

A: Spreadsheet tool for sizing VGHEs

Some of the sizing models that are used in Chapter seven have been developed in a VBA Excel spread sheet. A preliminary version of this tool is presented in this Appendix.

Figure A-1 presents the main menu of the spreadsheet. As can be seen, there are eight possible selections in the main menu. These selections correspond to individual worksheets in the spreadsheet: 1- enter the borehole locations, 2- enter the input parameters, 3 to 6- four types of sizing models, 7- generate g-functions for short and long time steps and 8- calculate temperature penalties.

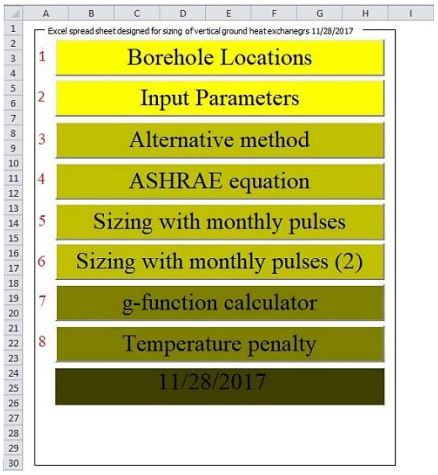

Figure A-1: Main menu of the Excel spreadsheet designed for sizing vertical boreholes

Figure A-2 illustrates the worksheet in which the user can enter the borehole locations. The borehole positions can be specified either as a rectangular pattern or with specific locations. By selecting the rectangular pattern option the user needs to enter the number of boreholes in the two directions as well as the borehole spacing. By clicking the save button the locations appear in columns A and B. The second option gives the user the ability to enter the individual borehole positions. After entering the number of boreholes, the program proposes the cells that should be filled in columns A and B. When clicking the save button, the program checks values and gives an alert when an invalid value is encountered.

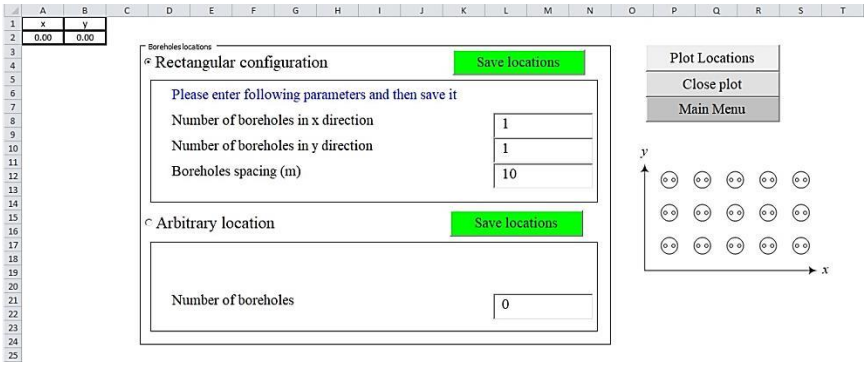

Figure A-2: Borehole locations user input worksheet

Figure A-3 shows the worksheet designed for entering the input parameters. It is divided into eight blocks. The first three blocks give the user the ability to enter the characteristics of the ground and borehole as well as the fluid properties. The fourth block is related to the parameters required for evaluating the short term g-functions. The fifth and sixth blocks give the user the opportunity to enter a constant value for the borehole thermal resistance or evaluate it during the sizing procedure. In this later case, the borehole thermal resistances are evaluated based on the first-order multipole method with three possible boundary conditions at the borehole wall: uniform heat flux, uniform wall temperature, or the mean of these two. The seventh block helps the user to estimate the borehole thermal resistance based on the zeroth order multipole method which could then be entered as a constant value in the fifth block if required. The eighth block is used to enter calculation parameters that are required by some sizing models.

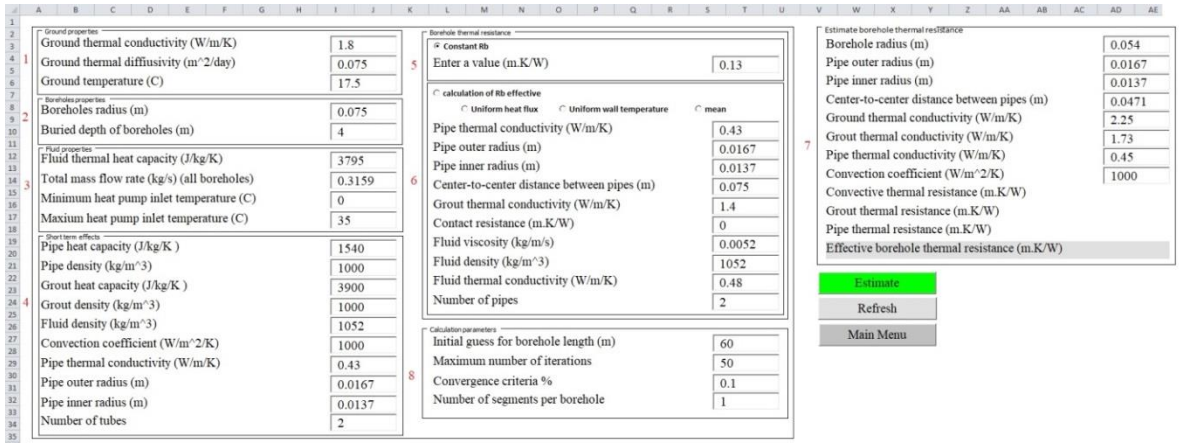

Figure A-3: The input parameters required for the ground, borehole, and fluid

As shown in Figure A-3, some parameters are required twice, for example the fluid density. This is due to the fact that these parameters are required for evaluating both the short term effects and

the variable borehole thermal resistance. If the user selects to calculate R_b effective as a variable during sizing, then parameters in block four will be hidden and only the first four values are used while the rest are read from the sixth block. When the user selects the constant borehole thermal resistance option, all parameters of block six are hidden and they are not used in the sizing calculations.

Figure A-4 shows the first sizing model developed in the spreadsheet. It is the alternative method described in chapters four and five (see equation 7.7). In the illustrated text boxes, the three ground loads (yearly, monthly and hourly) as well as their durations are entered. The ground loads should be entered as positive values for both heating and cooling modes. The only exception is for the case when the annual ground load imbalance is not in the same mode as the monthly average and peak loads. In this case, the monthly average and peak load pulses should be entered as positive values and the yearly load should be entered as a negative value.

The required g-functions are evaluated internally during the sizing procedure. The user should select whether the short term effects are used or not. The long term temperature responses can be evaluated with or without temporal superposition as described in chapter five. In Figure A-4, it is displayed that the borehole thermal resistance is kept constant in the three iterations and this shows that the user has selected the constant borehole thermal resistance option in the input parameters worksheet. It can also be seen that the method converges in just three iterations (column I). After completing the sizing procedure, two boxes pop up to show the average fluid temperature and the calculation time as shown in Figure A-4.

Figure A-5 illustrates three other sizing procedures. Two of these models use the modified ASHRAE equation as is suggested by Bernier (2006) (see equation 7.4). The only difference between these two models is related to the way the temperature penalties are evaluated using either (g_N-g_1) as shown in equation 7.5 or $((g/2\pi) - G)$ as shown in equation 7.6.

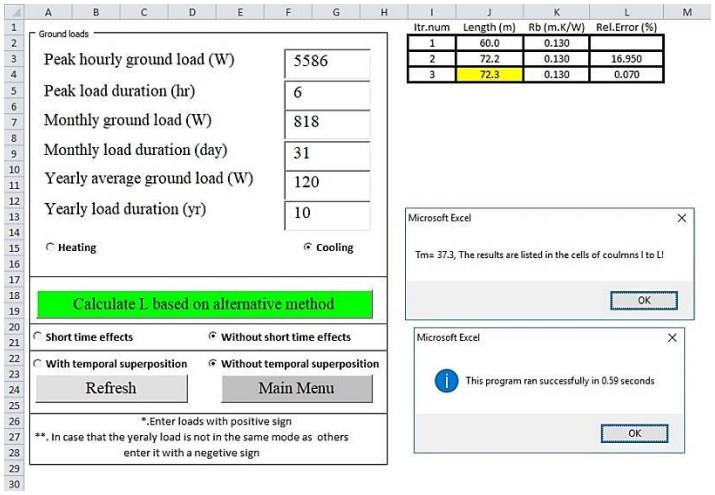

Figure A-4: Input parameters and sizing procedure for the alternative method

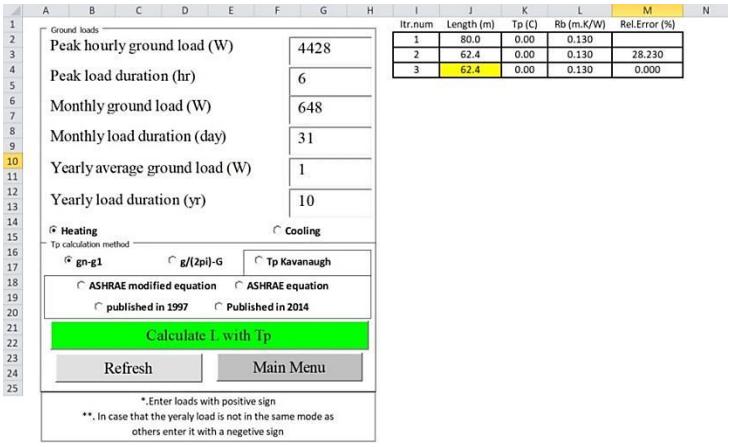

Figure A-5: Input parameters and sizing procedure for the ASHRAE modified method

The third model evaluates the temperature penalty based on the approach originally suggested by Kavanaugh and Rafferty (1997) or the modified approach, which accounts for heat transfer from the bottom of the bore field (Kavanaugh and Rafferty, 2015). Based on the methodology presented by Kavanaugh and Rafferty (1997) the temperature penalty is determined as follows:

$$T_p = \frac{N_4 + 0.5N_3 + 0.25N_2 + 0.1N_1}{N_b} t_{pl} \tag{A.1}$$

where N_1 to N_4 denote the number of boreholes that are surrounded by 1 to 4 neighboring boreholes, respectively. The modified approach (Kavanaugh and Rafferty, 2015) is given by:

$$T_p = \frac{N_4 + 0.75N_{3S} + 0.5N_{3C} + 0.5N_2 + 0.25\,N_1}{N_b \times C_{f,H}} t_{pl} \quad \text{(A.2)}$$

$$C_{f,H} = \frac{[L \times 2 \times (W_{Field} + L_{Field})] + [W_{Field} + L_{Field}]}{L \times 2 \times (W_{Field} + L_{Field})} t_{pl} \quad \text{(A.3)}$$

where $W_{Field} = (N_{Wide} - 1) \times B$ and $L_{Field} = (N_{Long} - 1) \times B$, L is the borehole length, N_{3S} is the number of boreholes surrounded by three boreholes on the side of the bore field (not on the corners), and N_{3C} is the number of boreholes surrounded by three boreholes and located on the corner of the bore field. These terms are illustrated in Figure A-6. The two equations are actually developed for rectangular bore field and N_{Wide} and N_{Long} are the number of boreholes in both directions. The methodology is iterative as T_p in both Equations A.2 and A.3 is dependent on the borehole length which is unknown *a priori*.

The evaluated temperature penalties can be applied to the classic ASHRAE equation (as presented in the ASHRAE Handbook (2011) (equation 7.3) or the one modified by Bernier (2006) (equation 7.4). Thus, four combinations can be used (two related to temperature penalties and two related to the sizing equations). Since the classic ASHRAE sizing equation has different input parameters than the modified one, based on the selected sizing model, the required input parameters are to be filled by the user while the others are hidden. This is the same for the temperature penalty models as each one need specific parameters. Figure A-6 shows the parameters that are required for the temperature penalty model suggested by Kavanaugh and Rafferty (2015) and the classical ASHRAE equation.

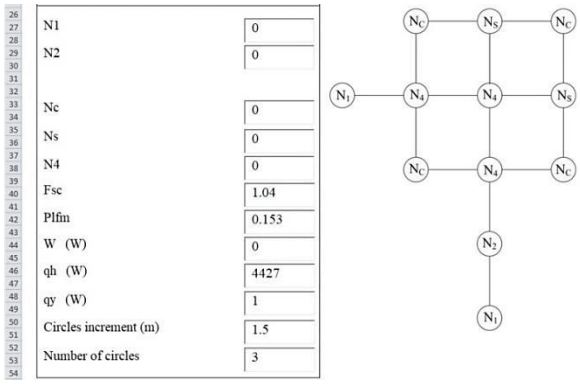

Figure A-6: Input parameters for the ASHRAE equation method

Figure A-7 illustrates the sizing procedure of three sizing models that accept monthly average and peak loads but size the bore field on the three load pulses method. These heat loads are, respectively, the average load of previous months, and the average and peak loads of the current month. The first method is based on the monthly version of the alternative method (see equation 7.12). The other two methods use the modified ASHRAE equation (see equation 7.11) and evaluate the temperature penalties based either on equation 7.5 or on equation 7.6 as explained earlier.

For design periods greater than one year, the model calculates two lengths: one for the first year of operation and the other for the last year. The maximum value between these two is the final value. The user can also select if short term effects are to be included. Finally, the long term g-functions can be evaluated with or without temporal superposition.

Figures A-8 and A-9 show the worksheet related to the two monthly sizing methods. These models evaluate the lengths based on equations 7.13a, 7.13b (or 7.14 when short term effects are considered) and 7.13d. The only difference between these models is that loads are superimposed by load aggregation in the time domain in the first method and in the spectral domain in the second. As can be seen in the Figures A-8 and A-9, the user can select a multi-year simulation in addition to sizing. This simulation is based on the length that is entered in the "input parameter" worksheet as the initial guessed length. The sizing methods use an optimization procedure to find the length. The objective function is the same as the one presented in chapter six and the optimization is based on the golden section search method. At the end of simulation/sizing, the user can plot the fluid temperature evolutions through the design period and the evolution of the required length from iteration to iteration can be plotted as shown in Figure A-9. The columns in the middle of Figure A-8 represent respectively the monthly average fluid temperature and the maximum and minimum peak fluid temperature in the boreholes and the corresponding maximum and minimum peak inlet fluid temperature to the heat pumps. The columns in the middle of Figure A-9 show the operational time period, the corresponding g-functions, the monthly changes of the load per unit length of boreholes, the Fast Fourier transform of the g-functions and the heat load rates and the inverse Fourier transform of their products. These terms are used to calculate the average and peak fluid temperatures in the boreholes as well as the peak fluid temperatures of the heat pumps.

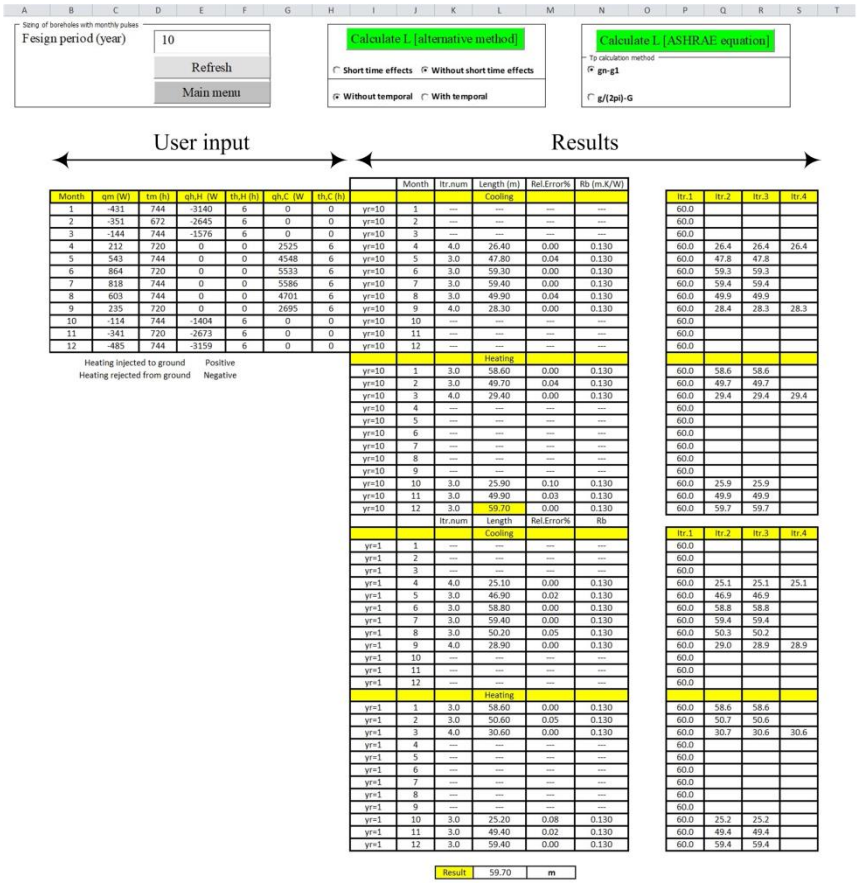

Figure A-7: Input parameters and sizing procedure for the monthly versions of the classic ASHRAE sizing equation and its alternatives

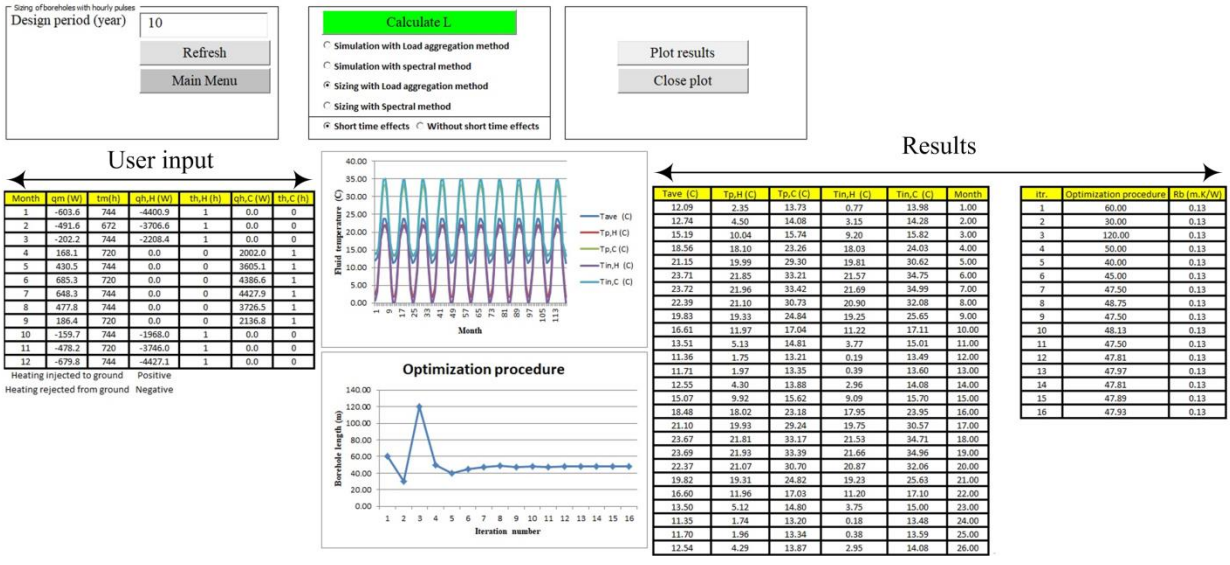

Figure A-8: Input parameters and sizing procedure for the monthly method with load aggregation

Figure A-10 shows the worksheet that is designed for the evaluation of the short and long term g-functions. The block of three columns in the center presents the g-function over selected value of $\ln(t/t_s)$ while the block of three columns on the right represent g-function values at every 0.1 hour. Figure A-11 shows the worksheet that is designed for evaluation of the temperature penalties using the methodology suggested by Bernier et al. (2008) (equation 7.5). The required input parameters should be entered directly in these worksheets and parameters entered in other worksheets are not used. The only exception is for the borehole locations that are read from the "borehole locations" worksheet.

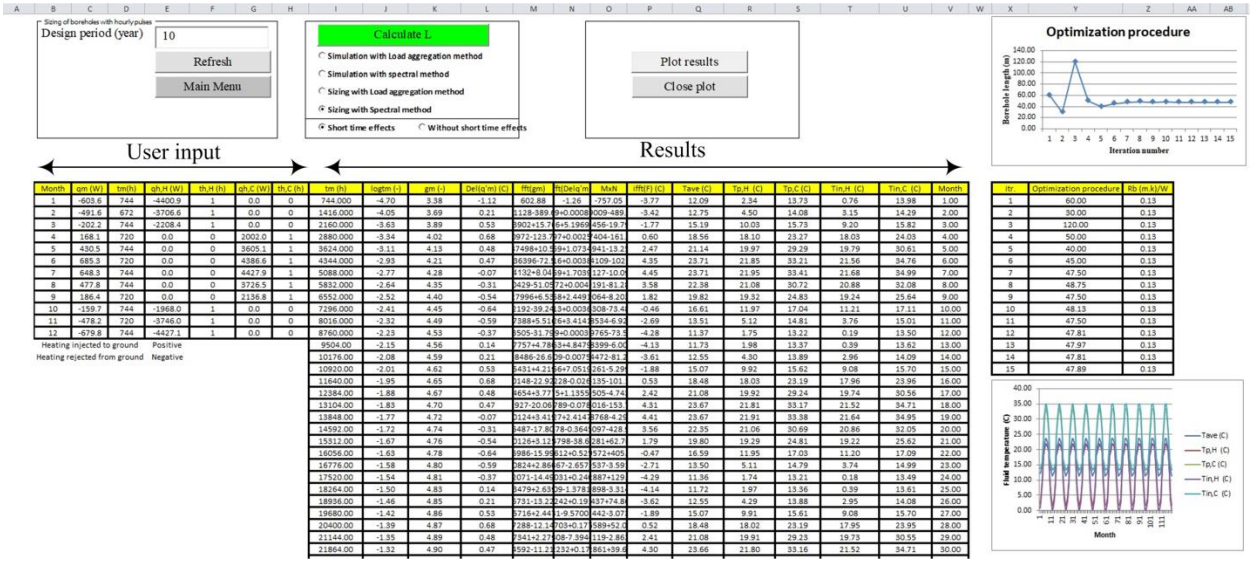

Figure A-9: Input parameters and sizing procedure for the monthly methods that use the spectral method

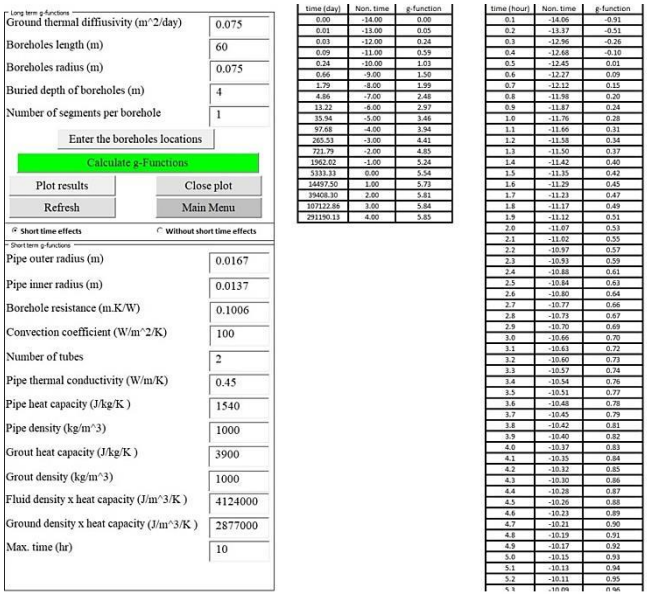

Figure A-10: Input parameters required for the evaluation of short and long-term g-functions

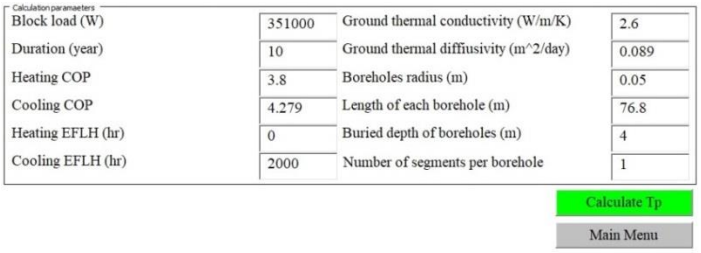

Figure A-11: Input parameters required for evaluating temperature penalties

Appendix B: Excel spreadsheet for the inter-model comparison

As mentioned in chapter seven, the input parameters and the results obtained in the inter-model comparison are reported in an Excel spreadsheet. A description of this spreadsheet is provided in this Appendix.

The spreadsheet has seven main tabs that show: the input parameters; the results of Test 1a, Test 1b, Test 2, Test 3, Test 4; a sensitivity analysis; and a nomenclature. Figure B-1 shows the symbols used throughout the spreadsheet.

Parameter	Symbol	Unit
hourly building or ground loads	q_h	(W)
cooling hourly building or ground peak loads	$q_{h,C}$	(W)
heating hourly building or ground peak loads	$q_{h,H}$	(W)
monthly building or ground loads	q_m	(W)
yearly building or ground loads	q_y	(W)
duration of cooling hourly peak loads	$t_{h,C}$	(h)
duration of heating hourly peak loads	$t_{h,H}$	(h)
total number of boreholes	N_b	(---)
distance between the boreholes	B	(m)
distance between the ground surface and the top of boreholes	D	(m)
borehole radius	rb	(mm)
outer and inner radius of U-pipe legs	$r_{p,o}$,$r_{p,i}$	(mm)
center-to-center spacing between the legs of a U-tube	$2d_p$	(mm)
flow rate of the circulating fluid	m_f	($kg.s^{-1}$)
density of the heat carrier fluid	ρ_f	($kg.m^{-3}$)
specific heat capacity of the circulating fluid	$c_{p,f}$	($kJ.kg^{-1}K^{-1}$)
viscosity of the heat carrier fluid	μ_f	($K.g.m^{-1}s^{-1}$)
fluid thermal conductivity	k_f	($W.m^{-2}K^{-1}$)
thermal capacity of the soil	$\rho c_{p,g}$	($kJ.m^{-3}K^{-1}$)
thermal capacity of the grout	$\rho c_{p,gr}$	($kJ.m^{-3}K^{-1}$)
thermal heat capacity of the pipe	$\rho c_{p,pipe}$	($kJ.m^{-3}K^{-1}$)
soil thermal diffusivity	α_g	($m^2.day^{-1}$)
soil thermal conductivity	k_g	($W.m^{-1}K^{-1}$)
thermal conductivity of the backfilling material	k_{gr}	($W.m^{-1}K^{-1}$)
initial temperature of the ground	T_g	(°C)
pipe thermal conductivity	k_p	($W.m^{-1}K^{-1}$)
minimum inlet fluid temperature to the heat pump	T_L	(°C)
maximum inlet fluid temperature to the heat pump	T_H	(°C)
effective thermal resistance of the boreholes	R_b	($m.K.W^{-1}$)
duration of simulation period	t	(yr)
contact thermal resistance	R_c	($m.K.W^{-1}$)
internal convection coefficient in pipes	h_{conv}	($W.m^{-2}K^{-1}$)
geothermal heat flux	q''_g	($W.m^{-2}$)
short circuit heat loss factor in the borehole	F_{sc}	(---)
heat pump coefficient of performances in cooling	COP_C	(---)
heat pump coefficient of performances in heating	COP_H	(---)

Figure B-12: Symbols used in the inter-model comparison Excel spreadsheet

Figure B-2 illustrates the various parts of the spreadsheet for a typical test. Various blocks of data can be found from left to right: Loads (in blue) are located on the left followed by input parameters (in violet) in the middle and results (in green) on the right. Various load profiles are used depending on the level of the method: Hourly ground loads can be found in column B, monthly average and monthly peak values are reported in columns D to I and loads used for three

pulse methods are given in column L. The hourly load profile is also plotted below the monthly values. Results are also plotted in the form of bar charts below the numerical results in the green region of the worksheet. Finally, on the bottom left corner, a table presents the impact of short-term effects.

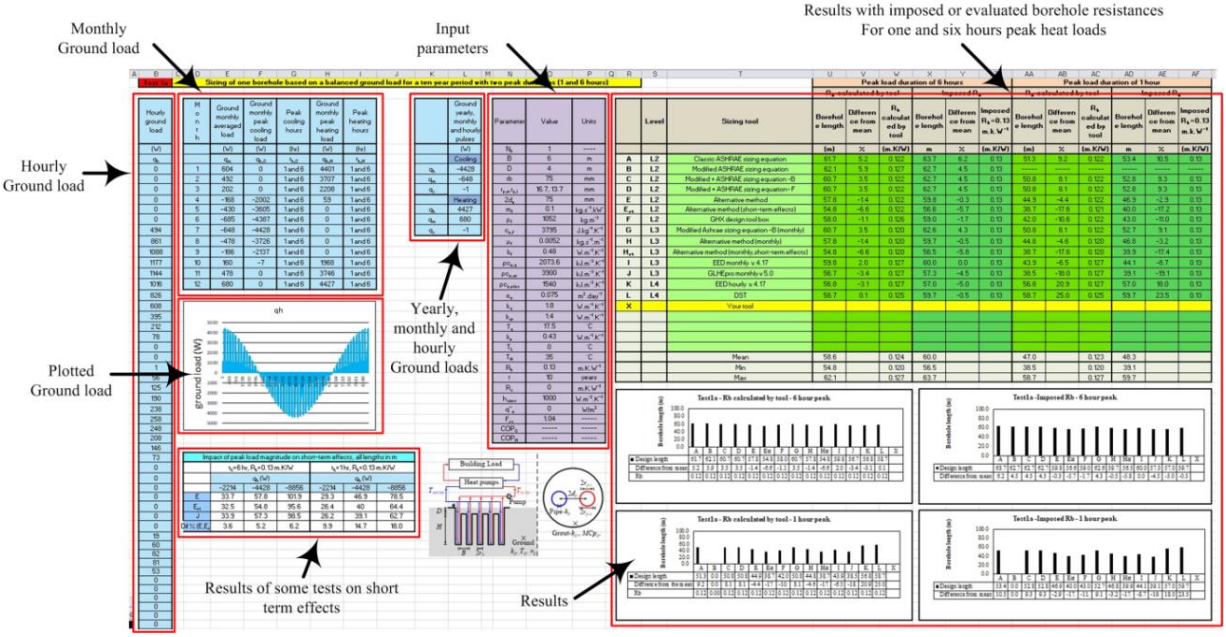

Figure B-13: Example of worksheets used for reporting the input parameters and the results of various sizing tests

For Test 1b and Test 4, which use building loads, additional columns (in red) are inserted as illustrated in Figure B-3.

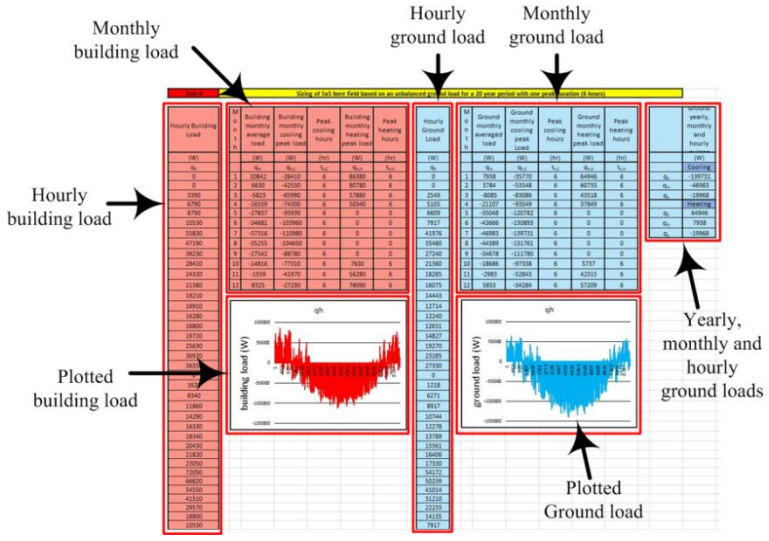

Figure B-14: Building and ground loads given for Test 4

Figure B-4 shows the input parameters and the results of the sensitivity analysis obtained based on Test 4. In this analysis, the input parameters are exactly the same as the ones considered for Test 4. In the results section, five parameters (peak magnitude, thermal conductivity, borehole spacing, ground temperature, number of boreholes) are varied one at a time to analyse their impact on borehole length for each tool. The resulting length is compared to Test 4 and the percentage difference between the two is reported in the table.

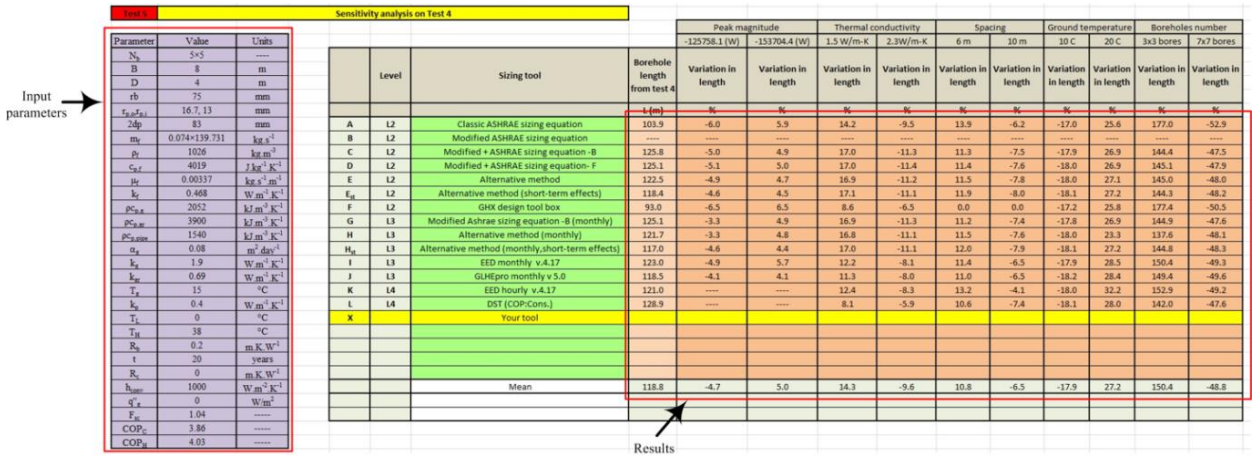

Test 5 — Sensitivity analysis on Test 4

Parameter	Value	Units
N_b	5×5	----
B	8	m
D	4	m
rb	75	mm
$r_{p,i}$,$r_{p,i}$	16.7, 13	mm
2dp	83	mm
m_f	0.074×139.731	kg s^{-1}
ρ_f	1026	kg m^{-3}
$c_{p,f}$	4019	J kg^{-1} K^{-1}
μ_f	0.00337	kg s^{-1} m^{-1}
k_f	0.468	W m^{-1} K^{-1}
$\rho c_{p,s}$	2052	kJ m^{-3} K^{-1}
$\rho c_{p,gr}$	3900	kJ m^{-3} K^{-1}
$\rho c_{p,grout}$	1540	kJ m^{-3} K^{-1}
α_s	0.08	m^2 day^{-1}
k_s	1.9	W m^{-1} K^{-1}
k_{gr}	0.69	W m^{-1} K^{-1}
T_g	15	°C
k_g	0.4	W m^{-1} K^{-1}
T_i	0	°C
T_H	38	°C
R_b	0.2	m.K.W^{-1}
t	20	years
R_c	0	m.K.W^{-1}
h_{open}	1000	W m^{-2} K^{-1}
q''_g	0	W/m^2
F_{sc}	1.04	-----
COP_c	3.86	-----
COP_h	4.03	-----

	Level	Sizing tool	Borehole length from test 4	Peak magnitude -125758.1 (W) Variation in length	Peak magnitude -153704.4 (W) Variation in length	Thermal conductivity 1.5 W/m-K Variation in length	Thermal conductivity 2.3W/m-K Variation in length	Spacing 6 m Variation in length	Spacing 10 m Variation in length	Ground temperature 10 C Variation in length	Ground temperature 20 C Variation in length	Boreholes number 3x3 bores Variation in length	Boreholes number 7x7 bores Variation in length
			L (m)	%	%	%	%	%	%	%	%	%	%
A	L2	Classic ASHRAE sizing equation	103.9	-6.0	5.9	14.2	-9.5	13.9	-6.2	-17.0	25.6	177.0	-52.9
B	L2	Modified ASHRAE sizing equation	----	----	----	----	----	----	----	----	----	----	----
C	L2	Modified + ASHRAE sizing equation -B	125.8	-5.0	4.9	17.0	-11.3	11.3	-7.5	-17.9	26.9	144.4	-47.5
D	L2	Modified + ASHRAE sizing equation- F	125.1	-5.1	5.0	17.0	-11.4	11.4	-7.6	-18.0	26.9	145.1	-47.9
E	L2	Alternative method	122.5	-4.9	4.7	16.9	-11.2	11.5	-7.8	-18.0	27.1	145.0	-48.0
E_d	L2	Alternative method (short-term effects)	118.4	-4.6	4.5	17.1	-11.1	11.9	-8.0	-18.1	27.2	144.3	-48.2
F	L2	GHX design tool box	93.0	-6.5	6.5	8.6	-6.5	0.0	0.0	-17.2	25.8	177.4	-50.5
G	L3	Modified Ashrae sizing equation -B (monthly)	125.1	-3.3	4.9	16.9	-11.3	11.2	-7.4	-17.8	26.9	144.9	-47.6
H	L3	Alternative method (monthly)	121.7	-3.3	4.8	16.8	-11.1	11.5	-7.6	-18.0	23.3	137.6	-48.1
H_d	L3	Alternative method (monthly,short-term effects)	117.0	-4.6	4.4	17.0	-11.1	12.0	-7.9	-18.1	27.2	144.8	-48.3
I	L3	EED monthly v.4.17	123.0	-4.9	5.7	12.2	-8.1	11.4	-6.5	-17.9	28.5	150.4	-49.3
J	L3	GLHEpro monthly v 5.0	118.5	-4.1	4.1	11.3	-8.0	11.0	-6.5	-18.2	28.4	149.4	-49.6
K	L4	EED hourly v.4.17	121.0	----	----	12.4	-8.3	13.2	-4.1	-18.0	32.2	152.9	-49.2
L	L4	DST (COP:Cons.)	128.9	----	----	8.1	-5.9	10.6	-7.4	-18.1	28.0	142.0	-47.6
X		Your tool											
		Mean	118.8	-4.7	5.0	14.3	-9.6	10.8	-6.5	-17.9	27.2	150.4	-48.8

Figure B-15: Worksheet used for the sensitivity analysis

Appendix C: Extended tests using the experimental data of the Valencia case

In chapter seven, the experimental data available in the literature for the so-called Valencia case was used for comparison with the results of Cullins et al. (2015). In this appendix, an extended set (for over 10 years) of the experimental data from the Valencia case is used to re-check the ASHRAE sizing equation and the DST-GenOpt tool. The author is grateful to Dr. Carla Montagud for providing this data.

The heating and cooling plant at the Department of Applied Thermodynamics at the Polytechnic University of Valencia, Spain, conditions a 250 m^2 space (Montagud et al., 2011). The heat pump system is linked to a 3 × 2 bore field. Each borehole has a length of 50 m depth and the borehole spacing is 3 m. The system started functioning on February 2005 and the data provided by Dr. Montagud extends up to June 2015. The data of some months of the first three years as well as some different days during the remaining years are not available due to maintenance operations or research activities. Also during the year 2009 and 2010, some optimization strategies were carried out which have resulted in changing of the heat pump temperature settings for both heating and cooling cases.

Data were collected every minute (every 20 seconds for the last four years). Figure C-1 shows a screenshot of the data for an averaging period of one hour.

			Outlet of the heat pump	Inlet of the heat pump	Inlet of the boreholes	Outlet of the boreholes	Internal circuit mass flow rate	Mass flow rate in boreholes	Power consumption of the external circuit	Power consumption of the internal circuit
	A	B	C	D	E	F	G	H	I	J
1	Day	Time	TinIC (ºC)	ToutIC (ºC)	TinEC (ºC)	ToutEC (ºC)	Mass Flow Rate IC (kg/h)	Mass Flow Rate EC (kg/h)	P_EC(kW)	P_IC(kW)
2	01/Apr/2005	0:01:55	40.344	44.096	19.259	19.242	0.157025	2785.26825	0.41572083	0.13423645
3	01/Apr/2005	0:02:55	40.242	44.035	19.262	19.248	0.136425	2784.2905	0.41572083	0.13423645
4	01/Apr/2005	0:03:55	40.184	43.99	19.265	19.251	0.1776	2784.3935	0.4156251	0.13427298
5	01/Apr/2005	0:04:55	40.037	43.872	19.269	19.253	0.1879	2784.44475	0.41561335	0.13427466
6	01/Apr/2005	0:05:55	39.977	43.816	19.273	19.259	0.151875	2784.3935	0.41565534	0.13425702
7	01/Apr/2005	0:06:55	39.938	43.755	19.277	19.26	0.2085	2785.31975	0.41558564	0.13428725
8	01/Apr/2005	0:07:55	39.791	43.684	19.279	19.264	0.120975	2785.37125	0.41556465	0.1342818
9	01/Apr/2005	0:08:55	39.719	43.628	19.285	19.27	0.162175	2786.555	0.41568809	0.13422008
10	01/Apr/2005	0:09:55	39.634	43.559	19.287	19.272	0.126125	2786.555	0.4156335	0.13424233

Figure C-16: Typical measured data collected for Valencia case

From the collected data, three parameters (flow rate, inlet and the outlet temperature of the boreholes, i.e. columns E, F and H in Figure C-1) are selected. Measurement errors such as negative flow rates or high meaningless fluid temperatures were removed from the data. Then,

the hourly average of the flow rate changes and the evolutions of the inlet and outlet temperature of the boreholes are calculated.

In the first use of this data, the averaged flow rate and borehole inlet temperatures are given as inputs to three simulation-based models: DST model in TRNSYS, as well as two in-house models developed by Godefroy (2014) known as Types 204 and 245. As shown in Figure C-2, the flow rate fluctuates between 0 to 3174.3 kg/hr and the inlet temperature varies between 7.9 °C and 39.3 °C. The borehole thermal resistance is 0.11 $m.K.W^{-1}$, the borehole buried depth is assumed to be 4 m and the fluid is considered pure water with a specific heat of 4174 $J.kg^{-1}.K^{-1}$ and a fluid density of 998.2 $kg.m^{-3}$. Other design parameters are reported in chapter seven.

Both Types 204 and 245 use g-functions which are evaluated based on the correct positions and lengths of the boreholes. Type 204 accepts the borehole thermal resistance as an input except for the internal convection coefficient which is evaluated internally at each time step. Type 245 is a TRC-type model and accounts for the thermal capacity inside the boreholes and is not possible to input the borehole thermal resistance directly.

In this test, the borehole outlet temperature predicted by the three models are compared against measured values.

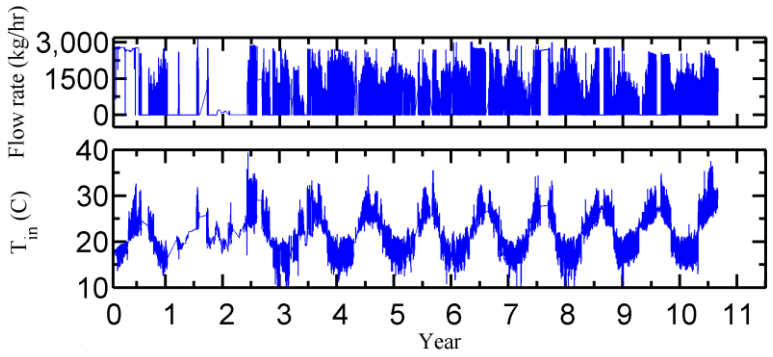

Figure C-17: The averaged measured a. fluid flow rate and b. inlet temperature of Valencia case

Figures C-2a to C-2c show the boreholes outlet temperatures evaluated respectively by the DST, Types 204 and 245 as well as the measured values. The outlet temperature evaluated by the DST varies between 13.8 °C and 31.1 °C while the variation for Types 245 and 204 range between 13.3°C and 31.8 °C and between 12.9 °C and 32.7 °C, respectively, as illustrated in Figures C-2b and C-2c. The hourly averaged measured outlet temperature changes between the minimum of 14.6 °C to 34.2 °C. The hourly difference between calculated and measured value can reach up to

10 °C. The maximum evaluated outlet temperatures are obtained in the tenth year of operation while the maximum measured temperature happened in the ninth year. The maximum measured value in the first three years is 33.9 °C which is lower than the value of 35.5 °C used in chapter seven since it has been averaged over the hour.

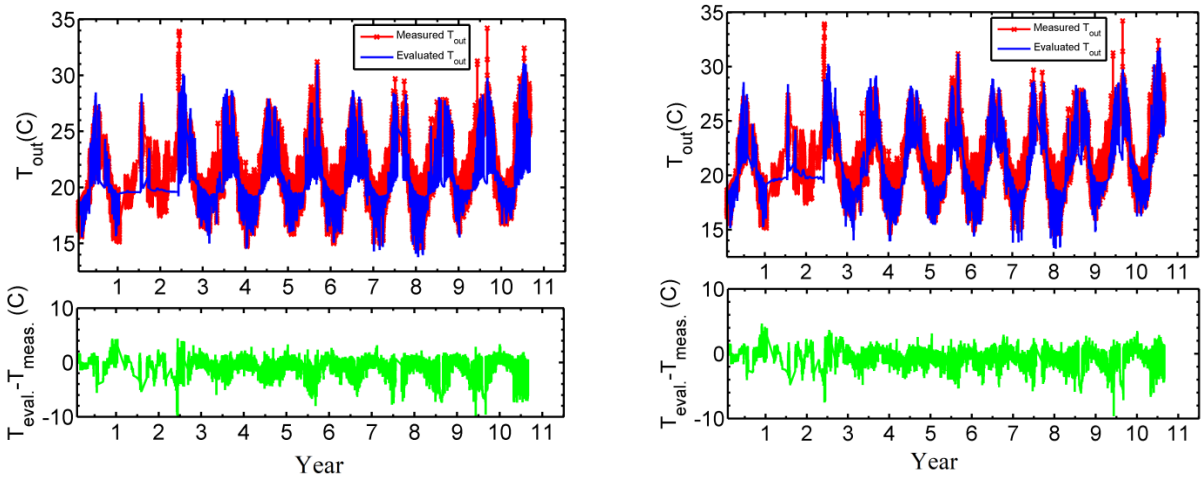

a. b.

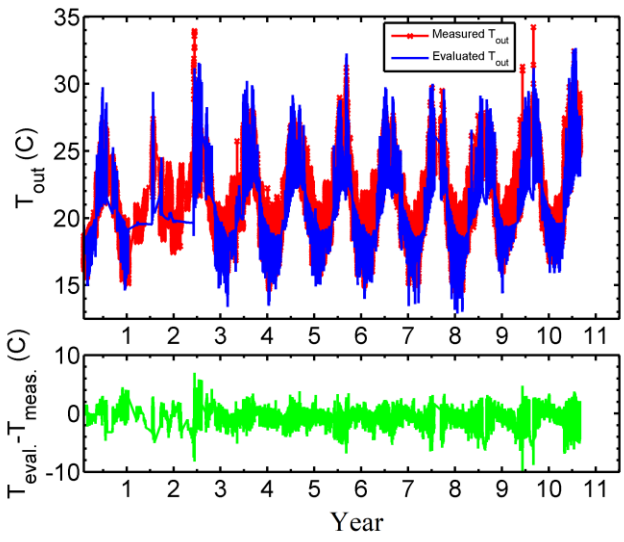

c.

Figure C-18: Evolution of the borehole outlet fluid temperature obtained by a. DST, b. Type 245 and c. Type 204 compared to measured values for the Valencia case

By comparing the results, it can be concluded that none of the three simulated temperature profiles are similar to the actual one and there are some significant differences especially for the peak values. A number of reasons may explain such differences. The ground thermal conductivity

used may be inaccurate. Indeed, Montagud et al. (2011) have mentioned that the ground thermal conductivity can have up to 20% uncertainty. Measurement errors can also be at the origin of the differences. In the simulations using DST and Types 204, the borehole thermal resistance is assumed constant. However in reality it varies.

The Valencia data is also used with the ASHRAE equation and the DST-GenOpt tool developed in this work. For the ASHRAE equation, three different sets of conditions are used. In the first condition, the average loads for the ten and a half years are used as well as the monthly peak load that happened in the month of July of the ninth year and the monthly average load for the same month. The design period is considered as ten and a half years. In the second condition, the loads of the first two and half years are neglected and the rest are used to evaluate the yearly average load and the boreholes are sized for eight years. The monthly averaged and the peak loads are the same as for the first condition. In the third condition, the load of the first three years is used. The monthly peak load occurred in the third year in July and so the average loads of July in the third year are used as the monthly averaged load. For all three conditions, the duration of the peak load is assumed to be one hour and the duration of the monthly average load is thirty days.

Table C-1 shows the input parameters and the results of these three conditions. In these calculations the ground thermal conductivity is 1.6 $W.m^{-1}K^{-1}$, the ground thermal diffusivity is 2250 $kJ.m^{-3}K^{-1}$, the ground temperature is 19.5 °C, the fluid flow rate is 0.76 $kg.s^{-1}$, the fluid thermal heat capacity is 4174 $J.kg^{-1}K^{-1}$, and the borehole radius is 0.075 m.

For the DST-GenOpt tool, the measured inlet and outlet temperatures and flow rates are used and the temperature limits of the heat pumps are assumed as 14.6 °C to 34.2 °C.

Results for the ASHRAE equation and the DST-GenOpt tool are shown on the last two lines of Table C-1. Remarkably, the ASHRAE equation for the first two conditions are very close to the actual length while the lengths determined by the DST-GenOpt tool are about 25% above the real lengths. Given that the DST-GenOpt tool is considered more accurate, this seems to indicate that the ASHRAE equation undersized the bore field for the first two sets of conditions. For the third condition, the effects of the time periods for which the measured data is not available is more significant and that is the reason that the reported result is oversized for the ASHRAE equation.

Table C-1: Three conditions used with the ASHRAE sizing equation for the Valencia case

Parameter	Units	Condition 1	Condition 2	Condition 3
q_h	kW	-21.0	-21.0	-33.0
$q_h \times PLF_m$	kW	-21.0×0.111	-21.0×0.111	-33.0×0.117
q_a	kW	-0.365	-0.389	-0.460
$R_h/R_m/R_y$	m.K.W^{-1}	0.059/0.270/0.241	0.059/0.270/0.228	0.059/0.270/0.180
R_b	m.K.W^{-1}	0.11	0.11	0.11
$t_h/t_m/t_a$	hours/days/years	1/30/10.5	1/30/8	1/30/3
T_{inhp}/T_{outhp}	°C	33.9/34.2	33.9/34.2	33.6/33.9
F_{SC}	-	1.04	1.04	1.04
T_p	°C	-0.35	-0.35	-0.20
L (ASHRAE equation)	m	50.7	50.7	80.6
L (DST-GenOpt)	m	62.8	62.8	58